LRP-1-dependent and -independent endocytic pathways of TIMP-3

Simone Dario Scilabra

A thesis submitted for the degree of Doctor of Philosophy to Imperial College London

September 2012

Department of Matrix Biology

The Kennedy Institute of Rheumatology Division

Faculty of Medicine

Imperial College London

Abstract

Tissue inhibitor of metalloproteinases-3 (TIMP-3) is an endogenous inhibitor of metalloproteinases (MMPs), adamalysins (ADAMs) and adamalysins with thrombospondin motifs (ADAMTSs), and consequently TIMP-3 is an important regulator of extracellular matrix (ECM) turnover. It has been shown that TIMP-3 levels in the tissue are regulated post-translationally by endocytosis. This study aimed to characterize the mechanism of TIMP-3 endocytosis in more detail.

In this thesis, I demonstrated that TIMP-3 is endocytosed and degraded by a number of cell types including chondrocytes, fibroblasts, and monocytes. I found that the endocytic receptor low-density lipoprotein receptor-related protein-1 (LRP-1) plays a major role in TIMP-3 endocytosis. Nevertheless, I found that TIMP-3 can also be internalized by LRP-1-null cells, indicating that an LRP-1-independent endocytic pathway also occurs. CHO-cells lacking heparan sulfate proteoglycans (HSPGs) efficiently endocytosed TIMP-3, indicating that HSPGs are not involved in its endocytosis.

Shedding of LRP-1 has been shown to reduce cell surface levels of the receptor, and hence to modulate endocytosis of its ligands. I demonstrated that LRP-1 shedding leads to accumulation of soluble LRP-1 (sLRP-1) in the medium of chondrosarcoma cells. sLRP-1 interacted with TIMP-3 and inhibited its endocytosis, but had no effect on TIMP-3 inhibition of target metalloproteinases, indicating that sLRP-1 negatively regulates TIMP-3 endocytosis.

TIMP-3 endocytosis was not affected by addition of GM6001, which inhibits interaction with target metalloproteinases, indicating that TIMP-3 can be internalized independently. Internalization of TIMP-3 in complex with a number of metalloproteinases occurred with the same kinetics as that of TIMP-3 alone. Furthermore, TIMP-3 promoted the endocytosis of MMP-1, suggesting that TIMP-3 can mediate the scavenging of metalloproteinases by cells.

The study thus identifies LRP-1 as a central mediator of TIMP-3 endocytosis, and indicates that this process regulates levels of TIMP-3 in the ECM, thus contributing to the maintenance of tissue homeostasis.

Table of Contents

Chapter 2: Materials and Methods

Chapter 3: TIMP-3 internalization by different cell types

List of Figures

List of Tables

Declaration

This PhD thesis is a result of my own work. All collaborations have been acknowledged in the appropriate place within the text.

Simone Dario Scilabra

London, 28-09-2012

Acknowledgements

I believe that many people can explain how a metalloproteinase works or correct a PhD thesis, but only few are able to explain "science" as Prof. Hideaki Nagase has done to me. All his "metaphors" will stick in my mind forever and they will contribute to make myself a good scientist. I would like to thank him for the great opportunity that he gave me and for all his teachings.

1975 times thanks to Dr. Linda Troeberg, one for each day I have spent in the Lab. Thank you for your sketches to explain me the experiments, for answering all my stupid questions and for cheering me up when my experiments failed.

I would like to thank all the people in Matrix Biology lab for making it a friendly place to work in, and especially Kazu, Rob, Salvo, Han and Szymon for our beerstormings (to be taken as friendship and contribution to my scientific development). Thanks to "my" scintillator for all the good results and to Dr. Lesley Rawlinson for dealing with my radioactive mess.

Finally, I would like to thank Prof. Maria Letizia Vittorelli, without whom all this could not have been possible.

Voglio ringraziare la mia famiglia che mi ha permesso di arrivare sin qui: mio padre che non mi ha fatto mai mancare il suo supporto, mia madre per avermi insegnato a fare per gioco quello che oggi faccio per lavoro e mio fratello che ha sempre creduto in me.

Grazie Fra', Pini, Saliba, Leo e Lazzarano (in rigoroso ordine di apparizione al KIR) per essere stati la mia "famigghia" negli ultimi sei anni. Grazie alla "Pizzica" e a tutti coloro che alla Pizzica hanno brindato con me, cantato con me, danzato con me. Grazie per avermi fatto sentire a casa quando mi sentivo solo, grazie per avermi tirato su il morale quando mi sentivo triste e grazie per avere riso con me quando mi sentivo felice. Il mio fegato vi ringrazia un po' meno....

Grazie Amore per aver aspettato pazientemente questo momento, finalmente coroneremo il nostro sogno.

alla nonna Vita e alla nonna Angela, che sarebbero state orgogliose di me.....

Abbreviations

α2M α2-macroglobulin
α2M* activated α2-macroglobulin
β-Me β-mercaptoethanol
Ab A-beta peptide
AD Alzheimer's disease
ADAM a disintegrin and metalloproteinase
ADAMTS a disintegrin and metalloproteinase with thrombospondin type I motifs
AP alkaline phosphatase
apoE apolipoprotein E
APP amyloid precursor protein
APS ammonium persulfate
AP-2 adaptor protein-2
ARF6 ADP-ribosylation factor 6
ATP adenosin-5'-triphosphate
BACE β site of APP-cleaving enzyme
BAR bin–amphiphysin–rvs
BBB blood-brain barrier
BSA bovine serum albumin
CaPPS calcium pentosan polysulfate
CD cluster of differentiation
Cdc42 Cell division control protein 42
CDE clathrin-dependent endocytosis
CIE clathrin-independent endocytosis
CHO Chinese hamster ovary
CLASPs clatrin-associated sorting proteins
COMP cartilage oligomeric protein
CR complement-type repeats
CS chondroitin sulfate
CTB cholera toxin B
CTGF connective tissue growth factor
DMEM Dulbecco's modified Eagle's medium
DMF N, N-dimethylformamide
DMSO dimethyl sulfoxide DS dermatan sulfate
ECM extracellular matrix
EDTA ethylenediaminetetraacetic acid
EGF epidermal growth factor
ER endoplasmic reticulum
ERC endosomal recycling compartment
ERK extracellular signal-regulated kinases
FCS fetal calf serum
FGF fibroblast growth factor
GAG glycosaminoglycan
GAPDH glyceraldehyde 3-phosphate dehydrogenase

GLUT glucose transporter
GPI glycosylphosphatidylinositol
GTP guanosine-5'-triphosphate
HA hylauronic acid
HEPES 4-(2-hydroxyethyl)-1-piperazineethanesulfonic acid
HIV human immunodeficiency virus
HMGB1 high mobility group box-1 protein
HRP horseradish peroxidase
HS heparan sulfate
HSC heat shock cognate
HSPG heparan sulfate proteoglycan
HUCF human uterine cervical fibroblasts
IFN-γ interferon-gamma
IGD interglobular domain
IKK IκB kinase
IL-1 interleukin-1
IL-17 interleukin-17
IL-18 interleukin-18
iNOS inducible nitric oxide synthase
KS keratan sulfate
kDa kilo Daltons
LDL low-density lipoprotein
LDL-R low-density lipoprotein receptor
LMP-1 latent membrane protein 1
L-NMA L-N-methyl-arginine
LPS lipopolysaccharides
LpL lipoprotein lipase
LPS lipopolysaccharides
LRAD3 LDL receptor class A domain containing 3
LRP low-density lipoprotein receptor-related protein
LRR leucine-rich repeat
MCF-7 Michigan Cancer Foundation - 7
mDab1 mammalian Disabled
MAPK mitogen-activated protein kinase
MEGF multiple EGF-like domain
Mek1 mitogen-activated protein kinase kinase 1
MHC major histocompatibility complex
miR micro-RNA
MMP matrix metalloproteinase
MT-MMP membrane-type MMP
MTT 3-(4,5-dimethylthiazol-2-yl)-2,5-diphenyl tetrazolium bromide
NaOH sodium hydroxate
NO nitric oxide
N-TIMP N-terminal domain of tissue inhibitor of metalloproteinase
OA osteoarthritis
OSM oncostatin M
PAI-1 plasminogen activator inhibitor type-1

PAGE polyacrylamide gel electrophoresis
PAMPs pathogen associated molecular patterns
PBS phosphate-buffered saline
PDGF platelet-derived growth factor
PDGFR PDGF-receptor
PFA paraformaldehyde
PI(4,5)P2 phosphatidylinositol 4,5-bisphosphate
PLAC protease and lacunin
PN-1 protease nexin-1
PTEN phosphatase and tensin homolog
PTH parathyroid hormone
PVDF polyvinylidene difluoride
RA rheumatoid arthrytis
Rac1 Ras-related C3 botulinum toxin substrate 1
RAGE receptor for advanced glycan endproducts
RAP receptor-associated protein
RPMI Roswell Park Memorial Institute
RT room temperature
sAPP soluble amyloid precursor protein
SDS sodium dodecyl sulfate
Sepp1 selenoprotein P, plasma, 1
SH3 Src homology 3
siRNA short interfering RNA
SLRPs small leucine-rich proteoglycans
SNAP soluble N-ethylmaleimide sensitive fusion protein (NSF) attachment protein
SNARE soluble N-ethylmaleimide sensitive fusion protein (NSF) attachment protein receptor
SNP sodium nitroprusside
SorLA sorting protein-related receptor containing LDLR class A repeats
Sp-1 specificity Protein 1
SV40 simian virus 40
$t_{1/2}$ half-life
TACE TNF-α converting enzyme
TBS Tris-buffered saline
TCA trichloroacetic acid
TEMED N, N, N', N'-Tetramethylethylenediamine
TFPI tissue factor pathway inhibitor
TGF transforming growth factor
TGFα transforming growth factor alpha
TGN *trans*-Golgi network
TIMPs inhibitor of metalloproteinases
TLR toll-like receptor
TM transmembrane domain
TNF-α tumour necrosis factor-alpha
TNFR TNF-receptor
tPA tissue-type plasminogen activator
TRAIL TNF-related apoptosis-inducing ligand

TS thrombospondin
TSP thrombospondin
TTP thrombocytic thrombocytopenic purpura
uPA urinary-type plasminogen activator
uPAR urinary-type plasminogen activator receptor
VWF von Willebrand factor
VEGF vascular endothelial growth factor
VLDL very low-density lipoprotein
VLDLR very low-density lipoprotein receptor
VSMC vascular smooth muscle cell

Equation of Life

人生・仕事の結果 = 考え方 × 熱意 × 能力

Kazuo Inamori, “Way of living”

Chapter 1

Introduction

Extracellular matrix (ECM) turnover is an important feature of several physiological processes such as development, organogenesis, wound healing and tissue remodeling. Timely degradation of the ECM is finely balanced under normal conditions (Brew and Nagase, 2010). Various types of proteinases are implicated in ECM turnover, but the major enzymes responsible for this process are considered to be the matrix metalloproteinases (MMPs), which include collagenases, gelatinases, stromelysins, matrilysins and membrane-type MMPs (Nagase and Woessner, 1999). The related metalloproteinases with a disintegrin domain (ADAMs) and ADAMs with thrombospondin motifs (ADAMTSs) are also involved in shedding of cell surface molecules and turnover of various ECM components respectively (Apte, 2009; Seals and Courtneidge, 2003). Under physiological conditions the activity of these metalloproteinases is precisely regulated at the levels of transcription, translation and post-translation, including zymogen activation, inhibition by endogenous inhibitors and clearance by receptor-mediated endocytosis (Murphy, 2009; Murphy and Nagase, 2008a; Nagase, 1997). Disruption of these balances may result in pathological conditions associated with enhanced ECM degradation such as arthritis, cancer and cardiovascular disorders (Egeblad and Werb, 2002; Murphy and Nagase, 2008b; Nagase et al., 2006; Newby et al., 2006).

Tissue inhibitors of metalloproteinases (TIMPs) inhibit MMPs, ADAMs and ADAMTSs (Brew and Nagase, 2010). Four TIMPs are known in mammals, and among them TIMP-3 plays a key role in the regulation of ECM turnover as it can uniquely inhibit MMPs and some ADAMs and ADAMTSs. Reduced levels of TIMP-3 are associated with different pathological conditions, including cancer and atherosclerosis (Cardellini et al., 2009; Cruz-Munoz et al., 2006a; Cruz-Munoz et al., 2006b). Conversely, overexpression of TIMP-3 inhibits tumor growth and invasion, and reduces the development of sclerotic plaques (Ahonen et al., 1998; Baker et al., 1999; Casagrande et al., 2012). It also blocks cartilage breakdown when it is added to porcine explants in culture (Gendron et al., 2003). This suggests a protective role of TIMP-3 in progression of a number of diseases.

In 2008, Troeberg *et al.* reported that TIMP-3 levels in the tissue are regulated post-translationally by endocytosis. This study aims to define in detail the endocytic pathways of TIMP-3, including identification of the major receptors

involved in the process, molecules that modulate the endocytosis and whether the inhibitor can scavenge proteinases from the ECM.

1.1 Endocytosis

Endocytosis is the process by which cells internalize a wide range of extracellular materials, such as liquids, small molecules (e. g. vitamins), macromolecules (e. g. proteins and glycoproteins), lipids, cell debris and microorganisms. In this process the cell membrane first invaginates to surround the particle due to be internalized, and then pinches off, forming a vesicle that contains the particle. This removal of membrane from the cell surface is balanced by recycling pathways that return much of the endocytosed proteins and lipids back to the plasma membrane. The balance between endocytic uptake and recycling controls the composition of the plasma membrane and contributes to diverse cellular processes, including nutrient uptake, cell adhesion, junction formation, cell migration, cytokinesis, cell polarity and signal transduction (Grant and Donaldson, 2009).

Ligands can be internalized by cells through a number of different endocytic pathways. Some of them are well characterized, while others are still poorly understood. Generally, endocytic pathways can be divided into two major categories: clathrin-dependent and clathrin-independent (Conner and Schmid, 2003; Doherty and McMahon, 2009; Sandvig et al., 2011; Sandvig et al., 2008). Receptor-mediated endocytosis is usually mediated by clathrin-dependent pathways. Transferrin and the receptors for low-density lipoproteins (LDLRs) are two classic examples of cargo proteins that undergo clathrin-dependent endocytosis (CDE) (Doherty and McMahon, 2009). The cytoplasmic tail of these transmembrane proteins contains sequences that are recognized by adaptor proteins that mediate the polymerization of a clathrin coat around the forming vesicle. In contrast, other ligands can enter the cells by clathrin-independent endocytosis (CIE), and being packaged in vesicles that are not clathrin coated. Regardless of the way of entry into the cell, internalized cargo is delivered to the early endosome, where sorting takes place. Some molecules are sorted to late endosomes and lysosomes for degradation, while others are recycled to the cell membrane (Grant and Donaldson, 2009). The

recycling route can be direct, where cargo is sorted directly to the cell membrane from the early endosome, or indirect, where cargo is firstly delivered to the *trans*-Golgi network before recycling to the membrane.

1.1.1 Clathrin-dependent endocytosis (CDE)

Many different cargoes can be endocytosed by CDE. In all cases budding of endocytic vesicles involves the construction of a clathrin lattice coat around them (Pearse, 1976). CDE has several different functions: it uptakes nutrients such as the iron carrier transferrin (Hopkins et al., 1985) and LDL particles (Maurer and Cooper, 2006), it regulates receptor availability on the cell surface and cellular responsiveness to external stimuli (Di Fiore and De Camilli, 2001). The recycling of vesicles from the plasma membrane also plays a key role in synaptic transmission by recycling membranes at the outer margin of the active zone. When neurons are stimulated to secrete neurotransmitters, vesicles containing neurotransmitters continuously fuse with the pre-synaptic plasma membrane. To prevent expansion of the plasma membrane, synaptic vesicles can be retrieved by CDE (Galli and Haucke, 2001). Many toxins and viruses are also reported to enter the cell via CDE (Harrison and McKnight, 2011; Nauwynck et al., 1999; Pho et al., 2000; Torgersen et al., 2001).

1.1.1.1 Clathrin coated vescicle cycle

This process includes nucleation, cargo selection, clathrin coat assembly, vesicle scission and depolymerization of clathrin-coated vesicles.

Nucleation. The first step in clathrin-coated endocytosis is the formation of an invagination of the membrane, called a pit, and the recruitment of the highly conserved adaptor protein 2 (AP2) to the plasma membrane. AP2 binds to the plasma membrane specific lipid phosphatidylinositol-4,5,-bisphosphate [PI(4,5)P2] (Honing et al., 2005) and endocytic motifs in cytoplasmic tails of receptors (Ohno et al., 1996; Ohno et al., 1995). Recent studies reported that recruitment of AP2 to the correct site at the plasma membrane, where the vesicle will bud, is mediated by a nucleation module, which includes the membrane-sculpting F-BAR domain-containing Fer/Cip4 homology domain-only proteins 1 and 2 (FCHo1/2), the epidermal growth factor receptor pathway substrate 15 (EPS15) homology domain proteins and intersectins (Henne et al., 2010). Depletion of any of these proteins has

been shown to inhibit clathrin coat recruitment, corroborating the crucial role played by these proteins in CDE (Henne et al., 2010).

Cargo selection. A wide range of accessory proteins [clathrin-associated sorting proteins (CLASPs)] drive the efficient sorting of specific cargoes into a clathrin-coated pit (Edeling et al., 2006). Like AP2, CLASPs recognize the cytoplasmic tail of specific receptors (Jung et al., 2007). For instance, NPXY-motifs, which are present in the cytoplasmic tails of all LDL receptor superfamily members, are recognized by adaptor proteins including Numb, ARH and Dab2 (Traub, 2003). These cargo-specific adaptor proteins bind AP2, which serves as a "hub" to connect PI(4,5)P2, cargo proteins, accessory proteins and clathrin. The efficient coat formation and release depend on the coordinated activity of PI kinases and phosphatases (Honing et al., 2005).

Clathrin coat assembly and vesicle scission. Purified clathrin has the form of a three-legged triskelion, where every leg contains one clathrin heavy (180 kDa) and one clathrin light chain (35-40 kDa). The clathrin heavy chain consists of multiple subdomains, starting with the N-terminal domain, followed by the ankle, distal leg, knee, proximal leg, and trimerization domains. After cargo selection and nucleation complex assembly, triskelia of clathrin are recruited to the budding vesicle and polymerize to form a lattice around the vesicle (Pearse, 1976). This lattice mediates membrane bending after the coated pit invaginates (Saffarian et al., 2009).

The GTPase dynamin is necessary for coated-vesicle formation, as blocking dynamin activity or depletion of the enzyme blocks membrane scission (Hinshaw and Schmid, 1995; Sweitzer and Hinshaw, 1998). Dynamin is recruited at the vesicle neck by BAR (Bin–Amphiphysin–Rvs) domain-containing proteins that recognize the curvature at the vesicle neck (Ferguson et al., 2009). The precise mechanism of how dynamin mediates vesicle pinching off from the plasma membrane is not clear. It seems to polymerize at the neck of the pit and induce membrane scission upon GTP hydrolysis (Stowell et al., 1999).

Depolymerization of clathrin-coated vesicles. After budding from the plasma membrane, vesicles need to be addressed to and fuse with the target endosome. For this reason the clathrin-coat needs to be disassembled from the vesicle. Depolymerization of clathrin is driven by the ATPase heat shock cognate 70 (HSC70) and by its cofactor auxilin (Schlossman et al., 1984; Schmid et al., 1984; Ungewickell

et al., 1995). After vesicle budding, auxilin binds to the terminal domains of clathrin triskelia, and it recruits HSC70 which binds to clathrin light chains and starts clathrin coat depolymerization by cycles of ATP hydrolysis (Rothnie et al., 2011).

Nucleation	Cargo selection	Coat assembly	Scission	Depolymerization
AP2 EPS15 FCHO1,2 Intersectin	Clathrin AP2 Adaptor proteins	Clathrin BAR proteins	Dynamin	Auxilin GAK

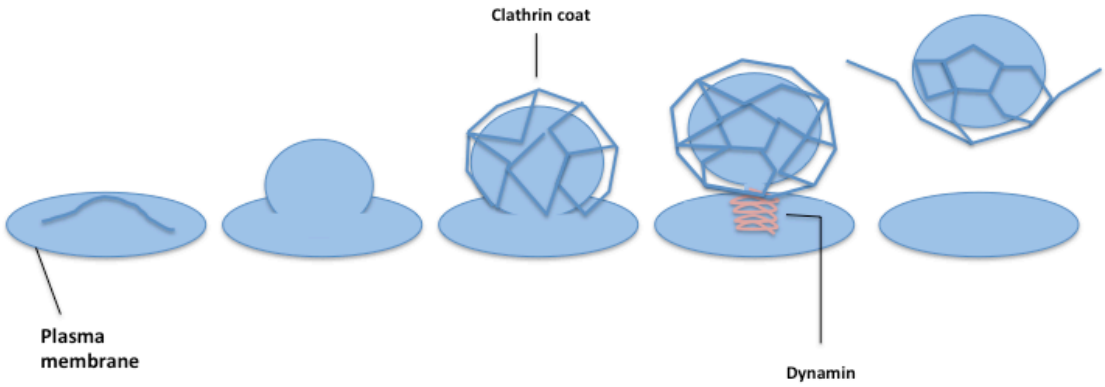

Figure 1. The clathrin coated vesicle cycle.
Schematic diagram demonstrating the stages and the proteins involved in the budding and scission of clathrin coated pits.

1.1.2 Receptor-mediated endocytosis and endocytic recycling

The endocytosis of ligands in a receptor-mediated manner requires the formation of clathrin-coated pits. The low-density lipoproteins (LDL) are endocytosed through LDL receptors through a classical example of receptor-mediated and clathrin-dependent endocytosis (Doherty and McMahon, 2009). The endocytic receptors contain specific sequences in their cytoplasmic domains that are recognized by adaptor proteins (Traub, 2009). Thus, after ligand-binding and subsequent activation, these receptors can trigger clathrin-coat assembly and vesicle formation. After endocytosis, membrane lipids and proteins have to return to the plasma membrane or move to intracellular compartments, such as late endosomes or the Golgi, to maintain cellular homeostasis (Maxfield and McGraw, 2004). This process is referred to as endocytic

recycling. Conversely, many of the ligands have to be sorted to late endosomes or lysosomes for degradation.

After budding, the newly generated vesicle fuses with a pre-existing sorting endosome (Traub, 2009). This process is mediated by proteins such as the GTPase Rab5, and by proteins that mediate vesicle fusion, including the early endosome antigen 1 (EEA1) and the "SNAP [Soluble N-ethylmaleimide sensitive fusion protein (NSF) Attachment Protein] REceptor" (SNARE) proteins (Cho et al., 2005; Dumas et al., 2001). The sorting endosome is an organelle formed by vesicles and tubules that usually localizes at the periphery of the cytoplasm. The pH of its lumen is about 6.0, and it becomes increasingly acidic during a process called endosome maturation due to the action of a vacuolar ATPase that pumps protons from the cytoplasm to the lumen (Huotari and Helenius, 2011; Lafourcade et al., 2008). The endosome maturation terminates with the generation of late endosomes from sorting endosomes. Late endosomes have a more acidic pH in the lumen and are not capable to accept plasma vesicles. The acidification of the lumen during the maturation from sorting to late endosome causes the release of many ligands from their receptors. After dissociation of ligands from their specific transmembrane receptors, vesicles containing ligands are sorted to lysosomes, where ligands are degraded. On the other hand, receptors usually undergo recycling (Maxfield and McGraw, 2004).

There are two different routes of receptor recycling, the rapid route and the slow route (Grant and Donaldson, 2009). In the rapid route, some receptors are recycled back to the plasma membrane directly from early endosomes. Alternatively, other receptors are first delivered to a tubular organelle, called the endosomal recycling compartment (ERC). The ERC sorts molecules to different destinations, but mostly to the plasma membrane, which is the case for LDLRs.

1.1.3 Caveolae/lipid raft-dependent endocytosis

Clathrin-dependent endocytosis represents the main mechanism for the internalization of extracellular ligands and plasma membrane components, however other clathrin-independent uptake mechanisms also exist. One of these pathways involves the formation of typical plasma membrane invaginations called “caveolae”

(Montesano et al., 1982). Caveolae are smaller in diameter than clathrin-coated vesicles (50-80 nm against 100 nm) and they appear flask-shaped (Stan et al., 1997). Almost all molecules that are known to be internalized in a clathrin-independent manner localize to defined microcompartments of the plasma membrane called "lipid rafts". Lipid rafts are enriched in cholesterol, glycosphingolipids, sphingomyelin, and several lipid-anchored proteins, such as GPI-linked proteins (Brown, 1998; Simons and Ikonen, 1997; Simons and Toomre, 2000; Simons and van Meer, 1988). Another factor to discriminate lipid rafts is their resistance to detergent solubilization (Heerklotz, 2002; Heerklotz et al., 2003).

The coat of caveolae is mainly composed of a protein called caveolin-1 (Rothberg et al., 1992). Caveolin-1 and the other two members of the family (caveolin-2 and -3), harbor a hairpin-like topology presenting both the C-terminus and N-terminus in the cytosolic side of the membrane (Cohen et al., 2004).

One of the best studied endocytic pathways mediated by caveolae is that of simian virus 40 (SV40) for its entry into the cell (Pelkmans et al., 2001). This pathway includes: i) sequestration and internalization; and ii) transport to caveosome.

Sequestration and internalization. After binding to MHC class I molecules, SV40 particles diffuse laterally until they are trapped in caveolae. When SV40 particles arrive in caveolae, an "endocytosis signal" is triggered by tyrosine kinase phosphorylation in proteins associated with caveolae (Pelkmans et al., 2002). One effect of this signal cascade is the disassembly of actin fibers in the proximity of the caveola-budding site on the plasma membrane, and their polymerization around the caveola with formation of a structure called the "actin tail" (Pelkmans et al., 2002). At this point dynamin is recruited to mediate pinching off of the caveola (Pelkmans et al., 2002).

Transport to caveosome. After efficient caveolae budding from the membrane, the actin tail is rapidly depolymerized and caveolae are targeted to more complex tubular organelles called "caveosomes", where SV40 particles accumulate (Pelkmans et al., 2002). Interestingly, caveosomes are directly transported to the smooth ER, bypassing all the other organelles involved in clathrin-dependent vesicle endocytosis (Kartenbeck et al., 1989).

1.1.4 Clathrin Independent Carriers- Dynamin dependent (CLIC-D)

Some lipid raft-dependent endocytic pathways are dynamin-dependent but do not require caveolins. Endocytosis of the IL-2 receptor and the gamma chain cytokine receptor are the most well established endocytic pathways falling within this category (Lamaze et al., 2001; Sauvonnet et al., 2005). Both pathways need the GTPase activity of Rho for budding, probably because it is involved in remodeling of the actin cytoskeleton and might therefore coordinate plasma membrane invagination.

1.1.5 Clathrin Independent Carriers- Dynamin Independent (CLIC-DI)

Some endocytic mechanisms require neither clathrin nor dynamin. Some of them use a different GTPase from dynamin, such as Cdc42, Rac or Arf6, and others are dependent on flotillins, a group of raft-associated, integral membrane proteins.

Cdc42 dependent uptake. SV40 and the cholera toxin B (CTB), which are internalized by cells via caveolae, have been reported to also be able to enter cells in a dynamin-independent manner (Damm et al., 2005; Kirkham et al., 2005). These pathways use Cdc42 as a GTPase and are reported to be dependent on lipid rafts for vesicle formation. Cdc42-dependent endocytosis is also responsible for the uptake of GPI-anchored proteins, also called GPI-Enriched Endocytic Compartments (GEEC) pathway (Sabharanjak et al., 2002).

Flotillin-dependent endocytosis. The lipid raft-associated proteins flotillin-1 and -2 are also reported to play a role in caveolin-independent endocytosis (Glebov et al., 2006). Flotillins have similar topology to caveolins, with both C- and N-termini in the cytosolic side of the plasma membrane. Interestingly, endocytic pathways involving flotillins can be either dynamin-dependent or -independent. For instance, endocytosis of heparan sulfate proteoglycans is flotillin- and dynamin-dependent, while endocytosis of GPI-anchored proteins are flotillin-dependent but does not need dynamin activity (Ait-Slimane et al., 2009; Payne et al., 2007). Flotillin-dependent endocytosis is slow, with a very low frequency of membrane-budding. Nevertheless, this process seems to be regulated by kinases (Riento et al., 2009).

Arf-6-associated endocytosis. ADP-ribosylation factor 6 (ARF6) is a member of the ADP ribosylation factor family of GTP-binding proteins. ARF6 has a variety of cellular

functions that are frequently involved in trafficking of membranes and endocytosis. Various proteins, including MHC class I proteins, β-integrins, the GPI-anchored protein CD59 and the glucose transporter GLUT1 have been reported to be internalized in ARF6-dependent manner (Brown et al., 2001; Naslavsky et al., 2004; Powelka et al., 2004; Radhakrishna and Donaldson, 1997).

Macropinocytosis. This involves membrane ruffling and formation of relatively large vesicles, called macropinosomes (Swanson and Watts, 1995). This mechanism is used by cells to endocytose liquid and solutes from the extracellular space. Macropinocytosis seems to be dynamin-independent and it requires GTPases such as Cdc42, Rac and ARF6 (Kerr et al., 2009).

1.1.6 Phagocytosis

Phagocytosis is an endocytic process used only by specialized cells such as monocytes, neutrophils and macrophages. Classically, phagocytosis has been considered to be the means through which macrophages remove “nonself” cells (such as invading microbes), “altered self” cells (for instance apoptotic or necrotic cells) and cell debris (Han and Ravichandran, 2011; Ishimoto et al., 2008). Phagocytosis has been also documented as a means of acquiring nutrients from the extracellular space. Phagocytosis in mammalian immune cells is activated by “eat-me signals”, namely pathogen associated molecular patterns (PAMPS), which lead to NF-κB activation (Fournier and Philpott, 2005). PAMPs are microbial structures, which upon interaction with elements of the host innate immune system trigger the initiation of host protective responses with the clearance of the pathogen by phagocytic cells (Elward and Gasque, 2003; Fournier and Philpott, 2005). Opsonins, which are molecules that target an antigen for immune response, such as antibodies or complement molecules, aid phagocytosis of pathogens (Rosenzweig and Holland, 2011). Engulfment of material is facilitated by the actin-myosin contractile system. The phagosome of ingested material is then fused with the lysosome, leading to degradation.

Following apoptosis, the dying cells need to be taken up into the surrounding tissues by macrophages in a process called efferocytosis. Apoptotic cells (and also necrotic cells) show on the cell surface molecules that usually are located

intracellularly, including calreticulin, oxidised LDL and annexin V. Phospholipids (such as phosphatidylserine) which are usually in the inner layer of the membrane can be relocated in the outer layer in apoptotic cells (Elward and Gasque, 2003). These molecules are recognised by specific receptors on the cell surface of the macrophage and trigger phagocytosis. Defects in apoptotic cell clearance are usually associated with impaired phagocytosis of macrophages. Accumulation of apoptotic cell remnants often causes autoimmune disorders, thus pharmacological potentiation of phagocytosis has a medical potential in treatment of certain forms of autoimmune disorders (Kruse et al., 2010).

Table 1: Examples of endocytic pathways

	Clathrin-dependent endocytosis	Caveolae-dependent endocytosis	CLIC-D	CLIC-DI		Flotillin-mediated endocytosis		Macropinocytosis	Phagocytosis
clathrin	✓	✘	✘	✘		✘	✘	✘	✘
caveolin	✘	✓	✘	✘		✘	✘	✘	✘
dynamin	✓	✓	✓	✘		✓	✘	✘	✓ for pseudopod extension
other GTPase involved in budding	✘	✘	Rho	Cdc42	Arf-6	✘	?	Cdc42, Rac, ARF6	?
ligands	LDL, transferrin, growth factors, glycoproteins, hydrolytic enzymes, toxins, hormones	viruses, cholera toxin, autocrine motility factor (AMF), sphingolipids, GPI-anchored proteins, endothelin, growth hormone	IL2 receptors, γc cytokine receptor	Simian Virus 40, GEEC,	MHC I proteins, β-integrins, CD59, GLUT1	Heparan Sulfate proteo-glycans	?	liquids and solutes	invading micro-organisms, apoptotic and necrotic cells

1.2 LDL receptor superfamily

The LDL receptor (LDLR) superfamily consists of several structurally homologous receptors, seven of which are very closely related: LDL receptor (LDLR), LDL receptor-related protein-1 (LRP-1), LRP-1b, megalin/LRP-2, very-low density lipoprotein receptor (VLDLR), LRP-4/multiple EGF-like domain 7 (MEGF7) and LRP8/apolipoprotein E receptor 2 (apoER2) (Figure 2). Other members are more distantly related such as sorting protein-related receptor containing LDLR class A repeats (SorLa/LRP11), LRP-5 and LRP-6. All members of the LDLR family are type 1 transmembrane receptors and consist of an extracellular N-terminal ligand binding domain, containing cysteine-rich ligand-binding repeats, epidermal growth factor (EGF)-like domains and β-propeller domains, a single transmembrane domain and all except LRP-5/-6 contain NPXY motifs in their cytoplasmic tail (Marzolo and Bu, 2009). The NPXY motifs mediate binding of the receptor to coated pits and have been shown to bind cytosolic adaptor proteins such as mammalian Disabled (mDab1) and FE65. The tyrosine of some NPXY motifs in LDL receptors is phosphorylated, indicating that they may activate intracellular signaling (Barnes et al., 2003; Hiesberger et al., 1999).

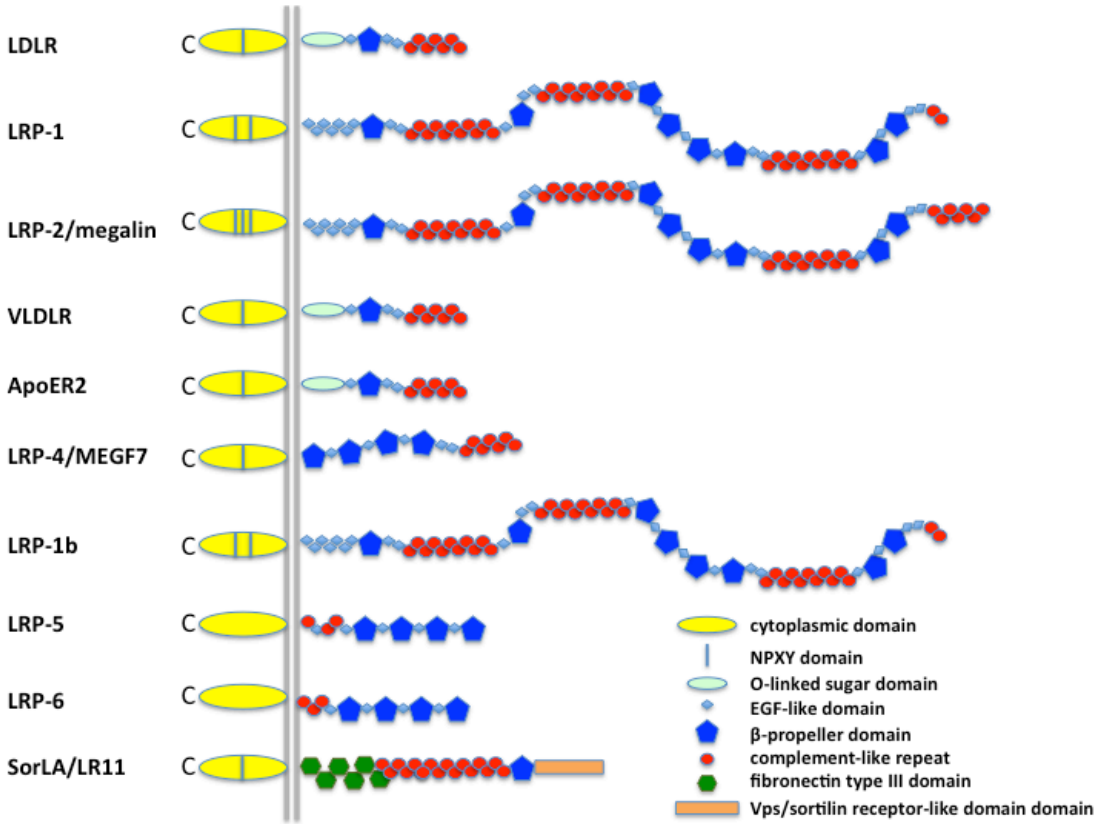

Figure 2. Modular domain organization of LDL receptor family members
Members of the LDL receptor family share the same common structural motifs. Ligand-binding domains contain between 2 and 12 complement-like repeats. These are interspersed with epidermal growth factor (EGF)-homology domains consisting of EGF and β-propeller domains. The receptors have a single membrane-spanning segment, followed by a cytoplasmic tail that contains at least one NPXY motif (except for LRP-5 and -6 which contain no NPXY domains in their cytoplasmic tail).

1.2.1 LDLR

The most characterized and founder member of the LDL receptor superfamily is the low-density lipoprotein receptor (LDLR), which was identified by Brown and Goldstein in 1974 (Brown and Goldstein, 1974). This receptor mediates the uptake of LDL from plasma and therefore regulates levels of cholesterol in circulation (Brown et al., 1986). LDLR binds to lipoproteins that contain apolipoprotein (Apo)B-100 or ApoE (Brown et al., 1986). Because of its role in modulating the uptake of cholesterol from the plasma and cholesterol content in the plasma membranes, LDLR expression needs to be finely regulated. Expression of newly synthesized LDLRs is suppressed by cholesterol with a negative feedback mechanism that therefore prevents further cellular entry of LDL and cholesterol overloading (Nimpf and Schneider, 2000).

Mutations within the LDLR gene cause familial hypercholesterolemia (Hobbs et al., 1990). In this condition, the clearance of lipoproteins from the bloodstream is impaired which results in increased LDL levels in the circulation. Ishibashi *et al.* (1993) generated a transgenic mouse in which the *LDLR* gene was inactivated by homologous recombination (Ishibashi et al., 1993). This mouse line has been widely used as a model for investigating atherosclerosis and cardiovascular diseases due to increased deposition of cholesterol in the arteries.

1.2.2 LRP-1

LRP-1, also known as CD91, was first described as the receptor for α_2-macroglobulin (α_2M) (Hanover et al., 1983). In 1988, Herz *et al.* screened a mouse lymphocyte cDNA library and identified a cell surface receptor with sequence similarity to the LDL-receptor, naming it LDL-receptor related protein (LRP) (Herz et al., 1988). Sequencing of both the α_2M receptor and LRP identified them as the same molecule (Strickland et al., 1990). LRP-1 is synthesized as a 600 kDa precursor which is cleaved in the trans-Golgi by a furin-like protease to produce a non-covalently associated receptor of 85 kDa and 515 kDa subunits (Willnow et al., 1996). The 85 kDa subunit contains a small ectodomain, single transmembrane domain and cytoplasmic tail and the 515 kDa extracellular subunit contains four ligand-binding sites, each of them consisting of several complement-type repeats (CRs) (Herz et al., 1990; Willnow and Herz, 1994). Each CR contains 40 amino acids and folds into a cage-like structure. Negatively charged residues drive the interaction with positive charged residues of ligands (Andersen et al., 2000). In several LRP-1 ligands, including receptor-associated protein (RAP) (Migliorini et al., 2003), lipoprotein lipase (Williams et al., 1994), α_2M (Arandjelovic et al., 2005), and plasminogen activator inhibitor-1 (PAI-1) (Stefansson et al., 1998), it has been shown that clusters of lysines and arginines interact electrostatically with CR domains.

Deletion of the LRP-1 gene is embryonic lethal as LRP-1-null mice die at around embryonic day 10 (Herz et al., 1992). LRP-1 expression is widespread: it is found abundantly in the placenta, liver and brain and is highly expressed in several cell types including hepatocytes, fibroblasts and macrophages (Moestrup et al., 1992; Zheng et al., 1994). Aside from activated α_2M, LRP-1 binds and internalizes a

variety of other ligands, including the matrix molecules decorin (Brandan et al., 2006) and fibronectin (Salicioni et al., 2002). Many proteases or molecules associated with regulating protease activity are also LRP-1 ligands including tissue-type plasminogen activator (tPA) (Bu et al., 1992), urokinase-type plasminogen activator (uPA) (Kounnas et al., 1993), tPA or uPA bound to plasminogen activator inhibitor type I (PAI-1) (Nykjaer et al., 1992a; Orth et al., 1994), MMP-2 (Emonard et al., 2004), MMP-9 (Hahn-Dantona et al., 2001) and MMP-13 (Barmina et al., 1999). LRP-1 is also the endocytic receptor for thrombospondin-1 and -2 (Chen et al., 1996; Mikhailenko et al., 1995), *Pseudomonas* exotoxin A (Kounnas et al., 1992) and the transcriptional transactivator HIV-1-Tat (Liu et al., 2000b). In addition, LRP-1 internalizes ApoE-enriched lipoproteins and lipoprotein lipase (LpL) (Beisiegel et al., 1989; Herz et al., 1988). LRP-1 has four ligand binding clusters (I-IV), of which ligand-binding clusters II and IV are recognized by the majority of LRP-1-ligands.

Table 2: List of a selection of LRP-1 ligands

Apolipoprotein E, Apolipoprotein B, β2-Glycoprotein, Apolipoprotein J/clusterin/Sp40,40 , Lipoprotein (a), Lipoprotein lipase, Hepatic lipase, Vitellogenin, Cubilin	**Proteins involved in lipoprotein metabolism**
RAP, HSP-96	**Protein involved in cell trafficking**
MMP-13, MMP-9, MMP-2-TIMP-2,TIMP-3, α2-Macroglobulin-protease-complexes	**Matrix metalloproteinases**
Pro-uPA, uPA-PAI-1, uPA-protease nexin-1, tPA, tPA-PAI-1	**Serine proteinases**
Thrombin-PAI-1, Thrombin-protease nexin 1, Thrombin-antithrombin III, Thrombin-heparin cofactor II, Trypsin-α1-antitrypsin, Coagulation factor VIII, Coagulation factor -α1-antichymotrypsin, Elastase-α1 antitrypsin	**Proteinases involved in blood coagulation**
IXa, Tissue factor pathway inhibitor (TFPI), Coagulation factor Xa-TFPI, Aprotinin, Cathepsin G	
Thrombospondin-1, Thrombospondin-2, Thrombospondin-2/MMP2, Decorin,Fibronectin, Complement C3	**ECM proteins**
PDGF, CTGF, TGF-β, midkine	**Growth factors**
Aβ-peptide derived from Alzheimer's precursor protein (APP)	**Proteins involved in AD**
Lactoferrin, Pseudomonas exotoxin A, Ricin A Saporin, Trichosanthin, Saposin, Circumsporozoite protein, HIV-Tat protein	**Others**

1.2.2.1 Cell trafficking of LRP-1 and role of RAP

Because LRP-1 recognizes such a variety of ligands, mechanisms exist to prevent newly translated LRP-1 from associating with ligands in the endoplasmic reticulum (ER), which would lead to aggregation and degradation instead of proper targeting to the plasma membrane. The LRP-1 ligand midkine, for example, is overexpressed in colorectal carcinomas and its premature binding to LRP-1 in the ER was found to interfere with LRP-1 maturation and secretion (Sakamoto et al., 2011). A chaperone, termed receptor associated protein (RAP), binds tightly to LRP-1 and other members of the LDL receptor family in the ER, enabling them to be correctly delivered to the plasma membrane (Williams et al., 1992). RAP is a 39 kDa protein which was identified co-purifying with LRP-1 (Ashcom et al., 1990). RAP binds to LRP-1 ligand-binding clusters II and IV with a K_d of 3 nM (Iadonato et al., 1993) and inhibits the binding and/or uptake of all known LRP-1 ligands (Bu et al., 1992; Herz et al., 1992; Nykjaer et al., 1992a).

$RAP^{-/-}$ mice showed a reduced abundance of LRP-1 in different tissues, such as liver and brain (Willnow et al., 1995). Conversely, overexpression of RAP in colorectal carcinomas promoted LRP1 maturation and secretion to the cell surface (Sakamoto et al., 2011). Site-directed mutagenesis showed that binding of RAP to LRP-1 is mediated by two critical lysines (K256 and K270). These two lysines interact with a pocket formed by two juxtaposed CRs and drive the high affinity binding of RAP to LRP-1. When only one of these two lysines is mutated to an arginine or alanine, the binding affinity decreased, but RAP could be still endocytosed by LRP-1 (van den Biggelaar et al., 2011). When both lysines are mutated to alanines or arginines, binding is completely lost and endocytosis impaired.

1.2.2.2 Endocytosis of MMPs

LRP-1 mediates endocytosis of different proteinases from the extracellular milieu and thus it plays a major role in the regulation of extracellular matrix turnover. LRP-1-dependent endocytosis has been shown to regulate levels of different metalloproteinases, including MMP-2, -9 and -13 (Barmina et al., 1999; Emonard et al., 2004; Hahn-Dantona et al., 2001; Van den Steen et al., 2006). The first MMP shown to be internalized by LRP1 was MMP-13 in 1999. Barmina *et al.* reported that

the endocytosis of MMP-13 occurred *via* a two-step mechanism. The proteinase first binds to a Ca^{2+}-sensitive receptor and then it is transferred to LRP-1, which mediates its internalization (Barmina et al., 1999). RAP did not inhibit binding of MMP-13 to cells, but impaired its internalization, and the enzyme was also able to bind the cell surface of LRP-1-null MEFs, supporting the involvement of an initial cell receptor other than LRP-1. LRP-1-mediated catabolism of MMP-13 was later shown to be impaired in human osteoarthritic chondrocytes *in vitro* (Walling et al., 2003), indicating that LRP-1-mediated endocytosis may be an important mechanism regulating the extracellular levels of MMP-13 in the cartilage matrix.

Subsequently, MMP-2 was also reported to be internalized by LRP-1, via a mechanism that involves the formation of a complex with thrombospondin-2 (Yang et al., 2001). Later, Emonard *et al.* (2004) showed that MMP-2 could also be endocytosed by cells in a thrombospondin-independent manner when in a pro-form (proMMP-2). Furthermore, proMMP-2 can be endocytosed by LRP-1 alone or in a complex with TIMP-2. Binding of the proMMP-2—TIMP-2 to the surface of HT1080 cells was not inhibited by RAP, whereas endocytosis and lysosomal degradation of pre-bound complex was inhibited by RAP (Emonard et al., 2004). The authors suggested that an unknown RAP-insensitive co-receptor might be involved in the initial binding of proMMP-2—TIMP-2 to the cell surface. This initial binding may function to concentrate ligands in specialized microdomains of the plasma membrane, which would facilitate transfer to LRP-1. Blocking the interaction of thrombospondin-1 with proMMP-2 by anti-thrombospondin antibodies inhibited LRP-1-mediated endocytosis of proMMP-2, but had no affect on the endocytosis of the proMMP-2—TIMP-2 complex (Emonard et al., 2004). Conversely, complexing of proMMP-2 with thrombospondin-1 accelerated the enzyme clearance (Emonard et al., 2004). This suggests that pro-MMP-2 and proMMP-2—TIMP-2 are internalized through a different mechanism (Emonard et al., 2004).

MMP-9 was also reported to be an LRP-1 ligand, either as a free enzyme or in complex with TIMP-1 (Hahn-Dantona et al., 2001). Another member of the LDL receptor family, megalin has also been shown to internalize MMP-9 through the enzyme's hemopexin domain (Van den Steen et al., 2006). Functions of LRP-1 in regulating growth and invasion of cancer cells have been investigated. Whether the

abrogation of LRP-1 activity induces increased invasiveness is still under debate. Neutralizing the endocytic function of LRP-1 has been shown to lead to increased invasiveness of human malignant cells (Sid et al., 2006; Webb et al., 2000). It is also reported that LRP-1 induces the expression of MMP-2 and MMP-9 and thereby promotes the migration and invasion of human glioblastoma cells. Knockdown of LRP-1 expression greatly decreased cell migration and invasion, which was rescued by the forced expression of a functional LRP-1 minireceptor (Song et al., 2009). However, Dedieu *et al.* (2008) showed that silencing LRP-1 in carcinoma cells prevents invasion despite a strong stimulation of proteolytic activity (Dedieu et al., 2008).

1.2.2.3 Endocytosis of proteinase-proteinase inhibitor complex and ECM proteins

In 1992, Nykjaer *et al*. showed that uPA had no affinity for LRP-1 when in a free form. However, when the protease was in complex with its specific inhibitor PAI-1, the affinity of uPA—PAI-1 complex was comparable to that of RAP. In the same year, Herz *et al*. showed that LRP mediates uptake and degradation of uPA—PAI-1 complexes. Interestingly, when uPA is in a pro-form it can also be internalized and degraded by cells independently from the interaction with PAI-1. In addition, another uPA-inhibitor, protease nexin-1 (PN-1), can mediate the LRP-1-dependent endocytosis of uPA (Conese et al., 1994). Similarly, tPA is poorly endocytosed when in a free form, but upon binding to PAI-1 the complex affinity for LRP-1 and subsequently its endocytosis is enhanced (Lee et al., 2010).

A number of ECM proteins are endocytosed via LRP-1. Thrombospondin-1 is a secreted glycoprotein located in the extracellular matrix that has been shown to be a potent inhibitor of angiogenesis (Lawler, 2002). Thrombospondin-1 was shown to be internalized by LRP-1 (Mikhailenko et al., 1995) and mediate VEGF scavenging by binding the growth factor and driving its uptake via LRP-1 (Greenaway et al., 2007). Thrombospondin-2 is also a LRP-1 ligand and, as already mentioned, it mediates the scavenging of MMP-2 (Yang et al., 2001). Extracellular levels of decorin are controlled by LRP receptor-mediated catabolism (Brandan et al., 2006). Decorin is a small proteoglycan that modulates the activity of TGF-β and other growth factors

and thereby influences the processes of proliferation and differentiation. LRP-1 can modulate signaling induced by several growth factors by receptor-mediated endocytosis. The platelet-derived growth factor (PDGF) binds to PDGF-receptor and triggers cell-division in fibroblasts and smooth muscle cells (Betsholtz et al., 2004). LRP-1 functions to reduce PDGF levels and PDGFR activation by directly binding to and mediating internalization of PDGF (Loukinova et al., 2002). TGF-β regulates several cellular processes in a context-dependent manner. LRP-1 was reported to bind to and endocytose TGF-β, therefore regulating its activity (Huang et al., 2003). LRP-1 mediates internalization and transcytosis of connective tissue growth factor (CTGF) in chondrocytes, determining the distribution of this growth factor in cartilage (Kawata et al., 2012; Segarini et al., 2001). Midkine is a heparin binding growth factor that has several biological functions including in cancer progression, neuronal survival and differentiation, and inflammation (Kadomatsu, 2005). LRP-1 mediates the internalization of midkine. Interestingly, after LRP-1-dependent endocytosis, midkine is not targeted for degradation but it binds to nucleolin and it translocates into nucleus, where it activates anti-apoptotic responses (Muramatsu et al., 2000; Shibata et al., 2002).

1.2.2.4 Clearance of plasma proteins

LRP-1 is highly expressed in the liver where it recognizes a variety of molecules in the circulation including proteinases-inhibitor complexes, activated coagulation factors and chylomicron remnants.

α_2M-protease complexes. α_2M is a general protease inhibitor capable of inhibiting different classes of proteinases. It has been found in the circulation of vertebrates and several invertebrate species (Sottrup-Jensen, 1989). In humans, α_2M circulates at relatively high plasma concentrations of 2–4 μM. α_2M is a tetramer of four identical 185 kDa subunits linked in pairs by disulfide bonds (Barrett et al., 1979). Each subunit has a "bait region", a segment of the α_2M that is particularly susceptible to cleavage by proteinases. The mechanism of protease inhibition involves protease cleavage of the bait region, which initiates a conformational change such that the α_2M engulfs the protease. In the resulting α_2M—protease complex, the active site of the protease is sterically shielded, but the trapped

protease remains active towards low molecular mass substrates. However, protease activity towards large molecular mass substrates is inhibited (Barrett and Starkey, 1973; Harpel, 1973; Starkey and Barrett, 1973). After the cleavage of the bait region and the conformational change, α_2M exposes a receptor-binding site, which enables the inhibitor-protease complex to interact with LRP-1 (Sottrup-Jensen et al., 1986). LRP-1 is therefore the key receptor for clearing α_2M—protease complexes. Indeed, cells genetically deficient in LRP-1 lack the ability to mediate endocytosis and degradation of ^{125}I-labeled α_2M—protease complexes (Poller et al., 1995). As discussed in section 1.2.2.1, RAP chaperones the correct folding of LRP-1. RAP-deficient mice display decreased hepatic levels of LRP-1 and consequently they have delayed clearance of α_2M—protease complexes from the circulation (Willnow et al., 1995). On the other hand, RAP was demonstrated to compete with ^{125}I-labeled α_2M—protease complexes when co-injected in mice and inhibit their clearance from the circulation, (Kounnas et al., 1996).

Aβ-peptide. The amyloid precursor protein (APP) is a type-1 integral membrane protein that is mainly expressed in neurons. APP can undergo proteolytic shedding through the action of two proteases, ADAM-10 and beta-site APP cleaving enzyme 1 (BACE1 or BACE), known as the α- or β-secretase respectively, which release two forms of the ectodomain into the extracellular space (Kuhn et al., 2010; Vassar et al., 1999). The secreted APP (sAPP) is the protease inhibitor protease nexin 2, with the serine protease inhibitory activity localized in a Kunitz domain within the APP molecule. After ectodomain shedding, the part of APP remaining associated to the cell membrane can be further processed by γ-secretase. This cleavage leads to the formation of two forms of Aβ: $A\beta_{40}$ and $A\beta_{42}$. The $A\beta_{42}$ form is highly fibrillogenic and its accumulation in the extracellular space provokes the formation of β-amyloid plaques, which are thought to be a possible cause of Alzheimer's disease (Deane et al., 2008). There is increasing interest in the role of LRP-1 in the development of Alzheimer's disease because it is responsible for the binding and the internalization of APP, the soluble ectodomain of APP (sAPP), Aβ and other molecules which have been genetically associated with Alzheimer's disease, such as apoE, lactoferrin, and α_2M (Herz and Strickland, 2001; Kounnas et al., 1995). A study by Ulery *et al.* (2001) showed that transfection of APP and LRP-1 in LRP-1-deficient cells led to a 3-fold

increase in Aβ, demonstrating that LRP-1 promotes APP endocytosis and APP processing to Aβ (Ulery et al., 2000). Other reports have also indicated that polymorphisms within the LRP-1 gene are associated with Alzheimer's disease and the levels of LRP-1 decrease with age (Kang et al., 2000; Kang et al., 1997; Kolsch et al., 2003). Knauer *et al*. (1996) showed that LRP-1 can internalize the membrane associated APP, although the mechanism by which LRP-1 mediates the internalization of APP is not yet well understood (Knauer et al., 1996). The ectodomains of LRP-1 and APP can interact, either directly or indirectly, after APP, through its Kunitz domain, binds to the binding protein for epidermal growth factor (EGFBP), which functions as a bridge between the two receptors (Kinoshita et al., 2001; Knauer et al., 1996). There is also some evidence that LRP-1 also indirectly interacts with APP in the cytoplasm, through adaptor proteins such as Fe65 (Kinoshita et al., 2001). LRP-1 was shown to bind the Aβ-peptide and mediate its transcytosis across the blood-brain barrier (BBB) from the brain to blood (Shibata et al., 2000). In the liver, LRP-1 mediates the systemic clearance of Aβ. Sagare *et al.* (2007) showed that the soluble form of LRP-1, which normally circulates in the plasma, binds to Aβ reducing its transcytosis across the BBB via receptor for advanced glycation endproducts (RAGE) and preventing its accumulation in the brain (Sagare et al., 2007).

Chylomicron remnants. Chylomicrons are lipoprotein particles composed of a core of triglycerides and cholesterol, surrounded by phospholipids and apolipoproteins. Chylomicrons are vehicles to transport hydrophobic lipids in the circulation (Hussain, 2000). They are adsorbed by the vascular endothelial cells of tissues that have a high requirement for triglycerides, such as skeletal and cardiac muscle (for the production of energy) and adipose tissue (for storage). Lipoprotein lipase, which is highly expressed in these cells, releases the triglycerides from the core of the chylomicron hydrolyzing them to fatty acids. The residual lipoproteins particles, deprived of triglycerides, are called chylomicron remnants. The apoE lipoprotein contained in chylomicron remnants has a binding site for LRP-1. Such remnants are therefore rapidly cleared by LRP-1 in the liver (Willnow et al., 1992). Indeed, deletion of

hepatic LRP-1 leads to increased plasma levels of remnant lipoproteins and accelerates atherosclerosis (Rohlmann et al., 1998).

Serpin-enzyme complexes. The serine proteinase inhibitors (serpins) are a family of proteins that inhibit serine proteases. Serpins are the largest family of protease inhibitors, with over 1000 member that have been identified in many different species, spanning from bacteria to humans. The first serpins identified in human were anti-thrombin and anti-trypsin (Bundy and Mehl, 1959; Rosenberg and Damus, 1973). After these, thirty-four other members have been added to the serpin family in human. Serpins play a key role in several biological processes, including coagulation, inflammation and tissue remodeling. Serpin complex formation with target serine proteinases that is initiated when a loop of the inhibitor is cleaved and the inhibitor undergoes a conformational change. The activated serpin-proteinase complex is recognized by a receptor system and directed to endocytosis and degradation (Ohlsson et al., 1971). LRP-1 is the main receptor mediating the hepatic clearance of serpin—enzyme complexes (Mast et al., 1991).

An interesting example of how serpin—protease complex formation mediates enzyme inhibition and its LRP-1-dependent clearance is that of uPA—PAI-1. Nykjaer *et al.* (1992) demonstrated that uPA can interact with LRP-1 only when it is complexed with PAI-1, whereas no binding was observed when uPA was in a free form (Nykjaer et al., 1992b). On the other hand, the tPA can bind to LRP-1 directly, in a manner that is independent from the formation of a complex with PAI-1 (Orth et al., 1994).

Factor VIII. After an injury to blood vessels, blood initiates the process of coagulation, which leads to the formation of blood clots. Coagulation is a very well orchestrated process that involves several proteins. Factor VIII is a key plasma protein and a member of the coagulation cascade, and its deficiency causes the well-characterized bleeding disorder hemophilia A in humans. Factor VIII normally circulates with its carrier, the von Willebrand factor, as an inactive cofactor (Fay and Jenkins, 2005). Upon injury within the vasculature, factor VIII is activated to factor VIIIa by thrombin and it dissociates from the von Willebrand factor and interacts with the cell-surface factor IX to form a macromolecular complex which plays a key

role in the coagulation cascade. The activated factor VIII forms with factor IX a complex called tenase, which, in turn, activates factor X. The activated factor X mediates the activation of pro-thrombin to thrombin. LRP-1 has been reported to mediate clearance of the activated factor VIII, and thus contributes to the maintenance of blood coagulation homeostasis (Lenting et al., 1999; Saenko et al., 1999).

1.2.2.5 Regulation of the plasma membrane proteome

While LRP-1 was originally believed to function only as an endocytic receptor, many other roles have now been reported for LRP-1 in different physiological and pathological conditions. LRP-1 plays a key role in regulating the composition of plasma membrane. In addition to diffusible proteins, it mediates the internalization of a number of transmembrane proteins, including integrins and the urokinase-type plasminogen activator receptor (uPAR). There is emerging evidence that this endocytic receptor can also trigger signaling pathways by its cytoplasmic tail. LRP-1 regulates levels of several plasma membrane-anchored proteins, including receptors, by endocytosis, and therefore it negatively modulates signal transduction triggered by other cell surface receptors. Well-characterized examples of this LRP-1 function are uPAR and integrins.

uPAR. uPAR is a glycosylphosphatidylinositol (GPI)-anchored protein found associated with lipid rafts/caveolae (Stahl and Mueller, 1995). It functions as receptor for both uPA and vitronectin (Kanse et al., 1996; Ploug et al., 1991). It has been reported that uPA bound to uPAR is stable on the cell surface. However, when the specific uPA inhibitor, PAI-1, binds covalently to uPAR-bound uPA, the ternary complex of uPAR, uPA and PAI-1 associates with LRP-1 and is sequestered in clathrin-coated pits for subsequent endocytosis (Jensen et al., 1990; Nykjaer et al., 1992b). In migrating cancer cells, uPAR localizes in lamellipodia where it assembles uPA molecules, promoting ECM degradation and cell migration (Conese and Blasi, 1995). RAP blocks the LRP-1-dependent catabolism of uPAR (Conese et al., 1995). Breast cancer cells cultured in the presence of RAP have been reported to have an increased level of cell surface uPAR, and therefore higher motility *in vitro* (Webb et al., 1999). In addition, uPAR can itself transduce cell signaling. Binding of uPA to

uPAR activates the ERK pathway and controls cell growth, apoptosis and migration (Nguyen et al., 2000). Through uPAR, vitronectin activates Rac1, which controls actin remodeling (Kjoller, 2002). Therefore, by mediating the catabolism of plasma membrane levels of uPAR through a mechanism that involves the formation of a ternary complex with uPA and PAI-1, LRP-1 suppresses uPAR-mediated activation of ERK and Rac1. This mechanism represents an example of how LRP-1 can influence cell-signaling indirectly.

Integrins. LRP-1 has been shown to facilitate the indirect endocytosis of integrins αvβ3 and α5β5, that form interactions with uPAR on the cell surface (Lillis et al., 2008). It was reported that LRP-1 interacts with integrin $\alpha_M\beta2$ in macrophages, mediating its internalization directly and therefore modulating the ability of macrophages to migrate towards sites of inflammation (Ranganathan et al., 2011a). Salicioni *et al.* (2004) reported that cell-surface levels of integrin β1 increase with the expression of LRP-1 (Salicioni et al., 2004). LRP-1 did not directly modulate endocytosis of the integrin, but the increase in integrin β1 on the cell surface was rather due to LRP-1-mediated promotion of its maturation and transport to the plasma membrane. This ability of LRP-1 to facilitate protein trafficking to the cell surface constitutes a novel mechanism by which LRP-1 regulates the plasma membrane composition.

1.2.2.6 Cell-signalling

The cytoplasmic tail of LRP-1 contains four tyrosine residues, two of which are present in a NPXY motif (Lillis et al., 2008). Intracellularly, LRP-1 was found to interact with some adapter proteins, including Dab-1 and Shc, and non-receptor tyrosines kinases such as Src and Fyn (Ranganathan et al., 2004). Interaction with such proteins and the presence of NPXY motifs in the cytoplasmic tail suggest that LRP-1 is able to transduce cell signals, although the exact mechanism by which this occurs has not been clearly elucidated. Such investigation is limited by the difficulties in cloning and expressing full-length LRP-1, which is a 600 kDa protein. Therefore, the majority of approaches are based on the use of chimeras containing the cytoplasmic domain of LRP-1 fused with different extracellular moieties. Barnes *et al.* (2003) showed that when an LRP-1-Myc chimera was expressed together with Src,

tyrosine 63 in the cytoplasmic domain of LRP-1 was phosphorylated (in this work residues were numbered starting at the first residue of the cytoplasmic domain, thus tyrosine 63 corresponds with 4473 in LRP-1 sequence). The phosphorylated tyrosine 63 was able to interact with Shc, a signaling protein involved in the activation of Ras (Barnes et al., 2003). Hu *et al.* (2006) showed that binding of tPA to LRP-1 induces tyrosine phosphorylation on the receptor which triggers the expression of MMP-9 through a cascade involving MAP (Mitogen-Activated Protein) Kinase/ERK (Extracellular Signal-Regulated Kinase) Kinase 1 (MEK1) and its downstream extracellular signal-regulated kinases 1 and 2 (ERK-1 and -2) (Hu et al., 2006). In addition, LRP-1 promotes glioblastoma cell migration and invasion by increasing the expression of MMP-2 and MMP-9 via an ERK-dependent signaling pathway (Song et al., 2009).

1.2.2.7 Inflammation and atherosclerosis

LRP-1 has been implicated in the regulation of inflammation. Gaultier *et al.* (2008b) showed that LRP-1-null macrophages had an aberrant activation of the IκB kinase (IKK)-NF-κB pathway, leading to a dysregulated secretion of pro-inflammatory cytokines. They reported that LRP-1 could indirectly downregulate this pro-inflammatory pathway by mediating the internalization of tumor necrosis factor receptor 1 (TNFR-1) (Gaultier et al., 2008b). Studies in LRP-1-null vascular smooth muscle cells (VSMC) and macrophages have indicated that LRP-1 has a protective role in atherosclerosis (Boucher et al., 2003). LRP-1 regulates smooth muscle cell proliferation by internalizing PDGF (Boucher et al., 2003). Mice carrying an LRP-1 deletion in VSMCs exhibited more atherosclerotic lesions and an aberrant activation of the PDGF-PDGFR pathway in VSMCs compared to wild-type animals, suggesting that LRP-1 plays a role in protecting the integrity of the vascular wall and preventing atherosclerosis by suppressing the PDGFR pathway (Boucher et al., 2003). In addition, a deficiency of LRP-1 in macrophages increased atherogenesis in hypercholesterolemic mice, with 40 % more atherosclerotic lesions being present compared to wild-type mice (Overton et al., 2007). In these studies, deletion of LRP-1 led to a decrease in the uptake of chylomicron remnants and VLDL, without altering plasma levels of triglycerides and cholesterol. MMP-9, which participates in

atherosclerosis progression due to its ability to degrade the ECM and promote VSMC invasion, was significantly upregulated in the absence of macrophage LRP-1. More recently, Yancey *et al.* (2011) confirmed previous findings by demonstrating increased atherogenesis in the absence of macrophages expressing functional LRP-1. This mutation enhances macrophage recruitment to the lesion site and their apoptosis (Yancey et al., 2011). In addition, LRP-1 plays a key role in maintaining the integrity of the blood-brain barrier. Endothelial cells present in the central nervous system form a barrier along all capillaries, which separates circulating blood from the brain extracellular fluid (Rubin and Staddon, 1999). This serrate barrier is maintained by specific tight junctions between adjacent endothelial cells and protects the brain from harmful substances circulating in the blood. The blood-brain barrier is carefully regulated under physiological conditions, and any dysregulation can lead to pathological conditions. LRP-1 is widely expressed by different cell-types in the brain, including VSMCs, pericytes, astrocytes and neurons (Lillis et al., 2008). Its function in maintaining the integrity of the blood-brain barrier was firstly reported by Yepes *et al*. (2003), who found that tPA regulates blood-brain barrier permeability through an as yet uncharacterized mechanism that may involve LRP-1-mediated cell-signaling (Yepes et al., 2003).

1.2.2.8 Shedding of LRP-1 and biological functions of sLRP-1

It has been reported that LRP-1 can undergo proteolytic shedding, in which the β-chain is cleaved near the plasma membrane. Thus, the soluble form of LRP-1 (sLRP-1) consists of the entire α-chain interacting with a small portion of the β-chain. sLRP-1 is still able to bind α_2M and tPA, suggesting that the ligand-binding clusters remain intact after LRP-1 shedding (Quinn et al., 1997). sLRP1 is found in human plasma (Quinn et al., 1997), in cerebral spinal fluid (Liu et al., 2009) and in the conditioned medium of HT1080 cultured cells (Selvais et al., 2011). Different metalloproteinases, such as ADAM10, ADAM12 and the tumor necrosis factor alpha (TNF-α) converting enzyme (TACE) and BACE have been shown to cleave the ectodomain of LRP-1 *in vitro* (Liu et al., 2009; Selvais et al., 2009; von Arnim et al., 2005), and sLRP-1 can also be further proteolytically fragmented by MT1-MMP (Rozanov et al., 2004). Both shedding and further degradation modulate the amount of functional LRP-1 on the

cell membrane, and consequently modulate the scavenging of LRP-1 ligands. The level of functional LRP-1 on the cell surface and consequent modulation of its clearance of ligands, such as MMP-2 and MMP-9, can be regulated by shedding in a "loss of function" manner (Selvais et al., 2011). Shedding of LRP-1 is induced by LPS and IFN-γ both *in vitro* and *in vivo* (Gorovoy et al., 2010), and it was observed that cholesterol prevents LRP-1 shedding in HT1080 cells (Selvais et al., 2011). sLRP-1 has been shown to bind directly to Schwann cells and to inhibit TNF-α-triggered signalling in a mouse model of nerve injury (Gaultier et al., 2008a). In addition, sLRP-1 induces signalling in macrophages with subsequent activation of the IKK-NF-κB pathway, leading to the expression of regulatory cytokines (Gorovoy et al., 2010).

1.2.3 LRP-2 or Megalin

Megalin was originally called glycoprotein 330 and identified as the pathogenic antigen of Heymann nephritis (Farquhar 1982). Because of its similarity with LRP-1 and the presence of homologous binding regions, Megalin was associated with the LDL endocytic receptor family (Saito et al., 1994). In fact, like LRP-1, megalin binds and internalizes serine proteinases and their complexes with serpins, including pro-uPA, uPA—PAI-1 and tPA—PAI-1. Nevertheless, unlike LRP-1, which is abundantly expressed in the liver, megalin is mainly expressed in the kidney, where it is involved in endocytosis and metabolism of several glomerular-filtered proteins and vitamin-protein complexes in the proximal tube (Christensen and Willnow, 1999). Protein—vitamin complexes that are endocytosed by megalin are then sorted to lysosomes where the proteins are degraded and the vitamins are returned to the circulation via peritubular capillaries. Similar to LRP-1, megalin seems to activate signaling pathways as it contains an NPXY sequence in the cytoplasmic tail and interacts with adaptor proteins such as Dab-2 (Hosaka et al., 2009).

Many of the biological functions of megalin were identified by Leheste *et al.* who generated megalin knockout mice (Leheste et al., 2003; Leheste et al., 1999). These mice die of pulmonary failure shortly after birth, indicating a role for megalin in development. In addition, megalin knockout mice showed brain malformations and vitamin D deficiency. Megalin was shown to bind and internalize the signaling factor BMP-4, which is a negative regulator of sonic hedgehog. Thus, sonic hedgehog

activity in the developing forebrain is reduced in megalin knockout mice leading to brain deformities, such as holoprosencephaly. In addition, lack of vitamin recovery by these mice led to greatly enhanced excretion of vitamin D in the urine. Another transgenic mouse line, carrying a deletion of megalin specifically in the kidney, was used to investigate the role of megalin in vitamin homeostasis. These studies indicated that as well as vitamin D, which is endocytosed by megalin in complex with the vitamin D binding protein, vitamin A and vitamin B12 are internalized by megalin in complex with their binding proteins. These vitamins are thus reabsorbed in the kidney, through a megalin-mediated mechanism. Megalin also acts as the endocytic receptor for parathyroid hormone (PTH) and thus has a role in PTH homeostasis (Bacic et al., 2003).

1.2.4 VLDLR

VLDLR is very similar to LDLR, with its structure differing from that of LDLR only by an additional ligand-binding repeat at the N-terminus (Sakai et al., 1994). Although LDLR and VLDLR show such similarity, the two genes are located on different chromosomes (chromosome 19 for LDLR and chromosome 9 for VLDLR) (Sakai et al., 1994), and their tissue distribution also differs, with VLDLR only scarcely expressed in the liver, where LDLR is highly abundant (Takahashi et al., 1992). VLDLR is mainly expressed in muscle, heart and brain (Takahashi et al., 1992). Two different forms of VLDLR are produced (type 1-VLDLR and type-2-VLDLR) as a result of alternative splicing (Iijima et al., 1998). VLDLR endocytoses proteins involved in lipoproprotein metabolism such as apoE and VLDL as well as several protease—inhibitor complexes including protease—anti-thrombin III and protease—PAI-1 complexes (Hussain et al., 1999). In contrast to LDLR, VLDLR is not downregulated by intracellular lipoproteins (Sakai et al., 1994; Suzuki et al., 1995). $VLDLR^{-/-}$ mice do not show any abnormalities in lipoprotein levels in plasma, although their adipose tissue mass is reduced (Frykman et al., 1995). The reason for this phenotype is mainly that VLDLR is the only lipoprotein receptor for VLDL triglycerides in peripheral tissues, while plasma lipoprotein levels depends mainly on LDLRs in the liver (Tacken et al., 2000).

1.2.5 ApoE receptor-2

The ApoER2 gene is differentially spliced and thus encodes for two forms of the same protein that originally were described as two different receptors: ApoER2 and LRP7/8 (Kim et al., 1996; Novak et al., 1996). The tissue expression pattern of ApoER2 is peculiar, as it is present only in brain, placenta and testis, unlike other LDL-receptor family members that have a much broader expression pattern (Nimpf and Schneider, 2000). One explanation of this unique pattern of expression is the involvement of apoER2 in the transport of selenium. Selenium is necessary for the synthesis of selenoproteins, but some tissues, including testis and brain, tolerate selenium deficiency better than others (Hill et al., 2003). The mechanism by which apoER2 transports selenium into the tissue has been recently characterized. The selenoprotein P, plasma, 1 (Sepp1) is an extracellular glycoprotein containing multiple selenocysteine (Sec) residues. ApoER2 was found to bind and endocytose Sepp1 and through this mechanism to regulate the homeostasis of selenium in the tissue (Kurokawa et al., 2012). Reelin is a large secreted glycoprotein that binds to ApoER2 and VLDLR (Hiesberger et al., 1999). Following ligand binding, the adaptor protein Dab1 associates with the receptor's C-terminal NPXY motifs, causing Dab1 to become tyrosine phosphorylated by members of the Src-family kinases, leading to transduction of the Reelin signal downstream (Benhayon et al., 2003). Reelin signaling through these receptors is required for a range of processes in the developing and adult brain, including neuronal migration (Andrade et al., 2007; Hiesberger et al., 1999), dendritic development (Niu et al., 2004), and synaptic plasticity (Beffert et al., 2006; Beffert et al., 2005; Weeber et al., 2002).

1.2.6 LRP-4 or MEGF7

MEGF7 was first identified by Nakayama and colleagues in 1998, who reported its similarity to some members of the LDL receptor family (Nakayama et al., 1998). MEGF7 is also known as LRP-4. Its size and structural complexity are in between that of the smaller LDL-receptors (LDLR, VLDLR and ApoER2) and the bigger members of this family (LRP-1, LRP-1b and Megalin). As with the other members, MEGF7 contains one NPXY motif in the cytoplasmic tail suggesting it plays a role in signaling transduction and receptor-mediated endocytosis. Nevertheless, its biological

functions are not yet fully understood. MEGF7 seems to play a pivotal role in the regulation of essential signaling pathways and it also appears to be involved in various other physiological functions such as brain development (May et al., 2007). Jonson *et al.* (2005) have recently generated a MEGF7 knockout mouse line, which provided some information about the biological functions of this receptor (Johnson et al., 2005). Homozygous knockout animals show fully penetrant polysyndactyly and a mild and incompletely penetrant form of craniofacial abnormalities, which are frequently associated with abnormal limb development in humans. These findings suggest a likely role for MEGF7 as a modulator of the signaling pathways that control limb development in the embryo.

1.2.7 LRP-1b

LRP-1b is approximately 600 kDa and shares 60 % amino acid identity with LRP-1 (Liu et al., 2000a). Due to this similarity, LRP-1b also binds several LRP-1 ligands, including RAP, uPA, tPA, PAI-1, uPAR, *Pseudomonas* exotoxin, although it mediates a slower rate of endocytosis than LRP-1 (Liu et al., 2001). Nevertheless, some ligands such as fibrinogen seem to be specific for LRP-1b (Haas et al., 2011). Unlike LRP-1, which is broadly expressed, LRP-1b has a restricted pattern of expression in human tissue. It is reported that its expression is high in brain and thyroid gland, with lower expression detected in skeletal muscle and testis. No expression was detected in other tissues including heart, kidney, lung and placenta (Haas et al., 2011). Deletion or inactivation of LRP-1b has been correlated with several cancers in humans (Liu et al., 2000a), including esophaegeal, urothelial, head and neck tumors, and B-cell lymphomas (Cengiz et al., 2007; Langbein et al., 2002; Nakagawa et al., 2006; Rahmatpanah et al., 2006; Sonoda et al., 2004). More recently it has been shown that its inactivation by epigenetic- and microRNA-mediated mechanisms confers cancer cells with an increased growth and invasion capacity (Prazeres et al., 2011). In addition, when activity of LRP-1b is restored, growth and invasiveness of cancer cells is inhibited in both *in vitro* and *in vivo* experimental models, with a decrease of MMP-2 levels in the tumor environment (Prazeres et al., 2011). Deletion of the LRP-1b gene is lethal in mice, although blastocysts carrying the same mutation can be propagated normally in culture. Interestingly, mice that express a truncated form of

LRP-1b missing the transmembrane and cytoplasmic domain, which are expected to secrete the entire extracellular domain (ECD) of LRP-1b, are viable and do not show any apparent phenotype (Dietrich et al., 2010). These discoveries highlight the role of LRP-1b in development and its potential role as a signal modulator in the extracellular space.

1.2.8 Other LRP related receptors

The LDL receptor family also includes additional members that are more distantly related: LRP5 and LRP6 that function as co-receptors in the Wnt canonical signaling pathway; sorLA/LR11 which plays a crucial role in trafficking APP and in the pathogenesis of Alzheimer's Disease (AD); and LRAD3 is involved in trafficking of APP.

1.2.8.1 LRP5/6

LRP5 and 6 were identified in 1998 and found to share high homology with members of LDL receptor family (Brown, 1998; Dong et al., 1998). However, rather than acting as endocytic receptors, LRP5 and LRP6 were found to be co-receptors for the Wnt canonical signaling pathway (Babij et al., 2003; Fujino et al., 2003). Both LRP5 and LRP6 ectodomains consist of four repeating units of a six-bladed β-propeller connected to an EGF-like domain, followed by three LDLR-type A repeats. Wnt proteins bind to either LRP5 or LRP6 and a frizzled receptor. This binding provokes phosphorylation of the LRP5/6 cytoplasmic tail with subsequent stabilization of β-catenin, which migrates into the nucleus and induces the expression of target genes. Both LRP5 and LRP6 play a role in development, with LRP6 appearing to be more critical than LRP5. In fact, LRP6 deletion is lethal in mice, while LRP5-null mice are fully viable, but show a high degree of osteoporosis (Holmen et al., 2004).

1.2.8.2 SorLA or LR11

SorLA, also known as LR11, is a 250 kDa receptor belonging to the LDL receptor family (Jacobsen et al., 1996). Similar to other LDL receptor family members SorLA binds ApoE, RAP and lipoprotein lipase. However, uniquely among LDLRs, SorLA contains a vacuolar protein sorting 10 protein (vps10p) domain, which indicates a role for SorLA in protein trafficking (Yamazaki et al., 1996). SorLA is mainly expressed

in brain, spinal cord and testis. Its expression is reduced in AD brains, suggesting that SorLA activity is linked with the pathogenesis of AD (Scherzer et al., 2004). In fact, in 2005 Andersen *et al.* reported that sorLA regulates processing of amyloid precursor protein. The overexpression of sorLA in neurons enhances the localization of APP in the Golgi and decreases it on the cell surface, thus diminishing the formation of Aβ. On the other hand, ablation of sorLA in mice provokes higher levels of APP on the cell surface and increases production of Aβ (Andersen et al., 2005). In 2006 Spoelgen and colleagues reported that sorLA can bind both APP and BACE through its cytoplasmic tail and that it can prevent interactions between APP and BACE and therefore Aβ production (Spoelgen et al., 2006).

1.2.8.3 LRAD3

Very little is known about LDL receptor class A domain containing 3 (LRAD3) which is the most recently identified member of the LDL receptors family (Ranganathan et al., 2011b). LRAD3 is a 50 kDa type I transmembrane receptor with an ectodomain containing three LDLa repeats, a transmembrane domain, a cytoplasmic domain of 151 amino acids, which, unlike most other members of the LDL receptor family, does not contain NPXY internalization sequences. However, the LRAD3 cytoplasmic domain contains a conserved dileucine motif which may mediate endocytosis (Ranganathan et al., 2011b). LRAD3 expression was found to be high in the brain, where it co-localizes with APP. It plays a role in modulating the processing of APP, as it was reported that coexpression of LRAD3 with APP decreases the levels of Aβ in the medium compared the expression of only APP (Ranganathan et al., 2011b).

1.3 Heparan sulfate proteoglycan-mediated endocytosis

Heparan sulfate proteoglycans (HSPGs) are glycoproteins that contain covalently attached heparan sulfate chains (HS) (Sarrazin et al., 2011). Heparan sulfates are glycosaminoglycans (GAGs) that consist of a repeating sequence of the disaccharide unit, glucuronic acid—N-acetylglucosamine, and differ for their level of sulfation. There are four groups of HSPGs according to their localization: transmembrane HSPGs, which includes the syndecan family, GPI-anchored HSPGs, which includes glypicans, and secreted HSPGs, such as perlecan and agrin (Sarrazin et al., 2011). The

proteoglycan serglycin falls into another group, which is the vesicle-associated HSPGs. The biosynthesis of heparan sulfate proteoglycans occurs in a number of steps and involves several enzymes that function sequentially. It starts with the transfer of xylose to serine residues of the protein core mediated by xylosyltransferase. After xylose, two molecules of galactose and one of glucuronic acid are added to form the link saccharide between protein and HS chain. After the link saccharide is positioned, alternate N-acetylglucosamine units and glucuronic acid units are added to the link, with the effect of elongating the HS chain. As the chain polymerizes, it undergoes several modifications that include deacetylation, sulfation and epimerisation. Esko *et al.* (1985) created a mutant cell line not expressing HSPGs due to inactivation of xylosyltransferase (Esko et al., 1985). The generation of this mutant cell line allowed functional studies that have shed light on many of the biological functions of HSPGs. To date, HSPGs are known (i) to be an important component of basal membranes, (ii) to function as extracellular storage sites for cytokines, growth factors and chemokines, (iii) to mediate cell-cell and cell-matrix adhesion, (iv) to trigger cell signaling, and (v) to act as co-receptors or as independent endocytic receptors (Couchman, 2010; Sarrazin et al., 2011).

1.3.1 HSPGs as co-receptors

HSPGs have been reported to function as co-receptors to the LDLR family for the internalization of a number of ligands. It is postulated that HSPGs may accumulate ligands in certain areas of the cell membrane rendering them more accessible for subsequent binding to LDL- receptors.

Wang *et al.* (2004) reported that thrombospondin 1, which is an LRP-1 ligand, requires prior high-affinity binding to cell surface HSPGs to be internalized (Wang et al., 2004). Tissue factor pathway inhibitor (TFPI) is an important regulator of coagulation by inhibiting both factor Xa and factor VIIa, two crucial enzymes of the coagulation cascade. TFPI is internalized by cells through a mechanism that involves both HSPGs and LRP-1 (Schwartz and Broze, 1997). The high amount of HSPGs on the cell surface compared to LRP-1 suggests that HSPGs serve to dock TFPI at the cell surface but do not mediate its uptake, and LRP-1 mediates TFPI internalization. The extracellular levels of coagulation factor VIII are also regulated by a similar

mechanism. The internalization of factor VIII is blocked in mutant cells lacking either LRP-1 or HSPGs (Sarafanov et al., 2001). As in the case of TFPI, firstly HSPGs mediate the binding of factor VIII to the cell surface, and secondly LRP-1 induces its endocytosis. Several other proteins involved in blood coagulation are internalized in a LRP-1- and heparin-sensitive manner, including uPA and protease nexin-1,(Crisp et al., 2000). Altogether these studies indicate the LRP-1/HSPGs axis functions as a key regulator of blood homeostasis.

Kanekyo *et al*. (2011) reported that another LRP-1 ligand, Aβ peptide, are internalized in such a manner that involves HSPGs as co-receptor. Both heparin, which antagonizes cell surface HSPGs, and heparinase treatment blocked the LRP-1-dependent internalization of Aβ by neurons, showing that HSPGs and LRP-1 function in a cooperative way for its internalization (Kanekiyo et al., 2011).

1.3.2 HSPGs as independent receptors

Membrane HSPGs can also act as independent receptors, although the precise mechanism is not completely understood yet. Clathrin, caveolin and dynamin are not involved in the process of internalization through HSPGs, and transmembrane HSPGs are internalized with a different kinetics compared to GPI-anchored HSPGs (Yanagishita, 1992). As was discussed in Section 1.2.2.4, LRP-1 plays a crucial role in the hepatic clearance of chylomicron remnants from plasma. Chylomicron remnants can also interact with HSPGs, which are abundant on the surface of hepatocytes (Mahley and Huang, 2007). HSPGs can either function as co-receptors to LRP-1 for the clearance of chylomicron remnants, or they can directly mediate the internalization of remnants. Recently, Stanford *et al.* (2009) reported that syndecan-1 is the primary heparan sulfate proteoglycan involved in the hepatic clearance of chylomicrons, showing that *Sdc*$^{-/-}$ mice accumulated plasma triglycerides (Stanford et al., 2009).

1.4 TIMPs

Many proteinases are involved in the degradation of the ECM, and the matrix metalloproteinases (MMPs) are thought to be of primary importance. MMPs, also called matrixins, belong to the metzincin superfamily of zinc-dependent proteinases (Nagase and Woessner, 1999). The disintegrin and metalloproteinases (ADAMs) and the disintegrin and metalloproteinases with thrombospondin domains (ADAMTSs) also form part of the metzincin superfamily (Apte, 2009; Edwards et al., 2008). While MMPs and ADAMTSs mainly degrade ECM components, affecting the cell environment, ADAMs cleaves cell surface proteins, including signaling receptors, adhesion molecules and pro-cytokines. The activity of MMPs, ADAMs and ADAMTSs in the tissue is finely orchestrated, and dysregulation of their activities leads to pathological conditions associated with uncontrolled ECM turnover, inflammation, cell growth and migration, such as arthritis, cancer, and cardiovascular diseases. Regulation of MMPs, ADAMs and ADAMTSs occurs at different levels, including transcriptional and post-transcriptional regulation, activation of inactive precursors and inhibition by the tissue inhibitors of metalloproteinases (TIMPs). (Murphy, 2009; Nagase et al., 2006; Werb et al., 1999). Consequently, TIMPs are involved in maintaining tissue homeostasis by controlling the activity of these metalloproteinases and therefore TIMPs are important in biological and physiological processes including embryogenesis, development and wound healing.

The first member of the TIMP family was discovered in the 1970s. It was found in different tissues like skin, cartilage tendon and serum, as an inhibitor of collagenases (Bauer et al., 1975; Vater et al., 1979; Woolley et al., 1975). Later, it was also found to be an inhibitor of gelatinases and stromelysins, and therefore named "tissue inhibitor of metalloproteinases" or "TIMP" (Cawston et al., 1981). Four TIMPs have been characterized in humans. All of them present some common structural features and the same mechanism of MMP inhibition. Nevertheless, the four TIMPs harbor some properties that render them unique among the family.

1.4.1 TIMPs: common features

All mammalian TIMPs consist of two distinct domains, an N-terminal domain of about 125 amino acid residues and a C-terminal domain of about 65 residues. The

global structure of each domain is maintained by three disulfide bonds (Williamson et al., 1990). Recombinant forms of the N-terminal domains of TIMPs, denominated N-TIMPs, have stable native structures and are fully active as inhibitors of MMPs (Murphy et al., 1991). The N-terminal domains consist of five β-strands connected by loops, and three α-helices, one at the N-terminus and two close to the C-terminus forming part of the interface with the C-domain (Figure 3) (Brew and Nagase, 2010).

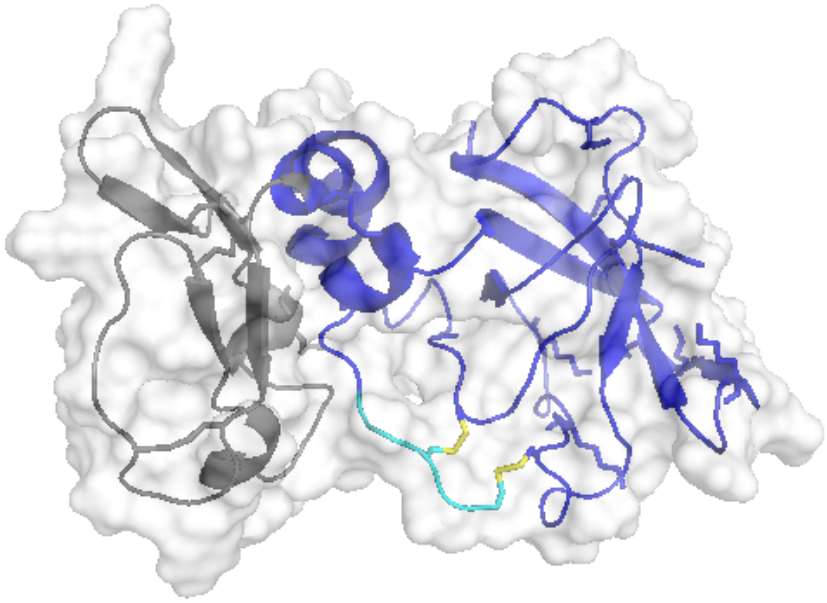

Figure 3, Common structure of mammalian TIMPs
A ribbon structure showing the common features of mammalian TIMPs: the N-terminal domain (blue) with the terminal five residues which make the majority of interactions with metalloproteinases (cyan), the conserved disulfide bonds Cys^{1}-Cys^{70} and Cys^{3}-Cys^{100} (yellow), and the C-terminal domain (grey) are indicated.

Although the four TIMPs bind tightly to most MMPs, some differences in inhibitory properties among the four different TIMPs have been reported. TIMP-1 is more limited in its inhibitory spectrum than the other three TIMPs, with low affinities for membrane-type MMPs (Murphy and Nagase, 2008a), whereas TIMP-2 and -3 are weaker than TIMP-1 in inhibiting MMP-3 and -7 (Hamze et al., 2007), and TIMP-3 unlike other TIMPs, is able to inhibit several members of the ADAMTS and ADAM metalloproteinase families (Amour et al., 1998; Kashiwagi et al., 2001).

Structures of TIMP-1, TIMP-2 and N-TIMP-3 in inhibitory complexes with their target metalloproteinases have been determined by X-ray crystallography (Fernandez-Catalan et al., 1998; Gomis-Rüth et al., 1997; Wisniewska et al., 2008). TIMPs appear as wedge-shaped, with a ridge which inserts into the metalloproteinase active site cleft in such a manner that the conserved N-terminal Cys^1 coordinates the catalytic Zn^{2+} of the metalloproteinases (Figure 4)(Gomis-Rüth et al., 1997). The bidentate coordination of the metal ion by the N-terminal α-amino group and carbonyl group of Cys^1 displaces the water molecules needed for peptide bond hydrolysis, and the majority of the interactions between TIMPs and a metalloproteinase are made by a continuous ridge formed by the N-terminal five residues (for instance Cys^1-Thr-Cys-Val-Pro^5 in TIMP-1) which are highly conserved among all TIMPs, and the loop connecting the β-strands C and D (CD loop).

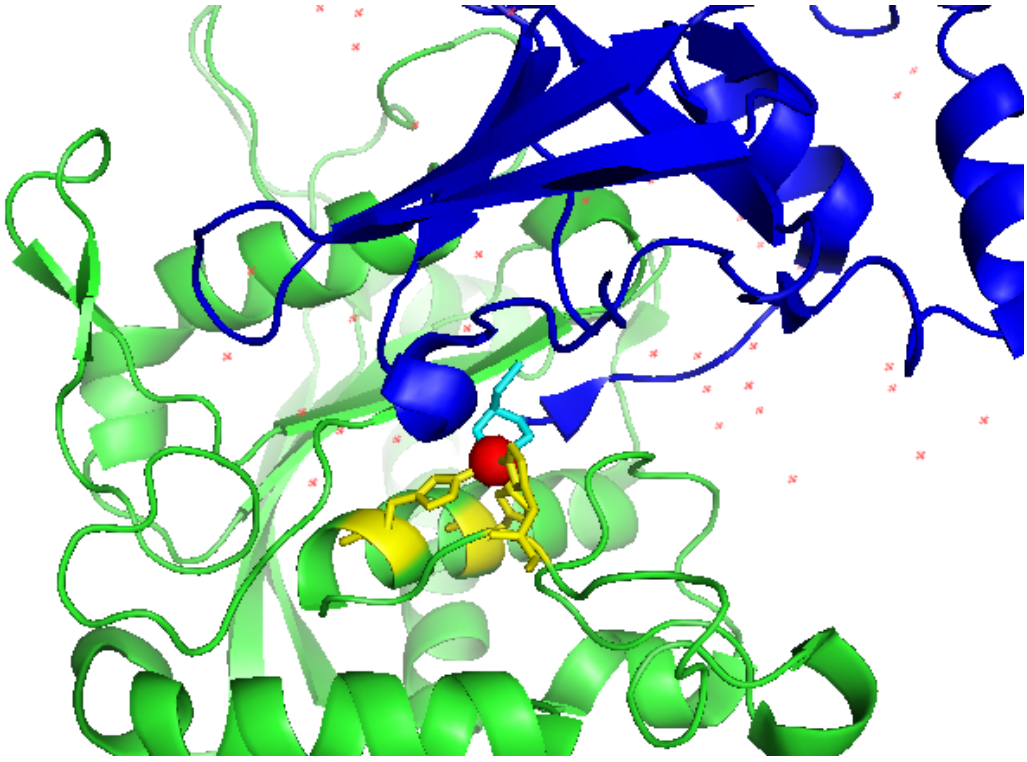

Figure 4, Common interactions between TIMPs and metalloproteinases
The conserved N-terminal Cys^1 (cyan) of the TIMP moiety (blue) coordinates the catalytic Zn^{2+} (red sphere), which is bound to the three conserved histidines (yellow) of the metalloproteinase (green).

1.4.1.1 TIMP-1

TIMP-1 was the first member of TIMP family to be discovered and purified (Bauer et al., 1975; Vater et al., 1979; Woolley et al., 1975). Compared to TIMP-3, it has a narrower specificity against the different groups of metzincins, being able to inhibit MMPs and only ADAM-10 among ADAM proteinases, but with a relatively low affinity for the membrane-type 1 matrix metalloproteinase (MT1-MMP) and MMP-19 (Amour et al., 2000; Brew and Nagase, 2010). TIMP-1 has several biological activities that influence cell behavior. Many of these activities are dependent on its metalloproteinase inhibitory capability, but others are independent from this inhibitory function. For example, TIMP-1 was shown to promote cell growth in various cell types including fibroblasts (Hayakawa et al., 1992). This is due to its interaction with a specific receptor, which is still unknown, and activation of MAPK signaling pathway (Wang et al., 2002). TIMP-1 has also been reported to have anti-apoptotic activity (Taube et al., 2006). Thus, high levels of TIMP-1 in serum and expression in cancer are associated with poor prognosis in many kinds of cancer (Kossakowska et al., 1991; Nakopoulou et al., 2002). The anti-apoptotic activity is mediated by the interaction of the inhibitor with CD63, a member of the tetraspanin family (Jung et al., 2006). The TIMP-1—CD63 complex interacts with integrin β1 and induces the activation of survival signaling through focal adhesion kinase, P13K and ERK (Liu et al., 2003; Liu et al., 2005).

1.4.1.2 TIMP-2

TIMP-2 was first purified from the cultural medium of human melanoma cells as a complex of proMMP-2—TIMP-2 (Stetler-Stevenson et al., 1989). Besides its inhibition of MMPs, the protein is capable of inhibiting angiogenesis (Moses et al., 1990). All four members of the TIMP family are reported to have anti-angiogenic activity, which is linked to their capability to inhibit metalloproteinases. However, compared to other TIMPs, TIMP-2 is unique in its ability to inhibit endothelial cells proliferation and migration in a manner which is independent from metalloproteinase inhibition and possibly mediated by binding to a cell-membrane receptor (Murphy et al., 1993a). As with TIMP-1, TIMP-2 induces cell growth. However, TIMP-2 triggers a different signaling pathway from that activated by TIMP-

1, and leads to the activation of the protein kinase A (PKA) (Wang et al., 2002). Inhibition of angiogenesis may be due to TIMP-2 interaction with $\alpha_3\beta_1$ integrin, which induces tyrosine-kinase phosphatase activity and suppresses growth factor-induced phosphorylation pathways (Feldman et al., 2004).

Another unique property of TIMP-2 is its ability to mediate activation of pro-MMP2. TIMP-2 can interact with the hemopexin domain of pro-MMP-2 by its C-terminal domain. A molecule of MT1-MMP can function as a membrane receptor for the pro-MMP-2—TIMP-2 complex. A second molecule of MT1-MMP, free of TIMP-2, homodimerizes with the molecule of MT1-MMP bound to pro-MMP-2—TIMP-2 complex. In this manner, the free MT1-MMP which is in close proximity to the trimolecular complex cleaves the pro-domain from pro-MMP-2 (Strongin et al., 1995).

1.4.1.3 TIMP-3

TIMP-3 harbors some unique properties among TIMPs. It was first reported as an ECM binding protein (Pavloff et al., 1992; Staskus et al., 1991; Yang and Hawkes, 1992) different from other TIMPs which are soluble in the extracellular milieu. Lee *et al.* (2007) identified the ECM-binding motif in TIMP-3 by extensive site-directed mutagenesis. Mutation of a cluster of lysine and arginine residues, situated on the opposite side of the molecule to the inhibitory ridge, to glutamine or glutamate residues, resulted in a soluble TIMP-3. This cluster of lysines and arginines is specific for TIMP-3. Furthermore, when this cluster of lysines and arginines was introduced into TIMP-1, the chimera inhibitor showed binding to the ECM (Lee et al., 2007).

TIMP-3 inhibits some members of the MMP, ADAM and ADAMTS families (Amour et al., 1998; Kashiwagi et al., 2001; Murphy et al., 1991). The ADAM metalloproteinases are a family of membrane-bound enzymes, which are also referred to as “sheddases” for their ability to cleave extracellular portions of transmembrane proteins, releasing the soluble ectodomains from the cell surface. TIMP-3 was first shown to inhibit ADAM-17, also called the tumor necrosis factor alpha (TNF-α) converting enzyme (TACE), which mediates the shedding of soluble TNF-α from its membrane-associated precursor (Amour et al., 1998). It also sheds others receptors such as TNF receptors, tumor growth factor alpha (TGFα) and L-

selectin (Le Gall et al., 2009; Wang et al., 2009). TIMP-3 is also an effective inhibitor of ADAMTS-4 and -5, also known as aggrecanase-1 and -2, respectively (Kashiwagi et al., 2001). The inhibition of TACE and aggrecanases suggest a leading role for TIMP-3 in regulating inflammatory processes and affecting the progression of diseases such as cancer, rheumatoid arthritis and osteoarthritis.

TIMP-3 shows a pro-apoptotic effect on several cell types (Ahonen et al., 1998; Baker et al., 1999). The pro-cell death function of TIMP-3 is located within the N-terminal domain and it correlates with its MMP-inhibitory activity (Bond et al., 2000). Bond *et al.* (2002) showed that TIMP-3 is involved in a type II apoptotic pathway initiated by FAS, by demonstrating that a dominant negative form of this death receptor inhibited the TIMP-3 induced apoptosis. TIMP-3 pro-apoptotic activity results from its ability to stabilize TNF receptors due to an inhibition of TACE-mediated shedding (Ahonen et al., 2003).

TIMP-3 is also a potent inhibitor of angiogenesis; this activity is dissociated from the metalloproteinase inhibiting activity and it is due to direct binding to VEGF receptor 2 which blocks the effect of VEGF on endothelial cells (Qi et al., 2003). TIMP-3 also binds to angiotensin II type-2 receptor, and overexpression of both TIMP-3 and angiotensin II type-2 receptor synergistically inhibits angiogenesis (Kang et al., 2008).

1.4.1.4 TIMP-4

Among four TIMPs, TIMP-4 is the last one identified (Greene et al., 1996). The primary sequence of TIMP-4 is 51% identical to that of TIMP-2 (Olson et al., 1998). Its tertiary structure is considered to be stabilized by six disulfide bridges, which is a structural signature of TIMPs. Despite its similarity to TIMP-2 and the capability to interact with pro-MMP-2, TIMP-4 does not induce the activation of the enzyme (Bigg et al., 2001). While other TIMPs are expressed in most tissues, the expression of TIMP-4 is largely confined to the heart, kidney and brain (Koskivirta et al., 2010). Table 3 shows the general properties of the four TIMPs.

Table 3: Schematic summery of the general properties of the four TIMPs

Property	TIMP-1	TIMP-2	TIMP-3	TIMP-4
nº of residues	184	194	188	194
M_r (Da)	20,709	21,755	21,690	22,329
Expression	Most tissue types	Most tissue types	Most tissue types	heart, kidney, brain
MMP inhibition	Weak for MMP-14, -16, -19 and -24	All	All	Most
Adamalysin inhibition	ADAM-10	ADAM-12	ADAM-10, -12, -17, -28, -33; ADAMTS-1, -2 (weak), -4, -5	ADAM-17, -28, -33 (weak)
Other partners	CD63	$\alpha_3\beta_1$	EFEMP1, VEGFR2 angiotensin II receptor	-
Pro-apoptotic	Negative	Positive Negative	Positive	Negative

1.4.2 Biological activity of TIMP-3

Studies with mice deficient in TIMP-3 have suggested the physiological and pathological functions of TIMP-3 *in vivo*. *Timp3*-null mice exhibit several abnormalities, including air space enlargement in the lungs, enhanced apoptosis during mammary gland involution, dilated cardiomyopathy, abnormal vascularization with enlarged capillaries and impaired bronchiole branching morphogenesis (Fata et al., 2001; Fedak et al., 2004; Gill et al., 2003; Leco et al., 2001). These abnormalities are due to enhanced matrix degradation caused by a lack of metalloproteinase inhibition. The *Timp3*-null mouse has additional defects related to excess ADAM and ADAMTS activity. *Timp3*-null mice release high levels of TNF-α upon challenge with partial hepatectomy, due to excess of ADAM-17 activity (Mohammed et al., 2004). These mice show signs of premature arthritis due to increased aggrecan degradation (Sahebjam et al., 2007). These studies indicate that TIMP-3 is a key endogenous regulator of metalloproteinases involved in ECM turnover and inflammation.

1.4.3 Regulation of TIMP-3 synthesis

The synthesis of TIMP-3 is regulated transcriptionally, which includes epigenetic regulation. More recent studies have shown that it is also regulated post-transcriptionally by microRNA (miRNA).

Transcriptional regulation. TGF-β1 is a multifunctional growth factor produced by different cell-types such as monocytes, platelets and chondrocytes. This factor is a potent inducer of chondrogenesis during development and ECM synthesis in cartilage. It has been shown to induce the expression of TIMP-3 in articular chondrocytes (Gunther et al., 1994; Su et al., 1996). Qureshi *et al.* (2005) reported that TGF-β1 induces the expression of TIMP-3 by activating the ERK-MAPK signaling pathway leading to phosphorylation of the Sp-1 transcription factor and its subsequent binding to the *TIMP3* promoter. More recently, Qureshi *et al.* (2008) also reported that TIMP-3 expression could be induced by TGF-β1 through a mechanism involving Smad-2, -3 and -4. Oncostatin M, a cytokine belonging to the IL-6 family, can also induce expression of TIMP-3 in human chondrocytes by activating the Janus Kinase/STAT signaling pathway (Li et al., 2001).

Epstein-Barr virus latent protein 1 (LMP-1) is a viral protein essential for the capability of Epstein-Barr virus to mediate growth transformation of B-cells. LMP-1 was shown to suppress TIMP-3 transcription by binding to the promoter of the TIMP-3 gene, thus promoting metastasis in EBV-negative nasopharyngeal carcinoma cells (Chang et al., 2008). Human hepatitis B virus suppresses TIMP-3 expression, but the molecular mechanism is still poorly understood (Kim and Kim, 2004).

Missense mutations in the p53 gene inactivate its growth suppressing activity and are observed in the majority of human tumors. Thomas *et al.* (2006) showed that missense mutations in p53 create a mutant p53 that gained the ability to bind to the TIMP-3 promoter and suppress its expression. Loss of TIMP-3 expression in cancer cells could lead to increase of metalloproteinase activity and therefore increased metastatic potential.

Epigenetic regulation. The epigenetic regulation of gene expression involves a number of mechanisms that are not dependent on gene sequence. Examples of such mechanisms are DNA methylation and histone modification. DNA methylation involves the addition of a methyl group to cytosines or adenines. DNA methylation

suppresses gene expression by affecting the binding of transcriptional factors to the gene. In addition, methylated DNA is recognized by methyl-CpG-binding domain proteins, which, in turn, recruit chromatin remodeling proteins, including histone deacetylases. Chromatin remodeling proteins modify histones and enhance the formation of compact and inactive chromatin. Aberrant methylation of the promoter region of TIMP-3 gene was found associated with primary cancer of the brain, kidney, colon, breast, etc (Bachman et al., 1999). This epigenetic regulation of the TIMP-3 gene therefore participates in cancer progression (Eads et al., 2001; Rohrs et al., 2009; Ueki et al., 2000).

Post-transcriptional regulation. Post-transcriptional regulation of TIMP-3 expression has been reported in both physiological processes and pathological conditions. Several miRNAs have been found to bind the 3'-UTR of the TIMP-3 mRNA resulting in the degradation of TIMP-3 transcripts and its gene silencing (Gabriely et al., 2008; Wang et al., 2010).

miR-21 is one of the most expressed micro-RNAs in many different tumors, including glioblastoma, and its expression often correlates with tumor grade and poor prognosis (Gabriely et al., 2008). miR-21 targets TIMP-3 mRNAs, leading to their degradation. Its ability to reduce TIMP-3 expression promotes tumor invasion (Gabriely et al., 2008; Selaru et al., 2009; Song et al., 2010). Regulation of TIMP-3 by miR-21 has also been observed in physiological processes, including wound healing (Yang et al., 2011). During skin wound healing, keratinocytes need to proliferate and migrate. Both keratinocyte proliferation and migration are favored by expression of miR-21, which attenuates TIMP-3 expression (Yang et al., 2011).

TIMP-3 mRNA is a validated target of miR-181b and miR-206 (Limana et al., 2011; Wang et al., 2010). miR-181b is upregulated by TGF-β and its expression is markedly suppressed in hepatocarcinomas. These data suggest that TGF-β can modulate TIMP-3 expression by miR-181b (Wang et al., 2010). miR-206-mediated downregulation of TIMP-3 promotes cardiac regeneration of chronically failing hearts (Limana et al., 2011).

miR-221 and miR-222 can downregulate the expression of TIMP-3. Garofalo *et al.* (2009) found that the hepatocyte growth factor/scatter factor upregulates miR-221 and miR-222 expression. This enhances tumorigenicity of lung and liver

cancer cells by downregulating the phosphatase and tensin homolog (PTEN) and TIMP3 (Garofalo et al., 2009; Song et al., 2007).

1.4.4 TIMP-3 in disease

Cell-specific overexpression of TIMP-3 has been shown to have a protective role in several pathologies, including arthritis, cancer and atherosclerosis. Gendron *et al*. (2003) showed that TIMP-3 inhibits glycosaminoglycan release from bovine nasal and porcine articular cartilage explants stimulated with interleukin-1 alpha (IL-1α) or retinoic acid, suggesting that TIMP-3 may be a candidate agent for use against cartilage degradation and a potential target for therapy of arthritis. Intra-articular injection of TIMP-3 similarly inhibited cartilage degradation in a rat meniscal tear model (Black et al., 2007).

Baker *et al.* (1999) initially showed that adenoviral-mediated overexpression of TIMP-3 in different cancer cell-lines, including MCF-7, HeLa and HT1080 cells, inhibited cell invasion by blocking MMP activity and inducing apoptosis (Baker et al., 1999). Several other groups have also investigated the ability of TIMP-3 to reduce tumor growth and invasiveness *in vivo*. Xenografts of human chronic myelogenous leukemia cells were less invasive when they overexpressed TIMP-3 (Yu et al., 2006). In a similar manner, TIMP-3 overexpression blocked growth and invasion of solid tumors (Anania et al., 2011; Zhang et al., 2010).

TIMP-3 levels in carotid atherosclerotic plaques are reduced, particularly in regions enriched with monocytes and macrophages (Cardellini et al., 2009). A deficiency in TIMP-3 leading to increased TACE activity may contribute to vascular disorders by increasing inflammatory mediators, such as TNF-α and monocyte chemoattractant protein-1, that recruit monocytes and T cells from the circulation (Fiorentino et al., 2010). The protective role of TIMP-3 in atherosclerosis was investigated by Casagrande *et al*. (2012) by generation of a mouse line which overexpresses TIMP-3 in the macrophages via the macrophage-specific gene Mac1. They were protected from the development of atherosclerotic plaques when these mice were crossbred with the LDLR knockout mouse (*MacT3/LDLR*$^{-/-}$). Atherosclerotic plaques in MacT3/LDLR$^{-/-}$ mice contained increased collagen content and decreased necrotic core formation, and fewer T cells and macrophages

(Casagrande et al., 2012). These results indicate that overexpression of TIMP-3 may be beneficial in prevention of plaque formation.

1.4.5 Metalloproteinases inhibited by TIMP-3

1.4.5.1 MMPs

The human genome encodes 23 MMPs, also called matrixins (Nagase and Woessner, 1999). All of the matrixins are multidomain zinc metalloproteinases, which share sequence homology in their catalytic domains (Bode et al., 1999). They are synthesized as pro-enzymes and their activity is regulated by zymogen activation. The pro-domain consists of three α-helices connected by loops. All the matrixins, except MMP-23, contain a "cysteine switch" motif PRCGXPD in the pro-domain. The thiol SH group of the cysteine coordinates the catalytic zinc. Upon cleavage of the prodomain, the Cys-Zn^{2+} coordination is disrupted and a water molecule coordinates the catalytic zinc, rendering the enzyme active for peptide hydrolysis (Van Wart and Birkedal-Hansen, 1990). The catalytic domain consists of one five-stranded β-sheet and 3 α-helices and connecting loops. It contains a conserved zinc-binding motif HEXXHXXGXXH, where three histidine residues coordinate a Zn^{2+} ion. The catalytic domain also contains a conserved methionine, which forms a "Met-turn", eight residues after the zinc-binding motif. The "Met-turn" forms the base of the active site cleft around the catalytic zinc (Bode et al., 1999) The catalytic domain is connected to a hemopexin domain by a linker region. The hemopexin domain is essential for collagenases to perform their collagenolytic activity, as it is necessary to unwind the triple helical structure of collagen and render the collagen cleavage site accessible to the catalytic domain (Chung et al., 2004).

MMPs are divided in 6 groups based on their domain organization and substrate preferences: i) collagenases, ii) gelatinases, iii) stromelysins, iv) matrilysins, v) membrane-type MMPs and vi) other MMPs. Tissue distribution and representative substrate of each MMPs are listed in Table 4.

Collagenases (MMP-1, MMP-8 and MMP-13) are capable of cleaving fibrillar collagens type I, II and III into characteristic 1/4 and 3/4 fragments. They can also cleave other ECM molecules, cytokines, chemokines, growth factors, binding proteins and cell adhesion molecules (Nagase et al., 2006).

Gelatinases (MMP-2 and MMP-9) have weak or no activity against fibrillar collagens respectively (Aimes and Quigley, 1995; Patterson et al., 2001). They can degrade denatured collagens, gelatins and other ECM molecules, such as laminin and aggrecan core protein.

Stromelysins (MMP-3, MMP-10 and MMP-11) share the same domain arrangement with collagenases, although they do not cleave fibrillar collagen. MMP-3 and -10 function as activators of proMMPs and degrade a number of ECM molecules. Differently from MMP-3 and -10, MMP-11 is not secreted as an inactive proMMP, but it is activated intracellularly by furin cleavage (Pei and Weiss, 1995). MMP-11 shows weak activity towards ECM molecules (Murphy et al., 1993b).

Matrilysins (MMP-7 and MMP-26) are the smallest members, lacking the hemopexin domain. MMP-7 is mainly synthesized in epithelial cells (Yu and Woessner, 2000). It can act as a sheddase, cleaving cell surface molecules including pro-TNF-α, Fas-ligand and syndecan-1 (Parks et al., 2004). MMP-26 is expressed in the endometrium and in some carcinomas, and it cleaves several ECM molecules (Marchenko et al., 2004).

Membrane-type MMPs are divided into two subgroups: the type-I transmembrane MMPs, including MMP-14 (MT1-MMP), MMP-15 (MT2-MMP), MMP-16 (MT3-MMP) and MMP-24 (MT5-MMP), and the GPI-anchored members, MMP-17 (MT4-MMP) and MMP-25 (MT6-MMP). All type-1 transmembrane MMPs can activate pro-MMP-2 (English et al., 2001), and MT1-MMP can activate MMP-13 (Knäuper et al., 1996).

Seven members of the MMP family cannot be associated with any of the above groups. MMP-12, -20 and -27 share a similar domain arrangement. MMP-12 is also referred to as metalloelastase (Shapiro et al., 1993). It was first identified in macrophages and it cleaves elastin and other ECM proteins (Shipley et al., 1996). MMP-20 is also called enamelysin and it is tooth-specific (Ryu et al., 1999). Little is known about mammalian MMP-27 (Yang and Kurkinen, 1998). MMP-19 is broadly expressed in human tissues and plays a role in tissue remodeling and wound healing (Pendas et al., 1997). MMP-23 is unique as it lacks the cysteine-switch in the prodomain and the hemopexin domain (Velasco et al., 1999). It is expressed mainly

in testis and ovary, suggesting a role in the reproductive process (Velasco et al., 1999). MMP-28, which is also known as epilysin, degrades casein. MMP-28 is expressed in different tissues, including testis, brain, intestine and skin, suggesting its involvement in tissue homeostasis and wound healing (Lohi et al., 2001; Marchenko and Strongin, 2001). Table 4 shows a list of all MMPs identified so far, their substrates and tissue where different MMPs are expressed.

.

Table 4: Description of the MMPs, their tissue expression and their substrates

MMP	Other Names	Human Tissue Expression	Substrates
MMP-1	Interstitial collagenase; fibroblast collagenase; collagenase 1	Most tissue types	Type I, II, III, X, XI collagens; fibronectin; aggrecan; link protein; gelatin; IGFBP-3; IL-1β precursor; monocyte chemoatractant protein-3; protease activated receptor 1
MMP-2	Gelatinase A; 72-kD gelatinase; type IV collagenase	Skin, gingival fibroblasts, cartilage	Type I, III, IV, X, XI collagens; fibronectin; SPARC; aggrecan; link protein; decorin; gelatin; IGFBP-3; laminin; IL-1β; monocyte chemoatractant protein-3; big endothelin; adrenomedullin; stromal cell-derived factor 1α
MMP-3	Stromelysin 1; transin; proteoglycanase	Synovial, gingival, and dermal fibroblasts; cartilage, endothelium, macrophages, vascular smooth muscle cells, osteoblasts, keratinocytes	Type III, IV, IX, X, XI collagens; fibronectin; SPARC; aggrecan; perlecan; link protein; decorin; gelatin; plasminogen; IGFBP-3; monocyte chemoatractant protein-3;
MMP-7	Matrilysin; PUMP-1	Glandular epithelium, mononuclear phagocytes, renal mesangial cells, cartilage	Type I, IV collagens; fibronectin; SPARC; aggrecan; link protein; decorin; IGFBP-3; E-cadherin; Fas ligand; pro-TNF-α; RANK ligand; heparin binding EGF;
MMP-8	Neutrophil collagenase; collagenase 2	Neutrophils, cartilage	Type I, II, III collagens; aggrecan

MMP	Other Names	Human Tissue Expression	Substrates
MMP-9	Gelatinase B; 92-kD gelatinase	Endometrium, bone, monocytes, neutrophils, T cells, cartilage, various cancers	Type IV, XI collagen; aggrecan; SPARC; link protein; decorin; galactin-3; gelatin; IL-1β precursor; precursor of TGFβ; ICAM-1
MMP-10	Stromelysin 2; transin 2	T cells, heart, kidney, menstrual endometrium, cartilage, various cancers	Type III, IV collagens; fibronectin; aggrecan; link protein
MMP-11	Stromelysin 3	Stromal tissues, various cancers	α1-proteinase inhibitor, α2-antiplasmin, plasminogen activator inhibitor 2.
MMP-12	Macrophage elastase; metalloelastase	Macrophages, placenta, cartilage	Type I, IV collagens; fibronectin; aggrecan; elastin
MMP-13	Collagenase 3	Cartilage, breast carcinoma	Type I, II, III, VI, IX, X collagens; fibronectin; SPARC; aggrecan; fibromodulin; monocyte chemoatractant protein-3;
MMP-14	Membrane-type 1 MMP	Monocytes, placenta, odontoblasts, cartilage, various cancers	Type I, II, III collagens; fibronectin; aggrecan; perlecan; CD44; laminin; MUC1
MMP-15	Membrane-type 2 MMP	Endometrium, placenta, odontoblasts, T lymphocytes, cartilage, various cancers	Type I collagen; fibronectin; perlecan; laminin; tenacin C
MMP-16	Membrane-type 3 MMP	T lymphocytes, brain, odontoblasts, cartilage, various cancers	-

MMP	Other Names	Human Tissue Expression	Substrates
MMP-17	Membrane-type 4 MMP	Brain, leukocytes, colon, reproductive tissues, odontoblasts, cartilage, cancers	gelatin
MMP-19	Rheumatoid arthritis synovial inflammation 1 (RASI-1)	Breast, cartilage, fibroblasts, capillary endothelium, macrophages, keratinocytes, myeloid cells	IGFBP-3; COMP; laminin
MMP-20	Enamelysin	Dental tissues	Amelogenin; COMP
MMP-21	-	Kidney, lung, liver, colon, leukocyte, ovary, testis, placenta, fetal brain, various cancers	α1-anti-trypsin
MMP-23	Cysteine array-MMP	Ovary, testis, prostate, cartilage	-
MMP-24	Membrane-type 5 MMP	Pancreas, kidney, lung, T lymphocytes, odontoblasts, cartilage, various cancers	-
MMP-25	Membrane-type 6 MMP	Leukocytes, lung, spleen, odontoblasts, cartilage, various cancers	Type IV collagen; fibronectin; fibrin; gelatin
MMP-26	Matrilysin 2; endometase	Endometrium, kidney, cartilage, cancers of epithelial origin	Gelatin; casein; fibrinogen; fibronectin
MMP-27	human MMP-22	B-cells, cartilage	-

MMP	Other Names	Human Tissue Expression	Substrates
MMP-28	Epilysin	Epidermis, heart, brain, placenta, lung, testes, prostate, intestine, T-cell, cancer	Casein

1.4.5.2 ADAMs

A disintegrin and metalloproteinases (ADAMs) also belong to the metzincins family of zinc-based proteinases (Murphy, 2008). Twenty-one ADAMs are found in human, but only thirteen of these harbor the metalloproteinases signature HEXXHXXGXXH sequence and thus have proteolytic potential. Cell membrane receptors, cytokines, growth factors and molecules that mediate cell-cell and cell-matrix interactions are among the physiological substrates of proteolytic ADAMs (Edwards et al., 2008; Murphy, 2008). Although little is still known about non-proteolytic ADAMs, their main expression in testis and a number of knockout studies suggests a role for these proteins in development (Edwards et al., 2008). The molecular structure of ADAMs consists of a pro-domain, catalytic domain, disintegrin domain, cysteine-rich domain, transmembrane domain and cytoplasmic tail. ADAMs are synthesized as inactive precursors and their activation usually occurs in compartments of the trans Golgi network (TGN) through cleavage by a furin pro-protein convertase (Lum et al., 1998). The cytoplasmic tail of several ADAMs presents binding sites for Src homology 3 (SH3)-containing proteins. The SH3 is a conserved domain shared by many adaptor proteins and tyrosine kinases, including Src and PI3 kinase, that are involved in cell signaling. The presence of binding sites for SH3 containing proteins, as well as a number of tyrosine and serine/threonine phosphorylation sites, suggest that the cytoplasmic tail of ADAMs may play a role in cell-signaling (Murphy, 2009). A soluble form, generated by alternative splicing, has been reported for some ADAMs, including ADAM-12 and ADAM-33 (Puxeddu et al., 2008; Wewer et al., 2006).

The biological functions of ADAMs have been investigated by the generation of knockout mouse lines for certain ADAM genes. ADAM-1 and ADAM-2 were the first two members of the family to be identified (Primakoff et al., 1987; Wolfsberg et al., 1993). Both of them were shown to be involved in sperm-egg fusion, and knockout mice for *Adam1* and *Adam2* show male infertility due to the inability of sperm to migrate and to bind the egg zona pellucida, respectively (Nishimura et al., 2004; Nishimura et al., 2007).

Some ADAMs are well studied, while only little information is available about the others. Table 5 shows a list of all ADAMs identified so far, their pattern of

expression and their substrates. Among them, ADAM-10 and ADAM-17 are widely characterized. TIMP-1 inhibits ADAM-10, TIMP-2 inhibits ADAM-12 and TIMP-3 inhibits ADAM-10, -12, -17, -28 and -33 (Brew and Nagase, 2010).

ADAM-10 plays a crucial role in Notch signaling, by RIPping (Regulation of Intramembrane Proteolysis) the intracellular domain of Notch (Hartmann et al., 2002). Notch is a transmembrane receptor, which triggers cell signaling events that are an important means of communication between cells. Notch signaling plays a crucial role in embryogenesis, development and cell differentiation. Notch ligands, including Delta, are also transmembrane proteins that initiate juxtacrine signaling by interacting with Notch expressed by the receiving cell. The interaction between Notch and Notch ligands induces a proteolytic cleavage that releases the ectodomain of the receptor. There is strong evidence that ADAM-10 is the major proteinase involved in the shedding of Notch, although other ADAMs, such as ADAM-17, are also known to be involved in this cleavage (Hartmann et al., 2002). After ADAM-mediated ectodomain shedding of Notch, a γ-secretase releases the Notch intracellular domain, which enters the nucleus and modulates gene expression (Schlondorff and Blobel, 1999). ADAM-10 is also the α-secretase involved in the processing of amyloid precursor protein (APP) in neurons (Kuhn et al., 2010), and it regulates cell adhesion by shedding of cadherins (Murphy, 2008).

ADAM-17, also known as tumor necrosis factor alpha (TNF-α) converting enzyme (TACE), is the most widely studied member of the ADAM family. TNF-α is produced as a transmembrane precursor. After proteolytic cleavage by ADAM-17, TNF-α is released and functions as a soluble cytokine (Black et al., 1997). For this reason, ADAM-17 plays a crucial role in inflammation and other processes that involve TNF-TNF receptor-mediated signaling. ADAM-17 is also involved in the regulation of epidermic growth factor receptor signaling, as all its ligands, including EGF, HB-EGF, TGF-β and amphiregulin are synthesized as transmembrane proteins which require ADAM-17-mediated shedding to become active (Lee et al., 2003).

Table 5: Description of the ADAMs, their tissue expression and their substrates

ADAM	Other Names	Human Tissue Expression	Substrates
ADAM-1			
ADAM-2	fertilin-β; PH-30β	Testis	-
ADAM-7	EAP1	Epididymis	-
ADAM-8	MS2, CD156a	granulocytes, monocytes	proTNF-α, RANKL, IL1RII, CHL1, SCF1, CD23, CD153, CX3CL1
ADAM-9	meltrin-γ, MDC9	Most tissue types	proHBEGF, oxytocinase, NGFR, murine splice variant of FGFR2
ADAM-10	kuzbanian, MADM, SU17	Most tissue types	proEGF, pro-β-cellulin, APP, ephrin A2 and A5, CX3CL1, CXCL16, IL6R, CD23, CD44, FASL, Slit, L1-CAM, NGFR, Notch, Delta-like 1, Jagged, N-cadherin, E-cadherin, VE-cadherin, protocadherin-γ, collagen XVII, LRP
ADAM-11	MDC	brain	-
ADAM-12	meltrin-α	Most tissue types	proHBEGF, proepiregulin, oxytocinase, Delta-like 1
ADAM-15	metargidin, MDC15	Most tissue types	proHBEGF, proepiregulin, proamphiregulin, CD23, E-cadherin
ADAM-17	TACE	Most tissue types	proTNF-α, proTGF-α, proHBEGF, proamphiregulin, proneuregulin, proNGF, TNFRI, TNFRII, ERBB4, CX3CL1, RANKL, IL6R, MUC1, SCF1 and 2, NGFR, CSFR, Notch, CD23, CD30, CD40, L-selectin, LDLR, LRP, VCAM1, ICAM1, APP
ADAM-18	tMDCIII	Testis	-
ADAM-19	meltrin-β, MADDAM	Most tissue types	RANKL, proneuregulin
ADAM-20	-	Testis	-
ADAM-21	-	Testis	-
ADAM-22	MDC2	Brain	-
ADAM-23	MDC3	Brain	-
ADAM-28	MDC-L	Epididymes, lung, lymphocytes	CD23

ADAM	Other Names	Human Tissue Expression	Substrates
ADAM-29	-	Testis	-
ADAM-30	-	Testis	-
ADAM-33	-	Most tissue types	CD23, SCF1

1.4.5.3 ADAMTSs

The family of ADAMTSs (a disintegrin and metalloproteinase with thrombospondin motifs) are closely related to ADAMs, but they do not have a transmembrane domain and are therefore secreted from the cells. Nineteen ADAMTSs are found in humans (Apte, 2009). All of these are translated as inactive pro-enzymes, with activation that involves cleavage of the prodomain by a furin-like pro-protein convertase. The structure of ADAMTSs includes a catalytic domain which shares structural similarity with that of MMPs, and ancillary domains consisting of a disintegrin-like domain, a central thrombospondin type-I (TS) domain, a cysteine-rich domain, a spacer domain and a variable number of trombospondin type-I repeats (that range from none to 14). Seven ADAMTS-like proteins that resemble ADAMTS ancillary domains but lack metalloproteinase domain are reported (Apte, 2009). The ancillary domains are important for substrate specificity and for the ability of ADAMTSs to bind to the ECM (Porter et al., 2005).

The ADAMTS family can be subdivided into four groups based on structural and functional similarities: i) proteoglycanases, ii) procollagen-N-proteinases, iii) von Willebrand factor (VWF)-cleaving proteinase and iv) other ADAMTS proteinases

Proteoglycanases (ADAMTS-1, -4, -5, -8, -9, -15, and -16) are able to cleave the core proteins of aggrecan, versican and/or brevican, and they are considered to play a role in ECM turnover. Among them, ADAMTS-4 and ADAMTS-5 have the highest aggrecanolytic activity and are implicated in the pathogenesis of arthritis (Bondeson et al., 2008). ADAMTS-1, -4 and -9 are able to cleave versican. The expression of ADAMTS-1 and -4 is high in atherosclerotic lesions, the former colocalises with endothelial cells and VSMCs, the latter with macrophages in atherosclerotic lesions (Wight and Merrilees, 2004). ADAMTS-4 is also able to cleave brevican (Haddock et al., 2007).

Procollagen-N-proteinases (ADAMTS-2, -3, and -14) remove N-terminal peptides from procollagen to form mature collagen (Porter et al., 2005). ADAMTS-2-null mice have a defect in forming type I collagen fibrils that leads to the development of fragile skin. ADAMTS-3 and -14 are thought to function in cartilage and tendons, respectively (Colige et al., 2002; Fernandes et al., 2001).

The VWF-cleaving protease has been purified and cloned and it is designated as ADAMTS-13 (Furlan et al., 1996). Von Willebrand factor (VWF) is a large multimeric glycoprotein that plays a crucial role in hemostasis (Bonthron et al., 1986). The endothelial cells of intact vessels control blood fluidity, secreting several molecules that prevent blood clotting and platelet aggregation. Following vessel injury, the endothelial cells stop the secretion of coagulation and aggregation inhibitors and VWF binds to exposed subendothelial collagen. In these conditions, the inactive globular conformation of VWF is unfolded in response to the shear forces exerted by the flowing blood. When in an unfolded string-like active conformation, VWF is able to bind and tether platelets (Sadler, 1998). VWF catabolism is mainly controlled by ADAMTS-13, which cleaves the Tyr^{1605}-Met^{1606} bond in VWF, breaking down the multimers into smaller units, which are degraded by other proteases (Fujikawa et al., 2001). In humans, deficiency in ADAMTS-13 activity leads to a pathological condition of the blood-coagulation system, called thrombotic thrombocytopenic purpura (TTP), which causes the formation of small blood clots throughout the body (Moake, 2004). TTP can be idiopathic or inherited. The idiopathic form of TTP is an autoimmune disease due to antibodies that target and inactivate ADAMTS-13. The inherited form of TTP is also known as Upshaw-Schülman syndrome and it is due to point mutations in the *ADAMTS13* gene (Levy et al., 2001).

There are a number of ADAMTSs, whose endogenous substrates are not well characterized. However, ADAMTS-7 and ADAMTS-12 have been identified to cleave the cartilage oligomeric matrix protein (COMP) and are upregulated in cartilage and synovium of patients with rheumatoid arthritis, suggesting a role for these enzymes in the progression of the disease (Liu et al., 2006a; Liu et al., 2006b). ADAMTS-7 was originally identified as an enzyme containing two TS domains and having a similar domain structure to ADAMTS-5, ADAMTS-6, and ADAMTS-8 (Hurskainen et al., 1999). A longer form of ADAMTS-7, called ADAMTS-7B, was then isolated and believed to be the full-length version of the enzyme (Somerville et al., 2004). ADAMTS-7B contains six additional TS domains, a mucin domain and a C-terminal PLAC (Protease and LACunin) domain. ADAMTS-6 and -10 have similar primary

structures, suggesting also their activities may be correlated (Hurskainen et al., 1999). TIMP-3 inhibits ADAMTS-1, -4, -5 and weakly ADAMTS-2 (Brew and Nagase, 2010). Tissue distribution and substrates of ADAMTSs are listed in Table 6

Table 6: Description of the ADAMTSs, their tissue expression and their substrates

ADAMTS	Other Names	Human Tissue Expression	Substrates
ADAMTS-1	Aggrecanase 3; METH-1	Most tissue types	Aggrecan; versican; α_2-macroglobulin
ADAMTS-2	Procollagen N-proproteinase	Skin, cartilage, liver, placenta, lung	Pro-collagen I, II, and III N-propeptides
ADAMTS-3	Procollagen N-proproteinase; KIAA0366	Skin, cartilage, placenta, heart, brain, lung, kidney	Pro-collagen II N-propeptides
ADAMTS-4	Aggrecanase 1; ADMP-1; KIAA0688	Uterus, stomach, spinal cord, skeletal muscle, ovary, heart, bladder, brain, cartilage	Aggrecan; versican; brevican; COMP; fibromodulin; decorin
ADAMTS-5	Aggrecanase 2; ADAMTS-11; ADMP-2	Bladder, cervix, esophagus, placenta, uterus, cartilage	Aggrecan; α2-macroglobulin
ADAMTS-6	-	Placenta, cartilage	-
ADAMTS-7	-	Pancreas, kidney, skeletal muscle, liver, heart	COMP; α_2-macroglobulin
ADAMTS-8	METH-2	Brain, heart, placenta, lung, smooth muscle, kidney, appendix	Aggrecan
ADAMTS-9	KIAA1312	Heart, placenta, skeletal muscle, kidney, pancreas, cartilage	Aggrecan; versican
ADAMTS-10	-	Cartilage	-
ADAMTS-12	-	Cartilage, fetal lung, gastrointestinal carcinomas	Aggrecan; COMP; α2-macroglobulin
ADAMTS-13	Von Willebrand factor-cleaving protease	Liver, brain, prostate, cartilage	von Willebrand factor

ADAMTS	Other Names	Human Tissue Expression	Substrates
ADAMTS-14	Procollagen N-proproteinase	Retina, brain, lung, placenta, prostate, skin, cartilage	-
ADAMTS-15	-	Liver, kidney, cartilage	Aggrecan
ADAMTS-16	-	Cartilage, brain, ovary, fetal lung, fetal kidney	Aggrecan
ADAMTS-17	-	Ovary, cartilage, fetal lung	-
ADAMTS-18	-	Endothelium, placenta, cartilage, fetal lung, fetal kidney, fetal brain, fetal liver	-
ADAMTS-19	-	Cartilage, fetal lung	-
ADAMTS-20	-	Breast, lung, testes, prostate, ovary, heart, placenta, pancreas, leukocytes, cartilage, various cancers	Aggrecan

1.5 Aims of the thesis

Troeberg *et al*. (2008) reported that levels of TIMP-3 in the extracellular milieu can be post-translationally regulated by endocytosis. It was postulated that this process is mediated by LRP-1, a member of the LDL receptor family. Since addition of calcium pentosan polysulfate or heparin to chondrocytes or HTB94 chondrosarcoma cells results in an accumulation of TIMP-3 in the medium, it was suggested that cell surface bound heparan sulfate proteoglycans (HSPGs) may serve as co-receptors for TIMP-3 endocytosis. The aim of this study is:

1. To elucidate TIMP-3 endocytosis in more details, which includes determining the kinetics of the process, the rate of endocytosis by number of cell lines and the distribution of endocytosed TIMP-3 among cell fractions.
2. To confirm the role of LRP-1 in TIMP-3 endocytosis and determine the involvement of other LDL receptors.
3. To investigate the involvement of LRP-1-independent pathways in TIMP-3 endocytosis
4. To investigate the role of heparan sulfate proteoglycans in the endocytosis of TIMP-3.
5. To elucidate whether TIMP-3 can mediate the scavenging of TIMP-3—MMP complexes.

To pursue these aims I set up a method to purify recombinant [^{35}S]radiolabeled TIMP-3-FLAG from the conditioned medium of human cells, and I optimized an assay to evaluate the internalization of [^{35}S]TIMP-3-FLAG by following the distribution of radioactivity among cell fractions.

Chapter 2

Materials and Methods

2.1 Reagents

2.1.1 Cultured cells

Human chondrosarcoma cells (HTB94), human epithelial cervical cancer cells (Michigan Cancer Foundation 7), human breast adenocarcinoma cell line (HeLa) and human acute monocytic leukemia cells (THP-1) were from American Culture Type Collection (Manassas, VA, USA). Human epithelial kidney (HEK-293/EBNA) cells were from Invitrogen (Paisley, UK). HEK-293/EBNA cells transfected with pCEP4-TIMP-3 and pCEP4-N-TIMP-3 constructs (Troeberg et al., 2009), HEK-293/EBNA cells transfected with pCEP4-ADAMTS4-2 construct (Kashiwagi et al., 2004), HEK-293/EBNA cells transfected with pCEP4-ADAMTS5-2 construct (Gendron et al., 2007) and HEK-293/EBNA cells transfected with pCEP4-MMP-1 construct (Visse R. and Nagase H., unpublished data) were from frozen cell stocks prepared by Dr. Linda Troeberg, Dr. Christi Gendron, Dr. Masahide Kashiwagi and Dr. Robert Visse, respectively. Human uterine cervical fibroblasts (HUCF) were kindly provided by Professor I. Ito from Tokyo University of Pharmacology and Life Science (Itoh et al., 1995). Mouse embryonic fibroblasts (MEF-1), and PEA-13 (homozygous LRP-1 deficient) cells were a kind gift from Professor D. Strickland from the University of Maryland, School of Medicine, Maryland, USA (Kounnas et al., 1992; Willnow and Herz, 1994). Syndecan-4-null and wild-type MEF cells were a kind gift from Professor J. R. Couchman from the University of Copenhagen, Denmark. CHO-745 cells, deficient in both chondroitin and heparan sulfate proteoglycans, and control CHO-K1 cells were a kind gift from Professor Jeffrey Esko from University of California, San Diego (Esko et al., 1985). Porcine metacarpophalangeal joints of 3-9 month-old-pigs were from Fresh Tissue (London, UK) and were used within 24 hours of slaughter.

2.1.2 Cell culture reagents

Materials were purchased from the following sources: Dulbecco's modified Eagle's medium (DMEM), DMEM without L-glutamine or phenol red, L-glutamine, Ham's F12, Roswell Park Memorial Institute (RPMI) medium, penicillin/streptomycin, hygromycin B, 4-(2-hydroxyethyl)-1-piperazineethanesulfonic acid (HEPES), amphotericin B and trypsin-ethylenediaminetetraacetic acid (EDTA) from PAA

Laboratories (Somerset, UK); fetal calf serum (FCS) from Gibco (Paisley, UK); DMEM without L-glutamine, cysteine, methionine or cystine from MP Biomedicals (CA, USA). Heparin, de-sulfated heparin, chondroitin sulfate, hyaluronic acid, sodium chlorate and collagenase from *Clostridium histolyticum* were from Sigma-Aldrich (Dorset, UK); dermatan sulfate from Calbiochem (Nottingham, UK); calcium pentosan polysulfate from Arthropharm (Sydney, Australia) and GM6001 from Elastin Products Co (Owensville, Missouri, USA); Pronase E from BDH (Dorset, UK).

2.1.3 SDS-PAGE and Western blot reagents

Materials were purchased from the following sources: 30% (w/v) acrylamide/bis-acrylamide from Severn Biotech (Worcestershire, UK); 2-amino-2-methyl-1,3-propanediol (ammediol) and the mouse monoclonal anti-FLAG M2 antibody from Sigma-Aldrich Company Ltd. (Dorset, UK); PageRuler™ Plus Prestained Protein Ladder for SDS-PAGE from Fermentas GmbH (St. Leon-Rot, Germany); 4-12% Tris-glycine polyacrylamide gradient gels and polyvinylidene difluoride (PVDF) membrane from Invitrogen (Paisley, UK); anti-rabbit alkaline phosphatase (AP)-linked antibody, anti-mouse AP-linked antibody, AP substrate (5-bromo-4-choloro-3-indolyl-1-phosphate and nitroblue tetrazolium), and horseradish peroxidase (HRP) substrate from Promega (Southampton, UK); anti-rabbit HRP-linked antibody and anti-mouse HRP-linked antibody from Dako (Ely, UK). Rabbit polyclonal anti-TIMP-3 (ab39184) was from Abcam (Cambridge, UK). Mouse monoclonal anti-LRP Heavy Chain (8G1) and Light Chain (5A6) were from Merck KGaA (Darmstadt, Germany). Mouse monoclonal syndecan-1 (DL-101) and syndecan-4 (5G9) were from Santa Cruz Biotechnology (Middlesex, UK). Anti-MMP-1 antibodies were prepared in sheep as reported (Ito and Nagase, 1988). HRP-conjugated streptavidin was from R&D (Abingdon, UK)

2.1.4 Protein chemistry reagents

Recombinant purified His-tagged N-TIMP-3 was obtained from Dr. Ngee Han Lim in this laboratory (Kashiwagi et al., 2001); recombinant His-tagged receptor-associated protein (RAP) was obtained from Dr. Linda Troeberg in this laboratory (Nielsen et al., 1995); recombinant purified MMP-1 catalytic domain (MMP-1 ΔC) was obtained

from Dr. Robert Visse in this laboratory (Chung et al. 2000). FLAG peptide (DYKDDDDK) was purchased from Advanced Biotechnology Centre (Imperial College, London, UK).

2.1.5 Radiochemical reagents

Pro-Mix™ L-[^{35}S] was from GE Healthcare (Buckinghamshire, UK) and Goldstar Multipurpose Liquid Scintillation Cocktail was from Meridian (Surrey, UK).

2.1.6 Molecular biology reagents

Materials were purchased from the following sources: AffinityScript One-Step RT-PCR Kit from Agilent Technologies UK Limited (Stockport, UK); RNeasy Mini Kit and QIAprep Spin Miniprep Kit from Qiagen (Crawley, UK); Luria-Bertani (LB) media, Lipofectamine2000™ and Opti-MEM medium from Invitrogen (Paisley, UK); *Pfu* DNA polymerase® from Amersham Biosciences UK Limited (Bucks, UK); SYBR green I from Molecular Probes (Cambridge, UK); siRNAs double-stranded RNA targeting human syndecan-1 (AM12432 and AM142557) from Ambion (Warrington, UK).

2.1.7 Immunofluorescence reagents

Materials were purchased from the following sources: goat serum from Dako (Ely, UK); Alexa-488 conjugated-goat anti-mouse and Alexa-568 conjugated-phalloidin from Molecular Probes (Leiden, Netherlands).

2.2 Cell culture

2.2.1 Cell line culture

Cells (HEK-293/EBNA, HTB94, MEF-1, PEA-10, PEA-13, HUCF, HeLa, MCF-7, syndecan-1-null and wild-type MEFs) were grown in DMEM supplemented with 100 U/ml penicillin, 100 µg/ml streptomycin and 10 % (v/v) FCS. CHO-K1 and CHO-745 cells were grown in Ham's F12 medium supplemented with 100 U/ml penicillin, 100 µg/ml streptomycin and 10 % (v/v) FCS. THP-1 cells were grown in RPMI medium supplemented with 100 U/ml penicillin, 100 µg/ml streptomycin and 5 % (v/v) FCS. HEK-293/EBNA cells transfected with pCEP4-TIMP-3 and pCEP4-N-TIMP-3 constructs were cultured in DMEM supplemented with 100 U/ml penicillin, 100 µg/ml

streptomycin and 10 % (v/v) FCS with the addition of 800 µg/ml hygromycin B. HEK-293/EBNA cells transfected with pCEP4-ADAMTS4-2, pCEP4-ADAMTS5-2 and pCEP4-MMP-1 constructs were cultured in DMEM supplemented with 100 U/ml penicillin, 100 µg/ml streptomycin and 10 % (v/v) FCS with the addition of 100 µg/ml hygromycin B. Cells were passaged every 3-4 days using trypsin-EDTA.

2.2.2 Primary chondrocyte isolation and culture

Porcine chondrocytes were isolated by digesting 1 g of porcine articular cartilage from metacarpophalangeal joints in 10 ml of DMEM with 10 % FCS and 0.25 mg/ml bacterial collagenase (over night at 37 °C with shaking). The chondrocytes were separated from undigested material by passing through a cell strainer into a 50 ml tube. Collected cells were washed twice and cultured in DMEM containing 100 U/ml penicillin, 100 mg/ml streptomycin, 2 mg/ml amphotericin B, 10 mM HEPES and 10% FCS.

2.3 SDS-PAGE and Western blots

2.3.1 SDS-PAGE

SDS-PAGE was run with or without reduction of samples using a modification of the ammediol/glycine/HCl buffer system of Wyckoff *et al*. (Wyckoff et al., 1977) or the Tris-glycine buffer system according to Laemmli (Laemmli, 1970). Polyacrylamide gels were made with 6-12 % total acrylamide, depending on the size of the proteins to be separated. Samples were diluted with an equal volume of 2 x sample buffer [42 mM ammediol or 0.125 mM Tris-HCl, 0.01 % (w/v) sodium azide, 2 % SDS, 0.1 % (w/v) bromophenol blue, 50 % (w/v) glycerol, 1 % with or without 1 % (v/v) β-mercaptoethanol]. Typically, ammediol gels were run at 200 V for 45-60 min and Tris-glycine gels were run at 150 V for 90 min.

2.3.2 Silver staining

Proteins were visualized in SDS-PAGE gels using silver staining (Shevchenko et al., 1996). Gels were first incubated with fixing solution [50 % (v/v) methanol and 5 % (v/v) acetic acid] for 20 min and washed for 10 min with 50 % (v/v) methanol. This was followed by 2 10 min washes in deionised water. Next, gels were

incubated with sensitizer [0.02 % (w/v) sodium thiosulfate] for 1 min, washed twice with deionised water, and incubated with cold silver reagent [0.1 % (w/v) silver nitrate] for 60 min at 4 °C. Following this incubation, gels were washed twice with distilled water prior the addition of developer [0.04 % (v/v) formalin and 2 % (w/v) sodium carbonate]. The developing reaction was stopped using 5 % (v/v) acetic acid when protein bands on the gels were clearly visualized.

2.3.3 Western Blotting

Proteins separated by SDS-PAGE were analysed by Western blotting using Novex Mini-cell (Invitrogen) or Mini-Trans-Blot cell (BIO-RAD) systems. The proteins were transferred to PVDF membranes at 350 mA for 1 h in transfer buffer [20 % (v/v) methanol, 12.6 mM Tris, 96 mM glycine and 0.1 % (w/v) SDS]. Pre-stained molecular weight markers were completely transferred in this time. The membrane was then blocked with either 5 % BSA in TBS or 5 % skimmed milk in TBS for 1 h at room temperature. In general, membranes were incubated overnight with primary antibodies (diluted depending on the antibody used) in either 1 % BSA-TBS or 1 % skimmed milk-TBS at 4 °C. The membrane was then washed three times with TBS containing 0.1 % Tween 20. After washing, a 1:1000 dilution of a AP-linked secondary antibody or HRP-linked secondary antibody in 1% BSA in TBS or 1% milk in TBS was added and incubated for 1 h at room temperature. The membrane was subsequently washed three times with TBS containing 0.1 % Tween 20 and then incubated with either the AP substrate until bands appeared or the HRP substrate for 1 min. Protein bands developed by HRP were detected by exposure to photographic film.

2.3.4 Densitometry

Gels and Western blots were scanned using a BioRad GS-710 imaging densitometer. Phoretix 1D software (Nonlinear Dynamics, Newcastle-upon-Tyne, UK) was used to quantify the pixel intensity of the protein bands. Unmodified 16-bit TIFF images were analysed and the background pixel intensity was subtracted using the “rolling ball” method.

2.4 Protein Purification

2.4.1 Purification of TIMP-3 and N-TIMP-3

Recombinant C-terminally FLAG-tagged TIMP-3 and N-TIMP-3 were purified following the procedure described by Troeberg *et al.* (Troeberg et al., 2009). HEK-293/EBNA cells stably transfected with either pCEP4-TIMP-3 or pCEP4-N-TIMP-3 construct were grown to confluence in the presence of hygromycin B (800 µg/ml). Next, the cells were washed and incubated in serum-free DMEM containing 30 mM sodium chlorate ($NaClO_3$). The conditioned medium was harvested after 4 days and centrifuged to remove cell debris prior to being applied to a 2 ml anti-FLAG M2-agarose column at room temperature. The column was washed with 10 column volumes of 1 M NaCl-TNC buffer [50 mM Tris-HCl (pH 7.5), 1 M NaCl, 10 mM $CaCl_2$] to remove non-specifically bound proteins. The column was then washed with 5 column volumes of TNC buffer [50 mM Tris-HCl (pH 7.5), 150 mM NaCl, 10 mM $CaCl_2$]. The proteins were eluted with 200 µg/ml FLAG peptide in TNC buffer [50 mM Tris-HCl (pH 7.5), 150 mM NaCl, 10 mM $CaCl_2$] and fractions were run on SDS-PAGE for subsequent silver staining and Western blotting with anti-FLAG primary antibody. TIMP-3 and N-TIMP-3 active concentrations were determined by titration against a known concentration of MMP-1 ΔC, using the Dnp (2,4-dinitrophenyl)-Pro-Leu-Gly-Pro-DL-Amp-D-Lys substrate (Knight, 1991).

2.4.2 Purification of ADAMTS4-2, ADAMTS5-2 and MMP-1

ADAMTS-4 and ADAMTS-5 are multidomain metalloproteinases with a similar domain arrangement, consisting of a prodomain, a catalytic metalloproteinase domain, a disintegrin (Dis) domain, a thrombospondin type I (TS) domain, a cysteine-rich (CysR) domain, and a spacer (Sp) domain. In addition, ADAMTS-5 contains an extra TS domain after the spacer domain (Gendron et al., 2007). ADAMTS4-2 is a C-terminal truncated form of ADAMTS-4 lacking of the spacer domain. ADAMTS5-2 is a C-terminal truncated form of ADAMTS-5 lacking of the second thrombospondin domain. HEK-293/EBNA cells stably transfected with FLAG-tagged pCEP4-ADAMTS4-2, pCEP4-ADAMTS5-2 and pCEP4-proMMP1 were grown to confluence in the presence of hygromycin B (200 µg/ml). Upon reaching confluence, the cells were

washed once with serum-free DMEM to remove serum and then incubated in serum-free DMEM. The conditioned medium was collected after 4 days and centrifuged to remove cell debris. The conditioned medium was applied to a 2 ml anti-FLAG M2-agarose column at 4 °C. The column was washed with 10 column volumes of 1 M NaCl-TNC buffer [50 mM Tris-HCl (pH 7.5), 1 M NaCl, 10 mM $CaCl_2$] to remove non-specifically bound proteins. The column was then washed with 5 column volumes of Tris-buffered-saline (TBS, pH 7.4). The protein was eluted with 200 µg/ml FLAG peptide in TNC [50 mM Tris-HCl (pH 7.5), 150 mM NaCl, 10 mM $CaCl_2$]. Fractions were run on SDS-PAGE and proteins were silver stained. proMMP-1 was activated as previously described (Chung et al., 2000). Active fractions of ADAMTS4-2, ADAMTS5-2 and MMP-1 were determined by titration against a kwown concentration of recombinant N-TIMP-3.

2.4.3 Purification of metabolically [^{35}S]labelled TIMP-3, N-TIMP-3 and MMP-1

[^{35}S]TIMP-3, [^{35}S]N-TIMP-3 and [^{35}S]MMP-1 were prepared by a modification of the procedure described in section 2.4.2. HEK-293/EBNA cells stably transfected with pCEP4-TIMP-3, pCEP4-N-TIMP-3 or pCEP4-MMP1 construct were grown to confluence in a 150 cm^2 flask, washed once and incubated in serum-free DMEM without L-glutamine, cysteine, methionine or cysteine for 2 hours and then incubated in serum-free DMEM without glutamine, cysteine, methionine or cystine containing [^{35}S]Met/[^{35}S]Cys (25 µCi/ml of Pro-Mix™ L-[^{35}S]). Conditioned media were collected after 4 days, centrifuged to remove cell debris, and applied to a 2 ml anti-FLAG M2-agarose column. The resin was extensively washed and bound protein eluted with 200 µg/ml FLAG peptide. The purity of recombinant proteins was confirmed by reducing SDS-PAGE (Bury and Roberts, 1982) and their active concentrations determined as mentioned in Section 2.4.2 and 2.4.3. Gels were dried and exposed to autoradiographic film for 4 days to confirm that the purified proteins were effectively radiolabeled.

2.5 Endocytosis assays

2.5.1 Western Blot assay to follow TIMP-3 clearance

Cells were grown to confluence in 6-well plates. After washing three-times with serum-free DMEM, cells were incubated for 1 h at 37 °C with DMEM containing 0.1 % BSA with or without GM6001 (10 µM), RAP (500 nM), heparin (5-500 µg/ml), calcium pentosan polysulfate (CaPPS), sodium pentosan polysulfate (NaPPS), chondroitin-4-sulfate, de-N-sulfated heparin or dermatan sulfate (all at 50 or 200 µg/ml). Following this, TIMP-3-FLAG (1 nM) was added and incubated for up to 24 h in a final volume of 2 ml. After incubation, the conditioned medium was removed and the protein was precipitated with TCA at the final concentration of 5 % (v/v) overnight at 4 °C. The TCA-soluble fraction was separated from the TCA-insoluble fraction by centrifugation at 13 000 rpm for 15 min at 4 °C and the TCA-insoluble fraction was re-suspended in 30 µl of 2 x reducing sample buffer. Samples (15 µl) were analysed by SDS-PAGE (10 % acrylamide) and Western blotting with the anti-FLAG-M2 antibody. The same assay was used to investigate N-TIMP-3 clearance by HTB94 cells.

2.5.2 Radioactivity-based assay

Cells were grown to confluence in a 6-well plate. After washing three-times with serum-free DMEM, cells were incubated for 1 h at 37 °C with DMEM containing 0.1 % BSA with or without GM6001 (10 µM), heparin, NaPPS, chondroitin sulfate, de-N-sulfated heparin or dermatan sulfate (all at 200 µg/ml), or hyaluronan (all at 250 µg/ml), or RAP (500 nM). As a control for agents diluted in DMSO, the equivalent dilution of DMSO was added to separate wells. Following this, 1 nM [^{35}S]TIMP-3 (unless differently stated) was added and cultured for up to 48 h in a final volume of 2 ml. After incubation, the conditioned medium was removed and the protein was precipitated with TCA (5 %) overnight at 4 °C. The TCA-soluble fraction was separated from the TCA-insoluble fraction by centrifugation at 13 000 rpm for 15 min at 4 °C. The cells were washed three-times with ice-cold PBS. The wash fractions were transferred into a scintillation vial and counted directly. The cell layer was incubated with 1M NaOH for 1h. The cell suspension was then moved into a

scintillation vial and counted. TCA-insoluble pellet was dissolved in 1 M NaOH (500 µl). Radioactivities in each fraction were counted using a HIDEX 300 SL Scintillation Counter (Sheffield, UK). The amount of radioactivity in all the different fractions was calculated as percentage of the total amount of radioactivity in all of any harvested sample. The percentage of TCA-soluble radioactivity in the preparation of labeled protein prior to incubation with cells was subtracted from the amount of TCA-soluble radioactivity. This corrected for any TCA-soluble radioactivity in the starting material. The same assay was used to investigate endocytosis of [^{35}S]N-TIMP-3 and [^{35}S]MMP-1. In these assays *n* refers to the repetitions of the entire experiment. The curves were generated by fitting the results to a one-phase exponential decay.

2.6 Molecular Biology

2.6.1 siRNA knockdown of syndecan-1 in HTB94 cells

siRNAs [two double-stranded RNA targeting syndecan-1 (AM12432 and AM142557) or scrambled] were transiently transfected into HTB94 cells using Lipofectamine 2000. Throughout the transfection procedure, penicillin and streptomycin were not added to the medium because these antibiotics reduce transfection efficiency. HTB94 cells were seeded at a density of 1-1.5x10^5 cells/well (6-well plate) in DMEM containing 10 % FCS. Cells were then washed and incubated in 500 µl of Opti-MEM. For each transfection, siRNA (10-100 nM) were diluted in serum-free Opti-MEM to a final volume of 50 µl. In a separate tube, 1 µl of Lipofectamine was diluted in 49 µl serum free Opti-MEM. The siRNA and Lipofectamine solutions were combined and incubated for 20 min at room temperature. The Lipofectamine-siRNA mixture (100 µl) was then gently pipetted into each well to ensure an even distribution of the siRNA in the medium. After 3 h the medium was replaced with 2 ml of DMEM containing 10 % FCS and the cells were grown to confluence.

2.6.2 RNA extraction and quantitative-PCR analysis of syndecan-1 knockdown

After siRNA transfection, confluent HTB94 cells were lysated and RNA extracted using a commercially available kit (RNeasy® Mini kit, Invitrogen), according to the manufacturer's instructions. Briefly, the cells were lysed in a highly denaturing

detergent-containing buffer and the lysates were directly applied to a spin column where RNA was specifically retained. After washing once with 700 µl of washing buffer, RNA was eluted using 50 µl of RNAse-free water and samples were quantified by spectrophotometry (A 260 nm) and stored at -80 °C until use. cDNA was made from total cell RNA using the affinityScript One-Step RT-PCR Kit, according to the manufacturer's instructions. Amplification reactions were performed in triplicate in an Applied Biosystems 7500 Real-Time PCR System. The primers used for syndecan 1 (*Sdc-1*) were 5'-GCCGCAAATTGTGGCTA-3' (forward) and 5'-AGCCGGAGAAGTTGTCAGAGTC-3' (reverse). Primers used for human glyceraldehyde 3-phosphate dehydrogenase (GAPDH) housekeeping gene were 5'-GCCCAAAGTCACCGTCAA-3' (forward) and 5'-TCCGAAGAGACCAAAGATCAC-3' (reverse). Data were normalized to the housekeeping control GAPDH and these are presented relative to control.

2.7 Immunofluorescence

2.7.1 Preparation of gelatin coated cover slips

Glass cover slips (18 mm in diameter) were coated with 5 mg/ml gelatin dissolved in distilled water and incubated for 15 min at room temperature. The gelatin solution was removed and fixed using 1% glutaraldehyde in TBS for 20 min at room temperature. Following fixation, the cover slips were incubated with 1 M ammonium chloride for 15 min to block any free glutaraldehyde. One cover slip was placed into one well of a 12-well plate, washed twice with 70% ethanol to ensure sterility, and then washed thrice with media containing 10% FCS before the cells were added.

2.7.2 Internalization of TIMP-3 followed by immunofluorescence

HTB94, MEF-1 and PEA-13 cells cultured on 18 mm cover glasses coated with gelatin were incubated at 37 °C in phenol-red free DMEM with 0.1% (v/v) FCS containing 1 µg/ml of non-radiolabeled recombinant FLAG-tagged TIMP-3 in the presence or absence of heparin (200 mg/ml) or RAP (500 nM). After 2 h cells were fixed with 3% paraformaldehyde in PBS for 10 min and blocked with 5% (v/v) goat serum and 3% (w/v) bovine serum albumin in PBS for 1 h at room temperature. Cells were

permeabilized with PBS containing 0.1% (v/v) Triton X-100 and then incubated with anti-FLAG M2 antibody (5 ml/ml) at room temperature for 2 h. Alexa Fluor-488–conjugated goat anti-mouse IgG was used to visualize the antigen signal. Actin was stained with Alexa Fluor-568-conjugated phalloidin. The signals were analyzed using a CCD camera-equipped microscope (Nikon TE-2000) with ×60 objective lens.

2.8 Study of binding of TIMP-3 to sLRP-1 by ELISA

2.8.1 Purification of sLRP-1 from plasma

sLRP-1 was isolated from fresh-frozen human plasma by a modification of previously published methods (Quinn et al., 1997). Plasma was diluted 5-fold with equilibration buffer (50 mM citrate, pH 6.0, 75 mM NaCl, 0.02 % NaN_3) supplemented with proteinase inhibitor cocktail (P8340, Sigma-Aldrich, Dorset, UK) and applied to a MacroPrep S ion exchange resin (Bio-Rad, Hemel Hempstead, UK) equilibrated in the same buffer. The resin was extensively washed in equilibration buffer to remove unbound material and bound proteins then eluted in a gradient of 75 to 500 mM NaCl in equilibration buffer over 10 column volumes. Eluted fractions were analyzed by SDS-PAGE with silver staining and immunoblotting for LRP-1 using the 8G1 antibody (Abcam, Cambridge, UK).

2.8.2 ELISA detection of TIMP-3 binding to sLRP-1

High-binding microtitre plates (Corning, NY, USA) were coated with 0.4 nmol sLRP-1 in 50 mM citrate, pH 6.0, 75 mM NaCl overnight. Wells were blocked using 3 % BSA-PBS (1 h, 37 °C) and washed in PBS containing 0.1 % (v/v) Tween 20 (Sigma-Aldrich, Dorset, UK) after this and each subsequent step. Wells were then incubated with recombinant TIMP-3 in blocking solution (0.15 - 20 nM, 3 h, 37 °C). Bound TIMP-3 was detected by incubation of wells with murine M2 anti-FLAG antibody (3 h, 37 °C) and then with an anti-mouse secondary antibody coupled to horseradish peroxidase (1 h, 37 °C) (DAKO, Ely, UK). Hydrolysis of tetramethylbenzidine substrate (KPL, Gaithersburg, MA, USA) was measured at 450 nm using a BioTek EL-808 absorbance microplate reader (BioTek, Winooski, VT, USA).

Chapter 3

TIMP-3 internalization by different cell types

3.1 Introduction

Our laboratory has recently shown that while no TIMP-3 is detectable in the medium of HTB94 cells in culture under normal conditions, TIMP-3 accumulates in the medium when heparin or calcium pentosan polysulfate (CaPPS) is added to the cells (Troeberg et al., 2008). Cytochalasin D, which is potent inhibitor of actin polymerization, also led to an accumulation of TIMP-3 in the medium (Troeberg et al., 2008). These data suggested that TIMP-3 can be rapidly internalized by cells after its secretion and that heparin and CaPPS interfere with its endocytosis leading to an accumulation of TIMP-3 in the conditioned medium. Other proteinases and proteinase—inhibitor complexes, such as MMP-13, MMP-9—TIMP-1, proMMP-2—TIMP-2 (Barmina et al., 1999; Emonard et al., 2004; Hahn-Dantona et al., 2001), uPA and uPA—uPAI-1(Higazi et al., 1996; Kounnas et al., 1993), and other ECM-associated proteins, such as connective tissue growth factor (CTGF) (Segarini et al., 2001), decorin (Brandan et al., 2006) and fibronectin (Salicioni et al., 2002) are known to be internalized by cells via a member of LDL receptor superfamily. To test the involvement of an LDL receptor in TIMP-3 endocytosis, Troeberg *et al*. (2008) treated HTB94 cells with the LDL receptor superfamily antagonist RAP, and they showed that this also led to an accumulation of TIMP-3 in the medium, suggesting that a member of LDL receptor superfamily is involved in TIMP-3 endocytosis.

In this chapter, this observation was further investigated to characterize the pathways involved in TIMP-3 endocytosis in more detail. Three different methods were used to study TIMP-3 endocytosis. i) Western blot analysis was used to follow clearance of exogenously added TIMP-3 from conditioned medium of cultured cells, ii) a radioactivity-based assay was used to investigate the kinetics of TIMP-3 endocytosis and iii) immunofluorescence was used to detect the presence of endocytosed TIMP-3 inside cells.

3.2 Results

3.2.1 Monitoring TIMP-3 and N-TIMP-3 disappearance from the medium of HTB94 cells by Western blot analysis

3.2.1.1 Preparation of conditioned medium containing recombinant FLAG tagged TIMP-3 or N-TIMP-3

HEK-293/EBNA cells transfected with a vector encoding FLAG-tagged TIMP-3 were grown to confluence and incubated in serum-free DMEM containing 30 mM sodium chlorate. Troeberg *et al*. (2009) showed that sodium chlorate ($NaClO_3$), which inhibits heparan sulfate proteoglycan sulfation, prevented TIMP-3 internalization and resulted in accumulation of soluble TIMP-3 in the medium of HEK-293/EBNA cells freshly transfected with a pCEP-4/TIMP-3-FLAG construct. Only a small amount of TIMP-3 was detected in the conditioned medium without adding $NaClO_3$ (Troeberg et al., 2009). After 4 days, the conditioned medium (250 ml) was collected, centrifuged for 5 min at 3000 g to eliminate cell debris and concentrated 10 times using Vivacell 250 filters (MWCO 5000). The medium was dialyzed using Slide-A-Lyzer Dialysis Cassettes (MWCO 3500) against TBS to remove the sodium chlorate.

Samples were taken after every step (1 ml or 100 μl after concentration) and TCA-precipitated (5 %). The TCA-insoluble pellets were re-suspended in 30 μl of 2 X SDS-PAGE buffer and the expression of TIMP-3 was analysed by Western blotting with anti-FLAG M2-antibody. As shown in Figure 5, TIMP-3 was detected in the conditioned medium. Conditioned medium containing FLAG tagged N-TIMP-3 was made in the same manner (data not shown). Inhibitory activity of both TIMP-3 and N-TIMP-3 was confirmed by titration against MMP-1 ΔC.

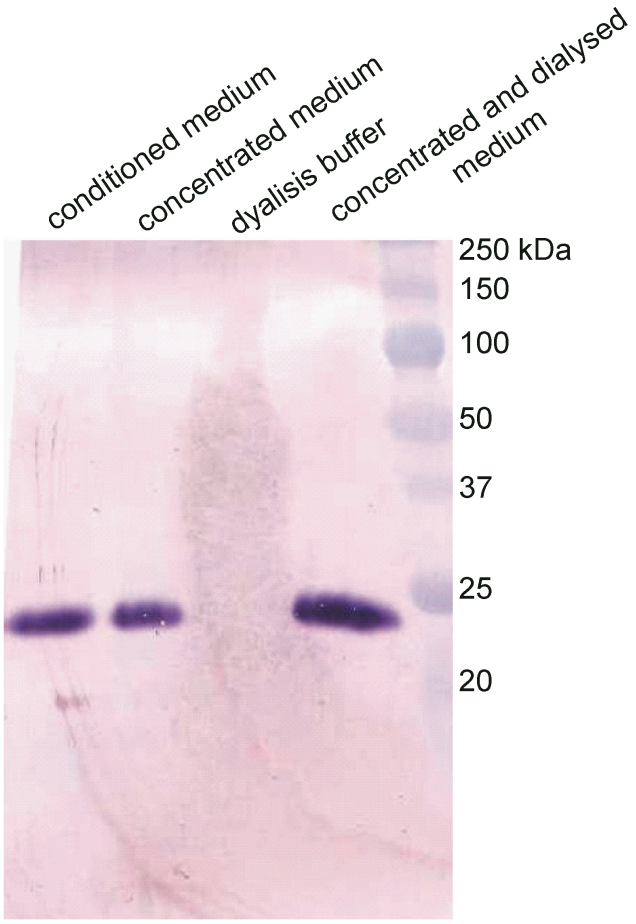

Figure 5, Western blot of conditioned medium containing TIMP-3-FLAG
Conditioned medium from HEK-293/EBNA cells transfected with pCEP4/TIMP-3-FLAG was harvested after 4 days of culture in serum-free DMEM with 30 mM $NaClO_3$, concentrated and dialyzed against TBS. Samples of conditioned medium (1 ml), concentrated medium (100 µl), dialysis buffer (1 ml) and concentrated and dialyzed medium (100 µl) were precipitated with TCA (5 %) and analysed by Western blotting using the anti-FLAG M2-antibody.

3.2.1.2 Time course of TIMP-3 disappearance from the medium of HTB94 cells

To investigate whether TIMP-3 could be endocytosed by HTB94 cells, the TIMP-3-FLAG containing medium, concentrated and dialyzed (prepared as described in Section 3.2.1.1), was added to HTB94 cells and the amount of recombinant FLAG

tagged TIMP-3 remaining in the medium of HTB94 cells over 24 h was examined by Western blotting.

HTB94 cells were grown to confluence in DMEM 10 % FCS, and then incubated in DMEM 0.1 % FCS supplemented with 100 µl of FLAG-tagged TIMP-3 containing medium. Cells were cultured for up to 24 h and the conditioned medium was harvested at the time points indicated, and concentrated by TCA precipitation. Equal volumes of all samples were analysed by Western blotting using the anti-FLAG-M2 antibody as described in Section 3.2.1.1.

Figure 6 shows that the amount of TIMP-3 in the medium of HTB94 cells reduced over a 24 h time period. To determine the half-life of TIMP-3 disappearance from the medium of HTB94 cells, the pixel volume of each band in Figure 6A was quantified using Phoretix software. A graph of pixel volume of TIMP-3 in the medium against time is shown in Figure 6B. The $t_{½}$ of TIMP-3 disappearance from the medium was about 6 h. TIMP-3 could not be detected in either the wash fractions or within the cells (results not shown).

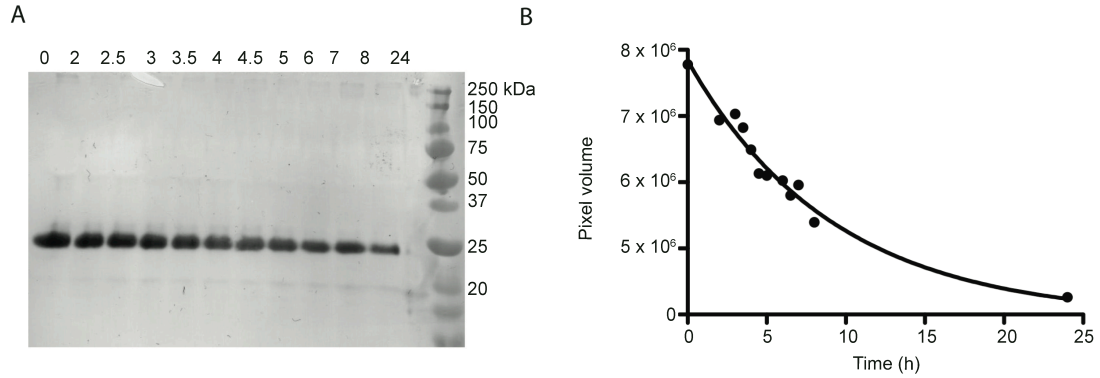

Figure 6, TIMP-3 disappearance from the medium of HTB94 cells
A. Conditioned medium containing TIMP-3 was added to HTB94 cells, harvested at indicated hours and precipitated with TCA (5 %). TCA-insoluble fractions were re-suspended in 2 X SDS-PAGE buffer and analysed by Western blotting using the anti-FLAG-M2 antibody. **B**. The pixel volume of each band from the Western blot was quantified using Phoretix software. The curve was generated by fitting to a one-phase exponential decay.

3.2.1.3 Time course of N-TIMP-3 disappearance from the medium of HTB94 cells

The same procedure was used to determine whether N-TIMP-3 could also be endocytosed. HTB94 cells were grown to confluence, then washed and incubated in N-TIMP-3-containing conditioned medium. Conditioned medium was harvested at the time points indicated and treated as previously described in Section 3.2.1.2 for TIMP-3. Figure 7A shows that the amount of N-TIMP-3 in the medium of HTB94 cells reduced over a 24 h time period. Graphs of pixel volume of N-TIMP-3 in the medium against time are shown in Figure 7B. The $t_{½}$ of N-TIMP-3 disappearance from the medium was about 6 h. As for TIMP-3, N-TIMP-3 could not be detected in either the wash fractions or within the cells (data not shown).

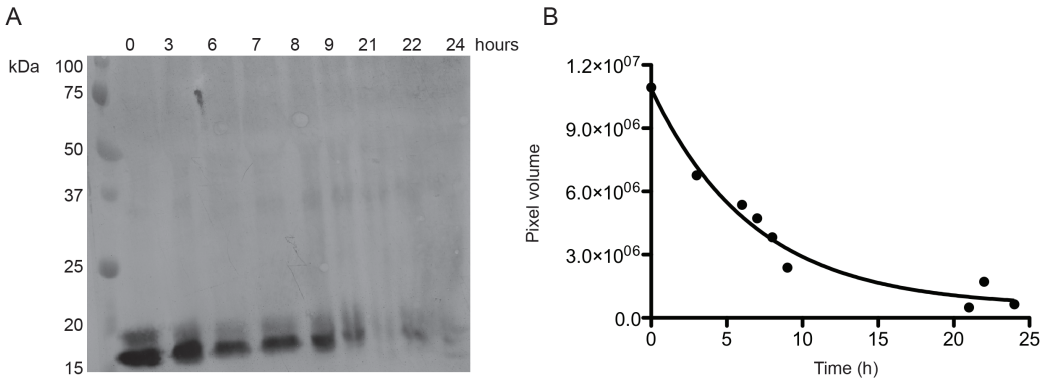

Figure 7, N-TIMP-3 disappearance from the medium of HTB94 cells
A. Conditioned medium containing N-TIMP-3 was added to HTB94 cells, harvested at the time points indicated and precipitated with TCA (5 %). TCA-insoluble fractions were re-suspended in 2 X SDS-PAGE buffer and analyzed by Western blotting using the anti-FLAG-M2 antibody. **B**. The pixel volume of each band corresponding at the amount of N-TIMP-3 remaining in the medium at each time was quantified using Phoretix software. The curve was generated by fitting to a one-phase exponential decay.

3.2.1.4 The effect of GAGs on TIMP-3 disappearance from the medium of HTB94 cells

Troeberg *et al.* (2008) showed that heparin and CaPPS induced accumulation of TIMP-3 in the conditioned media of cultured HTB94 cells. To determine if GAGs other that heparin and CaPPS could protect against TIMP-3 depletion, cells were treated with other GAGs, including de-N-sulfated heparin, dermatan sulfate and chondroitin-4-sulfate (at 50 μg/ml and 200 μg/ml) for 1 h prior to the addition of conditioned medium containing TIMP-3. After 8 h, the medium was precipitated with TCA (5 %) and analysed by Western blotting with the anti-FLAG-M2 antibody. Only heparin and CaPPS increased the amount of intact TIMP-3 remaining in the medium, the other GAGs tested did not show similar effects (Figure 8A and B).

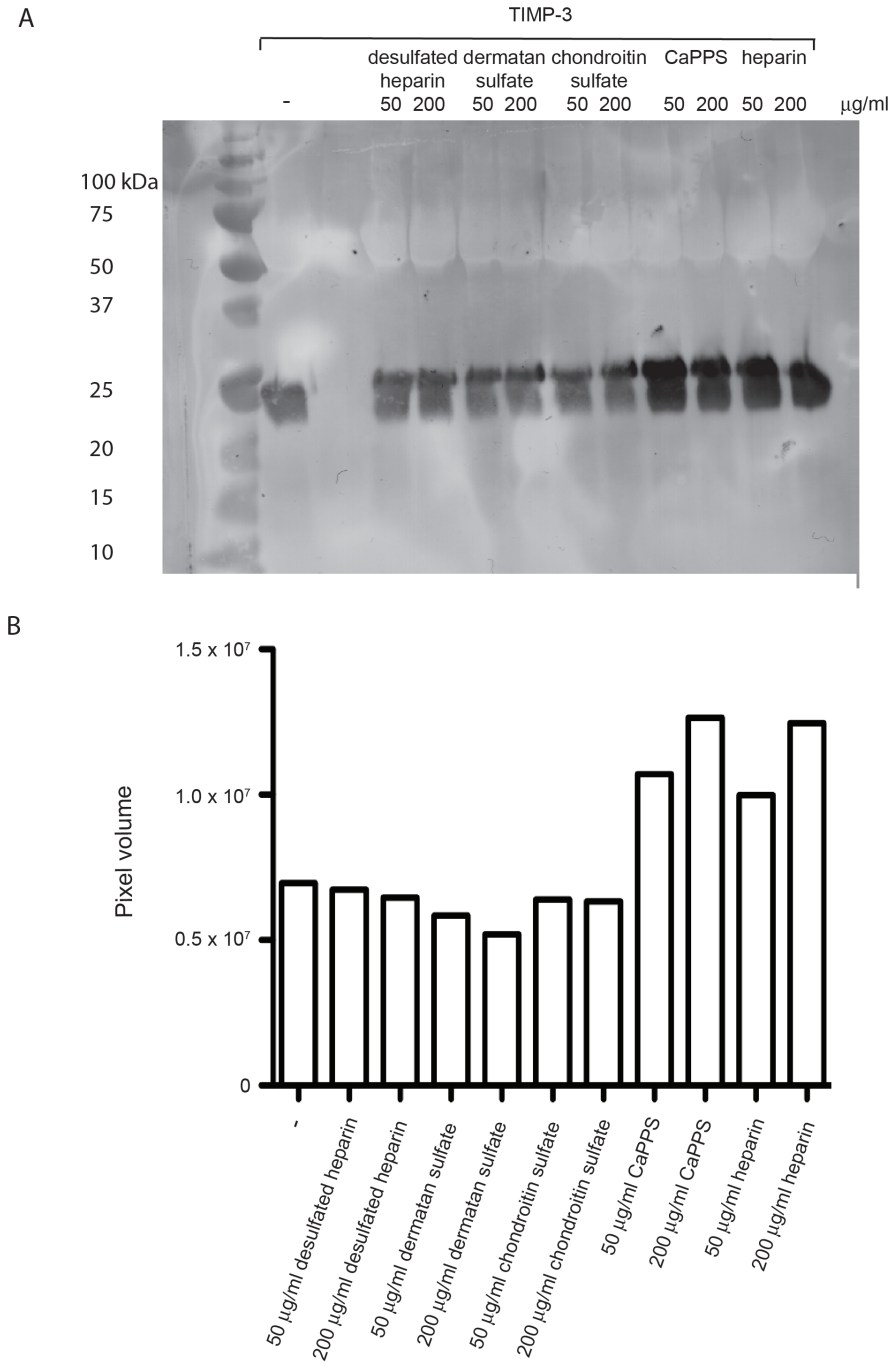

Figure 8, The effect of GAGs on TIMP-3 disappearance from the medium of HTB94 cells.

HTB94 cells were incubated with or without de-N-sulfated heparin, dermatan sulfate, chondroitin sulfate, calcium pentosan polysulfate or heparin (50 µg/ml and 200 µg/ml) for 1 h prior to addition of conditioned medium containing TIMP-3. After 8 h, the conditioned medium was harvested and precipitated with TCA (5 %). **A**. Each sample was analysed by Western blotting using anti-FLAG-M2 antibody. **B**. The pixel volume of each TIMP-3 band was quantifiied using Phoretix software.

3.2.1.5 The effect of RAP on TIMP-3 disappearance from the medium of HTB94 cells

To determine whether a member of the LDL family of receptors mediated TIMP-3 endocytosis, cells were treated with the LDL receptor family antagonist RAP (500 nM) for 1 h prior to the addition of conditioned medium containing TIMP-3. Media were harvested at the indicated time points and precipitated with TCA (5 %). TCA-insoluble fractions were analysed by Western blotting with the anti-FLAG-M2 antibody. Figure 9 shows that RAP protected against TIMP-3 disappearance from the medium at 8 h. This is in agreement with previous findings in our laboratory (Troeberg et al., 2008).

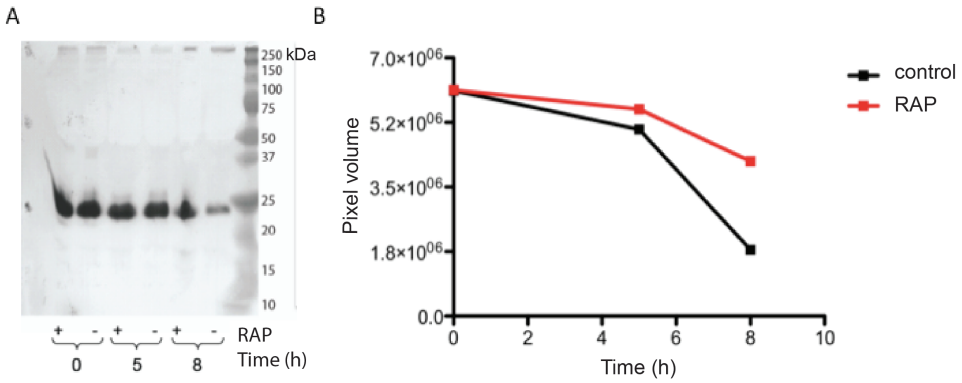

Figure 9, Effect of RAP on TIMP-3 disappearance from the medium
HTB94 cells were incubated with or without RAP (500 nM) for 1 h prior to addition of conditioned medium containing TIMP-3. At 0, 5 and 8 h the conditioned medium was harvested and precipitated with TCA. **A**. Each sample was analysed by Western blotting using anti-FLAG-M2 antibody. **B**. The pixel volume of each TIMP-3 band was quantified using Phoretix software.

3.2.2 Monitoring TIMP-3 endocytosis using a radioactivity-based assay

While Western blotting analysis was a useful initial tool to investigate disappearance of TIMP-3 from the medium, this technique was not sufficient to detect TIMP-3 within the cells. We thus established a more sensitive-quantitative radioactivity based assay to investigate TIMP-3 endocytosis.

3.2.2.1 Purification of [^{35}S]Met/[^{35}S]Cys-labeled TIMP-3 and N-TIMP-3

HEK-293/EBNA cells stably transfected with FLAG-tagged TIMP-3 were grown to confluence, and metabolically labeled with [^{35}S]Met/[^{35}S]Cys by incubation for 4 days in serum-free DMEM without cysteine, methionine or cystine, containing [^{35}S]Met/[^{35}S]Cys (25 µCi/ml). Sodium chlorate (30 mM) was added to ensure TIMP-3 accumulation in the medium (section 2.4.1).

[^{35}S]TIMP-3 and [^{35}S]N-TIMP-3 were purified from the conditioned medium using anti-FLAG M2 affinity chromatography and FLAG peptide elution (section 2.4.1). Aliquots of each sample were analysed by SDS-PAGE and silver staining. As the silver stain in Figure 10 shows, elution 1 contained two protein bands at a molecular weight of approximately 21 kDa and 24 kDa, corresponding to the non-glycosylated and glycosylated forms of TIMP-3 (Pavloff et al., 1992). Similarly, exposure to autoradiographic film indicated that the protein was labeled with [^{35}S] and that there were no other radioactive contaminants in the preparation. The purified protein was verified to be TIMP-3-FLAG by Western blot analysis with anti-FLAG M2 antibody. The same procedure was used to purify [^{35}S]N-TIMP-3 (data not shown). Active concentrations of [^{35}S]TIMP-3 were determined by titration against a known concentration of MMP-1 ΔC. Briefly, MMP-1 ΔC activity can be measured *in vitro* by following the hydrolysis of a cleavable fluorogenic substrate. 50 µl of 40 nM MMP-1 ΔC were incubated with serial dilutions of the [^{35}S]TIMP-3 preparation (50 µl) for 1 h at 37 °C to allow formation of stable 1:1 [^{35}S]TIMP-3—MMP-1 ΔC complexes. Then, 100 µl of Dnp (2,4-dinitrophenyl)-Pro-Leu-Gly-Pro-DL-Amp-D-Lys substrate (3 µM) were added. The amount of MMP-1 ΔC that remains uninhibited after incubation cleaves the fluoregenic substrate and TIMP-3 concentration can be determined from the maximum dilution (lowest concentration of TIMP-3) that gives a complete inhibition of MMP-1 ΔC. The dilution factor of [^{35}S]TIMP-3 preparation (X-axis) was plotted against the MMP-1 ΔC activity as row fluorescence units (Y-axis). The X-intercept gives the dilution of TIMP-3 preparation required to completely inhibit MMP-1 ΔC. Figure 10D shows that the X-intercept was about 0.150, thus elution 1 contained about 40 nM/0.150= 266 nM [^{35}S]TIMP-3.

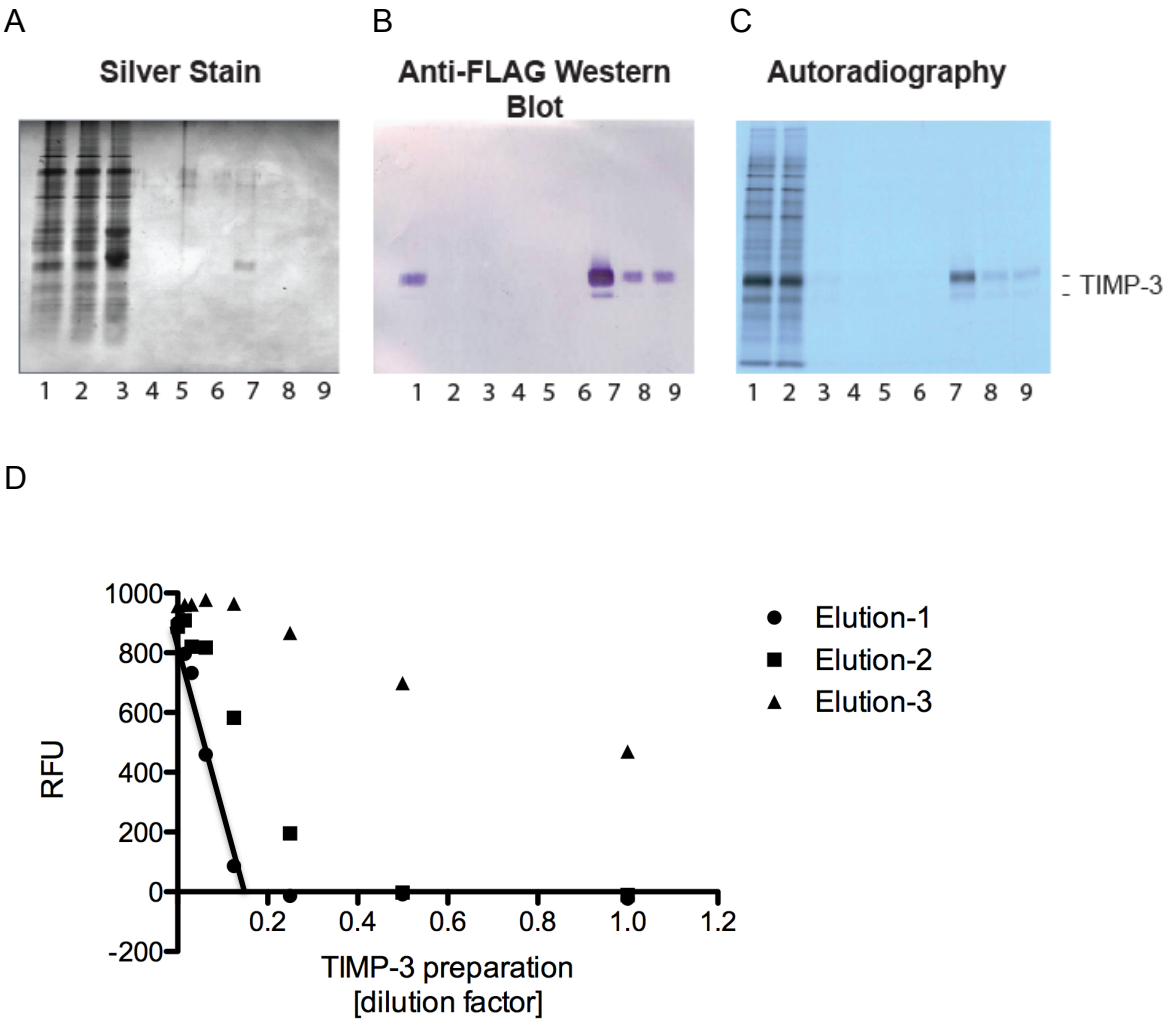

Figure 10, Purification of [^{35}S]TIMP-3-FLAG
A. HEK-293/EBNA cells transfected with TIMP-3-FLAG were metabolically labeled with [^{35}S]Met/[^{35}S]Cys for 4 days. The resulting conditioned medium (20 ml) was loaded onto an anti-FLAG M2-agarose column (2 ml). After washing with 1 M NaCl in TBS buffer (20 ml) and TBS (20 ml), the bound material was eluted with 200 µg/ml FLAG peptide in TBS in 3 ml fractions. **A**. Aliquots were analysed by SDS-PAGE (1. starting material, 2. unbound material, 3. NaCl wash-1, 4. NaCl wash-2, 5. TBS wash-1, 6. TBS wash-2, 7. elution-1, 8. elution-2, 9. elution-3) and silver staining. **B**. Western blot of [^{35}S]TIMP-3 using anti-FLAG M2-antibody. **C**. The gel was dried and exposed to autoradiographic film overnight. **D**. Titration of MMP-1 ΔC with dilutions of [^{35}S]TIMP-3 preparation.

3.2.2.2 Kinetics of [^{35}S]TIMP-3 internalization by HTB94 cells

2 ml of 1 nM [^{35}S]TIMP-3 were added to 1 x 10^6 cells/well HTB94 cells at 37 °C and the distribution of radioactivity in various cell fractions analyzed over 24 h. The amount of TCA-insoluble radioactivity in the conditioned medium decreased over 24 h, indicating that the amount of intact TIMP-3 was decreased. The amount of TCA-

soluble radioactivity increased, indicating that [^{35}S]TIMP-3 was degraded (Figure 11A). Radioactivity was also detected in the cell-associated fraction. It increased over the first 2 h and then reached a constant level . Treatment of the cell layer with pronase indicated that about half of cell-associated [^{35}S]TIMP-3 was detected on the cell surface (Figure 11B). Taken together, these data thus indicate that [^{35}S]TIMP-3 bound to the cell-surface, was internalized and degraded by the cells, with fragments released back into the medium.

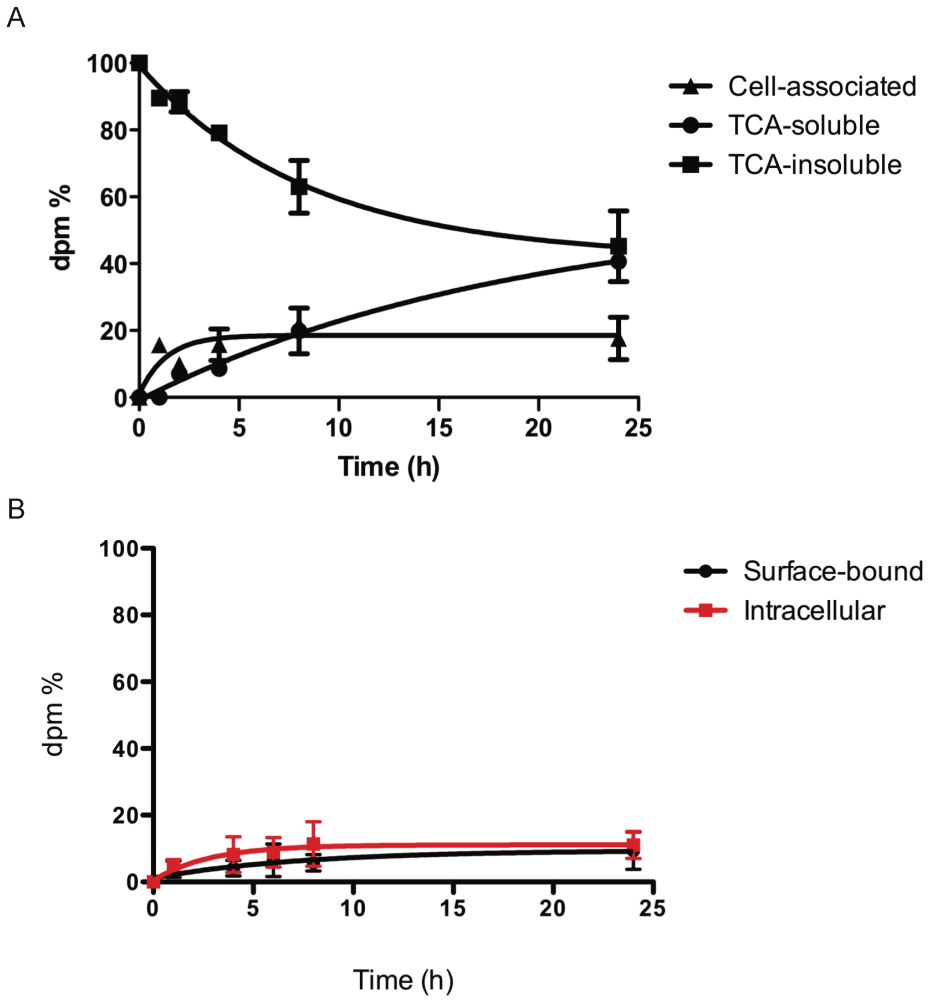

Figure 11, Time course of [^{35}S]TIMP-3 internalization by HTB94 cells
A. [^{35}S]TIMP-3 (1 nM) was added to HTB94 cells. After the indicated times, conditioned media were treated with 5 % TCA and centrifuged to separate TCA-soluble (●) radioactivity, that represents [^{35}S TIMP-3 fragments, from TCA-insoluble material (■), that represents intact [^{35}S TIMP-3. Cell-associated radioactivity (▲) was solubilized in NaOH. Radioactivity present in the different fractions was counted (*n=3*). **B**. Cells were released from the culture dish with pronase (10 min, on ice), then centrifuged to separate pronase-sensitive fraction (surface-bound, ●) from pronase-resistant fraction (intracellular, ■) (*n=3*).

3.2.2.3 Concentration-dependent endocytosis of [^{35}S]TIMP-3

To investigate the concentration-dependence of TIMP-3 clearance, [^{35}S]TIMP-3 was added at a range of concentrations (0.5 - 5 nM) and the medium was harvested at various time points. The TCA-insoluble fraction remaining at each concentration was expressed as % of the total counts for any time-point, normalized against the fraction at 0 h and plotted against time of incubation (Figure 12A). At each of the concentrations tested, [^{35}S] TIMP-3 disappeared from the medium at a similar rate. The TCA-soluble fraction also increased in the medium and all the concentrations tested increased at the same rate (Figure 12B).

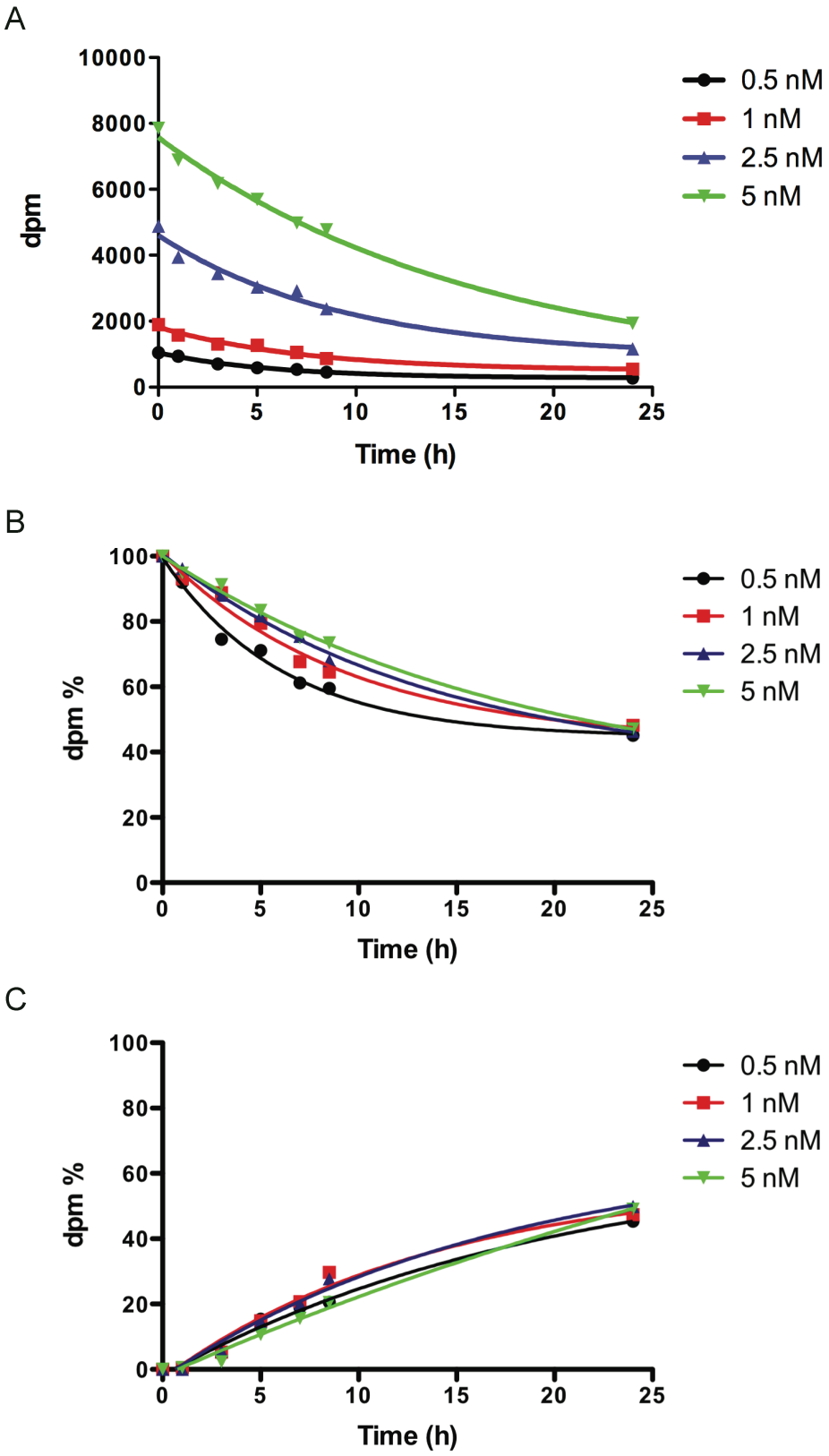

Figure 12, Concentration-dependent [^{35}S]TIMP-3 clearance by HTB94 cells
HTB94 cells were incubated for 1 h at 37 °C, then [^{35}S] TIMP-3 (0.5 nM, 1 nM, 2.5 nM, 5 nM) was added. At the time points indicated, the conditioned medium was removed and the TCA-soluble and TCA-insoluble fractions were harvested. **A**. TCA-insoluble fraction. **B.** TCA-insoluble fraction (%) **C.** TCA-soluble fraction (%).

3.2.2.4 Kinetics of [^{35}S]N-TIMP-3 internalization by HTB94 cells

To investigate whether the N-terminal inhibitory domain of TIMP-3 is also internalized, a time course experiment was performed, as described in section 3.2.2.2. HTB94 cells were plated at a density of 1x10^6 cells/well and grown overnight before incubation with DMEM containing 0.1 % FCS supplemented with 1 nM [^{35}S]N-TIMP-3. The radioactivity in the TCA-insoluble, -soluble and cell-associated fractions were measured as described in Section 3.2.2.2. As shown in Figure 13, [^{35}S]N-TIMP-3 seems to be cleared in a similar manner as [^{35}S]TIMP-3, with similar initial kinetics, but the rate of internalization and degradation was reduced after 5 h.

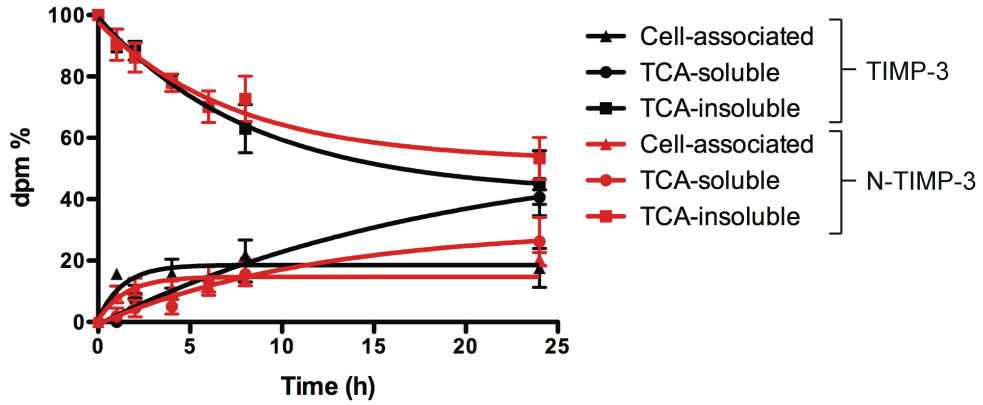

Figure 13, Time course of [^{35}S]N-TIMP-3 internalization by HTB94 cells
[^{35}S]N-TIMP-3 (1 nM) was added to HTB94 cells. After the indicated times, conditioned media were treated with 5 % TCA and centrifuged to separate TCA-soluble (●) radioactivity from TCA-insoluble material (■). Cell-associated radioactivity (▲) was solublised in NaOH. Radioactivity present in the different fractions was counted *(n=3)*. Data for TIMP-3 (black lines) are from Figure 11.

3.2.2.5 Endocyosis of [^{35}S]TIMP-3 at 4 °C and in Dynasore pre-treated HTB94 cells

To confirm that the decrease of radioactivity in the TCA-insoluble fraction is due to endocytosis rather than to non-specific binding of [^{35}S]TIMP-3 to cell or plate, an experiment was performed at 4 °C. HTB94 cells were seeded in a 6-well plate at a density of 1x10^6 cells, rested overnight and washed three-times in serum-free DMEM before incubation at 4 °C in DMEM containing 0.1 % FCS for 30 min. HTB94 cells were then incubated with [^{35}S]TIMP-3 (1 nM) at 4 °C. As shown in Figure 14A, at

4 °C radioactivity in the TCA-insoluble fraction slightly decreased over 6 h and degradation of [^{35}S]TIMP-3 was not observed (radioactivity in TCA-soluble fraction did not increase). Radioactivity in the cell-associated fraction increased over the first 2 h and then remained constant. These data suggested that [^{35}S]TIMP-3 was not endocytosed at 4 °C but that it still bound to the cell surface.

Dynasore is a cell-permeable inhibitor of dynamin, a large GTPase responsible for the scission of newly formed vesicles at the plasma membrane, and as such it is an inhibitor of dynamin-dependent endocytosis. Well-characterised clathrin- and caveolin-mediated pathways require dynamin and as a result are inhibited by Dynasore. Nevertheless, growing numbers of molecules are reported to be internalized in a dynamin-independent manner, such as GPI- anchored proteins (Mayor and Pagano, 2007), major histocompatibility complex I (Radhakrishna and Donaldson, 1997) and various bacterial toxins and viruses (Sandvig et al., 2008). To address the question of whether inhibition of dynamin could also affect TIMP-3 endocytosis, HTB94 cells were seeded in a 6-well plate at a density of 1x10^6 cells, rested overnight and washed three-times in serum-free DMEM before incubation with 80 μM Dynasore in DMEM 0.1 % FCS. After 30 min, 1 nM [^{35}S]TIMP-3 was added to the cells and samples harvested over 6 h. Figure 14B shows that in presence of Dynasore, radioactivity in the TCA-insoluble fraction slightly decreased and radioactivity associated with cells increased, indicating that [^{35}S]TIMP-3 bound to cells. Radioactivity associated with the TCA-soluble fraction also slightly increased, suggesting that a dynamin-independent endocytic pathway is involved in the internalization of TIMP-3.

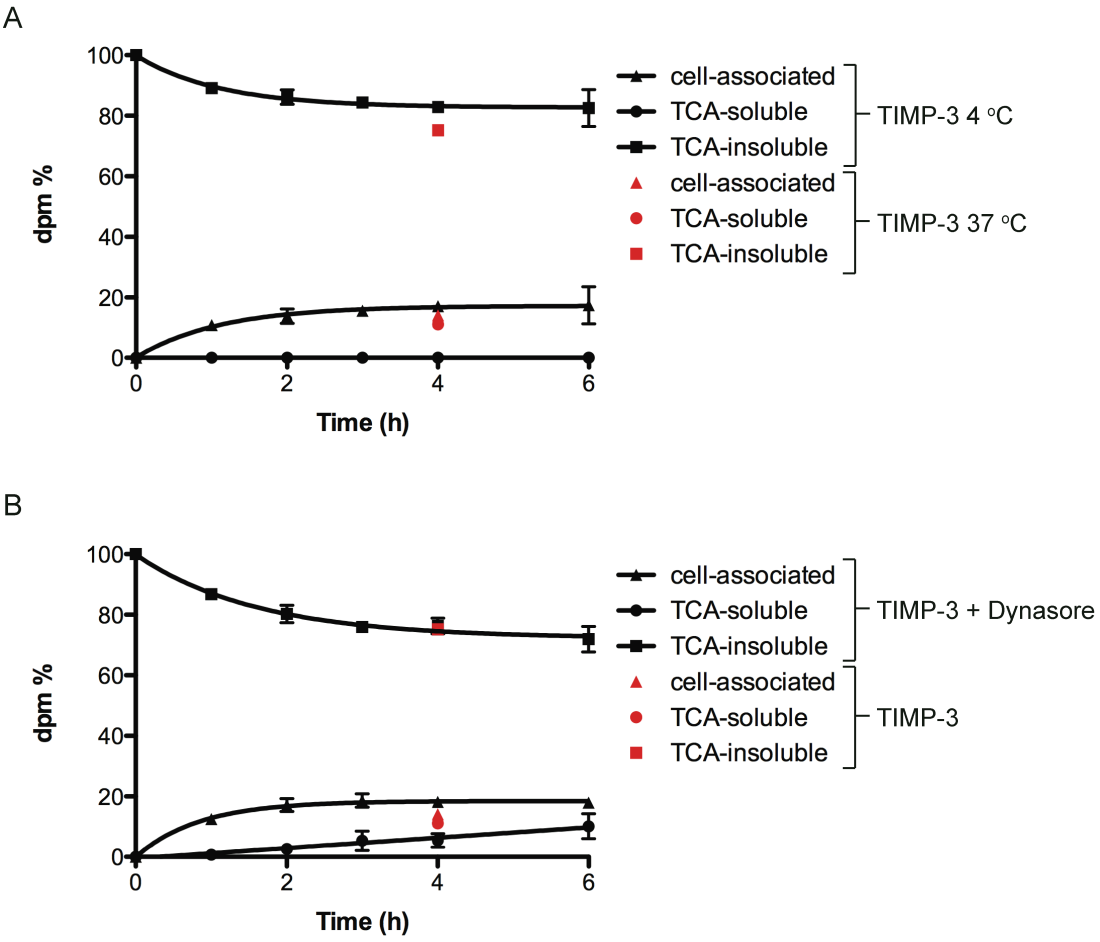

Figure 14, Inhibition of [^{35}S]TIMP-3 endocytosis at 4° C and in presence of Dynasore
A. HTB94 cells were seeded in a 6-well plate at a density of 1x10^6 cells, rested overnight and washed three-times in serum-free DMEM. Then, cells were incubated at 4 °C in DMEM containing 0.1 % FCS. After 30 min, 1 nM [^{35}S] TIMP-3 was added. At the time points indicated, the conditioned medium was harvested and radioactivity in TCA-insoluble (■), TCA-soluble (●) and cell-associated (▲) fractions was measured (*n=3*).
B. HTB94 cells were seeded in a 6-well plate at a density of 1x10^6 cells, rested overnight and washed three-times in serum-free DMEM. Cells were incubated with 80 μM Dynasore at 37 °C in DMEM containing 0.1 % FCS. After 30 min, 1 nM [^{35}S] TIMP-3 was added. At the time points indicated, the conditioned medium was harvested and radioactivity in TCA-insoluble (■), TCA-soluble (●) and cell-associated (▲) fractions was measured (*n=2*).

3.2.2.6 Effect of GAGs on [^{35}S]TIMP-3 endocytosis

3.2.2.6.1 Highly sulfated GAGs inhibited [^{35}S]TIMP-3 endocytosis

The effect of GAGs on TIMP-3 clearance was previously investigated by Western blot analysis (Figure 8). Here the inhibitory effect of GAGs on [^{35}S]TIMP-3 is investigated further. HTB94 cells were seeded in a 6-well plate at a density of 1x10^6 cells, rested overnight and washed three-times in serum-free DMEM before incubation at 37 °C in DMEM containing 0.1 % FCS and heparin or sodium pentosan polysulfate (NaPPS) or de-sulfated heparin or chondroitin sulfate or dermatan sulfate or hyaluronic acid (all at 200 μg/ml) for 1 h. HTB94 cells were then incubated with [^{35}S]TIMP-3 (1 nM). Media were harvested after 24 h and TCA precipitated as described before. TCA-insoluble fractions were transferred into scintillation vials and counted.

Figure 15 shows that heparin inhibited the decrease in TCA-insoluble radioactivity after 24 h, NaPPS similarly inhibited [^{35}S]TIMP-3 endocytosis, while de-sulfated heparin, dermatan sulfate, chondroitin sulfate and hyaluronic acid had minimal effects on TIMP-3 endocytosis.

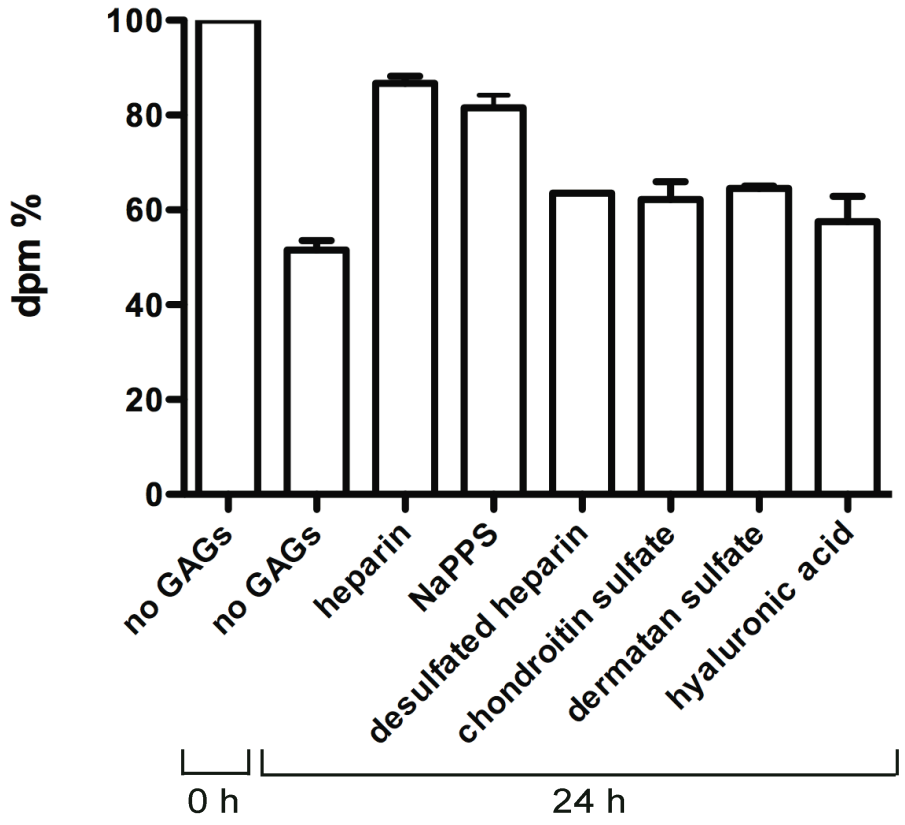

Figure 15, Effect of different GAGs on [^{35}S]TIMP-3 endocytosis
HTB94 cells were seeded in a 6-well plate at a density of 1x10^{6} cells, rested overnight and washed three-times in serum-free DMEM before incubation with indicated GAGs (200 μg/ml) for 1 h at 37 °C prior adding 1 nM [^{35}S]TIMP-3. After 24 h media were harvested and TCA-precipitated. Radioactivity associated with TCA-insoluble fractions was measured (*n=2*).

3.2.2.6.2 The effect of heparin on [^{35}S]TIMP-3 endocytosis

To understand the mechanism of heparin inhibition, a time course of [^{35}S]TIMP-3 internalization by HTB94 cells in the presence of heparin was performed. Figure 16 shows that the decrease in TCA-insoluble [^{35}S]TIMP-3 is inhibited by heparin compared to untreated control. Also, the appearance of radioactivity in TCA-soluble and cell-associated fractions was inhibited compared to control. Heparin also blocked the internalization of [^{35}S]N-TIMP-3 in a similar manner (data not shown), suggesting that in both cases heparin interfered with TIMP-3 binding to the cell surface and subsequent endocytosis.

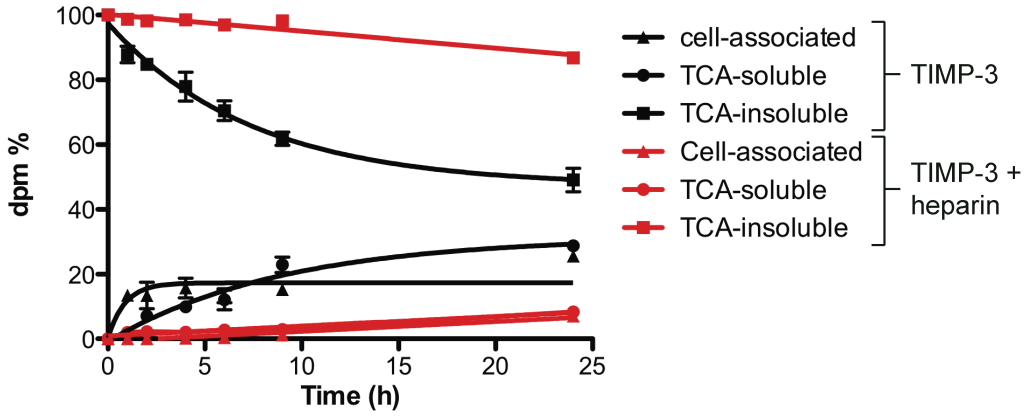

Figure 16, Effect of heparin on [^{35}S]TIMP-3 endocytosis.
HTB94 were incubated at 37 °C with heparin (200 µg/ml). After 1 h, 1 nM [^{35}S]TIMP-3 was added. The conditioned medium was harvested at different time points over 24 h and TCA-precipitated. Radioactivity in TCA-insoluble (■), TCA-soluble (●) and cell-associated (▲) fractions was measured and compared to that of samples non-treated with heparin (black symbols and lines) (*n=3*).

3.2.2.7 RAP inhibits [^{35}S]TIMP-3 endocytosis

We showed that RAP inhibited endocytosis using Western blot (section 3.2.1.5). We therefore investigated whether it also inhibits the endocytosis of [^{35}S]TIMP-3. HTB94 cells were incubated with RAP (500 nM) for 1 h at 37 °C and then [^{35}S]TIMP-3 (1 nM) was added. Fractions were harvested at various time points as previously described. Figure 17 shows that RAP inhibited the decrease of TCA-insoluble [^{35}S]TIMP-3, and inhibited the appearance of TCA-soluble and cell-associated fractions compared to the controls. These results suggest that an LRP-dependent pathway is involved in TIMP-3 endocytosis. RAP was, however, less effective at blocking TIMP-3 endocytosis than heparin (Figure 16), suggesting that LRP-independent pathways may also be involved TIMP-3 endocytosis. RAP inhibited [^{35}S]N-TIMP-3 endocytosis in a similar manner (not shown).

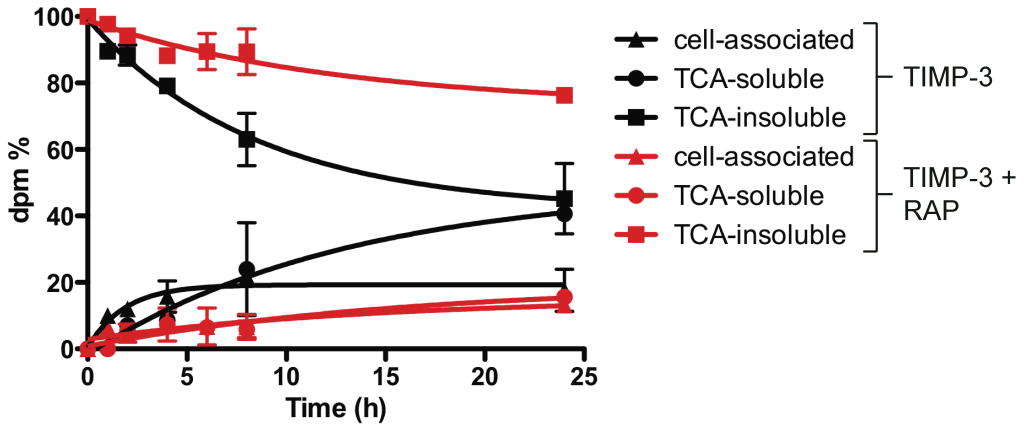

Figure 17, Effect of RAP on [^{35}S]TIMP-3 endocytosis by HTB94 cells
HTB94 cells were incubated at 37 °C in DMEM containing 0.1 % FCS and RAP 500 nM. After 1 h, [^{35}S]TIMP-3 (1 nM) was added, and the conditioned medium was removed at different time points and TCA-precipitated. Radioactivity in TCA-insoluble (■), TCA-soluble (●) and cell-associated (▲) fractions was measured and compared to that of samples non-treated with RAP (black symbols and lines) (*n=3*).

3.2.3 Visualisation of TIMP-3 endocytosis by immunofluorescent microscopy

To visualize TIMP-3 internalized by cells, HTB94 cells were cultured on 18 mm cover glasses coated with gelatin. 1 µg/ml of non-radiolabeled recombinant FLAG-tagged TIMP-3 was added to cells either alone or in combination with heparin (200 µg/ml) or RAP (500 nM) in phenol-red free DMEM with 0.1 % FCS. Cell-associated TIMP-3-FLAG was visualized with anti-FLAG M2 antibody (5 µg/ml) at RT for 2 h. Actin was stained with Alexa Fluor-568-conjugated phalloidin.

An intense and punctate staining was observed inside cells supplemented with TIMP-3-FLAG (Figure 18). In the presence of heparin, the staining was completely abolished, and in the presence of RAP the labeling was strongly reduced but not completely abolished.

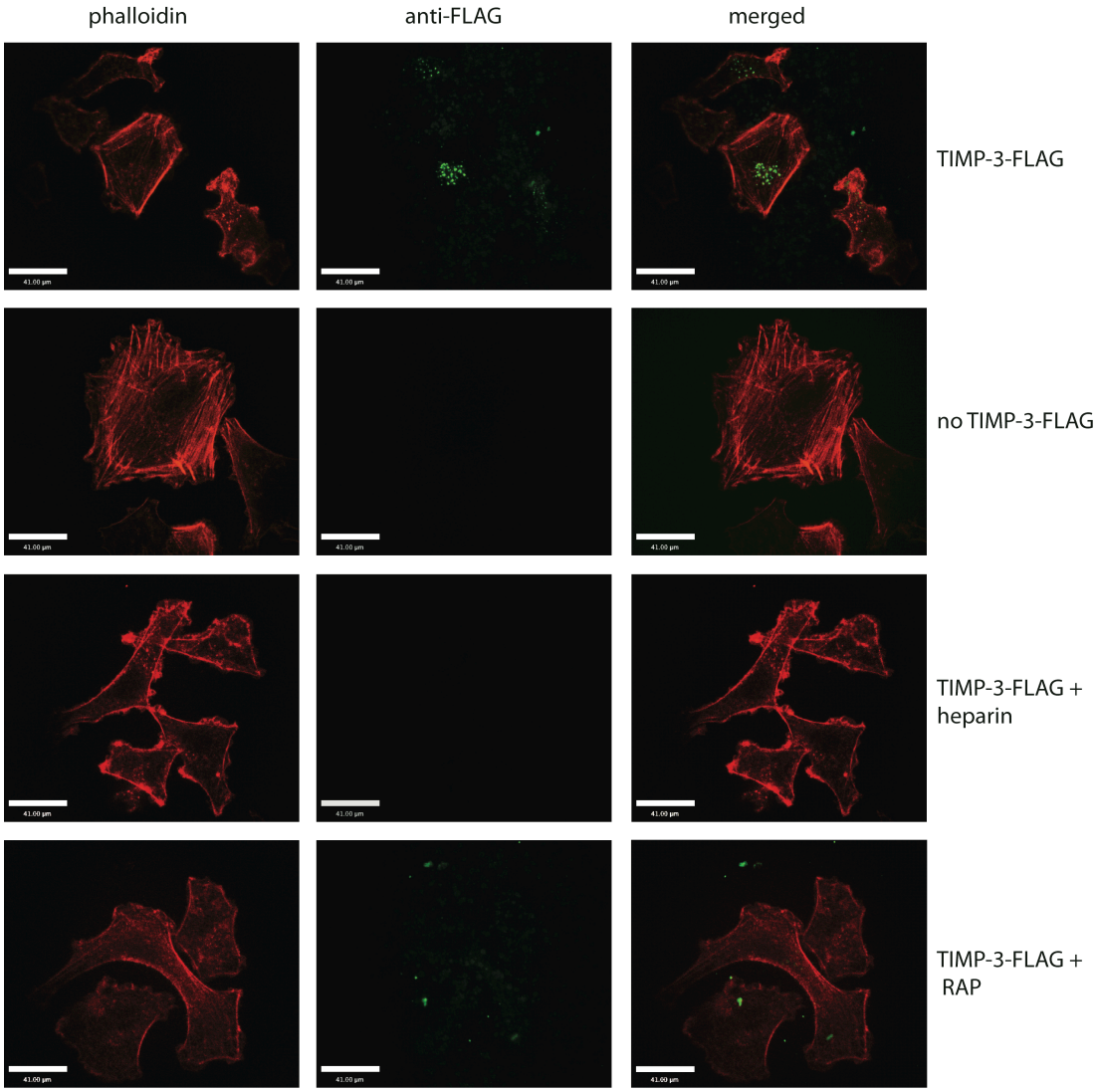

Figure 18, Detection of TIMP-3-FLAG within HTB94 cells
HTB94 cells were incubated at 37 °C with 1 µg/ml of FLAG-tagged TIMP-3 for 2 h in the presence or absence of heparin (200 µg/ml) or RAP (500 nM) and then permeabilised and immunostained for the presence of TIMP-3-FLAG inside the cells using an M2 anti-FLAG antibody and an Alexa 468-labelled secondary antibody (green channel). The cytoskeleton was visualized using Alexa 568-labelled phalloidin (red channel). Control samples were not supplemented with TIMP-3-FLAG.

3.2.4 Internalization of [^{35}S]TIMP-3 by different cell types

We investigated whether TIMP-3 endocytosis was a general phenomenon occurring in other cell-types different from HTB94 cells. Primary chondrocytes were isolated from pig cartilage, as described in Section 2.2.2, and then incubated with 1 nM [^{35}S]TIMP-3 at 37 °C. The distribution of radioactivity in different cell-fractions was analysed over 24 h. The amount of TCA-insoluble radioactivity in the conditioned medium decreased over 24 h, and radioactivity in the TCA-soluble and cell-associated fractions increased (Figure 19B) showing kinetics of internalization similar to that of HTB94 cells (Figure 19A). [^{35}S]TIMP-3 (1 nM) incubated with human uterine cervical fibroblasts (HUCF) was internalized and degraded as well as chondrocytes (Figure 19C). THP-1 cells (human acute monocytic leukemya) supplemented with 1 nM [^{35}S]TIMP-3 showed a slower internalization of the inhibitor compared to chondrocytes and fibroblasts, but internalization still occurred (Figure 19D).

Clearance of TIMP-3 by carcinoma cell lines showed a distinct profile. Incubation of [^{35}S]TIMP-3 with both MCF-7 cells (human breast adenocarcinoma cell line) and HeLa (human epithelial cervical cancer) cells resulted in a similar radioactivity distribution among cell-fractions over 24 h. The amount of TCA-insoluble radioactivity in the conditioned medium decreased over time; but surprisingly the amount of radioactivity in the TCA-soluble fraction did not increase over 24 h and a high amount of radioactivity was found associated with cells. These data suggest that TIMP-3 binds to the Hela and MCF-7 cell-surface, but it is not internalized nor degraded and released back in the medium (Figure 19E and F).

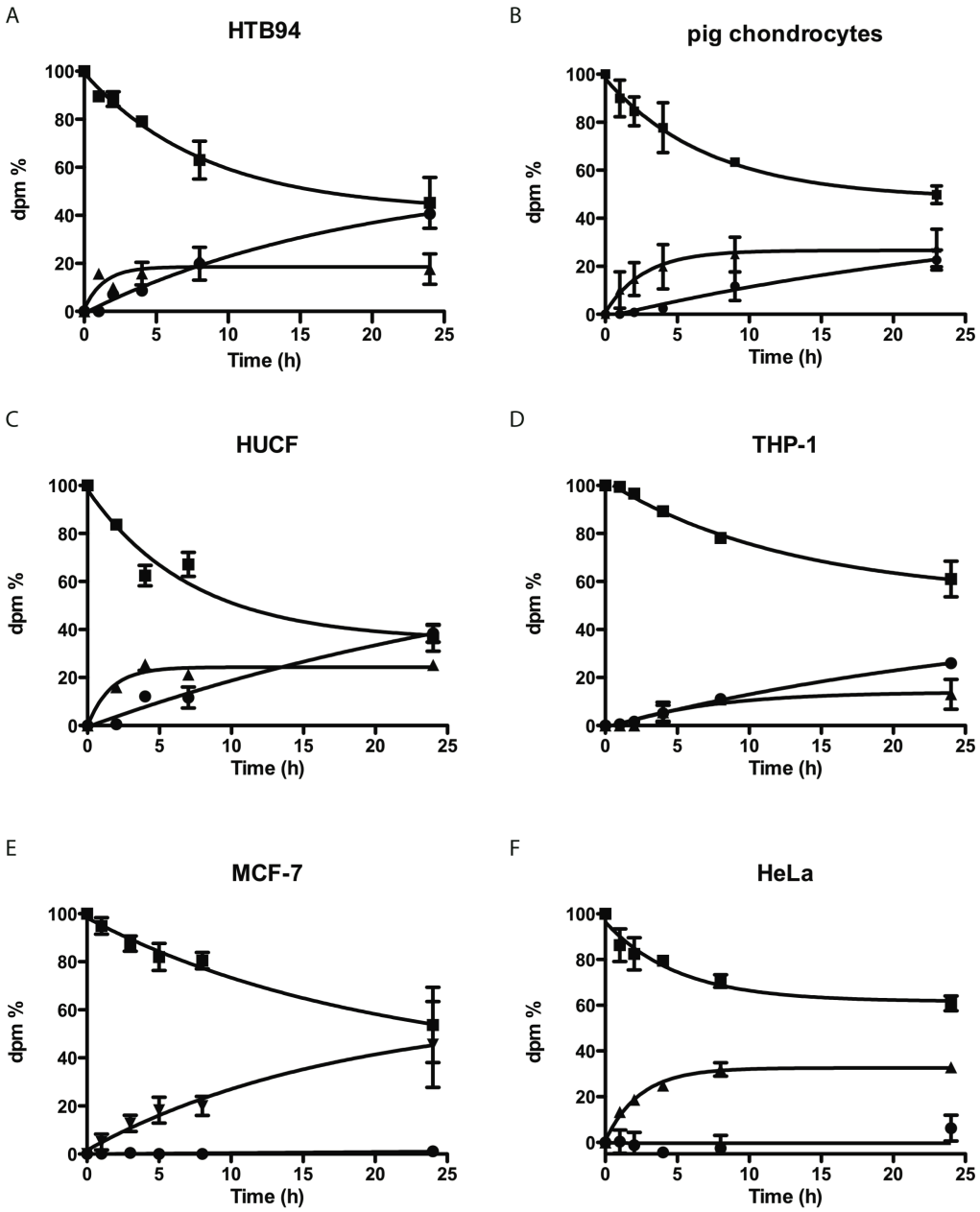

Figure 19, Internalization of TIMP-3 by different cell-types

1 nM [^{35}S]TIMP-3 was added to different cell-lines and TCA-insoluble (■), TCA-soluble (●) and cell-associated (▲) radioactivity analysed at various times over 24 h (*n=2*).

3.3 Discussion

Troeberg *et al*. (2008) showed that TIMP-3 accumulated in the medium of HTB94 cells or pig articular chondrocytes in culture when cells were treated with highly sulfated GAGs such as heparin or CaPPS. The fact that cytochalasin D, which is an

inhibitor of actin polymerization and as such an inhibitor of endocytic processes, also led to accumulation of TIMP-3 in the medium, prompted Troeberg *et al*. (2008) to postulate that TIMP-3 was rapidly internalized by cells after secretion. It was postulated that this process is mediated by a member of the LDL receptor-related protein (LRP) family as the LRP ligand antagonist, RAP, caused an accumulation of TIMP-3 in the medium of treated cells. Furthermore, it was also suggested that cell surface heparan sulfate proteoglycans (HSPGs) may be also involved in TIMP-3 endocytosis, since addition of CaPPS or heparin resulted in an accumulation of TIMP-3 in the medium,

In this chapter, I confirmed that TIMP-3 is internalized by HTB94 cells confirmed by following the clearance of exogenously added recombinant TIMP-3 by Western blotting and by detecting endocytosed TIMP-3 within cells by immunofluorescence microscopy. Using a radioactivity-based assay, I followed TIMP-3 internalization over time, and showed that TIMP-3 is internalized by HTB94 cells and degraded into fragments, which were released back into the medium. This method was proven to be useful to study the kinetics of TIMP-3 internalization. The inhibitor was endocytosed with a rate that is not constant but changed over 24 h, being faster at earlier time points and slower at later time points. Exogenously added TIMP-3 was not completely internalized by cells over 24 h, with about 50 % of the starting material remaining in the medium at 24 h. N-TIMP-3 was internalized in a similar manner to full length TIMP-3, suggesting that the N-terminal domain contains the minimal residues required for internalization. TIMP-3 internalization reached a plateau after about 10 h; only a very small amount of TIMP-3 was taken up after 10 h. This plateauing phenomenon will be investigated in more detail in chapter 5.

Highly sulfated GAGs blocked the endocytosis of TIMP-3, while de-sulfated heparin, dermatan sulfate, chondroitin sulfate and hyaluronic acid did not. We hypothesized that highly sulfated GAGs could directly bind to the TIMP-3 molecule, interfering with TIMP-3 binding to the cell surface HSPGs, which have been reported to act as co-receptors for the internalization of some LRP ligands such as TSP, lipoprotein lipase and Aβ peptide (Chappell et al., 1993; Kanekiyo et al., 2011;

Mikhailenko et al., 1995). The role of HSPGs in TIMP-3 endocytosis will be further investigated in Chapter 4.

RAP inhibits binding and uptake of all the ligands of all the LDL receptor family members (Bu, 1998). LRP-1 contains four ligand-binding regions, with regions II and IV being the major binding site for LRP-1 ligands. RAP is able to bind regions II, III and IV (Migliorini et al., 2003). We speculate that similarly to other LRP-1 ligands, TIMP-3 binds to regions II and IV. When RAP was added to HTB94 cells, TIMP-3 endocytosis was strongly inhibited, but not completely. These data suggest that a member of the LDL receptor family is involved in the internalization of TIMP-3 and the possibility that an LRP-independent mechanism is also involved.

The members of the LDLR family bind and internalize ligands with a clathrin-dependent mechanism (Brown and Goldstein, 1979; Chen et al., 1990). While cytochalasin D and low temperature completely blocked TIMP-3 endocytosis, Dynasore, an inhibitor of all dynamin-dependent endocytic pathways, only partially inhibited TIMP-3 endocytosis, suggesting that a dynamin-independent pathway might be also involved.

Porcine articular chondrocytes internalized TIMP-3 with similar kinetics to HTB94 cells, showing that endocytosis might be an important regulatory mechanism to control TIMP-3 concentration in cartilage. TIMP-3 endocytosis is a general phenomenon, as many different cell-types, including human fibroblasts, murine embryo fibroblasts, human monocytes, COS-7 cells and others, effectively internalize TIMP-3. Interestingly, among all the tested cell-types, only two types of cell lines (HeLa and MCF-7 cells) failed to internalize TIMP-3; these are both carcinoma cell lines. In these cell-lines TIMP-3 binds to the cell-surface without being taken up inside. It was reported that LDLR and VLDLR expression was downregulated in MCF-7, HeLa and Hep-G2 cells at both message and protein levels (Shen et al., 2011). Overexpression of midkine and its premature interaction with LRP-1 in the Golgi leads the receptor to proteosomal degradation and interruption of its maturation in human colorectal carcinomas, resulting in a decrease in the number of mature receptors on the cell surface (Sakamoto et al., 2011). The decrease of mature LRP-1 on the cell surface might explain the lack of TIMP-3 endocytosis by these cell lines.

Hypoxia stimulates LRP-1 expression through hypoxia-inducible factor-1α in human vascular smooth muscle cells (Castellano et al., 2011) and mouse embryonic stem cells (Lee et al., 2011). It will be investigated whether the hypoxic condition induces LRP-1 expression in carcinoma cells and rescues TIMP-3 endocytosis, which may allow carcinoma cells to escape from an oncosuppressor effect of TIMP-3 (Cruz-Munoz et al., 2006a).

Chapter 4

Analysis of receptors involved in endocytosis of TIMP-3

4.1 Introduction

As shown in Chapter 3, receptor-associated protein (RAP), which is an antagonist of all members of the LDL receptor superfamily, reduced TIMP-3 internalization by HTB94 cells. These data prompted us to postulate that a member of the LRP family of receptors plays a key role in the endocytosis of TIMP-3. As already mentioned, many proteinases and proteinases—inhibitor complexes are endocytosed by LRP-1, a scavenging receptor member of the LDL receptors. In this chapter, LRP-1-null mouse embryonic fibroblasts (PEA-13 cells) (Kounnas et al., 1992) were used to investigate whether or not LRP-1 is the member of the LDL receptor superfamily involved in TIMP-3 endocytosis. PEA-13 cells and their wild-type counterparts (MEF-1 cells) represent a perfect tool to study LRP-1-mediated endocytosis as they have been well characterised and used to investigate the LRP-1-mediated endocytosis of several ligands (Willnow and Herz, 1994).

Although RAP reduced TIMP-3 endocytosis by HTB94 cells, some endocytosis still occurred in the presence of RAP, indicating that TIMP-3 is internalized by an LRP-independent mechanism. Many ligands that are internalized by LDLRs also undergo LRP-independent internalization, which is mediated by HSPGs in several cases (Mahley and Huang, 2007). Highly sulfated GAGs, such as heparin and CaPPS completely blocked TIMP-3 endocytosis. These discoveries led me to further investigate the involvement of HSPGs in TIMP-3 endocytosis. Esko *et al.* (1985) generated Chinese hamster ovary cell mutants (CHO-745) defective in the biosynthesis of glycosaminoglycans by genetic disruption of the enzyme xylosyl-transferase, which is responsible for the initiation of chondroitin sulfate and heparan sulfate biosynthesis (Esko et al., 1985). In this chapter, the involvement of HSPGs was assessed by testing the ability of CHO-745 to internalize TIMP-3 compared to that of their wild-type counterparts (CHO-K1).

4.2 Endocytosis of [^{35}S]TIMP-3 by LRP-1-deficient PEA-13 cells and the wild-type MEF-1 cells

4.2.1 Endocytosis of [^{35}S]TIMP-3 is inhibited in PEA-13 cells

To further investigate the role of LRP-1 in TIMP-3 endocytosis, [^{35}S]TIMP-3 endocytosis by wild-type mouse embryonic fibroblasts (MEF-1) and by LRP-1-deficient mouse embryonic fibroblasts (PEA-13) were compared. As shown in Figure 20, the decrease in TCA-insoluble radioactivity and the increase in TCA-soluble radioactivity were less by PEA-13 (Figure 20B) cells compared to either HTB94 (Figure 20C) or MEF-1 cells (Figure 20A), suggesting that LRP-1 contributes to TIMP-3 endocytosis. However, cell-associated [^{35}S]TIMP-3 was only slightly decreased in PEA-13 cells compared to MEF-1 cells, indicating that [^{35}S]TIMP-3 can bind the cell surface even in absence of LRP-1. The slow internalization of [^{35}S]TIMP-3 by LRP-1-deficient PEA-13 cells indicates that an LRP-1-independent pathway also occurs.

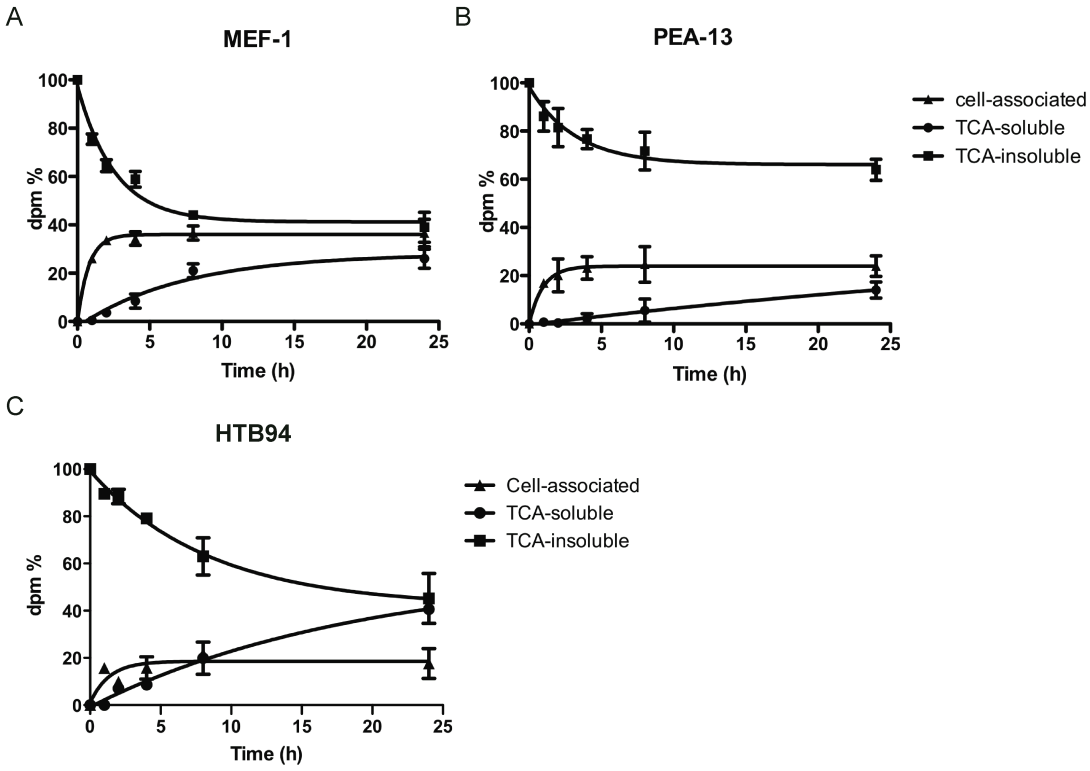

Figure 20, Time course of [^{35}S]TIMP-3 clearance by MEF-1 and PEA-13 cells
MEF-1 and PEA-13 cells were incubated at 37 °C in DMEM containing 0.1 % FCS and 1 nM [^{35}S]TIMP-3. At the time points indicated, the conditioned medium was removed and cell-associated, TCA-soluble and TCA-insoluble fractions were harvested as described before (*n=3*). **A**. Graph of [^{35}S]TIMP-3 endocytosis in MEF-1 cells. **B**. Graph of [^{35}S]TIMP-3 endocytosis in PEA-13 cells. **C**. Graph of [^{35}S]TIMP-3 endocytosis in HTB94 cells (from chapter 3).

4.2.2 Immunofluorescence analysis also indicates LRP-1 involvement

MEF-1 and PEA-13 cells were incubated with 40 nM FLAG-tagged TIMP-3 for 2 h at 37 °C. After fixation, labeling of the permeabilized cells with an anti-FLAG monoclonal antibody detected with an Alexa-488 secondary antibody showed green fluorescence. Immunolocalization of TIMP-3-FLAG was greatly reduced in PEA-13 cells No staining was observed inside cells not incubated with TIMP-3-FLAG, indicating that the signal was specific (Figure 21). These results indicate that TIMP-3-FLAG is internalized through LRP-1.

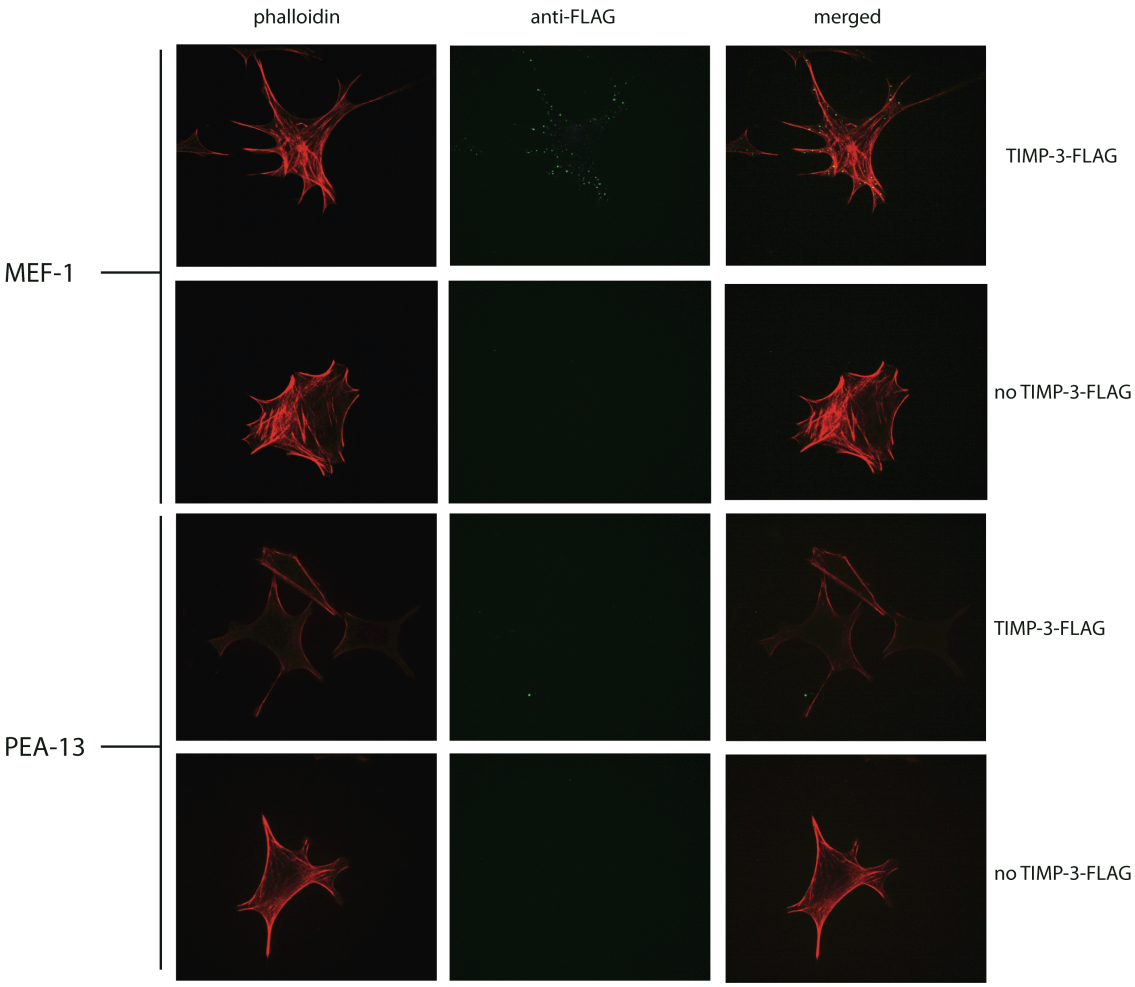

Figure 21, Internalization of TIMP-3 by PEA-13 cells and MEF-1 cells detected by confocal microscopy
MEF-1 and PEA-13 cells were incubated at 37 °C with 40 nM of FLAG-tagged TIMP-3 for 2 h and then permeabilsed and immunostained for the presence of TIMP-3-FLAG inside the cells. Control samples were not supplemented with TIMP-3-FLAG

4.2.3 Effects of heparin and RAP on [^{35}S]TIMP-3 endocytosis by MEF-1 cells and PEA-13 cells

MEF-1 cells and PEA-13 cells were preincubated with heparin (200 µg/ml) for 1 h before addition of 1 nM [^{35}S]TIMP-3. In both MEF-1 and PEA-13 cells, heparin inhibited the decrease in TCA-insoluble radioactivity as well as the increase in TCA-soluble and cell-associated radioactivity. Heparin inhibited endocytosis of [^{35}S]TIMP-3 by PEA-13 cells as effectively as that by HTB94 or MEF-1 cells. This indicates that heparin is an effective inhibitor of both LRP-1-dependent and LRP-1-independent internalization (Figure 22A and Figure 22B).

MEF-1 cells and PEA-13 cells were then incubated with 500 nM RAP for 30 min before addition of [^{35}S]TIMP-3 (1 nM). As shown in Figure 22C shows, RAP reduced the uptake of the TCA-insoluble [^{35}S]TIMP-3 by MEF-1 cells and the radioactivity in the TCA-soluble fraction. Cell-associated [^{35}S]TIMP-3 was slightly higher in RAP-treated cells. The kinetics of [^{35}S]TIMP-3 internalization by RAP-treated MEF-1 cells was very similar to that by PEA-13 cells. The slower rate of [^{35}S]TIMP-3 internalization in RAP-treated MEF-1 and PEA-13 suggests that LRP-1 plays a key role in [^{35}S]TIMP-3 endocytosis, but also that an LRP-1-independent endocytic pathway occurs in these cells. RAP-treated PEA-13 cells internalized [^{35}S]TIMP-3 with the same kinetics as non-RAP-treated PEA-13 cells (Figure 22D), confirming that an LRP-1-independent and RAP-insensitive pathway is also involved in [^{35}S]TIMP-3 internalization.

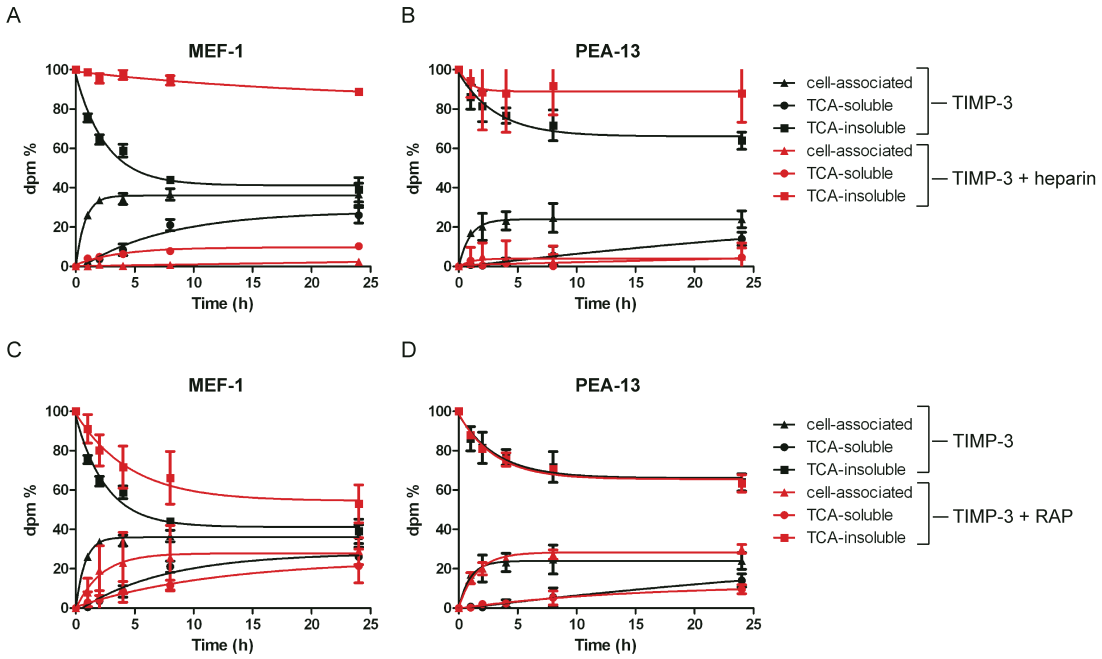

Figure 22, Effects of heparin and RAP on TIMP-3 internalization by MEF-1 and PEA-13 cells.

[^{35}S]TIMP-3 (1 nM) was added to MEF-1 or PEA-13. TCA-soluble (●), TCA-insoluble (■) and cell-associated (▲) radioactivity analysed at various times (*n=3*). **A**. Internalization of [^{35}S]TIMP-3 by MEF-1 cells in the presence (red symbols) and absence (black symbols) of 200 µg/ml of heparin. **B**. Internalization of [^{35}]TIMP-3 by PEA-13 cells in the presence (red symbols) and absence (black symbols) of 200 µg/ml of heparin. **C**. Internalization of [^{35}S]TIMP-3 by MEF-1 cells in the presence (red symbols) and absence (black symbols) of 500 nM RAP. **D**. Internalization of [^{35}S]TIMP-3 by PEA-13 cells in the (red symbols) and absence (black symbols) of 500 nM RAP.

4.2.4 Absence of LRP-1 does not affect TIMP-3 surface binding, but decreases TIMP-3 internalization and degradation

Previous experiments suggested that the absence of LRP-1 in PEA-13 cells did not affect TIMP-3 binding to the cell. Radioactivity in the cell-associated fraction of PEA-13 cells was very similar as that of MEF-1 cells at the time points analyzed. To confirm these data, a surface-binding experiment was performed at 4 °C. MEF-1 and PEA-13 cells were grown to confluence in a 6-well plate, then washed three-times and incubated in ice cold DMEM with 0.1 % FCS for 30 min. Next, 1 ml of 40 nM [^{35}S]TIMP-3 in ice cold TBS was added to cells and [^{35}S]TIMP-3 allowed to bind to cells for 2 hours at 4 °C. To assess cell binding at 4 °C, cells were washed twice in TBS and collected with 1 ml of 1M NaOH for scintillation counting. To assess internalization of surface bound [^{35}S]TIMP-3, other cells were washed in TBS and incubated in pre-warmed DMEM with 0.1 % FCS for 2 h at 37 °C. After 2 h, media were harvested and TCA-precipitated as described previously. The cell layers were treated with 0.1 % pronase solution on ice for 10 min to release surface ligands and detach cells from the plate. Cells were separated from the pronase-sensitive fraction by centrifugation and collected with 1 ml of 1M NaOH. Radioactivity in the TCA-insoluble fraction (intact TIMP-3 in the medium), TCA-soluble fraction (degraded TIMP-3 in the medium), surface-bound fraction (pronase-sensitive counts of cell fraction) and cell-associated fraction (pronase-resistent counts of cell fraction) fraction was measured. Figure 23A shows that a similar amount of [^{35}S]TIMP-3 bound to MEF-1 and PEA-13 cells at 4 °C, indicating that TIMP-3 binds to a cell surface molecule other than LRP-1. After 2 h incubation with DMEM 0.1 % FCS at 37 °C, both MEF-1 and PEA-13 cells internalized [^{35}S]TIMP-3 as shown by the decrease of radioactivity in their surface-bound fractions and by the presence of intracellular radioactivity and degradation products. Once again, [^{35}S]TIMP-3 internalization by MEF-1 cells was higher compared to that by PEA-13 cells, indicating that LRP-1 plays a key role in TIMP-3 internalization, but that an LRP-1-mediated pathway is not the only one involved. Interestingly, some intact [^{35}S]TIMP-3 molecules were released back into the media during the incubation at 37 °C, as we could detect radioactivity in the TCA-insoluble fractions.

A time course of surface-bound [^{35}S]TIMP-3 internalization and degradation by MEF-1 and PEA-13 was performed. MEF-1 and PEA-13 cells were first incubated with 40 nM [^{35}S]TIMP-3 at 4 °C for 2 h to allow surface binding. After washing, cells were further incubated with fresh DMEM 0.1 % FCS pre-warmed at 37 °C. At the indicated time points, degraded [^{35}S]TIMP-3 was measured. Degradation of surface-bound [^{35}S]TIMP-3 by MEF-1 was higher than that by PEA-13 cells over 5 h (Figure 23B).

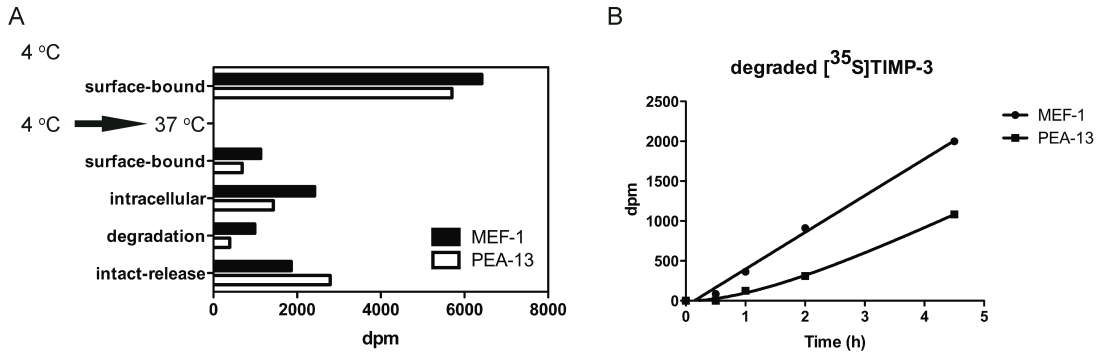

Figure 23, [^{35}S]TIMP-3 surface-binding to MEF-1 and PEA-13 cells

A. MEF-1 (solid bars) and PEA-13 (open bars) cells were incubated with 40 nM [^{35}S]TIMP-3 at 4 °C for 2 h to allow surface binding. After washing, some cultures were directly lysed to quantify cell-associated radioactivity. Alternatively, dishes were reincubated with fresh medium pre-warmed at 37 °C. Surface-bound ligand (pronase-sensitive radioactivity), intracellular (pronase-resistant), degraded (TCA-soluble counts in the medium) and intact-released (TCA-insoluble counts in the medium) [^{35}S]TIMP-3 were measured after 2 h at 37 °C. Surface binding of [^{35}S]TIMP-3 to MEF-1 and PEA-13 cells is similar, but endocytosis and degradation of [^{35}S]TIMP-3 by PEA-13 cells is lower than by MEF-1 cells. This result is representative of two separate experiments.

B. MEF-1 and PEA-13 cells were first incubated with 40 nM [^{35}S]TIMP-3 at 4 °C for 2 h to allow surface binding. After washing, cells were further incubated with fresh DMEM 0.1 % FCS pre-warmed at 37 °C. At the indicated times, degraded [^{35}S]TIMP-3 (TCA-soluble counts in the medium) was measured. This experiment was performed twice with similar results.

4.3 Investigation of HSPGs as potential receptors involved in the LRP-1-independent pathway

4.3.1 Internalization of [^{35}S]TIMP-3 by syndecan-4-deficient cells

Echtemeyer *et al.* (2009) showed that syndecan-4 is overexpressed in chondrocytes in osteoarthritis, and postulated that this leads to the increase in activity of ADAMTS-5 observed both *in vitro* and *in vivo*, leading to the appearance of an osteoarthritic phenotype in animal models (Echtermeyer et al., 2009). They postulated that the increase of ADAMTS-5 activity is due to cell-signalling triggered by syndecan-4.

We investigated whether syndecan-4 has a role in the endocytosis of TIMP-3 by using the radioactivity-based assay of [^{35}S]TIMP-3 endocytosis using syndecan-4 deficient mouse embryonic fibroblasts. Both syndecan-4-deficient and wild-type MEFs clearly internalized [^{35}S]TIMP-3, as radioactivity in TCA-insoluble fractions went down over 24 h, and radioactivity in cell-associated and TCA-soluble fractions increased with a similar kinetics (Figure 24). These data suggested that syndecan-4 is not involved in TIMP-3 internalization.

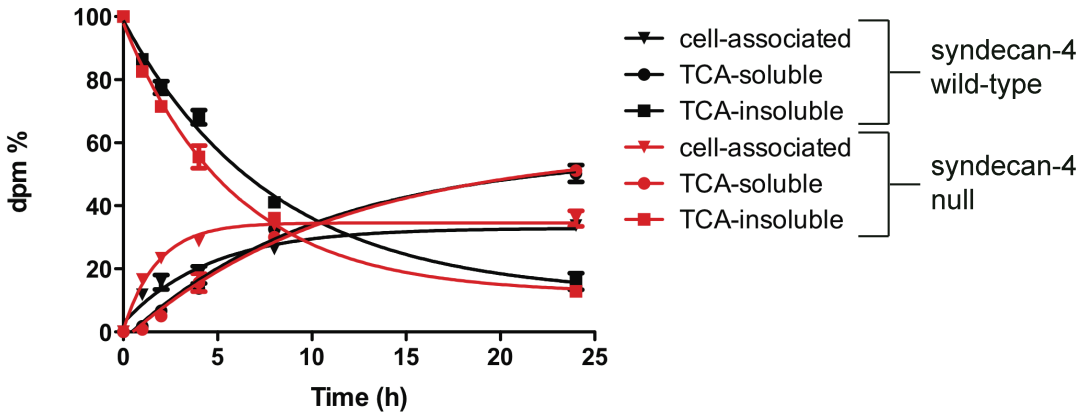

Figure 24, TIMP-3 endocytosis by Syndecan-4-deficient and -wild-type MEFs
Syndecan-4-deficient and wild-type MEFs were incubated at 37 °C in DMEM containing 0.1 % FCS and 1 nM [^{35}S]TIMP-3. At the time points indicated, the conditioned medium was removed and cell-associated, TCA-soluble and TCA-insoluble fractions were harvested as described before. The graph shows a time course of [^{35}S]TIMP-3 endocytosis by wild-type MEFs (black symbols) and syndecan-4-deficient MEFs (red symbols) (*n=2*).

4.3.2 Internalization of [^{35}S]TIMP-3 by syndecan-1 silenced HTB94 cells

Other ligands of LDLR family, such as triglyceride-rich lipoproteins and ApoE-VLDLs, can be also internalized in an LRP-independent manner via syndecan-1, through a process which is clathrin-independent and heparin-sensitive (Stanford et al., 2009; Wilsie et al., 2006). I hypothesized that this could also be the case for TIMP-3. I therefore silenced *Sdc-1* in HTB94 cells and tested whether the lack of *Sdc-1* has an effect on TIMP-3 internalization.

4.3.2.1 siRNA silencing of *Sdc-1*

To silence *Sdc-1* in HTB94 cells, two *Sdc-1* small interfering RNA (siRNA) specific for human *Sdc-1* gene were purchased from Ambion (catalog no. 12432 and 142557). These two siRNAs have been shown to inhibit Sdc-1 mRNA for more than 90 % in different cell lines, such as PC3, LNCaP and EJ-1 cells (Hu et al., 2010; Ogawa et al., 2007). To establish the conditions for *Sdc-1* knockdown, HTB94 cells were transfected overnight in a 6-well plate with scrambled siRNA, *Sdc-1* siRNA 12432, *Sdc-1* siRNA 142557 or a combination of both targeting siRNAs, all at 10-100 nM. Lipofectamine 2000 was used for the transfection as described in Section 2.6.1. Cells were harvested after 24 h and 48 h in culture, total RNA was extracted using a RNeasy® Mini kit (Invitrogen) and a q-PCR to assess *Sdc-1* expression compared to the housekeeping gene GAPDH was performed. Figure 25 shows that *Sdc-1* expression was reduced by about 70 % compared to scrambled siRNA 24 h after transfection with 10 nM siRNA 12432, by about 80 % with 10 nM siRNA 142557 and by more than 80 % with a combination of *Sdc-1* siRNAs 12432 and 142557. The same percentage of silencing was maintained 48 h after transfection. When the siRNAs concentration was increased to 50 nM, a slightly higher knockdown of about 90 % was obtained 24 h after transfection with siRNA 12432, siRNA 142557 and a combination of both siRNAs. 48 h after transfection with *Sdc-1* targeting siRNAs, *Sdc-1* expression drops down by > 90 %. Transfection with either 100 nM siRNA 12432 or siRNA 142557 or a combination of the two, led to a decrease of *Sdc-1* expression of more than 90 % compared to transfection with a scrambled siRNA, which was maintained between 24 and 48 h.

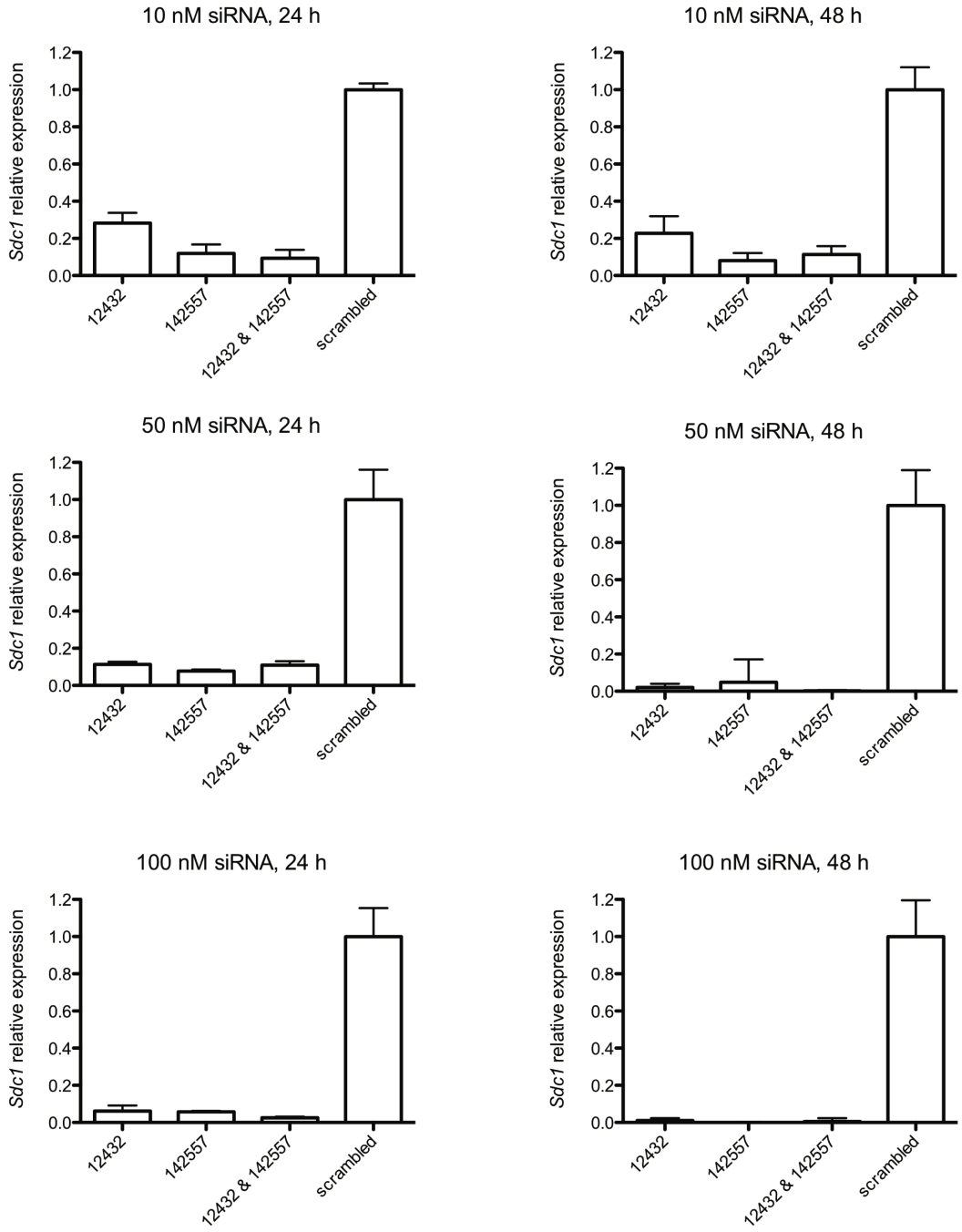

Figure 25, Sdc-1 knockdown in HTB94 cells

For transfection, either 10 or 50 or 100 nM of either siRNA 12432, 142557 or a combination of both, was added to 1-1.5 x 10^5 HTB94 cells in 6-well plate using Lipofectamine 2000. Control cells were transfected with scrambled siRNA. At 4 h after transfection, each well was supplemented with 3 ml of complete growth medium; at 24 h and 48 h after transfection, the cells were harvested, total RNA extracted and expression of *Sdc-1* evaluated in comparison with GAPDH housekeeping gene. Percentage of *Sdc-1* expression after transfection with 10 or 50 or 100 nM siRNAs at 24 h and 48 h is shown. Two siRNAs specific for human *Sdc-1* were designed by Ambion; each and a combination of them silence *Sdc-1* expression by 80 % - 90 %.

4.3.2.2 Internalization of [^{35}S]TIMP-3 by Sdc-1 silenced HTB94 cells

A combination of 12432 and 142557 siRNAs (50 nM) was used to silence *Sdc-1*, as these conditions resulted in a knockdown of *Sdc-1* expression of more than 90 %. A time course of [^{35}S]TIMP-3 endocytosis was started 24 h after *Sdc-1* targeting siRNAs transfection. As shown in Figure 26A, HTB94 cells transfected with *Sdc-1* targeting siRNAs internalized [^{35}S]TIMP-3 in a similar manner to HTB94 transfected with scrambled siRNAs. In both cases, radioactivity in the TCA-insoluble fraction decreased similarly, and radioactivity in the TCA-soluble fraction and associated with cells increased at the same rate. Non-transfected HTB94 cells thus showed the same kinetics of internalization as HTB94 cells transfected with *Sdc-1* targeting siRNAs (Figure 26B). These data indicate that syndecan-1 is not involved in the internalization of TIMP-3.

A

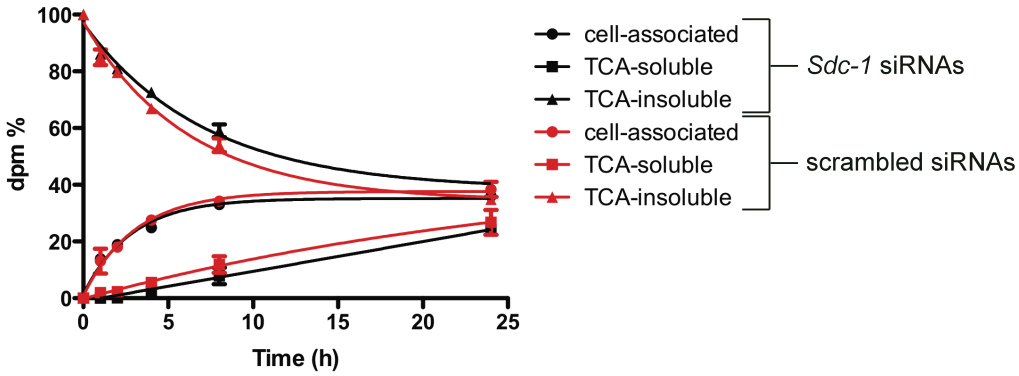

B

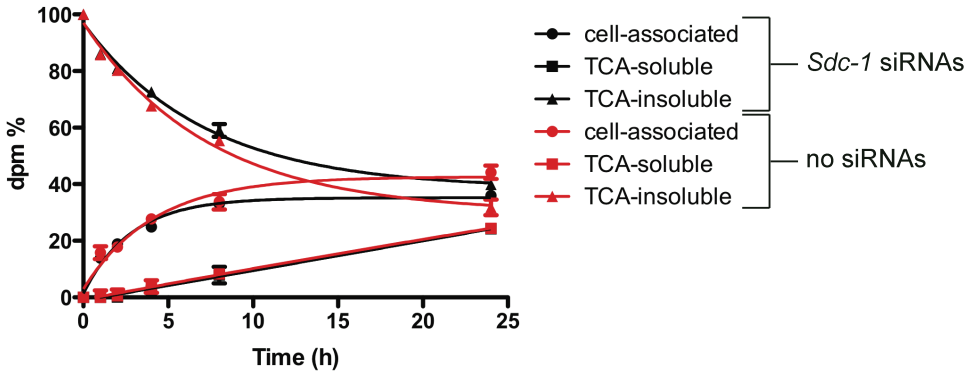

Figure 26, The effect of *Sdc-1* silencing on TIMP-3 internalization by HTB94 cells
HTB94 cells were transfected with a combination of two *Sdc-1* targeting 50 nM siRNAs from Ambion: 12432 and 142557. 24 h after transfection cells were incubated at 37 °C in DMEM containing 0.1 % FCS and 1 nM [^{35}S]TIMP-3 and [^{35}S]TIMP-3 endocytosis monitored. At the indicated time points, media were collected and TCA precipitated, and cells harvested. Radioactivity in TCA-insoluble, -soluble and cell-associated fractions was measured. **A**. Kinetics of [^{35}S]TIMP-3 internalization by HTB94 cells transfected with *Sdc-1* targeting siRNAs (black symbols and lines) and with scrambled siRNAs (red symbols and lines). **B**. Kinetics of [^{35}S]TIMP-3 internalization by non-transfected control HTB94 cells (red symbols and lines) and transfected with *Sdc-1* targeting siRNAs (black symbols and lines).

4.3.3 Internalization of [^{35}S]TIMP-3 by CHO-745 and wild-type CHO-K1

Four distinct syndecan proteins are known in mammals. There is some evidence that when a certain syndecan protein is lacking, its activity may be compensated for by other syndecans, other transmembrane proteoglycans, or even members of the glypican family (Couchman, 2010). Both syndecan-4-null cells and *Sdc-1*-silenced HTB94 cells internalized TIMP-3 as well as their wild-type counterparts. To exclude

that compensation among HSPGs could occur for TIMP-3 endocytosis, non-HSPG-expressing CHO-745 and wild-type CHO-K1 cells were chosen as a model system to test TIMP-3 internalization.

CHO-745 cells are deficient in xylosyl transferase, the enzyme which initiates heparan sulfate biosynthesis by catalyzing the attachment of xylose to a serine residue of a core protein (Esko et al., 1985). As a result, CHO-745 cells are deficient in both CS- and HS- proteoglycans. CHO-K1 and CHO-745 cells were incubated with 1 nM [^{35}S]TIMP-3 at 37 °C for 24 h. Radioactivity in the TCA-insoluble fractions of both CHO-KI and CHO-745 decreased over 24 h, and cell-associated and TCA-soluble radioactivity increased, suggesting that both cell-types internalize, degrade and release fragments of [^{35}S]TIMP-3 (Figure 27A and B). The kinetics of internalization by CHO-KI and CHO-745 were very similar (Figure 27C), indicating that cell-surface CS- and HS- proteoglycans are not required for TIMP-3 endocytosis. Nevertheless, the decrease in TCA-insoluble radioactivity was slightly reduced in CHO-745 compared to CHO-K1 cells, and the cell-associated radioactivity was slightly higher. These data indicate that TIMP-3 might bind to HSPGs on the cell surface, but its endocytosis is not significantly different in absence or presence of HSPGs.

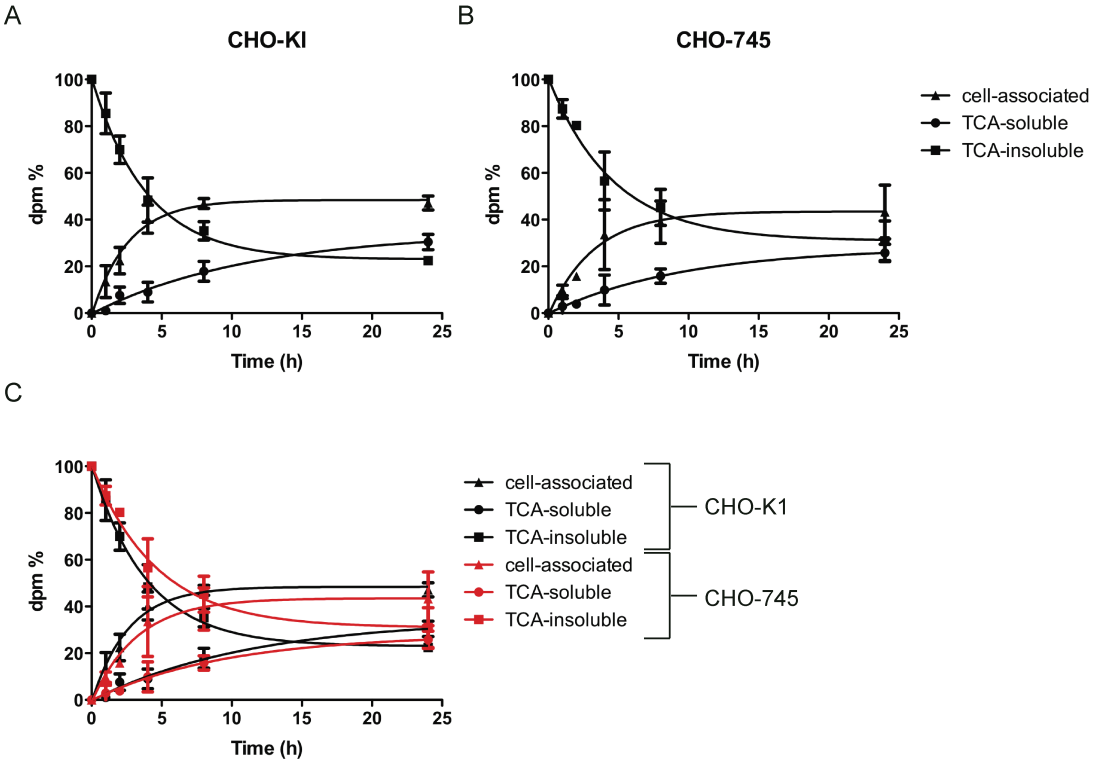

Figure 27, Internalization of TIMP-3 by CHO-KI and CHO-745 cells
CHO-KI and CHO-745 cells were incubated at 37 °C in DMEM containing 0.1 % FCS and 1 nM [^{35}S]TIMP-3. At the time points indicated, the conditioned medium was removed and cell-associated, TCA-soluble and TCA-insoluble fractions were harvested as described before. **A**. Time course of [^{35}S]TIMP-3 endocytosis by CHO-KI. **B**. Time course of [^{35}S]TIMP-3 endocytosis by CHO-745. **C**. Superimposed kinetics of [^{35}S]TIMP-3 internalization by CHO-KI (black symbols and lines) and CHO-745 (red symbols and lines) cells (*n=3*).

4.3.3.1 Effects of heparin and RAP on [^{35}S]TIMP-3 endocytosis by CHO-KI and CHO-745 cells

CHO-KI and CHO-745 cells were preincubated with heparin (200 µg/ml) for 1 h before addition of [^{35}S]TIMP-3. In both cell types, heparin inhibited the decrease in TCA-insoluble radioactivity as well as the increase in TCA-soluble radioactivity over 24 h (Figure 28A and B). Heparin inhibited endocytosis by both CHO-KI and CHO-745, showing that heparin inhibition of TIMP-3 endocytosis is not related to the presence of GAGs on the cell surface.

CHO-KI and CHO-745 cells were incubated with RAP (500 nM) for 30 min before addition of [^{35}S]TIMP-3 (1 nM). Figure 28C and Figure 28D show that RAP reduced the uptake of the TCA-insoluble [^{35}S]TIMP-3 by both cell types, indicating

that TIMP-3 is internalized in a LRP-dependent manner also by these cells. Kinetics of [^{35}S]TIMP-3 internalization by RAP treated CHO-KI and CHO-745 cells was very similar suggesting that the LRP-1-dependent pathway is the main mechanism of TIMP-3 internalization and that the LRP-1-independent mechanism is not mediated by cell-surface HSPGs.

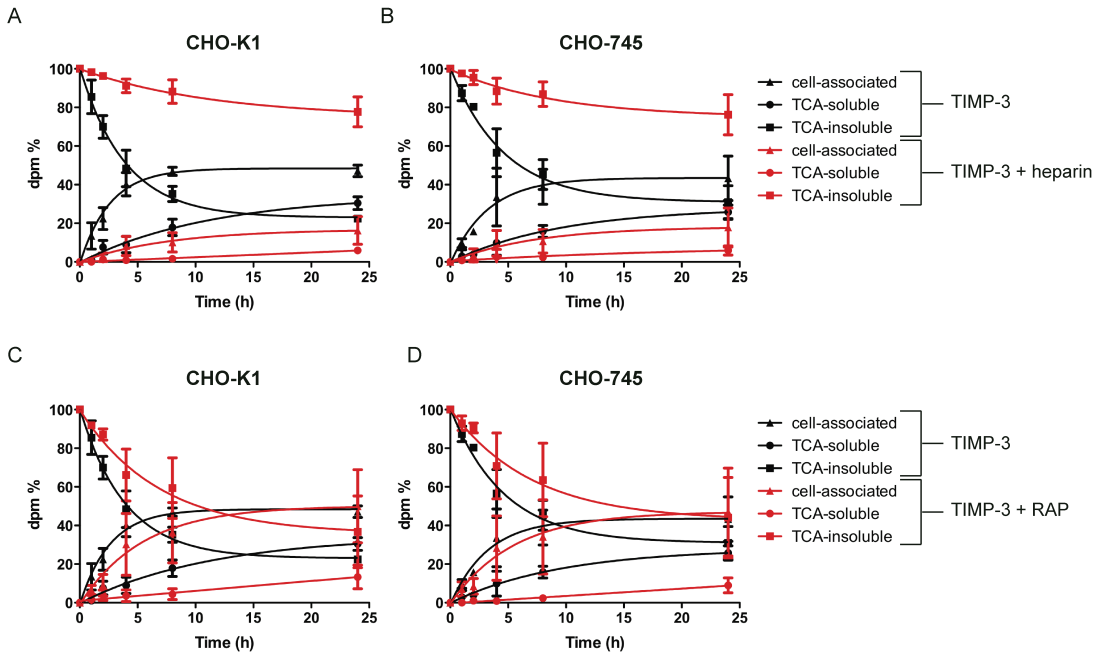

Figure 28, [^{35}S]TIMP-3 endocytosis by CHO-KI and -745 cells in presence of heparin or RAP

[^{35}S]TIMP-3 (1 nM) was added to CHO-KI or CHO-745 cells, and TCA-soluble (●), TCA-insoluble (■) and cell-associated (▲) radioactivity analysed at various times. **A**. Internalization of [^{35}S]TIMP-3 by CHO-KI cells in the presence (red symbols and lines) and absence (black symbols and lines) of 200 µg/ml of heparin. **B**. Internalization of [^{35}S]TIMP-3 by CHO-745 cells in the presence (red symbols and lines) and absence (black symbols and lines) of 200 µg/ml of heparin. **C**. Internalization of [^{35}S]TIMP-3 by CHO-KI cells in the presence (red symbols and lines) and absence (black symbols and lines) of 500 nM RAP. **D**. Internalization of [^{35}S]TIMP-3 by CHO-745 cells in the (red symbols and lines) and absence (black symbols and lines) of 500 nM RAP.

4.3.3.2 The effect of sodium chlorate on [^{35}S]TIMP-3 endocytosis

To understand the role of highly sulfated GAGs in TIMP-3 endocytosis, HTB94 cells were pre-treated with 30 mM sodium chlorate, which prevents GAG sulfation (Baeuerle and Huttner, 1986), for 24 h prior incubation with 1 nM [^{35}S]TIMP-3. Figure 29 shows that radioactivity in the TCA-insoluble fraction of sodium chlorate treated samples decreased indistinguishable from that of non-treated samples; radioactivity

associated with cells and TCA-soluble fraction of treated samples increased in a similar manner as that of non-treated control samples, suggesting that sulfation of GAGs is not essential for [^{35}S]TIMP-3 endocytosis.

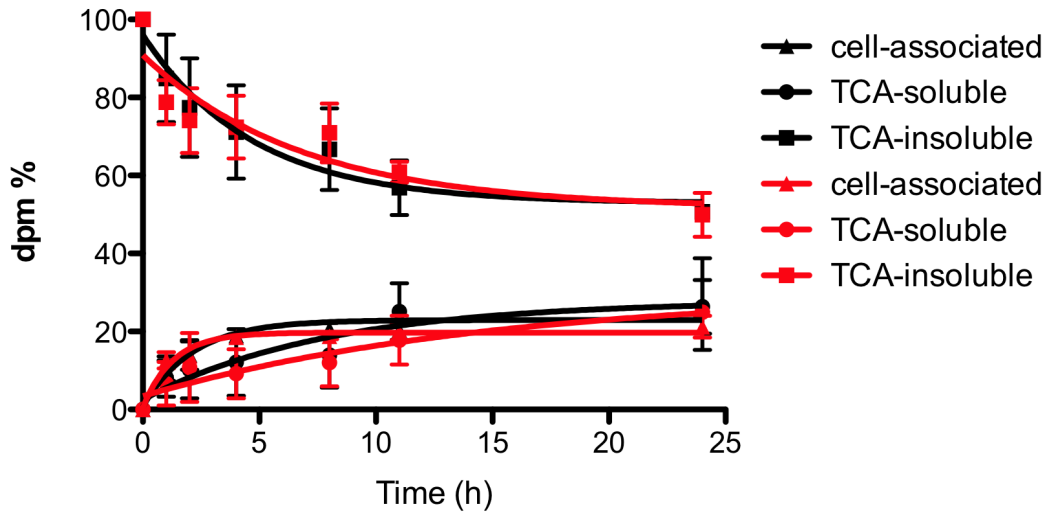

Figure 29, The effect of sodium chlorate on [^{35}S]TIMP-3 endocytosis.
HTB94 were pre-treated with 30 mM sodium chlorate for 24 h at 37 °C prior adding [^{35}S]TIMP-3 (1 nM). The conditioned medium was collected at indicated time points and harvested as described before. TCA-insoluble [^{35}S]TIMP-3 clearance is not affected by sodium chlorate (■) compared to untreated control (■). Appearance of [^{35}S]TIMP-3 TCA-soluble and cell-associated fractions (● and ▲, respectively) increase in a similar manner to controls (● and ▲) (*n=2*).

4.4 Discussion

As discussed in the Chapter 3, RAP treated HTB94 cells internalized TIMP-3 with a slower rate compared to non-treated controls, suggesting that members of the LDL receptor superfamily play a key role in TIMP-3 endocytosis, but that an LDL receptor-independent pathway also occurs. I investigated which member of the LDLR family was involved in TIMP-3 internalization. Many proteinases, proteinase inhibitors or molecules that play a role in the ECM turnover, are internalized by cells *via* LRP-1. I postulated that it could also be the case for TIMP-3, and therefore I tested TIMP-3 endocytosis by LRP-1-null mouse embryonic fibroblasts (PEA-13). TIMP-3 binding to the cell surface of MEF-1 and PEA-13 was comparable, but internalization and degradation of TIMP-3 by PEA-13 cells was approximately half as much as that in

MEF-1 cells. These data confirmed our hypothesis that TIMP-3 could be endocytosed *via* LRP-1, and that another as yet uncharacterized internalization pathway is also involved. RAP-treated PEA-13 cells internalized TIMP-3 with the same kinetics as non-treated controls, indicating that LRP-1 is the only member of LDLR family involved in this process.

Heparin completely blocked TIMP-3 endocytosis either in presence or in absence of LRP-1. I postulated that an HSPG might be the primary binding site for TIMP-3 and that it may function as a co-receptor for the LRP-1-mediated endocytosis, as it occurs for other LRP-1 ligands (Chappell et al., 1993; Mikhailenko et al., 1995). In the absence of LRP-1, HSPG might directly mediate internalization as has been shown for the Aβ peptide (Kanekiyo et al., 2011). Members of the syndecan family were thought to be possible candidates for their high degree of sulfation and for their involvement in the endocytosis of LRP ligands either as co-receptors or proper receptors (Stanford et al., 2009; Wilsie et al., 2006). It was shown that syndecan-4-null mice are protected from osteoarthritis in experimental models (Echtermeyer et al., 2009). We hypothesized that if syndecan-4 was involved in TIMP-3 internalization, then TIMP-3 levels would be increased in syndecan-4-null mice, which may explain their resistance to osteoarthritis. Surprisingly, syndecan-4-null cells internalized TIMP-3 as well as wild-type cells. Similar results were obtained testing TIMP-3 internalization by syndecan-1-silenced cells. Redundancy among members of the syndecan family can occur and syndecans can compensate for each other (Couchman, 2010). To exclude this possibility in our studies, we tested the internalization of TIMP-3 in CHO-745 cells, which are defective in the biosynthesis of glycosaminoglycans as they lack xylosyl-transferase (Esko et al., 1985). TIMP-3 was effectively internalized by CHO-745 cells, with similar kinetics to wild-type CHO-K1 cells, implying that HSPGs are not involved in TIMP-3 endocytosis. Sodium chlorate is known to be an *in vitro* inhibitor of ATP–sulfurylase, the first enzyme in the biosynthesis of 3'-phosphoadenosine 5'-phosphosulfate, the high-energy sulphate donor in biological reactions inhibits the sulfation (Baeuerle and Huttner, 1986). Treatment of various cell cultures with sodium chlorate resulted in inhibition of proteoglycan sulfation (Baeuerle and Huttner, 1986). Sodium chlorate-treated

HTB94 cells internalized TIMP-3 as well as non-treated controls, further indicating that HSPGs are not involved in internalization of TIMP. RAP effectively reduced internalization in both CHO-745 and CHO-K1 cells, suggesting that the LRP-1-mediated pathway of TIMP-3 endocytosis is also active in these cells. Heparin also completely blocked TIMP-3 endocytosis by CHO-745 cells, indicating that heparin did not protect TIMP-3 from endocytosis by preventing its binding to HSPGs. Highly sulfated GAGs may block TIMP-3 binding to LRP-1 either directly binding to TIMP-3 or binding to a receptor. Some other molecules on the cell surface which have been shown binding TIMP-3 may be possible candidates for its LRP-independent internalization. TIMP-3 may bind to membrane-associated metalloproteinases (MT-MMPs or ADAMs), but, as it will be shown in Chapter 6, the presence of the metalloproteinases inhibitor GM6001 did not block TIMP-3 binding to the cell surface, therefore this possibility is unlikely. TIMP-3 has been shown to interact with VEGFR-2 (Qi et al., 2003). VEGFR-2 is internalized by a clathrin-dependent mechanism upon binding of its ligand VEGF (Lampugnani et al., 2006), thus this receptor may be the TIMP-3 binding partner that mediates its LRP-1-independent internalization.

Chapter 5

Investigation of plateau in TIMP-3 internalization

5.1 Introduction

I observed that the rate of TIMP-3 endocytosis by different cell types was initially fast, but that it then gradually decreased over time and became minimal around 10 h after addition of the inhibitor to the cells. In this chapter, I investigated possible causes of this "plateau" in TIMP-3 internalization.

Firstly, I examined whether the decreased rate of TIMP-3 endocytosis was due to TIMP-3-induced apoptosis of the cells. It is well established that TIMP-3 induces apoptosis in a variety of cell types, primarily through its ability to inhibit metalloproteinase-mediated shedding of death receptors, such as tumor necrosis factor receptor-1 (TNFRI), FAS receptor, and TNF-related apoptosis inducing ligand receptor-1 (TRAIL-R1) (Ahonen et al., 2003; Bond et al., 2002). Inhibition of death receptors shedding by TIMP-3 results in an increased stabilization of these receptors on the cell surface, and a higher cell responsiveness to apoptosis induced by TNF-α, anti-Fas-antibodies or TRAIL. Secondly, I investigated whether the decrease in TIMP-3 endocytosis was caused by shedding of LRP-1 from the surface of endocytosing cells. Several studies indicate that LRP-1 can undergo proteolytic shedding. For example, a truncated, soluble form of LRP-1 is found in human plasma (Quinn et al., 1997) and in the conditioned medium of HT1080 cultured cells (Selvais et al., 2011). Different metalloproteinases, such as ADAM-10, ADAM-12, BACE and TACE, have been shown to cleave the ectodomain of LRP-1 *in vitro* (Liu et al., 2009; Selvais et al., 2009; von Arnim et al., 2005). The released LRP-1 ectodomain, or so called soluble LRP-1 (sLRP-1), maintains its ligand-binding ability (Quinn et al., 1997). sLRP-1 can also be further proteolytically fragmentated by MT1-MMP (Rozanov et al., 2004). Both shedding and further degradation modulate the amount of functional LRP-1 on the cell-membrane, and consequently modulate the scavenging of LRP-1 ligands, such as MMP-2 and MMP-9 (Selvais et al., 2009).

5.2 Results

5.2.1 [^{35}S]TIMP-3 does not impair cell viability

Ahonen *et al.* (2003) showed that TIMP-3 induced apoptosis in melanoma cell lines at concentrations above 25-50 nM (Ahonen et al., 2003), whereas, previous work in

our laboratory found that N-TIMP-3 did not induce apoptosis in porcine chondrocytes even at the concentration of 1 µM (Gendron et al., 2003). We investigated whether [^{35}S]TIMP-3 could impair viability of HTB94 cells, since such event may lead to a decrease in [^{35}S]TIMP-3 internalization. For this purpose we used the MTT (3-(4,5-Dimethylthiazol-2-yl)-2,5-diphenyltetrazolium bromide) assay. The MTT is a yellow tetrazole that is reduced to purple formazan in living cells. The absorbance of this purple product can be then quantified by measuring at a certain wavelength using a spectrophotometer.

HTB94 cells were incubated with or without 1 nM [^{35}S]TIMP-3 in DMEM containing 0.1 % FCS. Cells fixed in 3 % PFA in PBS (10 min, RT) were used as a negative control. At the indicated time points, the medium was replaced with phenol red-free DMEM containing 0.5 mg/ml MTT reagent (10 min, 37 °C). Then, the reaction was stopped by addition of 10 % SDS in 10 mM HCl (over night, 37 °C) and absorbance at 574 nm measured. Figure 30 shows that [^{35}S]TIMP-3 (1 nM) had no detectable effect on cell viability over 24 h.

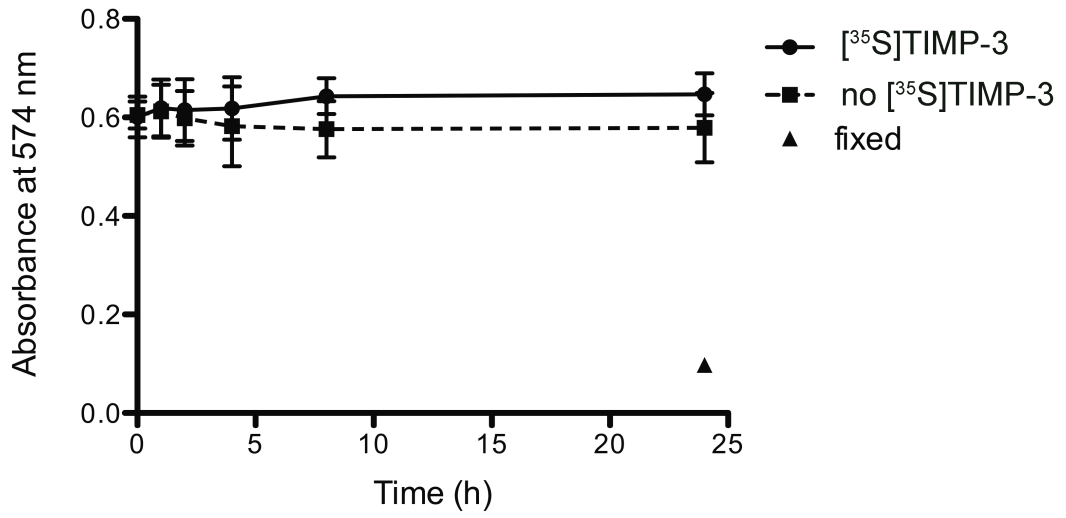

Figure 30, MTT assay of [^{35}S]TIMP-3 treated HTB94 cells

HTB94 cells were incubated with (●) or without (■) [^{35}S]TIMP-3 (1 nM) in DMEM containing 0.1 % FCS (0-24 h). At the indicated period of time, the medium was replaced with MTT reagent in phenol red-free DMEM (10 min, 37 °C). The reaction was stopped by addition of 10 % SDS in 10 mM HCl and absorbance at 574 nm determined. HTB94 cells fixed in 3 % PFA in PBS (10 min, RT) were used as negative control (▲) (*n=3*).

5.2.2 Pre-treatment of HTB94 cells with TIMP-3 has no effect on subsequent [^{35}S]TIMP-3 endocytosis

To test whether the decrease in TIMP-3 endocytosis was due to a decrease in availability of endocytic receptors on the cell surface, HTB94 cells were incubated with or without non-radioactive TIMP-3 (1 nM) for 24 h, before the addition of [^{35}S]TIMP-3 (1nM). As shown in Figure 31, the decrease in TCA-insoluble radioactivity and the increase in TCA-soluble and cell-associated radioactivity of cells pre-treated with TIMP-3 was similar to that of non-treated cells, indicating that the pre-treatment of HTB94 cells with TIMP-3 had no effect on the subsequent rate of [^{35}S]TIMP-3 endocytosis.

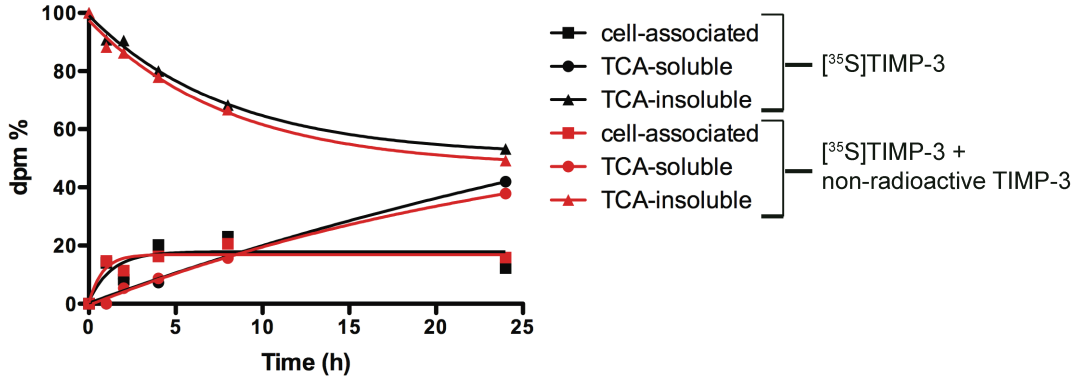

Figure 31, The effect of non-radioactive TIMP-3 pre-treatment on [^{35}S]TIMP-3 internalization by HTB94 cells.
HTB94 cells were pre-treated with TIMP-3 (1 nM) (red symbols and lines) or serum-free DMEM (black symbols and lines) for 24 h. Both conditioned media were then replaced with [^{35}S]TIMP-3 (1 nM) in DMEM 0.1 % FCS (24 h, 37 °C) and TCA-soluble (●,●), TCA-insoluble (■,■) and cell-associated (▲,▲) radioactivity was analysed at various periods of time. This experiment was performed twice with similar results.

5.2.3 TIMP-3 remnants are protected from internalization

I analyzed whether [^{35}S]TIMP-3 remaining in the medium after 24 h incubation with HTB94 cells (referred to as [^{35}S]TIMP-3 remnants) could be internalized by fresh cells. [^{35}S]TIMP-3 (1 nM) was incubated with HTB94 cells for 24 h. At the indicated time, a portion of conditioned media was harvested and the distribution of radioactivity between TCA-insoluble, TCA-soluble and cell-associated fraction were analyzed.

After 24 h, the rest of conditioned medium was harvested as the [^{35}S]TIMP-3 remnants, which were transferred to fresh HTB94 cells, and their endocytosis monitored over the subsequent 24 h. As shown in Figure 32A, [^{35}S]TIMP-3 was rapidly endocytosed by HTB94 cells initially, but the rate of endocytosis was greatly reduced after 10 h. When the [^{35}S]TIMP-3 remnants were transferred to fresh HTB94 cells, no further endocytosis was detectable (Figure 32B). The decrease in TCA-insoluble radioactivity and the increase in TCA-soluble radioactivity were minimal, with the distribution of radioactivity in these samples remaining constant. These data suggest that [^{35}S]TIMP-3 remnants had become resistant to endocytosis by HTB94 cells. [^{35}S]TIMP-3 binding to the cells was detectable but the amount of this binding was greatly reduced compared to the freshly added [^{35}S]TIMP-3, suggesting that the ability of [^{35}S]TIMP-3 remnants to bind to the cell surface was also impaired.

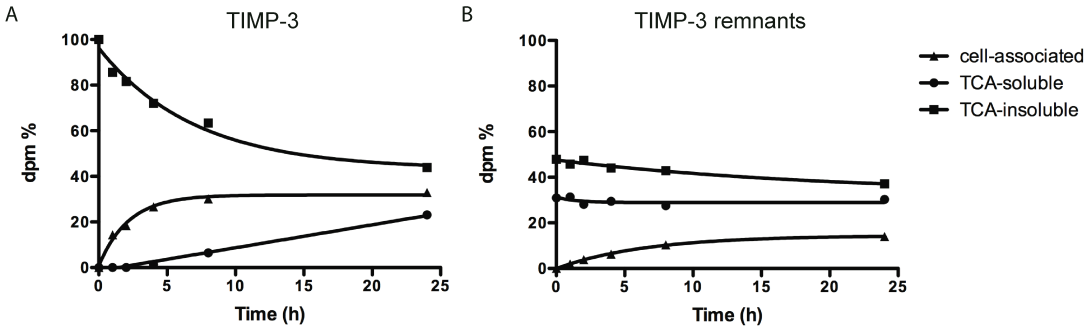

Figure 32, Endocytosis of [^{35}S]TIMP-3 remnants by fresh HTB94 cells
HTB94 cells were incubated with [^{35}S]TIMP-3 (1 nM) in DMEM containing 0.1 % FCS at 37 °C, and [^{35}S]TIMP-3 endocytosis monitored over 24 h. After 24 h, conditioned media containing [^{35}S]TIMP-3 remnants were collected and transferred to fresh HTB94 cells. At the indicated time points, the conditioned medium was collected and TCA-precipitated, and cells harvested. Radioactivity in the TCA-insoluble (■), TCA-soluble (●) and cell-associated (▲) fractions was measured. This result is representative of two separate experiments.

5.2.4 TIMP-3 remnants inhibit ADAMTS-4

HTB94 cells were incubated with 10 nM TIMP-3 in DMEM containing 0.1 % FCS. After 24 or 48 h incubation, TIMP-3 remnants were harvested and incubated with 1 nM ADAMTS-4 (1 h, 37 °C) to test their inhibitory activity. **Figure 33** shows that at 0 h, 10 nM TIMP-3 in DMEM containing 0.1 % FCS completely inhibited 1 nM ADAMTS-4,

compared to plain conditioned medium taken as a negative control. The activity of ADAMTS-4 was inhibited less by TIMP-3 containing medium harvested after 24 and 48 h, but these conditioned media still inhibited ADAMTS-4 activity effectively compared to control conditioned media which were not supplemented with TIMP-3. These data indicate that TIMP-3 remnants retained their ability to inhibit ADAMTS-4, indicating that their overall structure had been maintained. The lower inhibitory activity of TIMP-3 remnants at 48 h and 24 h compared to that at 0 h is in line with the internalization kinetics of TIMP-3 that is shown in Section 3.2.2.2

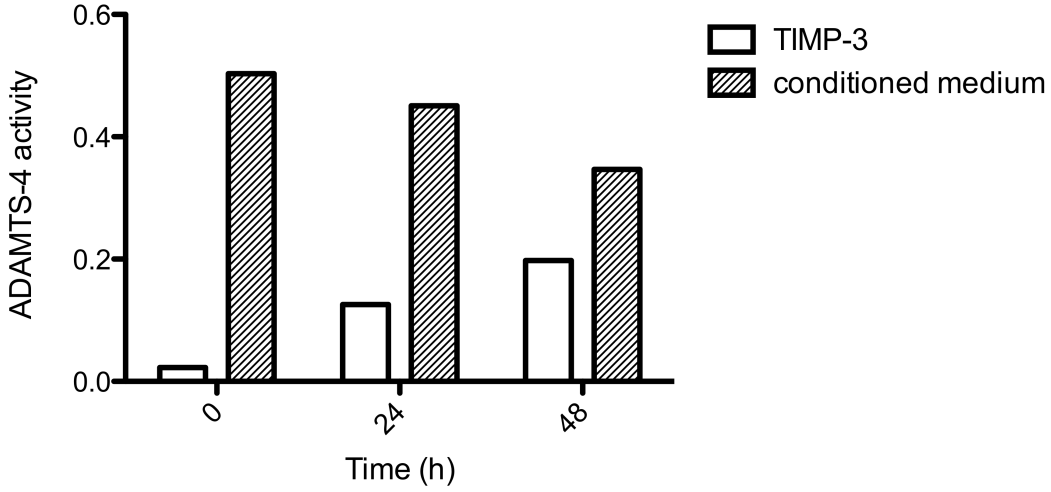

Figure 33, Inhibitory activity of TIMP-3-remnants
HTB94 cells were incubated with TIMP-3 (10 nM) in DMEM containing 0.1 % FCS. After 0, 24 and 48 h, the medium was collected and inhibition of ADAMTS-4 (1 nM) by residual [^{35}S]TIMP-3 analyzed. Conditioned medium (100 µl) was incubated (1h, 37 °C) with ADAMTS-4 (1nM) and its residual activity was measured against a fluorescent peptide as row fluorescence units (18h, 37 °C) (Troeberg et al., 2009). This result is representative of two separate experiments.

5.2.5 [^{35}S]TIMP-3 remnants are not truncated nor degraded

HTB94 cells in 6-well plate were incubated with [^{35}S]TIMP-3 (1 nM) in DMEM containing 0.1 % FCS. Cells were cultured up to 24 h and the conditioned medium was harvested at the time points indicated and TCA-precipitated. Equal volumes of all samples were analysed by reducing SDS-PAGE and subsequent autoradiography. Figure 34 shows the decreased intensity of [^{35}S]TIMP-3 band over time, indicating that [^{35}S]TIMP-3 was endocytosed by the cells. It is also notable that [^{35}S]TIMP-3

remained in the medium (remnants) exhibited essentially the same molecular weight from the original [^{35}S]TIMP-3. [^{35}S]TIMP-3 remnants ran as a single band on reducing SDS-PAGE, indicating that [^{35}S]TIMP-3 was not degraded during incubation on the cells.

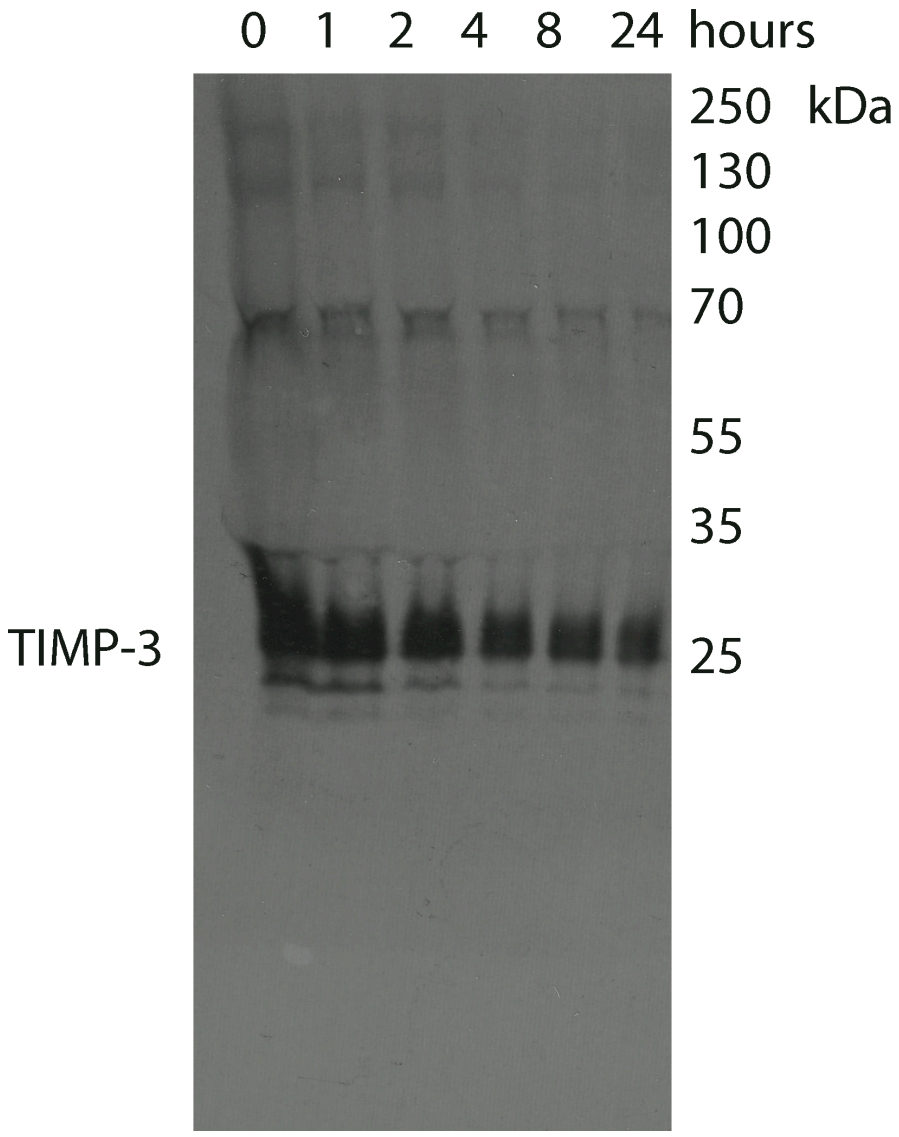

Figure 34, Autoradiographic analysis of [^{35}S]TIMP-3 after exposure to HTB94 cells
[^{35}S]TIMP-3 (1 nM) was added to HTB94 cells, and media harvested at the indicated time points and precipitated with TCA (5 %). TCA-insoluble fractions were re-suspended in 2 X reducing SDS-PAGE buffer and analysed by SDS-PAGE and autoradiography.

5.2.6 Incubation of [^{35}S]TIMP-3 with conditioned medium from HTB94 cells impairs its internalization

Since [^{35}S]TIMP-3 remained in the medium of HTB94 cells after a 24 h incubation did not show any apparent changes in its molecular weight, I hypothesized that [^{35}S]TIMP-3 may bind to a protein released by HTB94 cells and that such complexes are resistant to endocytosis. To test this hypothesis, HTB94 cells were incubated with DMEM containing 0.1 % FCS for 24 h at 37 °C. Then, the conditioned medium was collected, incubated with 1 nM [^{35}S]TIMP-3 (overnight, RT) and transferred to fresh confluent HTB94 cells in a 6-well plate. As a control, 1 nM [^{35}S]TIMP-3 incubated with DMEM containing 0.1 % FCS was added to HTB94 cells. At the indicated time points, the distribution of radioactivity in the TCA-insoluble, TCA-soluble and cell-associated fractions was analysed. As shown in Figure 35, pre-incubation of [^{35}S]TIMP-3 with HTB94 conditioned medium greatly reduced endocytosis of the protein. The decrease in TCA-insoluble was minimal, and the increase in the TCA-soluble and cell-associated fractions was also lower compared to that of [^{35}S]TIMP-3 incubated with DMEM. These data suggest that HTB94 cells release molecules that inhibit the endocytosis of [^{35}S]TIMP-3.

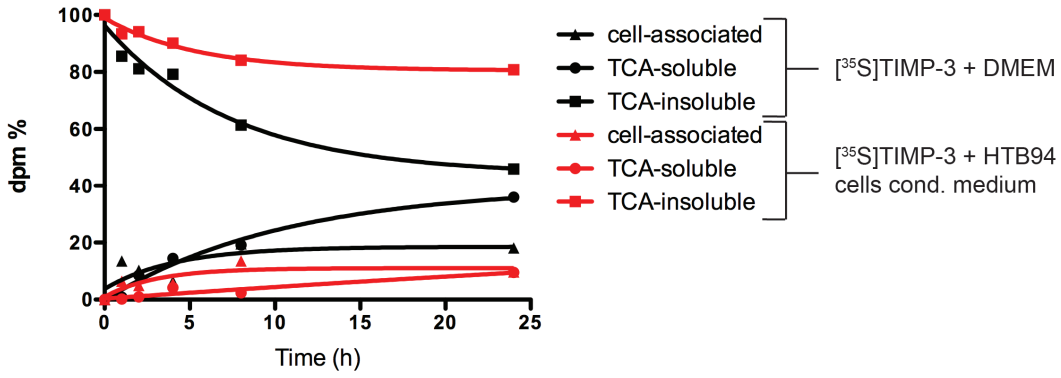

Figure 35, The effect of HTB94 cell-conditioned medium on [^{35}S]TIMP-3 internalization

[^{35}S]TIMP-3 (1 nM) was incubated with either DMEM containing 0.1 % FCS (black lines and symbols) or the conditioned medium from HTB94 cells (red lines and symbols) overnight at room temperature. After 24 h, these [^{35}S]TIMP-3-containing media were transferred to fresh HTB94 cells and the amount of TCA-soluble (●), TCA-insoluble (■) and cell-associated (▲) radioactivity quantified at various time points.

5.2.7 [^{35}S]TIMP-3 remnants from LRP-1-deficient cells are endocytosed by fresh LRP-1 wild-type cells

As LRP-1 has been shown to undergo proteolytic shedding (Quinn et al., 1997; Selvais et al., 2011), we investigated whether shed LRP-1 (sLRP-1) could bind to TIMP-3 and interfere with its endocytosis. [^{35}S]TIMP-3 (1 nM) was incubated with either MEF-1 or PEA-13 cells in DMEM containing 0.1 % FCS. After 24 h, conditioned media containing [^{35}S]TIMP-3 remnants were collected from both cell types and transferred to fresh MEF-1 cells.

As shown in Figure 36A, remnants from MEF-1 cells were not endocytosed by fresh MEF-1 cells, similar to the results we obtained in HTB94 cells (see Figure 32). Radioactivity in the TCA-soluble fraction remained constant over 24 h, indicating that no detectable endocytosis and degradation of [^{35}S]TIMP-3 occurred. Radioactivity in the TCA-insoluble fraction decreased slightly, and radioactivity in the cell-associated fraction increased slightly, indicating that some of [^{35}S]TIMP-3 remnants bound to the cell surface and ECM.

However, [^{35}S]TIMP-3 remnants from PEA-13 cells were effectively internalized by fresh MEF-1 cells (Figure 36B). Radioactivity in the TCA-insoluble fraction decreased and radioactivity in TCA-soluble and cell-associated fractions increased over 24 h.

Since incubation of [^{35}S]TIMP-3 on wild-type cells, but not on LRP-1-deficient cells, rendered [^{35}S]TIMP-3 resistant to endocytosis, we reasoned that shed LRP-1 may bind to TIMP-3 and inhibit its endocytosis.

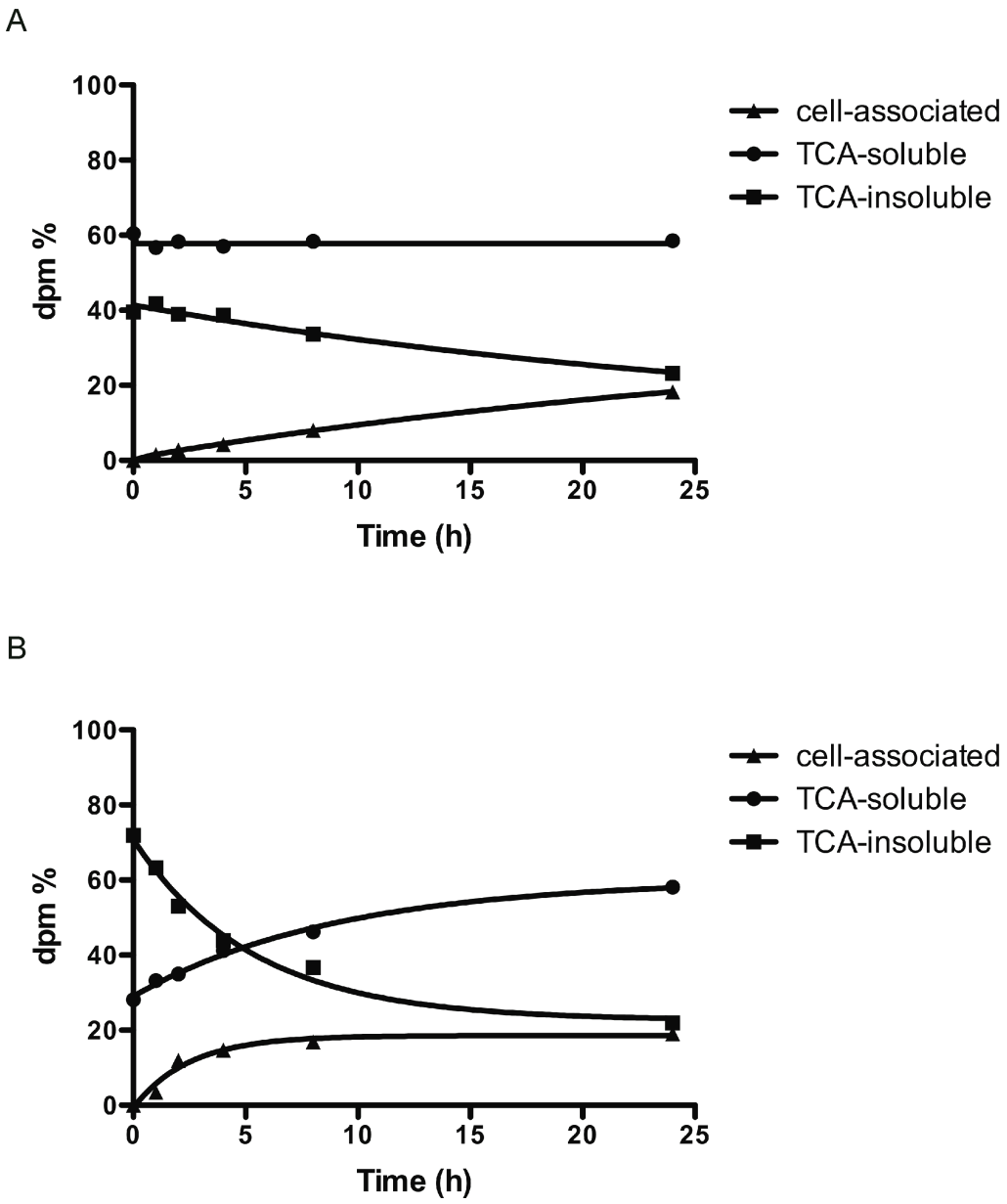

Figure 36, [^{35}S]TIMP-3 remnants from PEA-13 but not those from MEF-1 cells are endocytosed by fresh MEF-1 cells

[^{35}S]TIMP-3 (1 nM in DMEM with 0.1 % FCS) was incubated with either wild-type (**A**) or LRP-1-deficient PEA-13 MEFs (**B**). After 24 h, conditioned media containing residual [^{35}S]TIMP-3 was transferred to fresh wild-type cells and the amount of TCA-soluble (●), TCA-insoluble (■) and cell-associated (▲) radioactivity quantified at various time points. This experiment was repeated twice with similar results.

5.2.8 sLRP-1 accumulates in the medium of HTB94 cells

To test whether sLRP-1 was released from the HTB94 cell surface and accumulated in the conditioned medium, confluent HTB94 cells were incubated with DMEM containing 0.1 % FCS, in the absence or presence of 1 nM TIMP-3 (37 °C). Cells were cultured for up to 26 h and conditioned media were harvested at the time points indicated and TCA-precipitated. Pellets were re-suspended in 2X non-reducing SDS-PAGE buffer and analysed by Western blot using an anti-LRP-1 antibody. Figure 37 shows that bands corresponding to LRP-1 accumulated in the medium over time, either in the absence or presence of 1 nM TIMP-3. This indicates that LRP-1 was shed from HTB94 cells and its soluble ectodomain accumulated in the conditioned medium. Shedding was not affected by addition of 1 nM TIMP-3.

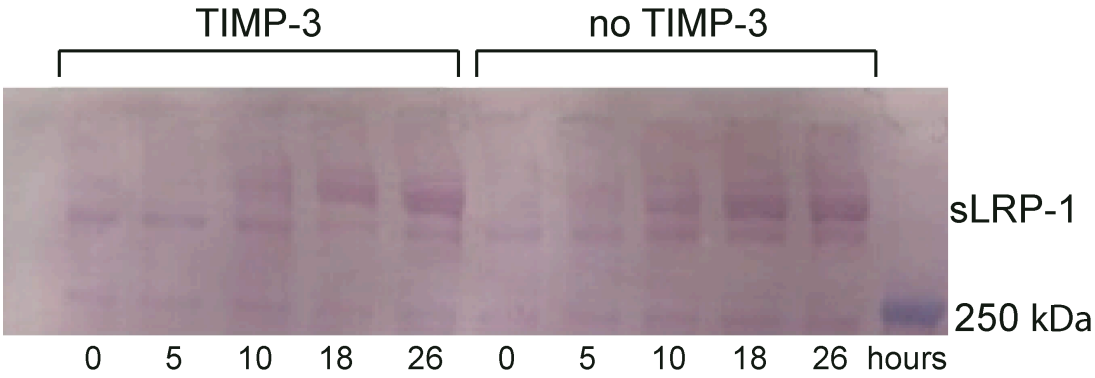

Figure 37, Accumulation of sLRP-1 in the medium of HTB94 cells
HTB94 cells were incubated with DMEM 0.1 % FCS (26 h, 37 °C) either in the absence or presence of 1 nM TIMP-3. Conditioned media were harvested at the indicated time points, precipitated with TCA (5 %) and analysed by Western blot using an anti-LRP-1 antibody. This result is representative of two separate experiments.

5.2.9 Co-immunoprecipitation of sLRP-1 with TIMP-3

We investigated whether complexes of TIMP-3 and sLRP-1 could be isolated from the conditioned medium of HTB94 cells. Conditioned medium from HTB94 was incubated with TIMP-3-FLAG (1 nM, 18 h, RT) and applied to an M2 anti-FLAG M2-agarose resin. Conditioned medium not incubated with TIMP-3 FLAG was used as a control. The column was washed with 10 volumes of TNC buffer, and then sequentially eluted with TNC buffer containing 1 M NaCl (2 X 0.5 ml) and then 200 µg/ml FLAG peptide (2 X 0.5 ml). Eluted samples were precipitated with TCA (5 %) and pellets re-suspended in SDS-PAGE buffer and analysed by Western blotting using an anti-FLAG M2 and an anti-LRP-1 antibodies. As shown in Figure 38, immunoblotting of the eluted material indicated that sLRP-1 eluted with TIMP-3, indicating that they are present as a complex in the HTB94 medium.

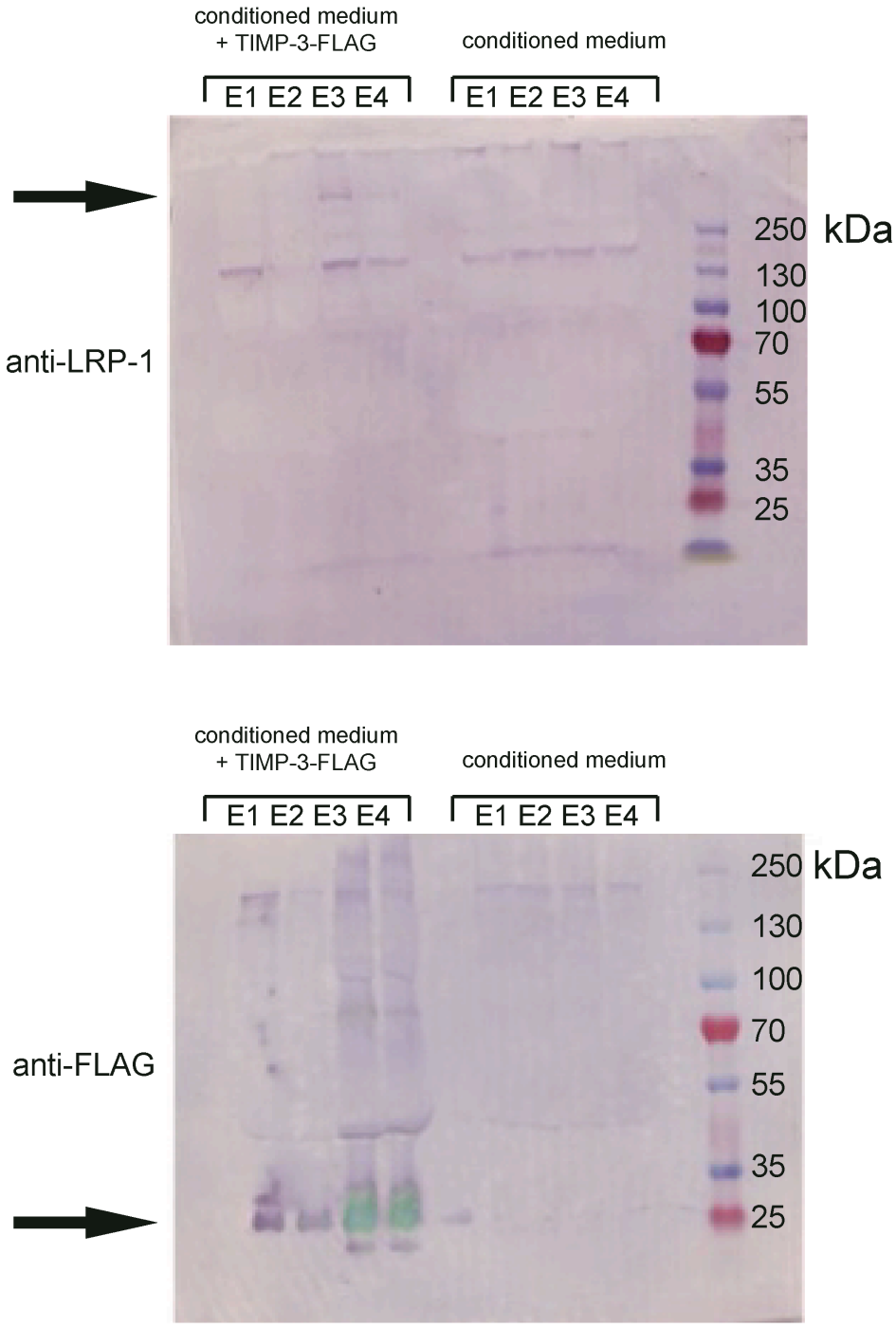

Figure 38, Co-Immunoprecipitation of sLRP-1 with TIMP-3-FLAG
Conditioned medium from HTB94 cells was incubated with FLAG-tagged TIMP-3 (1 nM, 18 h, RT) and then applied to an M2 anti-FLAG affinity resin (1 ml) equilibrated in TNC. The resin was extensively washed with TNC and then sequentially eluted with TNC containing 1 M NaCl (2 x 0.5 ml, E1 and E2) and 200 μg/ml FLAG peptide (2 x 0.5 ml, E3 and E4). Samples were analyzed by immunoblotting using anti-LRP-1 and anti-FLAG antibodies.

In a second experiment, TIMP-3 incubated with HTB94 conditioned medium was similarly applied to an M2 anti-FLAG affinity resin, and bound materials were then eluted with TNC buffer containing 200 µg/ml FLAG peptide (4 X 0.5 ml). Elution samples were precipitated with TCA (5 %) and then subjected to SDS-PAGE analysis by silver staining. As shown in Figure 39, a band with the molecular weight of sLRP-1 was detected in E1, the first fraction eluted with the FLAG peptide. This band was excised and analysed by mass spectrometry by Dr Jan Enghild at the University of Aarhus, Denmark. This analysis confirmed that the detected band was LRP-1.

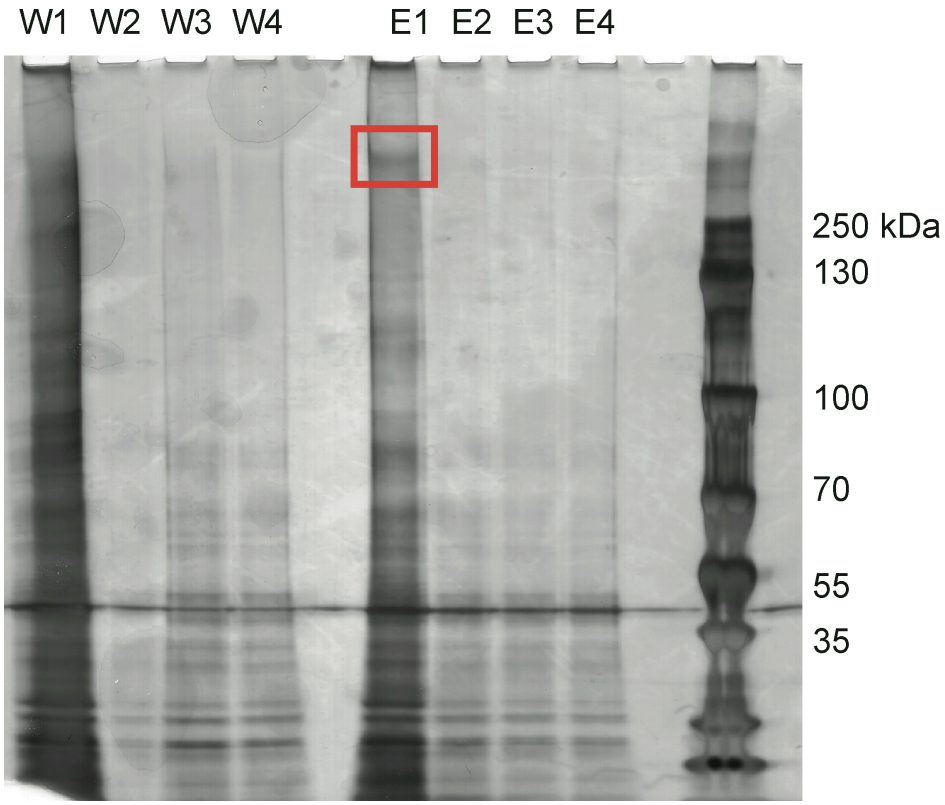

Figure 39, Silver stain of co-immunoprecipitation of sLRP-1 with TIMP-3-FLAG
Conditioned medium from HTB94 cells was incubated with FLAG-tagged TIMP-3 (1 nM, 18 h, RT) and then applied to M2 anti-FLAG affinity resin (1 ml) equilibrated in TNC. The resin was washed with TBS and then with TNC containing 1 M NaCl (10 x 2 ml). Samples were taken throughout the washing (W1, W2, W3 and W4). Finally, the column was eluted with TNC containing FLAG peptide (4 x 0.5 ml, E1, E2, E3 and E4). Samples were analysed silver staining. The detected band with the correct molecular weight was analysed by mass-spectrometry which confirmed that it was LRP-1.

5.3 Discussion

When exogenous TIMP-3 was added to a variety of cell types, it was rapidly endocytosed in the first 5 hours after addition, but after that the rate of its endocytosis gradually decreased and only a minimal amount of TIMP-3 was endocytosed by 10 h after addition. In this chapter, I investigated a possible mechanism for this decreased TIMP-3 endocytosis.

TIMP-3 induces apoptosis in melanoma cells at 25-50 nM (Ahonen et al., 2003), nevertheless, TIMP-3 does not cause it in porcine chondrocyte at concentrations up to 1 µM (Gendron et al., 2003). While the concentration of TIMP-3 used in the endocytosis assays (1nM) was much lower than that shown to induce apoptosis in melanoma cells, I examined the possibility that decreased endocytosis was due to cell death. Treatment of HTB94 cells with 1 nM TIMP-3 had no effect on viability over 24 h, indicating that the plateauing out the endocytic was not due to apoptosis induced by TIMP-3.

Reduced endocytosis due to a decrease in active receptors on the cell surface was also considered. LRP-1 is a scavenging receptor that binds over 30 different ligands and delivers them to lysosomes for degradation (Lillis et al., 2005). LRP-1 is constitutively endocytosed from the membrane and recycled back to the cell surface (van Kerkhof et al., 2005). To test the possibility that the decrease in TIMP-3 endocytosis was due to a decrease in the amount of cell surface LRP-1, HTB94 cells were pre-treated with non-radioactive TIMP-3 for 24 h. Then, [^{35}S]TIMP-3 was added and its endocytosis monitored. Such pre-treatment of cells had no effect on endocytosis of [^{35}S]TIMP-3, indicating that the decrease in internalization rate over time is not due to slowing down recycling of LRP-1 receptors on the cell surface. However, I found that TIMP-3 remaining in the conditioned medium (TIMP-3 remnants) was not internalized by fresh HTB94 cells. I considered that TIMP-3 might have undergone chemical modifications during its incubation with cells which rendered it resistant to internalization. However, TIMP-3 remnants were still active against ADAMTS-4 after 48 h of incubation with HTB94 cells, and they appeared indistinguishable from purified recombinant TIMP-3 on autoradiography after

reducing SDS-PAGE. These data suggested that TIMP-3 remnants resistance to endocytosis was not due structural modification of TIMP-3.

It has been reported that LRP-1 is shed by MT1-MMP and ADAMs (Quinn et al., 1997; Rozanov et al., 2004). Intact soluble LRP-1 (namely sLRP-1) has been shown to accumulate in human plasma (Quinn et al., 1997) and has been identified at the blood-brain barrier in ischemia (Polavarapu et al., 2007). I investigated whether sLRP-1 accumulated in the medium after shedding and whether sLRP-1 could interact with TIMP-3 and prevent its internalization. We verified that HTB94 cells constitutively shed LRP-1, and that sLRP-1 accumulates in the medium over time in a TIMP-3-independent manner. Incubation of TIMP-3 with the conditioned medium from HTB94 cells impaired endocytosis of the inhibitor. To further investigate whether LRP-1 played a role in this reduction in endocytosis, TIMP-3 was incubated with LRP-1-null mouse fibroblasts and with the wild-type fibroblasts for 24 h and remnants from both cell types transferred to fresh LRP-1-positive wild-type cells. Only TIMP-3 remnants collected from LRP-1-null cells were internalized, while TIMP-3 remnants from LRP-1 wild-type cells were not internalized by fresh mouse fibroblasts, suggesting that sLRP-1 interacts with TIMP-3 and blocks endocytosis. Using co-immunoprecipitation and mass spectrometry analysis, we confirmed that sLRP-1 was complexed with TIMP-3 in the medium of HTB94 cells.

Shedding of LRP-1 has been shown to modulate extracellular matrix turnover. For example, LRP shedding regulates the internalization of MMP-2 and MMP-9 in a "loss of function" manner. Cyclic elimination of the endometrium functional layer through menstrual bleeding is due to intense tissue breakdown by MMP-2 and MMP-9 (Selvais et al., 2009), which follows the fall of estrogen and progesterone that occurs in the absence of pregnancy. Selvais *et al.* (2009) showed that the fall of estrogen and progesterone increases mRNA level of ADAM-12 in human endometrium, and ADAM-12 is an LRP-1 sheddase. During the fall of estrogen and progesterone, LRP-1 is shed by ADAM-12 and the clearance of MMP-2 and MMP-9 is blocked, although LRP-1 mRNA expression remains constant throughout the cycle. More recently, Selvais and colleagues reported that metalloproteinase-dependent shedding of LRP-1 can be impaired by overloading fibroblastoid HT1080 cells with

cholesterol (Selvais et al., 2011). It is proposed that cholesterol could increase compartmentalization between LRP-1 and its sheddases in distinct areas within the cell membrane and reduces shedding events.

LRP-1 plays a key role in Aβ peptide clearance from the brain (Shibata et al., 2000). sLRP-1 is found in human brain tissue, in the cerebral spinal fluid and other tissues such as human plasma and placenta (Liu et al., 2009). Levels of sLRP-1 in the cerebral spinal fluid increase with age and LRP-1 shedding is induced by the Aβ peptide. These evidences suggest that LRP-1 shedding during age might contribute to the pathogenesis of Alzheimer Disease.

In this chapter, I have demonstrated that LRP-1 shedding may also regulate extracellular matrix turnover in a different manner. sLRP-1 released from the cell surface can interact with TIMP-3 in the extracellular milieu preventing it from being internalized. Importantly, the TIMP-3—sLRP-1 complex retains the metalloproteinase inhibitory activity of TIMP-3. Therefore, shed LRP-1 can protect the tissue from metalloproteinase-mediated degradation of the extracellular matrix.

Chapter 6

Effect of metalloproteinase complex formation on

[^{35}S]TIMP-3 endocytosis

6.1 Introduction

LRP-1 can modulate ECM turnover and consequently cell behavior, by regulating the clearance of different classes of proteinases and their endogenous inhibitors, including metzincins and TIMPs, and serine proteases and serpins. Among the metzincins, MMP-13 was the first member that was reported to be internalized by LRP-1 (Barmina et al., 1999). ProMMP-2, through its hemopexin domain, interacts with the C-terminal domain of TIMP-2, thus forming a proMMP-2—TIMP-2 complex. This complex is also endocytosed by LRP-1 (Emonard et al., 2004). Emonard *et al.* (2004) reported that both proMMP-2 and TIMP-2 harbor binding determinants for LRP-1 recognition and therefore they can also be internalized by this receptor in a free form. Hahn-Dantona *et al.* (2001) showed that MMP-9 interacts with LRP-1 and that it can be internalized alone or in complex with TIMP-1. However, differently from TIMP-2, TIMP-1 does not bind to LRP-1, thus it can be endocytosed by the receptor only when in complex with the enzyme.

Analogous examples can also be found among serine proteases and serpins. uPA is synthesized as an inactive zymogen precursor, pro-uPA, which is activated by plasmin (Dano et al., 1985). Both pro-uPA and uPA bind with high affinity to the cell surface receptor uPAR. uPAR can mediate the slow internalization of uPA in a clathrin- and dynamin-independent manner, by a mechanism which shares many features with macropinocytosis (Cortese et al., 2008). Nykjaer et al. (1992) reported that when uPA is in a complex with its specific inhibitor PAI-1, uPA endocytosis occurs at a higher rate (Nykjaer et al., 1992b). They showed that the uPA—PAI-1 complex interacts with uPAR at the cell surface, recruiting LRP-1, which mediates internalization of the complex. PAI-1 also increased the rate of tPA endocytosis.

In this chapter, I investigated endocytosis of TIMP-3 in complex with various MMPs and ADAMTSs. The aim of these experiments is to determine whether TIMP-3 can be internalized only in a free form or also in complex with its target enzymes, and also to determine whether TIMP-3 can promote the endocytosis of its target enzymes in a similar way to that reported for PAI-1.

6.2 TIMP-3 is internalized in a free form

Cultured HTB94 cells release a variety of metalloproteinases, and we considered that [^{35}S]TIMP-3 may be endocytosed in complex with these enzymes. To investigate this possibility, we examined endocytosis of [^{35}S]TIMP-3 in the presence of the broad-spectrum metalloproteinase inhibitor GM6001, which would block interaction of [^{35}S]TIMP-3 with such metalloproteinases released by HTB94 cells.

HTB94 cells were plated at a density of 1x10^{6} cells/well and grown overnight before incubation with DMEM containing 0.1 % FCS supplemented with 10 µM GM6001 for 1 h at 37 °C. Next, 1 nM [^{35}S]TIMP-3 was added and radioactivity distribution among the TCA-insoluble, TCA-soluble and cell-associated fractions monitored over 24 h. TCA-insoluble [^{35}S]TIMP-3 decreased both in the presence and in the absence of GM6001 with similar kinetics, and the TCA-soluble and cell-associated radioactivity also followed similar kinetics (Figure 40). These results suggest that TIMP-3 can be internalized in a free form by HTB94 cells, without formation of a complex with metalloproteinases.

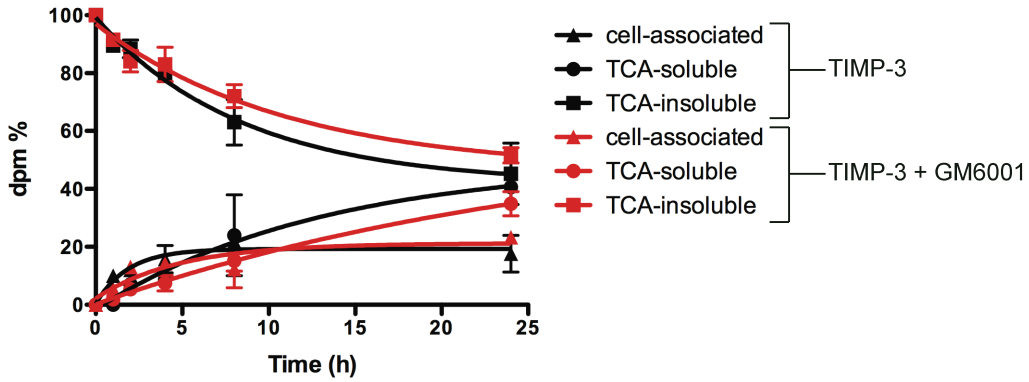

Figure 40, Effect of GM6001 on [^{35}S]TIMP-3 internalization
[^{35}S]TIMP-3 (1 nM) was added to HTB94 cells (0 to 24 h) in the absence (black symbols and lines) or presence (red symbols and lines) of 10 µM GM6001, and radioactivity in the cell-associated, and TCA-soluble and TCA-insoluble fractions of the conditioned media quantified by scintillation counting (*n=3*).

6.2.1 TIMP-3 binds directly to LRP-1

To confirm that TIMP-3 could directly bind to LRP-1, I measured binding of TIMP-3 to immobilized sLRP-1 purified from plasma by ELISA. As shown in Figure 41, TIMP-3 bound readily to LRP-1, compared to control wells. Heparin is reported to antagonize the binding of different LRP-1 ligands to LRP-1, including lipoprotein lipase (Williams et al., 1994), α_2M (Arandjelovic et al., 2005), and PAI-1 (Stefansson et al., 1998). To test whether or not this was also the case for TIMP-3, I incubated TIMP-3 (0.1-20 nM) with 100 µg/ml heparin before adding it to the sLRP-1 coated wells. Upon pre-incubation with heparin, binding of TIMP-3 to LRP-1 was completely abolished.

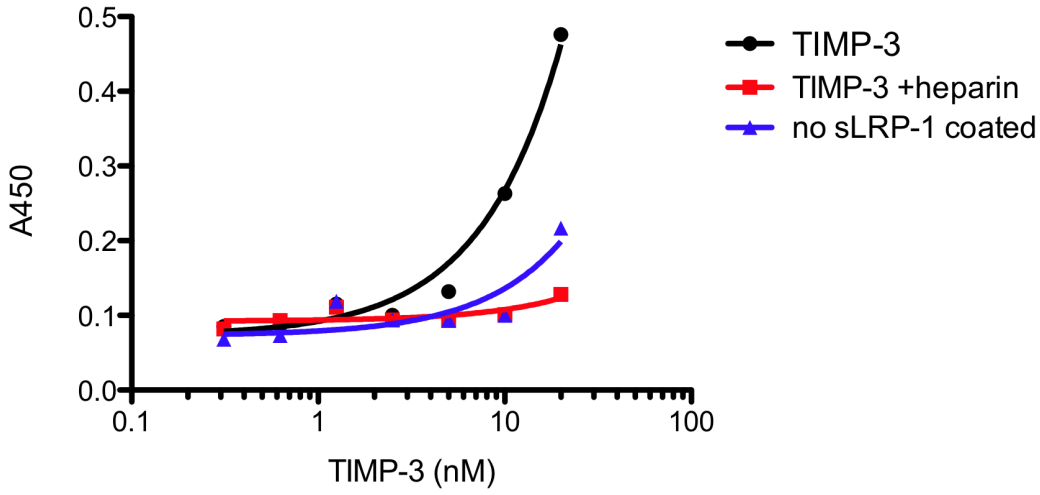

Figure 41, Interaction of TIMP-3 with sLRP-1 measured by ELISA
Shed LRP-1 purified from human plasma was coated onto microtitre plates and binding of TIMP-3 (0.1 – 20 nM) in the absence (●) and presence (■) of 100 µg/ml heparin was measured using an M2 anti-FLAG antibody and a HRP-conjugated secondary antibody. Control wells (▲) were not coated with sLRP.

6.3 Effect of complex formation with prototypic metzincins on TIMP-3 endocytosis

6.3.1 Formation of a complex with ADAMTS4-2 or ADAMTS5-2 does not affect TIMP-3 endocytosis

ADAMTS4-2 is a C-terminal spacer domain truncated form of ADAMTS-4, and ADAMTS5-2 is a truncated form of ADAMTS-5 that lacks of the C-terminal TS-2 domain (Gendron et al., 2007; Kashiwagi et al., 2004). To investigate whether formation of a complex with these proteinases had an effect on TIMP-3 internalization, [^{35}S]TIMP-3—ADAMTS4-2 or [^{35}S]TIMP-3—ADAMTS5-2 complexes were made *in vitro* by incubating 10 nM ADAMTS4-2 or ADAMTS5-2 with 10 nM [^{35}S]TIMP-3 for 1 h at 37 °C. Either [^{35}S]TIMP-3—ADAMTS4-2 or [^{35}S]TIMP-3—ADAMTS5-2 was added to HTB94 cells plated in a 6-well plate in DMEM containing 0.1 % FCS, and the distribution of radioactivity among the cell fractions was monitored over 24 h. The decrease in TCA-insoluble radioactivity of [^{35}S]TIMP-3—ADAMTS4-2 or [^{35}S]TIMP-3—ADAMTS5-2 wells was similar to that of [^{35}S]TIMP-3 alone (Figure 42). These data suggest that the formation of a complex with ADAMTS-4 or ADAMTS-5 has no effect on the rate of [^{35}S]TIMP-3 endocytosis.

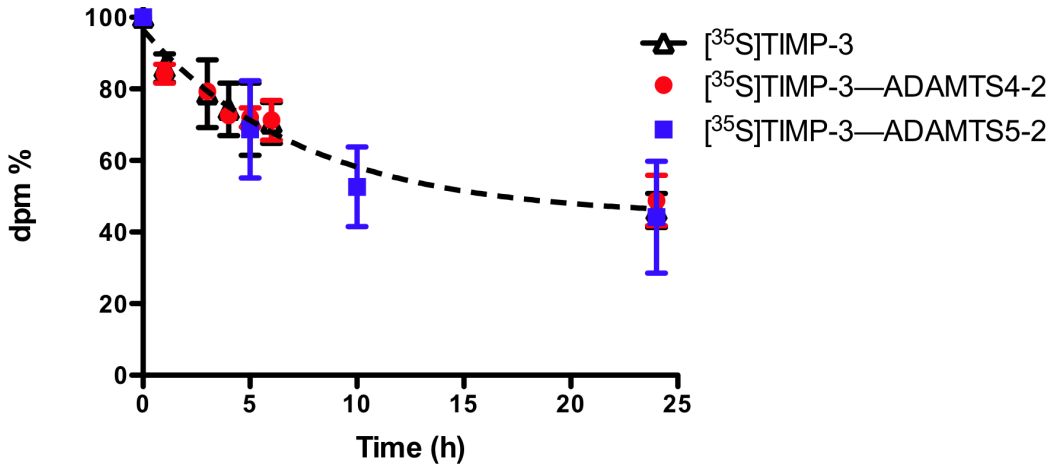

Figure 42, Internalization of [35S]TIMP-3—ADAMTS4-2 and [35S]TIMP-3—ADAMTS5-2 complexes
[35S]TIMP-3 (10 nM) was incubated *in vitro* with ADAMTS4-2 or ADAMTS5-2(10 nM, 1 h, 37 °C) and either [35S]TIMP-3—ADAMTS4-2 or [35S]TIMP-3—ADAMTS5-2 complex added to HTB94 cells. At the indicated time points, the conditioned medium was harvested and precipitated with TCA (5 %). Radioactivity in the TCA-insoluble fraction of [35S]TIMP-3—ADAMTS4-2 (red symbols) or [35S]TIMP-3—ADAMTS5-2 (blue symbols) was measured and compared to that of [35S]TIMP-3 supplemented controls (open symbols, dotted line) (*n=3*).

6.3.2 Formation of TIMP-3—MMP-1 complexes does not affect TIMP-3 endocytosis

To investigate whether complex formation with MMP-1 had an effect on TIMP-3 endocytosis, [35S]TIMP-3—MMP-1 complex was generated *in vitro* by incubating 10 nM of MMP-1 with 10 nM [35S]TIMP-3 for 1 h at 37 °C. Mantuano *et al.* (2008) reported that MMP-9 interacts with LRP-1 by its hemopexin domain. Thus, we also made a complex of [35S]TIMP-3 with the catalytic domain of MMP-1 (MMP-1 ΔC), in a similar manner as for full length MMP-1, to evaluate the effect of the hemopexin domain of MMP-1 in this process. Either [35S]TIMP-3—MMP-1 or [35S]TIMP-3—MMP-1 ΔC complex was added to HTB94 cells and radioactivity in TCA-insoluble fraction followed over 24 h. The decrease in TCA-insoluble radioactivity in cells treated with [35S]TIMP-3—MMP-1 or [35S]TIMP-3—MMP-1 ΔC complex had the same kinetics as that of [35S]TIMP-3, suggesting that the formation of a complex between TIMP-3 and MMP-1 does not affect TIMP-3 internalization, and that the hemopexin domain of MMP-1 does not alter this process.

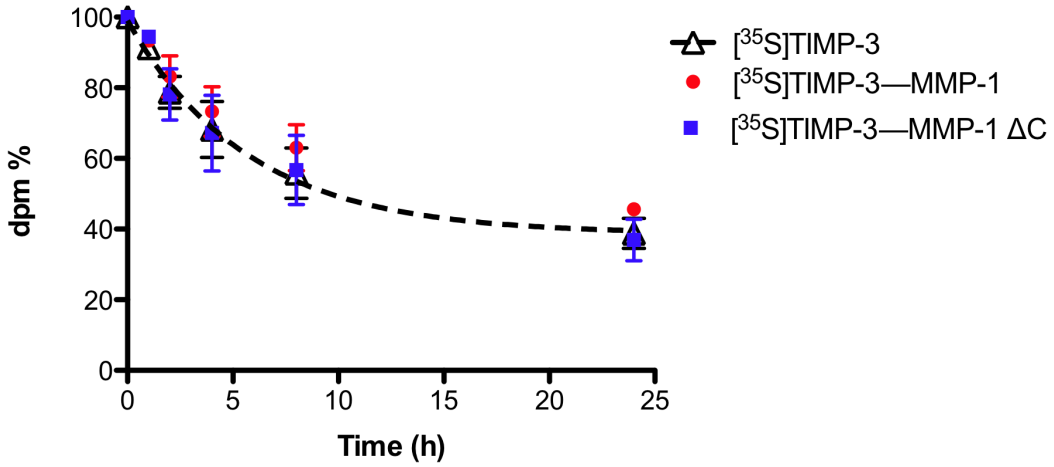

Figure 43, Effect of a MMP-1 and MMP-1ΔC complex formation on [35S]TIMP-3 endocytosis
[35S]TIMP-3 (10 nM) was complexed *in vitro* with MMP-1 or MMP-1 ΔC (10 nM, 1 h, 37 °C) prior to being added to HTB94 cells. At the indicated time points, the conditioned medium was harvested and precipitated with TCA (5 %), and radioactivity in the TCA-insoluble fraction of [35S]TIMP-3—MMP-1 treated cells (red symbols) and [35S]TIMP-3—MMP-1 ΔC treated cells (blue symbols) was compared to that of [35S]TIMP-3 treated cells (open symbols and dotted lines) (*n=3*).

6.3.3 MMP-1 is internalized in complex with TIMP-3

Our laboratory has recently shown that ADAMTS-5 and ADAMTS-4 can be internalized by LRP-1 independently from TIMP-3. Both enzymes have the LRP-1 binding determinants and we found that they directly interact with LRP-1 *in vitro* (Yamamoto et al., submitted; Owen and Nagase, unpublished observations). I investigated whether MMP-1 itself could be endocytosed. HTB94 cells were incubated with 10 nM [35S]MMP-1 at 37 °C for 24 h, and at the indicated time points, medium was harvested and precipitated with TCA (5 %). Radioactivity present in the cell fractions was measured. As shown in Figure 44A, TCA-insoluble radioactivity decreased and TCA-soluble and cell-associated radioactivity increased over 24 h, but with a slower kinetics compared to that of TIMP-3. This data suggest that although [35S]MMP-1 is internalized by HTB94 cells, the mechanism of internalization may be different from that of TIMP-3.

When [^{35}S]MMP-1 was in a [^{35}S]MMP-1—TIMP-3 complex, its internalization showed similar kinetics as that of TIMP-3 alone (Figure 44B). To investigate whether MMP-1 can be internalized in a free form not complexed with TIMP-3, I incubated [^{35}S]MMP-1 with HTB94 cells at 37 °C for 24 h in the presence of 10 µM GM6001, to inhibit binding of [^{35}S]MMP-1 with endogenous TIMP-3. In these conditions, radioactivity in the TCA-insoluble fraction minimally decreased, and radioactivity in the TCA-soluble and cell-associated fractions also minimally increased over 24 h, suggesting that MMP-1 can be internalized only efficiently in complex with TIMP-3 and not as a free enzyme (Figure 44C).

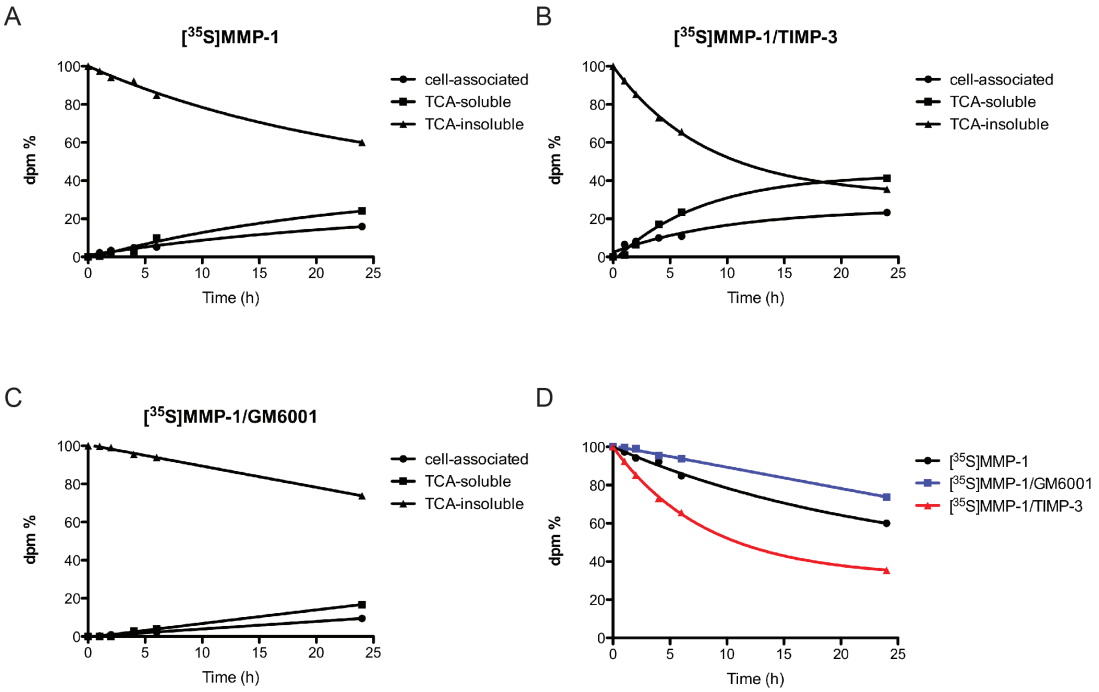

Figure 44, MMP-1 is minimally internalized by HTB94 cells, but it is taken up in complex with TIMP-3

10 nM [^{35}S]MMP-1 was added to HTB94 cells in a 6-well plate either alone (**A**) or in complex with TIMP-3 (**B**) or in the presence of GM6001 (**C**). At the indicated time points, the medium was harvested and precipitated with TCA (5 %), and cells collected with 1 ml of NaOH (1 N). Radioactivity in TCA-insoluble, TCA-soluble and cell-associated fractions was measured (this result is representative of 2 separate experiments). **D**, Comparison of the radioactivity decrease in the TCA-insoluble fraction of [^{35}S]MMP-1 treated cells, [^{35}S]MMP-1—TIMP-3 treated cells and [^{35}S]MMP-1 treated cells in the presence of GM6001.

6.3.4 MMP-1 does not interact with LRP-1

To investigate whether MMP-1 can directly bind to LRP-1 or only when in complex with TIMP-3, an ELISA was performed. MMP-1-FLAG (0.1-40 nM) was added to sLRP-1 purified from plasma, which was previously immobilized onto microtitre wells. Binding was measured by an M2 anti-FLAG primary antibody and an HRP-conjugated anti-mouse secondary antibody. TIMP-3-FLAG (0.1-40 nM) was added to control wells and binding measured in a similar manner. Compared to TIMP-3, which clearly bound to sLRP-1, MMP-1 did not show any binding to the receptor (Figure 45).

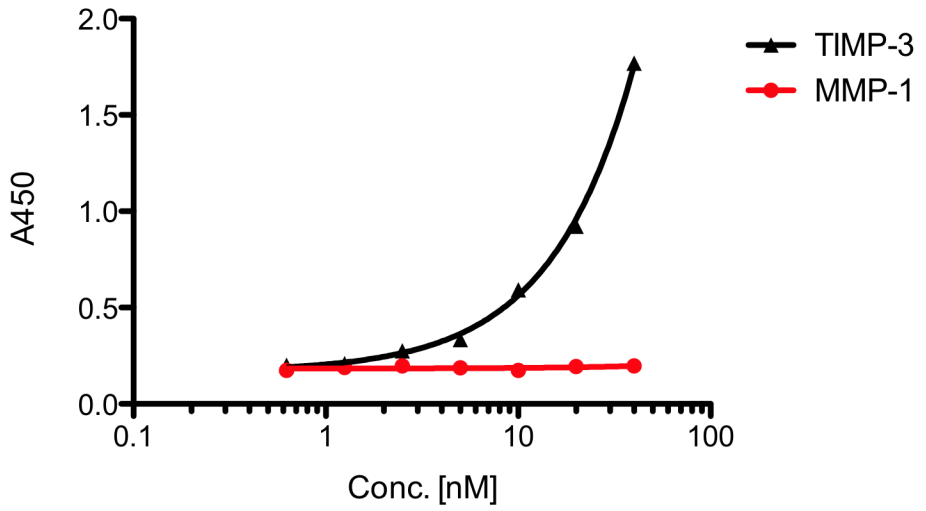

Figure 45, MMP-1 does not bind to LRP-1.
Shed LRP-1 purified from human plasma was coated onto microtitre plates and binding of TIMP-3-FLAG (0.1 – 20 nM) (▲) and MMP-1-FLAG (0.1 – 20 nM) (●) was measured using an M2 anti-FLAG antibody and an HRP-conjugate secondary antibody.

6.3.5 TIMP-3 bridges MMP-1 to LRP-1

In section 6.3.3 I showed that MMP-1 internalization by HTB94 cells is increased upon formation of a complex with TIMP-3. To demonstrate that this is due to the TIMP-3 capability of mediating the interaction between MMP-1 and LRP-1, I measured the binding of MMP-1 to immobilized sLRP-1 in the presence and absence of TIMP-3. Two different approaches were used. TIMP-3-FLAG (40 nM) was immobilized onto sLRP-1 coated microtitre plates. Then, either (i) biotinylated MMP-1 (E200A) (0.1-40 nM) was added to wells and binding detected by incubation of wells with HRP-conjugated streptavidin (Figure 46A), or (ii) MMP-1-FLAG (0.1-40 nM)

was added and binding detected with an anti-MMP-1 antibody and then with an anti-sheep secondary antibody conjugated with HRP (Figure 46B). In both cases, MMP-1 bound to sLRP-1 only in the presence of TIMP-3, suggesting that the inhibitor can bridge enzyme and receptor and mediate the LRP-1-dependent internalization of MMP-1.

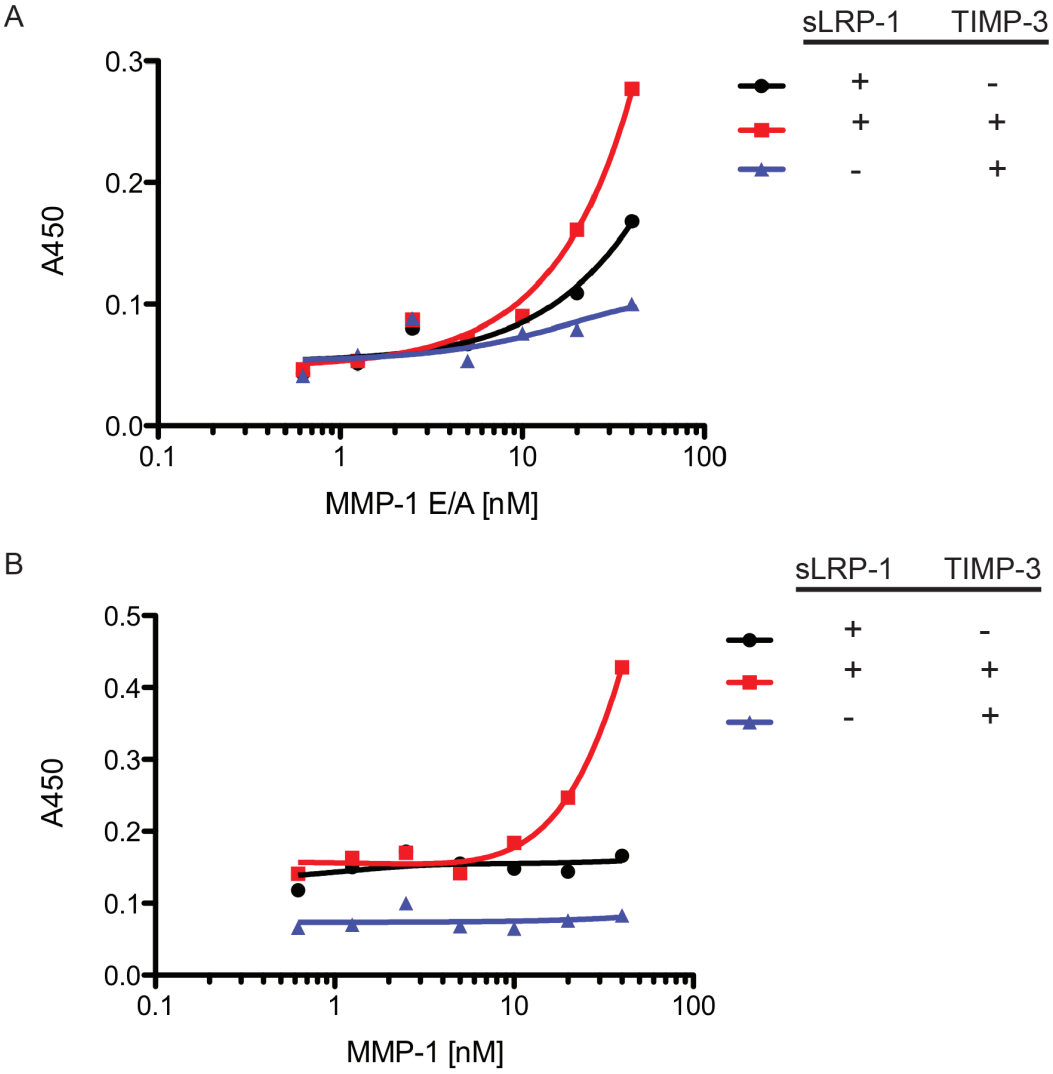

Figure 46, TIMP-3 mediates binding of MMP-1 to LRP-1.
Shed LRP-1 was coated onto microtitre plates and incubated with TIMP-3-FLAG (40 nM) at 37 °C for 2h. Then, (**A**) biotinylated MMP-1 E200A (0.1 – 40 nM) was added to sLRP-1 coated wells and binding detected by HRP-conjugated streptavidin (■). Control wells were either not incubated with TIMP-3-FLAG (●) or not coated with sLRP-1 and incubated with TIMP-3 (▲). Alternatively, (**B**) FLAG-tagged MMP-1 (0.1 – 40 nM) was added to sLRP-1 coated wells and binding detected by an anti-MMP-1 and anti-sheep HRP-conjugated antibody (■). Control wells were either not incubated with TIMP-3-FLAG (●) or not coated with sLRP-1 and incubated with TIMP-3 (▲).

6.4 Effect of other MMPs on TIMP-3 endocytosis

To test whether TIMP-3 could also be endocytosed in complex with classes of MMPs other than collagenases, such as stromelysins and membrane-type metalloproteinases, a complex of [35S]TIMP-3 with the catalytic domain of MMP-3 and MMP-14 was made *in vitro*. 10 nM of MMP-3 ΔC or MMP-14 ΔC was incubated with [35S]TIMP-3 (10 nM) for 1 h at 37 °C. Resultant [35S]TIMP-3—MMP-3 ΔC or [35S]TIMP-3—MMP-14 ΔC complex was added to HTB94 cells in a 6-well plate in DMEM containing 0.1 % FCS, and radioactivity in the TCA-insoluble fraction was monitored over 24 h. As shown in Figure 47, in both cases, the TCA-insoluble radioactivity of [35S]TIMP-3-enzyme samples decreased with similar kinetics as [35S]TIMP-3 alone, indicating that the formation of a complex with these metalloproteinases does not affect TIMP-3 endocytosis.

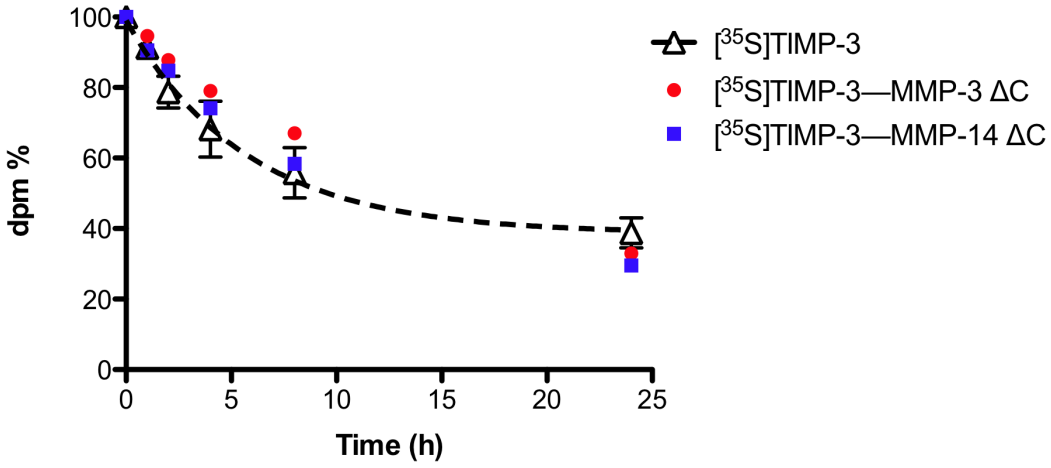

Figure 47, Effect of MMP-3 ΔC or MMP-14 ΔC on [35S]TIMP-3 endocytosis
10 nM [35S]TIMP-3 was incubated with MMP-3 ΔC (red symbols) or MMP-14 ΔC (blue symbols) (10 nM, 1 h, 37 °C), and the complex then added to HTB94 cells for up to 24 h. At the indicated time points, the conditioned medium was harvested, and radioactivity in the TCA-insoluble fraction compared to that of [35S]TIMP-3 alone (open symbols, dotted line), data for [35S]TIMP-3 are from Figure 43)

6.5 Discussion

As discussed in the Introduction, LRP-1 can mediate the cellular uptake of metalloproteinases and TIMPs, thus regulating their levels in the tissue and controlling biological processes, including cell migration. MMP-2, MMP-9 and MMP-

13 contain binding determinants for LRP-1, therefore they can interact directly with the receptor. It is reported that MMP-2 and MMP-9 can also be internalized by LRP-1 when in complex with their endogenous inhibitor TIMP-2 and TIMP-1, respectively. Interestingly, while TIMP-2 also harbors a binding site for LRP-1 and it can be internalized without MMP-2, TIMP-1 does not bind to LRP-1 when in a free form and it can be taken up only in complex with MMP-9. In this chapter, I investigated whether TIMP-3 can be internalized in a free form and/or in a complex with its target metalloproteinases. To answer this question, I firstly used the hydroxamate-based inhibitor of metalloproteinases, GM6001, which did not inhibit the internalization of TIMP-3 indicating that TIMP-3 does not require formation of a complex with secreted metalloproteinases to be internalized. Secondly, I confirmed that TIMP-3 harbors the binding determinants for LRP-1 by detecting direct binding of TIMP-3 to LRP-1 *in vitro*. These results suggested that TIMP-3 endocytosis is a way to control levels of this inhibitor in the extracellular environment. Therefore, TIMP-3 endocytosis may protect tissues from accumulation of an excess of free inhibitor, which may be detrimental as it induces cellular apoptosis. On the other hand, in response to specific stimuli, the cell can increase levels of TIMP-3 in the tissue by blocking its endocytosis. The activation of sheddases that cleave LRP-1 may be a potential mechanism for reducing endocytosis. Tissue levels of TIMP-3 may be regulated by controlling the cycle of secretion/endocytosis of the inhibitor. This process, which would be energetically expensive for the cell, may be explained by the fact that it enables cells to respond more rapidly to specific stimuli, rather than synthesizing TIMP-3 *de novo*.

As discussed in the Chapter 5, highly sulfated GAGs inhibit the internalization of TIMP-3 and this is not due to the involvement of HSPGs or CSPGs in the endocytic machinery. Several LRP-1 ligands, including ApoE (Lalazar et al., 1988), RAP (Migliorini et al., 2003), lipoprotein lipase (Williams et al., 1994), PAI-1 (Rodenburg et al., 1998; Stefansson et al., 1998) and α_2-macroglobulin—protease complexes (Arandjelovic et al., 2005; Dolmer and Gettins, 2006) are reported to interact with the receptor through clusters of positively charged arginine and lysine residues. Heparin has been shown to directly inhibit interaction of some of these ligands to

LRP-1. In this chapter, I verified that heparin could also block the direct binding of TIMP-3 to LRP-1, shedding light on the mechanism underlying the inhibition of TIMP-3 endocytosis by highly sulfated GAGs. Lee *et al.* identified a cluster of lysines and arginines residues involved in TIMP-3 binding to the ECM (Lee et al., 2007). I speculate that the determinants for LRP-1 binding are located in this cluster of positively charged residues on the TIMP-3 molecule, overlapping with the binding site for GAGs. Our laboratory plans to determine which of these individual residues is involved in the TIMP-3-LRP-1 interaction by site-directed mutagenesis.

It is reported that tPA and uPA are endocytosed by LRP-1 only when in complex with PAI-1. PAI-1 interacts directly with LRP-1, forming a bridge between the receptor and these proteases. Thus, I investigated whether TIMP-3 could mediate the LRP-1-dependent uptake of metalloproteinases that do not directly interact with the receptor. Differently from ADAMTS-4 and -5, which are two LRP-1 ligands (Yamamoto et al.; Owen and Nagase, unpublished obsarvations), MMP-1 showed no affinity for LRP-1 *in vitro*. However, when MMP-1 was in complex with TIMP-3, it was internalized with similar kinetics to the free inhibitor. TIMP-3 was shown to bridge binding of the enzyme to LRP-1 and to mediate its scavenging by cells. In this manner, TIMP-3 not only inactivates its target metalloproteinases in the tissue but also mediates their internalization and degradation by cells.

Chapter 7

General Discussion and Future Prospects

7.1 LRP-1 is the major receptor for TIMP-3 endocytosis

Studies in *Timp3*$^{-/-}$ mice have reported the crucial role of this inhibitor in maintaining tissue homeostasis by regulating the activity of several metalloproteinases (Fata et al., 2001; Fedak et al., 2004; Mohammed et al., 2004; Sahebjam et al., 2007). TIMP-3 has a protective role in pathological conditions characterized by enhanced ECM degradation, inflammation, cell growth and migration, including arthritis, atherosclerosis and cancer (Ahonen et al., 1998; Baker et al., 1999; Cardellini et al., 2009; Casagrande et al., 2012; Cruz-Munoz et al., 2006a; Gendron et al., 2003). Therefore, there is an increasing interest in understanding the mechanisms that regulate levels of TIMP-3 in the tissue. TIMP-3 expression can be regulated at different levels by different factors: (i) transcriptionally, by cytokines and growth factors, including TGF-β and oncostatin M (Li et al., 2001; Qureshi et al., 2005); (ii) post-transcriptionally, due to the action of a number of micro RNAs including miR-21, miR-221, miR-222, miR181b and miR206 (Gabriely et al., 2008; Garofalo et al., 2009; Limana et al., 2011; Song et al., 2010; Wang et al., 2010); and (iii) epigenetically by histone deacetylases and promoter methylation (Anania et al., 2011; Cardellini et al., 2009). Furthermore, my study has revealed a new mechanism for regulating levels of TIMP-3 in the extracellular space.

In 2008, Troeberg *et al.* reported the first evidence that TIMP-3 levels in the extracellular space can be post-translationally regulated by endocytosis, with TIMP-3 accumulating in the conditioned medium of chondrocytes and chondrosarcoma HTB94 cells in the presence of RAP. I investigated the mechanism of TIMP-3 endocytosis using three different approaches: immunoblotting, confocal microscopy and purified [^{35}S]radiolabeled TIMP-3. By following the distribution of purified [^{35}S]radiolabeled TIMP-3 among cell fractions after its exogenous addition to cultured cells, I could investigate the kinetics of TIMP-3 endocytosis. This methodology also allowed me to discover that TIMP-3 is degraded by cells after its endocytosis, with fragments released into the conditioned medium. I investigated the kinetics of endocytosis and degradation of [^{35}S]TIMP-3 by LRP-1-deficient PEA-13 mouse fibroblasts. These cells represent a widely used model for investigating the involvement of LRP-1 in diverse cell processes, including endocytosis and signalling

(Willnow and Herz, 1994). TIMP-3 endocytosis was clearly reduced in LRP-1-deficient PEA-13 cells compared to wild-type cells, indicating that LRP-1 is the major component of TIMP-3 endocytic machinery. RAP did not further decrease the residual internalization of the TIMP-3 by PEA-13 cells, indicating that among the LDL receptor family, LRP-1 is the only one involved in this process.

7.2 The LRP-1/sLRP-1 ratio regulates levels of TIMP-3 in the tissue

I compared the kinetics of TIMP-3 endocytosis by a number of cell types, including chondrosarcoma cells, porcine articular chondrocytes, fibroblasts and monocyte-like THP-1 cells. In all cases, the rate of TIMP-3 endocytosis was not constant over time. TIMP-3 endocytosis was initially rapid, then slowing down to reach a plateau after around 10 h, after which only a minimal amount of TIMP-3 was internalized. I investigated the causes of this decrease in endocytosis and demonstrated that it is due to the interaction of TIMP-3 with a soluble form of LRP-1, generated by proteolytic shedding of the transmembrane receptor. Shedding is an important way of regulating concentrations of LRP-1 on the cell surface. A number of sheddases have been reported to release the ectodomain of LRP-1, including ADAM-10, ADAM-12, ADAM-17 and BACE (Gorovoy et al., 2010; Liu et al., 2009; Polavarapu et al., 2007; Rozanov et al., 2004; Selvais et al., 2009; von Arnim et al., 2005). LRP-1 is shed by cleavage in the β-chain, which induces the release of the α-chain and part of the β-chain. MT1-MMP was also reported to cleave LRP-1, but, differently from the mentioned sheddases that generate a soluble form of the entire LRP-1 ectodomain, it provokes a fragmentation of the receptor (Rozanov et al. 2004). The specific sites at which these enzymes cleave have not yet been identified.

A number of stimuli are reported to induce LRP-1 shedding, and different stimuli can activate different sheddases in a cell-specific manner. Generally, inflammation seems to regulate this process. Increased levels of sLRP-1 are detectable in the plasma of patients with rheumatoid arthritis, systemic lupus erythematous (Gorovoy et al., 2010) and liver disease (Quinn et al., 1997). Molecules involved in inflammation, such as interferon γ and LPS stimulate LRP-1 shedding by

ADAM-17 (Gorovoy et al., 2010). sLRP-1 itself is a mediator of inflammation, being able to activate the IKK-NF-κB patway through its N-terminus (Gorovoy et al., 2010). Cholesterol depletion has also been found to stimulate LRP-1 shedding by MT1-MMP and ADAM-12 (Selvais et al., 2011). I observed the accumulation of sLRP-1 in the conditioned medium of HTB94 cells in the absence of any pro-inflammatory stimuli. Since a number of the proposed LRP-1 'sheddases' are metalloproteinases, production of sLRP-1 should be inhibited by metalloproteinase inhibitors such as TIMP-3 and GM6001. However, the concentration of [^{35}S]TIMP-3 that we used in endocytosis assays (1 nM) is an order of magnitude lower than the TIMP-3 concentration previously shown to inhibit MT1-MMP and ADAM12-mediated shedding (Selvais et al., 2011). GM6001 has been shown to inhibit LRP-1 shedding (Gorovoy et al., 2010; Wygrecka et al., 2011), but we found that GM6001 had no effect on the rate of [^{35}S]TIMP-3 endocytosis by HTB94 cells. This suggests that a GM6001-insensitive sheddase may mediate LRP-1 shedding in HTB94 cells. More interestingly, some preliminary experiments that I performed recently show that TIMP-3 itself can induce LRP-1 shedding in a concentration-dependent manner, with the generation of two fragments of 150 kDa and 250 kDa. Sheddases responsible for LRP-1 constitutive shedding in HTB94 cells and the mechanisms underlying TIMP-3-induced shedding of LRP-1 are currently under investigation in our laboratory.

Shedding of LRP-1 has numerous consequences. Firstly, it can reduce endocytosis of LRP-1 ligands in a loss-of-function manner by reducing the number of endocytic receptors on the cell surface (Rozanov et al., 2004; Selvais et al., 2011; Wygrecka et al., 2011). Secondly, sLRP-1 can bind to and inhibit endocytosis of its ligands, as has been reported for tPA, MMP-2 and MMP-9 (Quinn et al., 1997; Wygrecka et al., 2011). By antagonizing LRP-1-mediate endocytosis, sLRP-1 can increase the half-life of TIMP-3 in the extracellular space. More importantly, I found that the TIMP-3-sLRP-1 complex is still able to inhibit metalloproteinases, therefore the ratio between cell surface LRP-1 and sLRP-1 is an important factor that regulates the bioavailability of TIMP-3 to inhibit metalloproteinases in the extracellular space, thus controlling ECM proteolysis and proteolysis of cell surface molecules.

Heparin has been shown to directly inhibit interaction of other ligands, including factor IXa (Neels et al., 2000), apolipoproteins (Nilsson et al., 2007), C4b-

binding protein (Westein et al., 2002) and PAI-1 (Nykjaer et al., 1992b), with LRP-1. In the case of PAI-1, the heparin-binding and LRP-binding regions have been found to overlap (Horn et al., 1998; Stefansson et al., 1998). Binding of proteins to heparin is commonly mediated by clusters of positively charged residues (Gandhi and Mancera, 2008). Similarly, binding of protein ligands to LRP and related LDL receptors is often mediated by positive residues, as has been demonstrated for RAP (Fisher et al., 2006; van den Biggelaar et al., 2011), α_2M (Arandjelovic et al., 2005), PAI-1 (Rodenburg et al., 1998; Jensen et al., 2009; Skeldal et al., 2006), apolipoprotein E (Lalazar et al., 1988), lipoprotein lipase (Williams et al., 1994) and factor VIII (Meems et al., 2011). In the case of RAP, crystallography and mutagenesis studies have confirmed that K256 and K270 mediate binding to acidic pockets in the ligand binding motifs of the receptor (Fisher et al., 2006; van den Biggelaar et al., 2011). I found that heparin blocks the direct binding of TIMP-3 to sLRP-1 purified from plasma. This suggests that, as in the case of PAI-1, the heparin-binding and LRP-binding sites of TIMP-3 may overlap. The crystal structure of full-length TIMP-3 is currently unavailable, but the protein is predicted to contain an extended patch of basic residues, located on the opposite face of the protein to the inhibitory ridge that interacts with metalloproteinases. Mutagenesis indicates that this region mediates binding to the extracellular matrix and to sulfated proteoglycans (Lee et al., 2007). Residues in this region may also mediate binding to LRP. Binding of TIMP-3 to sLRP-1, which inhibits the TIMP-3 uptake by competing with the endocytic transmembrane LRP-1, may also prevent TIMP-3 from binding to the ECM. Therefore, sLRP-1 can regulate the bioavailability of TIMP-3 in the extracellular space by increasing its half-life and by competing for binding of TIMP-3 to the ECM.

7.3 LRP-1-independent endocytosis of TIMP-3

In addition to the LRP-1-mediated pathway, I observed an LRP-1-independent endocytosis of TIMP-3 in PEA-13 cells and RAP-treated HTB94, MEFs and CHO cells. Although this is a slower process compared to the LRP-1-mediated endocytosis, it is also likely to be receptor-mediated. Endocytosis of TIMP-3 in all tested cell types was almost completely inhibited by heparin, which is known to antagonize the binding of

proteins to HSPGs and CSPGs. I hypothesized that members of these two families could be involved in the LRP-1-independent pathway. In agreement with this hypothesis, HSPGs have been demonstrated to mediate endocytosis of ligands including lipoproteins (Stanford et al., 2009), and endocytosis mediated by HSPGs does not require dynamin, as it was the case for the LRP-1-independent endocytosis of TIMP-3. Alternatively, HSPG might act as co-receptors of LRP-1-mediated endocytosis, concentrating ligands on the cell surface for the subsequent LRP-1-mediated internalization. A similar endocytic mechanism was proposed for thrombospondin 1 (Wang et al., 2004), tissue factor pathway inhibitor (Schwartz and Broze, 1997), amyloid-β (Kanekiyo et al., 2011) and factor VIII (Sarafanov et al., 2001). Based on these reports I hypothesized that TIMP-3 could be internalized by two different pathways: i) TIMP-3 initially binds to an HSPG on the cell surface that functions as a co-receptor and transfers the inhibitor to LRP-1 for subsequent endocytosis; or ii) TIMP-3 binds to an HSPG which itself mediates the inhibitor endocytosis. However, I found that TIMP-3 endocytosis was not affected in xylosyltransferase-deficient CHO-745 cells, indicating that sulfated cell surface proteoglycans are not required for TIMP-3 endocytosis. In line with this finding, TIMP-3 endocytosis was also unimpaired in sodium chlorate treated cells, and in syndecan-4-null and syndecan-1-silenced cells. I therefore conclude that cell surface HSPG or CSPG do not mediate the LRP-1-independent pathway of TIMP-3 endocytosis. The receptor that mediates the LRP-1-independent endocytosis of TIMP-3 is yet to be identified. Members belonging to the macrophage mannose receptor protein family may be possible candidates as they have been shown to internalize some LRP-1 ligands and play a crucial role in ECM turnover. For instance, urokinase plasminogen activator receptor-associated protein/endocytic recycling protein Endo180 is expressed in chondrocytes and fibroblasts and is involved in collagen internalization (Engelholm et al., 2003; Kjoller et al., 2004), and the macrophage mannose receptor mediates internalization of ADAMTS-13 by dendritic cells (Sorvillo et al., 2012).

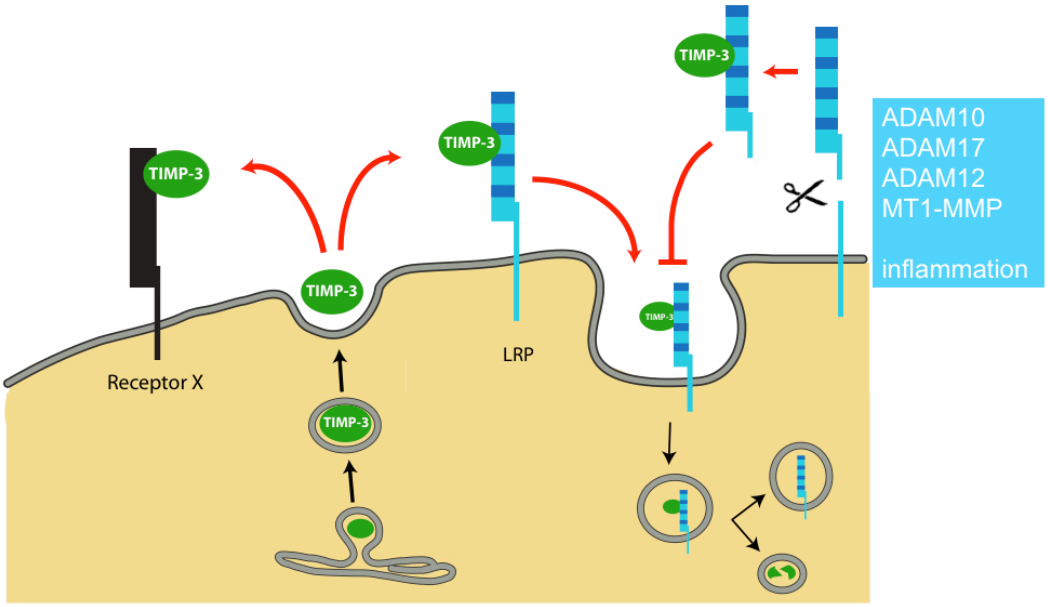

Figure 48. Model for TIMP-3 endocytosis.

7.4 LRP-1: a master regulator of ECM turnover

I investigated what the biological significance of TIMP-3 endocytosis is, whether it is a means to scavenge inactive metalloproteinases in TIMP-3—enzyme complexes or whether it is a mechanism to control levels of free inhibitor in the tissue. The internalization of TIMP-3 was not altered in the presence of the metalloproteinase inhibitor GM6001, which prevents TIMP-3 from forming a complex with metalloproteinases. This suggests that TIMP-3 can be internalized in a free form and that its endocytosis is a mechanism to control levels of this physiological and pathologically important inhibitor in the extracellular space. TIMP-3 has been reported to induce apoptosis by stabilizing death receptors; therefore accumulation of TIMP-3 in the extracellular space may be detrimental for the cell (Ahonen et al., 2003; Baker et al., 1999).

I found that TIMP-3 can be internalized in complex with metalloproteinases without any significant change in kinetics compared to free TIMP-3. As discussed above, a patch of positive residues that may drive the binding of TIMP-3 to LRP-1 is located in the opposite face to the inhibitory ridge. I hypothesize that the LRP-1 binding determinants on the TIMP-3 molecule are not sterically shielded when the

inhibitor is in complex with metalloproteinases. As shown for MMP-2, -9, -13 and ADAMTS-4 and -5, some metalloproteinases harbor LRP-1 binding determinants and they can be internalized by LRP-1 independently from binding to TIMP-3 or other TIMPs (Barmina et al., 1999; Emonard et al., 2004; Hahn-Dantona et al., 2001). On the other hand, I found that MMP-1 does not have affinity for LRP-1 and it is minimally endocytosed by cells. When in complex with TIMP-3, the internalization of MMP-1 occurs at a higher rate, suggesting that TIMP-3 can bridge binding of the enzyme to LRP-1. Other classes of MMPs (eg. stromelysins and membrane-type MMPs) are also internalized in complex with TIMP-3, indicating that the inhibitor can generally mediate the scavenging of metalloproteinases. Scavenging of inhibited metalloproteinases may have some biological consequences. Firstly, it may prevent accumulation of inactive enzymes in the ECM that may compete with other molecules for specific binding sites in the ECM, including proteoglycans. Secondly, binding of TIMP-3—metalloproteinase complexes to LRP-1 could activate cell-signalling and modulate gene expression. In agreement with this hypothesis, it has been reported that MMP-9 activates ERK1/2 and Akt in Schwann cells upon binding to LRP-1, and that LRP-1 activates ERK1/2 and inhibits JNK in cancer cells, promoting their migration (Langlois et al., 2010; Mantuano et al., 2008).

The capability of LRP-1 to internalize metalloproteinases and metalloproteinase inhibitors, controlling their levels in the extracellular space, renders it a master regulator of the ECM. Altered levels of this receptor on the cell surface affect the cell environment and can lead to pathological conditions. For example, low levels of LRP-1 in chondrocytes are associated with OA (Yamamoto et al., 2012). Interestingly, despite our finding that the presence of RAP induces accumulation of TIMP-3 in the conditioned medium of cultured porcine articular chondrocytes, the addition of RAP to porcine articular cartilage explants promotes cartilage degradation, primarily due to an increase in ADAMTS-5 activity (Yamamoto et al., 2012). Silencing of LRP-1 in carcinoma cells enhances pericellular proteolysis (Dedieu et al., 2008). Interestingly, overexpression of LRP-1 also increases pericellular proteolysis in human glioblastoma cells, by inducing the expression of MMP-2 and MMP-9 via ERK signalling (Song et al., 2009). These examples show the importance of LRP-1 in controlling proteolysis in the ECM both in terms of increasing

net proteolysis, and decreasing net proteolysis. Due to the high number of heterogeneous LRP-1 ligands, ranging from metalloproteinases to growth factors, it is impossible to connect lack of LRP-1 activity with an effect of only one of these ligands. Furthermore, LRP-1-induced cell signalling may affect the cell environment, and inactivation of the receptor would also inactivate the LRP-1-mediated responses. More than forty LRP-1 ligands have been identified so far and many of them lead to opposite biological effects, such as proteinases and their endogenous inhibitors. The mechanism how LRP-1 induces a specific cell response by internalizing opposing effectors and how levels of these effectors are interconnected is not well understood yet and represents fascinating research for the future.

7.5 Concluding remarks

TIMP-3 has been shown to have protective effects in a number of diseases: (i) TIMP-3 inhibits cartilage degradation in both *in vitro* and in an *in vivo* model of osteoarthritis. (ii) TIMP-3 overexpression in cancer cells is protective against tumor growth and invasion, and (iii) TIMP-3 overexpression in macrophages decreases the incidence of vascular diseases in an atherogenic mouse model. Therefore, understanding how levels of TIMP-3 are regulated in the tissue may lead to therapeutic targets for these diseases. TIMP-3 levels in the ECM, and therefore its metalloproteinase inhibitory activity, have been shown to be regulated at different levels. TIMP-3 expression can be modulated by epigenetic mechanisms, cytokines, growth factors and micro-RNAs. Recently, work from our laboratory has shown that TIMP-3 levels in the ECM can also be post-translationally regulated by endocytosis.

In this thesis, I found that the endocytic receptor LRP-1 is the major regulator of TIMP-3 levels in the tissue. The shed form of LRP-1 also interacts with TIMP-3, preventing it from binding cell surface LRP-1, thus increasing the bioavailability of the inhibitor in the extracellular space. When TIMP-3 is bound to sLRP-1, it is still capable of inhibiting proteinases, therefore the equilibrium between sLRP-1 and cell-surface LRP-1 is crucial in controlling ECM proteolysis in the tissue. This discovery may be used in development of novel therapies for those pathologies associated with enhanced ECM degradation. A current study in our laboratory aims to generate

a TIMP-3 mutant that does not interact with LRP-1 and to test this mutant for its capability to inhibit cartilage breakdown in models of OA. In addition, we have planned to evaluate the effects of overexpression of sLRP-1 in different biological systems, such as in cartilage, vessels and cancer cells.

Chapter 8

References

Ahonen, M., Baker, A.H., and Kahari, V.M. (1998). Adenovirus-mediated gene delivery of tissue inhibitor of metalloproteinases-3 inhibits invasion and induces apoptosis in melanoma cells. Cancer Res *58*, 2310-2315.

Ahonen, M., Poukkula, M., Baker, A.H., Kashiwagi, M., Nagase, H., Eriksson, J.E., and Kahari, V.M. (2003). Tissue inhibitor of metalloproteinases-3 induces apoptosis in melanoma cells by stabilization of death receptors. Oncogene *22*, 2121-2134.

Aimes, R.T., and Quigley, J.P. (1995). Matrix metalloproteinase-2 is an interstitial collagenase. Inhibitor-free enzyme catalyzes the cleavage of collagen fibrils and soluble native type I collagen generating the specific 3/4- and 1/4-length fragments. J Biol Chem *270*, 5872-5876.

Ait-Slimane, T., Galmes, R., Trugnan, G., and Maurice, M. (2009). Basolateral internalization of GPI-anchored proteins occurs via a clathrin-independent flotillin-dependent pathway in polarized hepatic cells. Mol Biol Cell *20*, 3792-3800.

Amour, A., Knight, C.G., Webster, A., Slocombe, P.M., Stephens, P.E., Knauper, V., Docherty, A.J., and Murphy, G. (2000). The in vitro activity of ADAM-10 is inhibited by TIMP-1 and TIMP-3. FEBS Lett *473*, 275-279.

Amour, A., Slocombe, P.M., Webster, A., Butler, M., Knight, C.G., Smith, B.J., Stephens, P.E., Shelley, C., Hutton, M., Knauper, V.*, et al.* (1998). TNF-alpha converting enzyme (TACE) is inhibited by TIMP-3. FEBS Lett *435*, 39-44.

Anania, M.C., Sensi, M., Radaelli, E., Miranda, C., Vizioli, M.G., Pagliardini, S., Favini, E., Cleris, L., Supino, R., Formelli, F.*, et al.* (2011). TIMP3 regulates migration, invasion and in vivo tumorigenicity of thyroid tumor cells. Oncogene *30*, 3011-3023.

Andersen, O.M., Christensen, L.L., Christensen, P.A., Sorensen, E.S., Jacobsen, C., Moestrup, S.K., Etzerodt, M., and Thogersen, H.C. (2000). Identification of the minimal functional unit in the low density lipoprotein receptor-related protein for binding the receptor-associated protein (RAP). A conserved acidic residue in the complement-type repeats is important for recognition of RAP. J Biol Chem *275*, 21017-21024.

Andersen, O.M., Reiche, J., Schmidt, V., Gotthardt, M., Spoelgen, R., Behlke, J., von Arnim, C.A., Breiderhoff, T., Jansen, P., Wu, X.*, et al.* (2005). Neuronal sorting protein-related receptor sorLA/LR11 regulates processing of the amyloid precursor protein. Proc Natl Acad Sci U S A *102*, 13461-13466.

Andrade, N., Komnenovic, V., Blake, S.M., Jossin, Y., Howell, B., Goffinet, A., Schneider, W.J., and Nimpf, J. (2007). ApoER2/VLDL receptor and Dab1 in the rostral migratory stream function in postnatal neuronal migration independently of Reelin. Proc Natl Acad Sci U S A *104*, 8508-8513.

Apte, S.S. (2009). A disintegrin-like and metalloprotease (reprolysin-type) with thrombospondin type 1 motif (ADAMTS) superfamily: functions and mechanisms. J Biol Chem *284*, 31493-31497.

Arandjelovic, S., Hall, B.D., and Gonias, S.L. (2005). Mutation of lysine 1370 in full-length human alpha2-macroglobulin blocks binding to the low density lipoprotein receptor-related protein-1. Arch Biochem Biophys *438*, 29-35.

Ashcom, J.D., Tiller, S.E., Dickerson, K., Cravens, J.L., Argraves, W.S., and Strickland, D.K. (1990). The human alpha 2-macroglobulin receptor: identification of a 420-kD cell surface glycoprotein specific for the activated conformation of alpha 2-macroglobulin. J Cell Biol *110*, 1041-1048.

Babij, P., Zhao, W., Small, C., Kharode, Y., Yaworsky, P.J., Bouxsein, M.L., Reddy, P.S., Bodine, P.V., Robinson, J.A., Bhat, B.*, et al.* (2003). High bone mass in mice expressing a mutant LRP5 gene. J Bone Miner Res *18*, 960-974.

Bachman, K.E., Herman, J.G., Corn, P.G., Merlo, A., Costello, J.F., Cavenee, W.K., Baylin, S.B., and Graff, J.R. (1999). Methylation-associated silencing of the tissue inhibitor of metalloproteinase-3 gene suggest a suppressor role in kidney, brain, and other human cancers. Cancer Res *59*, 798-802.

Bacic, D., Capuano, P., Gisler, S.M., Pribanic, S., Christensen, E.I., Biber, J., Loffing, J., Kaissling, B., Wagner, C.A., and Murer, H. (2003). Impaired PTH-induced endocytotic down-regulation of the renal type IIa Na+/Pi-cotransporter in RAP-deficient mice with reduced megalin expression. Pflugers Arch *446*, 475-484.

Baeuerle, P.A., and Huttner, W.B. (1986). Chlorate--a potent inhibitor of protein sulfation in intact cells. Biochem Biophys Res Commun *141*, 870-877.

Baker, A.H., George, S.J., Zaltsman, A.B., Murphy, G., and Newby, A.C. (1999). Inhibition of invasion and induction of apoptotic cell death of cancer cell lines by overexpression of TIMP-3. Br J Cancer *79*, 1347-1355.

Barmina, O.Y., Walling, H.W., Fiacco, G.J., Freije, J.M., Lopez-Otin, C., Jeffrey, J.J., and Partridge, N.C. (1999). Collagenase-3 binds to a specific receptor and requires the

low density lipoprotein receptor-related protein for internalization. J Biol Chem *274*, 30087-30093.

Barnes, H., Ackermann, E.J., and van der Geer, P. (2003). v-Src induces Shc binding to tyrosine 63 in the cytoplasmic domain of the LDL receptor-related protein 1. Oncogene *22*, 3589-3597.

Barrett, A.J., Brown, M.A., and Sayers, C.A. (1979). The electrophoretically 'slow' and 'fast' forms of the alpha 2-macroglobulin molecule. Biochem J *181*, 401-418.

Barrett, A.J., and Starkey, P.M. (1973). The interaction of alpha 2-macroglobulin with proteinases. Characteristics and specificity of the reaction, and a hypothesis concerning its molecular mechanism. Biochem J *133*, 709-724.

Bauer, E.A., Stricklin, G.P., Jeffrey, J.J., and Eisen, A.Z. (1975). Collagenase production by human skin fibroblasts. Biochem Biophys Res Commun *64*, 232-240.

Beffert, U., Durudas, A., Weeber, E.J., Stolt, P.C., Giehl, K.M., Sweatt, J.D., Hammer, R.E., and Herz, J. (2006). Functional dissection of Reelin signaling by site-directed disruption of Disabled-1 adaptor binding to apolipoprotein E receptor 2: distinct roles in development and synaptic plasticity. J Neurosci *26*, 2041-2052.

Beffert, U., Weeber, E.J., Durudas, A., Qiu, S., Masiulis, I., Sweatt, J.D., Li, W.P., Adelmann, G., Frotscher, M., Hammer, R.E.*, et al.* (2005). Modulation of synaptic plasticity and memory by Reelin involves differential splicing of the lipoprotein receptor Apoer2. Neuron *47*, 567-579.

Beisiegel, U., Weber, W., Ihrke, G., Herz, J., and Stanley, K.K. (1989). The LDL-receptor-related protein, LRP, is an apolipoprotein E-binding protein. Nature *341*, 162-164.

Benhayon, D., Magdaleno, S., and Curran, T. (2003). Binding of purified Reelin to ApoER2 and VLDLR mediates tyrosine phosphorylation of Disabled-1. Brain Res Mol Brain Res *112*, 33-45.

Betsholtz, C., Lindblom, P., Bjarnegard, M., Enge, M., Gerhardt, H., and Lindahl, P. (2004). Role of platelet-derived growth factor in mesangium development and vasculopathies: lessons from platelet-derived growth factor and platelet-derived growth factor receptor mutations in mice. Curr Opin Nephrol Hypertens *13*, 45-52.

Bigg, H.F., Morrison, C.J., Butler, G.S., Bogoyevitch, M.A., Wang, Z., Soloway, P.D., and Overall, C.M. (2001). Tissue inhibitor of metalloproteinases-4 inhibits but does not support the activation of gelatinase A via efficient inhibition of membrane type 1-matrix metalloproteinase. Cancer Res *61*, 3610-3618.

Black, R.A., Castner, B., Slack, J., Tocker, J., Eisenman, J., Jacobsen, E., Delaney, J., Winters, D., Hecht, R., and Bendele, A. (2007). Injected TIMP-3 protects cartilage in a rat meniscal tear model. Osteoarthritis and Cartilage, S23-24.

Black, R.A., Rauch, C.T., Kozlosky, C.J., Peschon, J.J., Slack, J.L., Wolfson, M.F., Castner, B.J., Stocking, K.L., Reddy, P., Srinivasan, S.*, et al.* (1997). A metalloproteinase disintegrin that releases tumour-necrosis factor-alpha from cells. Nature *385*, 729-733.

Bode, W., Fernandez-Catalan, C., Tschesche, H., Grams, F., Nagase, H., and Maskos, K. (1999). Structural properties of matrix metalloproteinases. Cell Mol Life Sci *55*, 639-652.

Bond, M., Murphy, G., Bennett, M.R., Amour, A., Knauper, V., Newby, A.C., and Baker, A.H. (2000). Localization of the death domain of tissue inhibitor of metalloproteinase-3 to the N terminus. Metalloproteinase inhibition is associated with proapoptotic activity. J Biol Chem *275*, 41358-41363.

Bond, M., Murphy, G., Bennett, M.R., Newby, A.C., and Baker, A.H. (2002). Tissue inhibitor of metalloproteinase-3 induces a Fas-associated death domain-dependent type II apoptotic pathway. J Biol Chem *277*, 13787-13795.

Bondeson, J., Wainwright, S., Hughes, C., and Caterson, B. (2008). The regulation of the ADAMTS4 and ADAMTS5 aggrecanases in osteoarthritis: a review. Clin Exp Rheumatol *26*, 139-145.

Bonthron, D.T., Handin, R.I., Kaufman, R.J., Wasley, L.C., Orr, E.C., Mitsock, L.M., Ewenstein, B., Loscalzo, J., Ginsburg, D., and Orkin, S.H. (1986). Structure of pre-pro-von Willebrand factor and its expression in heterologous cells. Nature *324*, 270-273.

Boucher, P., Gotthardt, M., Li, W.P., Anderson, R.G., and Herz, J. (2003). LRP: role in vascular wall integrity and protection from atherosclerosis. Science *300*, 329-332.

Brandan, E., Retamal, C., Cabello-Verrugio, C., and Marzolo, M.P. (2006). The low density lipoprotein receptor-related protein functions as an endocytic receptor for decorin. J Biol Chem *281*, 31562-31571.

Brew, K., and Nagase, H. (2010). The tissue inhibitors of metalloproteinases (TIMPs): an ancient family with structural and functional diversity. Biochim Biophys Acta *1803*, 55-71.

Brown, F.D., Rozelle, A.L., Yin, H.L., Balla, T., and Donaldson, J.G. (2001). Phosphatidylinositol 4,5-bisphosphate and Arf6-regulated membrane traffic. J Cell Biol *154*, 1007-1017.

Brown, M.S., and Goldstein, J.L. (1974). Familial hypercholesterolemia: defective binding of lipoproteins to cultured fibroblasts associated with impaired regulation of 3-hydroxy-3-methylglutaryl coenzyme A reductase activity. Proc Natl Acad Sci U S A *71*, 788-792.

Brown, M.S., and Goldstein, J.L. (1979). Receptor-mediated endocytosis: insights from the lipoprotein receptor system. Proc Natl Acad Sci U S A *76*, 3330-3337.

Brown, R.E. (1998). Sphingolipid organization in biomembranes: what physical studies of model membranes reveal. J Cell Sci *111 (Pt 1)*, 1-9.

Brown, S.A., Via, D.P., Gotto, A.M., Jr., Bradley, W.A., and Gianturco, S.H. (1986). Apolipoprotein E-mediated binding of hypertriglyceridemic very low density lipoproteins to isolated low density lipoprotein receptors detected by ligand blotting. Biochem Biophys Res Commun *139*, 333-340.

Bu, G. (1998). Receptor-associated protein: a specialized chaperone and antagonist for members of the LDL receptor gene family. Curr Opin Lipidol *9*, 149-155.

Bu, G., Williams, S., Strickland, D.K., and Schwartz, A.L. (1992). Low density lipoprotein receptor-related protein/alpha 2-macroglobulin receptor is an hepatic receptor for tissue-type plasminogen activator. Proc Natl Acad Sci U S A *89*, 7427-7431.

Bundy, H.F., and Mehl, J.W. (1959). Trypsin inhibitors of human serum. II. Isolation of the alpha 1-inhibitor and its partial characterization. J Biol Chem *234*, 1124-1128.

Bury, A.F., and Roberts, R.C. (1982). Comparison of the polypeptide composition of cystic fibrosis plasma with normal plasma by high resolution electrophoresis. Clin Chim Acta *118*, 45-55.

Cardellini, M., Menghini, R., Martelli, E., Casagrande, V., Marino, A., Rizza, S., Porzio, O., Mauriello, A., Solini, A., Ippoliti, A*., et al.* (2009). TIMP3 is reduced in

atherosclerotic plaques from subjects with type 2 diabetes and increased by SirT1. Diabetes *58*, 2396-2401.

Casagrande, V., Menghini, R., Menini, S., Marino, A., Marchetti, V., Cavalera, M., Fabrizi, M., Hribal, M.L., Pugliese, G., Gentileschi, P.*, et al.* (2012). Overexpression of tissue inhibitor of metalloproteinase 3 in macrophages reduces atherosclerosis in low-density lipoprotein receptor knockout mice. Arterioscler Thromb Vasc Biol *32*, 74-81.

Castellano, J., Aledo, R., Sendra, J., Costales, P., Juan-Babot, O., Badimon, L., and Llorente-Cortes, V. (2011). Hypoxia stimulates low-density lipoprotein receptor-related protein-1 expression through hypoxia-inducible factor-1alpha in human vascular smooth muscle cells. Arterioscler Thromb Vasc Biol *31*, 1411-1420.

Cawston, T.E., Galloway, W.A., Mercer, E., Murphy, G., and Reynolds, J.J. (1981). Purification of rabbit bone inhibitor of collagenase. Biochem J *195*, 159-165.

Cengiz, B., Gunduz, M., Nagatsuka, H., Beder, L., Gunduz, E., Tamamura, R., Mahmut, N., Fukushima, K., Ali, M.A., Naomoto, Y.*, et al.* (2007). Fine deletion mapping of chromosome 2q21-37 shows three preferentially deleted regions in oral cancer. Oral Oncol *43*, 241-247.

Chang, S.H., Chang, H.C., and Hung, W.C. (2008). Transcriptional repression of tissue inhibitor of metalloproteinase-3 by Epstein-Barr virus latent membrane protein 1 enhances invasiveness of nasopharyngeal carcinoma cells. Oral Oncol *44*, 891-897.

Chappell, D.A., Fry, G.L., Waknitz, M.A., Muhonen, L.E., and Pladet, M.W. (1993). Low density lipoprotein receptors bind and mediate cellular catabolism of normal very low density lipoproteins in vitro. J Biol Chem *268*, 25487-25493.

Chen, H., Strickland, D.K., and Mosher, D.F. (1996). Metabolism of thrombospondin 2. Binding and degradation by 3t3 cells and glycosaminoglycan-variant Chinese hamster ovary cells. J Biol Chem *271*, 15993-15999.

Chen, W.J., Goldstein, J.L., and Brown, M.S. (1990). NPXY, a sequence often found in cytoplasmic tails, is required for coated pit-mediated internalization of the low density lipoprotein receptor. J Biol Chem *265*, 3116-3123.

Cho, W.J., Jeremic, A., and Jena, B.P. (2005). Size of supramolecular SNARE complex: membrane-directed self-assembly. J Am Chem Soc *127*, 10156-10157.

Christensen, E.I., and Willnow, T.E. (1999). Essential role of megalin in renal proximal tubule for vitamin homeostasis. J Am Soc Nephrol *10*, 2224-2236.

Chung, L., Dinakarpandian, D., Yoshida, N., Lauer-Fields, J.L., Fields, G.B., Visse, R., and Nagase, H. (2004). Collagenase unwinds triple-helical collagen prior to peptide bond hydrolysis. Embo J *23*, 3020-3030.

Chung, L., Shimokawa, K., Dinakarpandian, D., Grams, F., Fields, G.B., and Nagase, H. (2000). Identification of the (183)RWTNNFREY(191) region as a critical segment of matrix metalloproteinase 1 for the expression of collagenolytic activity. J Biol Chem *275*, 29610-29617.

Cohen, A.W., Hnasko, R., Schubert, W., and Lisanti, M.P. (2004). Role of caveolae and caveolins in health and disease. Physiol Rev *84*, 1341-1379.

Colige, A., Vandenberghe, I., Thiry, M., Lambert, C.A., Van Beeumen, J., Li, S.W., Prockop, D.J., Lapiere, C.M., and Nusgens, B.V. (2002). Cloning and characterization of ADAMTS-14, a novel ADAMTS displaying high homology with ADAMTS-2 and ADAMTS-3. J Biol Chem *277*, 5756-5766.

Conese, M., and Blasi, F. (1995). The urokinase/urokinase-receptor system and cancer invasion. Baillieres Clin Haematol *8*, 365-389.

Conese, M., Nykjaer, A., Petersen, C.M., Cremona, O., Pardi, R., Andreasen, P.A., Gliemann, J., Christensen, E.I., and Blasi, F. (1995). alpha-2 Macroglobulin receptor/Ldl receptor-related protein(Lrp)-dependent internalization of the urokinase receptor. J Cell Biol *131*, 1609-1622.

Conese, M., Olson, D., and Blasi, F. (1994). Protease nexin-1-urokinase complexes are internalized and degraded through a mechanism that requires both urokinase receptor and alpha 2-macroglobulin receptor. J Biol Chem *269*, 17886-17892.

Conner, S.D., and Schmid, S.L. (2003). Differential requirements for AP-2 in clathrin-mediated endocytosis. J Cell Biol *162*, 773-779.

Cortese, K., Sahores, M., Madsen, C.D., Tacchetti, C., and Blasi, F. (2008). Clathrin and LRP-1-independent constitutive endocytosis and recycling of uPAR. PLoS One *3*, e3730.

Couchman, J.R. (2010). Transmembrane signaling proteoglycans. Annu Rev Cell Dev Biol *26*, 89-114.

Crisp, R.J., Knauer, D.J., and Knauer, M.F. (2000). Roles of the heparin and low density lipid receptor-related protein-binding sites of protease nexin 1 (PN1) in urokinase-PN1 complex catabolism. The PN1 heparin-binding site mediates complex retention and degradation but not cell surface binding or internalization. J Biol Chem *275*, 19628-19637.

Cruz-Munoz, W., Kim, I., and Khokha, R. (2006a). TIMP-3 deficiency in the host, but not in the tumor, enhances tumor growth and angiogenesis. Oncogene *25*, 650-655.

Cruz-Munoz, W., Sanchez, O.H., Di Grappa, M., English, J.L., Hill, R.P., and Khokha, R. (2006b). Enhanced metastatic dissemination to multiple organs by melanoma and lymphoma cells in timp-3-/- mice. Oncogene *25*, 6489-6496.

d'Ortho, M.P., Will, H., Atkinson, S., Butler, G., Messent, A., Gavrilovic, J., Smith, B., Timpl, R., Zardi, L., and Murphy, G. (1997). Membrane-type matrix metalloproteinases 1 and 2 exhibit broad-spectrum proteolytic capacities comparable to many matrix metalloproteinases. Eur J Biochem *250*, 751-757.

Damm, E.M., Pelkmans, L., Kartenbeck, J., Mezzacasa, A., Kurzchalia, T., and Helenius, A. (2005). Clathrin- and caveolin-1-independent endocytosis: entry of simian virus 40 into cells devoid of caveolae. J Cell Biol *168*, 477-488.

Dano, K., Andreasen, P.A., Grondahl-Hansen, J., Kristensen, P., Nielsen, L.S., and Skriver, L. (1985). Plasminogen activators, tissue degradation, and cancer. Adv Cancer Res *44*, 139-266.

Deane, R., Sagare, A., and Zlokovic, B.V. (2008). The role of the cell surface LRP and soluble LRP in blood-brain barrier Abeta clearance in Alzheimer's disease. Curr Pharm Des *14*, 1601-1605.

Dedieu, S., Langlois, B., Devy, J., Sid, B., Henriet, P., Sartelet, H., Bellon, G., Emonard, H., and Martiny, L. (2008). LRP-1 silencing prevents malignant cell invasion despite increased pericellular proteolytic activities. Mol Cell Biol *28*, 2980-2995.

Di Fiore, P.P., and De Camilli, P. (2001). Endocytosis and signaling. an inseparable partnership. Cell *106*, 1-4.

Dietrich, M.F., van der Weyden, L., Prosser, H.M., Bradley, A., Herz, J., and Adams, D.J. (2010). Ectodomains of the LDL receptor-related proteins LRP1b and LRP4 have anchorage independent functions in vivo. PLoS One *5*, e9960.

Doherty, G.J., and McMahon, H.T. (2009). Mechanisms of endocytosis. Annu Rev Biochem *78*, 857-902.

Dolmer, K., and Gettins, P.G. (2006). Three complement-like repeats compose the complete alpha2-macroglobulin binding site in the second ligand binding cluster of the low density lipoprotein receptor-related protein. J Biol Chem *281*, 34189-34196.

Dong, Y., Lathrop, W., Weaver, D., Qiu, Q., Cini, J., Bertolini, D., and Chen, D. (1998). Molecular cloning and characterization of LR3, a novel LDL receptor family protein with mitogenic activity. Biochem Biophys Res Commun *251*, 784-790.

Dumas, J.J., Merithew, E., Sudharshan, E., Rajamani, D., Hayes, S., Lawe, D., Corvera, S., and Lambright, D.G. (2001). Multivalent endosome targeting by homodimeric EEA1. Mol Cell *8*, 947-958.

Eads, C.A., Lord, R.V., Wickramasinghe, K., Long, T.I., Kurumboor, S.K., Bernstein, L., Peters, J.H., DeMeester, S.R., DeMeester, T.R., Skinner, K.A*., et al.* (2001). Epigenetic patterns in the progression of esophageal adenocarcinoma. Cancer Res *61*, 3410-3418.

Echtermeyer, F., Bertrand, J., Dreier, R., Meinecke, I., Neugebauer, K., Fuerst, M., Lee, Y.J., Song, Y.W., Herzog, C., Theilmeier, G*., et al.* (2009). Syndecan-4 regulates ADAMTS-5 activation and cartilage breakdown in osteoarthritis. Nat Med *15*, 1072-1076.

Edeling, M.A., Smith, C., and Owen, D. (2006). Life of a clathrin coat: insights from clathrin and AP structures. Nat Rev Mol Cell Biol *7*, 32-44.

Edwards, D.R., Handsley, M.M., and Pennington, C.J. (2008). The ADAM metalloproteinases. Molecular aspects of medicine *29*, 258-289.

Egeblad, M., and Werb, Z. (2002). New functions for the matrix metalloproteinases in cancer progression. Nat Rev Cancer *2*, 161-174.

Elward, K., and Gasque, P. (2003). "Eat me" and "don't eat me" signals govern the innate immune response and tissue repair in the CNS: emphasis on the critical role of the complement system. Mol Immunol *40*, 85-94.

Emonard, H., Bellon, G., Troeberg, L., Berton, A., Robinet, A., Henriet, P., Marbaix, E., Kirkegaard, K., Patthy, L., Eeckhout, Y*., et al.* (2004). Low density lipoprotein receptor-related protein mediates endocytic clearance of pro-MMP-2.TIMP-2

complex through a thrombospondin-independent mechanism. J Biol Chem *279*, 54944-54951.

Engelholm, L.H., List, K., Netzel-Arnett, S., Cukierman, E., Mitola, D.J., Aaronson, H., Kjoller, L., Larsen, J.K., Yamada, K.M., Strickland, D.K.*, et al.* (2003). uPARAP/Endo180 is essential for cellular uptake of collagen and promotes fibroblast collagen adhesion. J Cell Biol *160*, 1009-1015.

English, W.R., Holtz, B., Vogt, G., Knauper, V., and Murphy, G. (2001). Characterization of the role of the "MT-loop": an eight-amino acid insertion specific to progelatinase A (MMP2) activating membrane-type matrix metalloproteinases. J Biol Chem *276*, 42018-42026.

Esko, J.D., Stewart, T.E., and Taylor, W.H. (1985). Animal cell mutants defective in glycosaminoglycan biosynthesis. Proc Natl Acad Sci U S A *82*, 3197-3201.

Fata, J.E., Leco, K.J., Voura, E.B., Yu, H.Y., Waterhouse, P., Murphy, G., Moorehead, R.A., and Khokha, R. (2001). Accelerated apoptosis in the Timp-3-deficient mammary gland. J Clin Invest *108*, 831-841.

Fay, P.J., and Jenkins, P.V. (2005). Mutating factor VIII: lessons from structure to function. Blood Rev *19*, 15-27.

Fedak, P.W., Smookler, D.S., Kassiri, Z., Ohno, N., Leco, K.J., Verma, S., Mickle, D.A., Watson, K.L., Hojilla, C.V., Cruz, W.*, et al.* (2004). TIMP-3 deficiency leads to dilated cardiomyopathy. Circulation *110*, 2401-2409.

Feldman, A.L., Stetler-Stevenson, W.G., Costouros, N.G., Knezevic, V., Baibakov, G., Alexander, H.R., Jr., Lorang, D., Hewitt, S.M., Seo, D.W., Miller, M.S.*, et al.* (2004). Modulation of tumor-host interactions, angiogenesis, and tumor growth by tissue inhibitor of metalloproteinase 2 via a novel mechanism. Cancer Res *64*, 4481-4486.

Ferguson, S.M., Raimondi, A., Paradise, S., Shen, H., Mesaki, K., Ferguson, A., Destaing, O., Ko, G., Takasaki, J., Cremona, O.*, et al.* (2009). Coordinated actions of actin and BAR proteins upstream of dynamin at endocytic clathrin-coated pits. Dev Cell *17*, 811-822.

Fernandes, R.J., Hirohata, S., Engle, J.M., Colige, A., Cohn, D.H., Eyre, D.R., and Apte, S.S. (2001). Procollagen II amino propeptide processing by ADAMTS-3. Insights on dermatosparaxis. J Biol Chem *276*, 31502-31509.

Fernandez-Catalan, C., Bode, W., Huber, R., Turk, D., Calvete, J.J., Lichte, A., Tschesche, H., and Maskos, K. (1998). Crystal structure of the complex formed by the membrane type 1-matrix metalloproteinase with the tissue inhibitor of metalloproteinases-2, the soluble progelatinase A receptor. Embo J *17*, 5238-5248.

Fiorentino, L., Vivanti, A., Cavalera, M., Marzano, V., Ronci, M., Fabrizi, M., Menini, S., Pugliese, G., Menghini, R., Khokha, R.*, et al.* (2010). Increased tumor necrosis factor alpha-converting enzyme activity induces insulin resistance and hepatosteatosis in mice. Hepatology *51*, 103-110.

Fisher, C., Beglova, N., and Blacklow, S.C. (2006). Structure of an LDLR-RAP complex reveals a general mode for ligand recognition by lipoprotein receptors. Mol Cell *22*, 277-283.

Fournier, B., and Philpott, D.J. (2005). Recognition of Staphylococcus aureus by the innate immune system. Clin Microbiol Rev *18*, 521-540.

Frykman, P.K., Brown, M.S., Yamamoto, T., Goldstein, J.L., and Herz, J. (1995). Normal plasma lipoproteins and fertility in gene-targeted mice homozygous for a disruption in the gene encoding very low density lipoprotein receptor. Proc Natl Acad Sci U S A *92*, 8453-8457.

Fujikawa, K., Suzuki, H., McMullen, B., and Chung, D. (2001). Purification of human von Willebrand factor-cleaving protease and its identification as a new member of the metalloproteinase family. Blood *98*, 1662-1666.

Fujino, T., Asaba, H., Kang, M.J., Ikeda, Y., Sone, H., Takada, S., Kim, D.H., Ioka, R.X., Ono, M., Tomoyori, H.*, et al.* (2003). Low-density lipoprotein receptor-related protein 5 (LRP5) is essential for normal cholesterol metabolism and glucose-induced insulin secretion. Proc Natl Acad Sci U S A *100*, 229-234.

Furlan, M., Robles, R., and Lammle, B. (1996). Partial purification and characterization of a protease from human plasma cleaving von Willebrand factor to fragments produced by in vivo proteolysis. Blood *87*, 4223-4234.

Gabriely, G., Wurdinger, T., Kesari, S., Esau, C.C., Burchard, J., Linsley, P.S., and Krichevsky, A.M. (2008). MicroRNA 21 promotes glioma invasion by targeting matrix metalloproteinase regulators. Mol Cell Biol *28*, 5369-5380.

Galli, T., and Haucke, V. (2001). Cycling of synaptic vesicles: how far? How fast! Sci STKE *2001*, re1.

Gandhi, N.S., and Mancera, R.L. (2008). The structure of glycosaminoglycans and their interactions with proteins. Chem Biol Drug Des *72*, 455-482.

Garofalo, M., Di Leva, G., Romano, G., Nuovo, G., Suh, S.S., Ngankeu, A., Taccioli, C., Pichiorri, F., Alder, H., Secchiero, P.*, et al.* (2009). miR-221&222 regulate TRAIL resistance and enhance tumorigenicity through PTEN and TIMP3 downregulation. Cancer Cell *16*, 498-509.

Gaultier, A., Arandjelovic, S., Li, X., Janes, J., Dragojlovic, N., Zhou, G.P., Dolkas, J., Myers, R.R., Gonias, S.L., and Campana, W.M. (2008a). A shed form of LDL receptor-related protein-1 regulates peripheral nerve injury and neuropathic pain in rodents. J Clin Invest *118*, 161-172.

Gaultier, A., Arandjelovic, S., Niessen, S., Overton, C.D., Linton, M.F., Fazio, S., Campana, W.M., Cravatt, B.F., 3rd, and Gonias, S.L. (2008b). Regulation of tumor necrosis factor receptor-1 and the IKK-NF-kappaB pathway by LDL receptor-related protein explains the antiinflammatory activity of this receptor. Blood *111*, 5316-5325.

Gendron, C., Kashiwagi, M., Hughes, C., Caterson, B., and Nagase, H. (2003). TIMP-3 inhibits aggrecanase-mediated glycosaminoglycan release from cartilage explants stimulated by catabolic factors. FEBS Lett *555*, 431-436.

Gendron, C., Kashiwagi, M., Lim, N.H., Enghild, J.J., Thogersen, I.B., Hughes, C., Caterson, B., and Nagase, H. (2007). Proteolytic activities of human ADAMTS-5: comparative studies with ADAMTS-4. J Biol Chem *282*, 18294-18306.

Gill, S.E., Pape, M.C., Khokha, R., Watson, A.J., and Leco, K.J. (2003). A null mutation for tissue inhibitor of metalloproteinases-3 (Timp-3) impairs murine bronchiole branching morphogenesis. Dev Biol *261*, 313-323.

Glebov, O.O., Bright, N.A., and Nichols, B.J. (2006). Flotillin-1 defines a clathrin-independent endocytic pathway in mammalian cells. Nat Cell Biol *8*, 46-54.

Gomis-Rüth, F.X., Maskos, K., Betz, M., Bergner, A., Huber, R., Suzuki, K., Yoshida, N., Nagase, H., Brew, K., Bourenkov, G.P.*, et al.* (1997). Mechanism of inhibition of the human matrix metalloproteinase stromelysin-1 by TIMP-1. Nature *389*, 77-81.

Gorovoy, M., Gaultier, A., Campana, W.M., Firestein, G.S., and Gonias, S.L. (2010). Inflammatory mediators promote production of shed LRP1/CD91, which regulates cell signaling and cytokine expression by macrophages. J Leukoc Biol *88*, 769-778.

Grant, B.D., and Donaldson, J.G. (2009). Pathways and mechanisms of endocytic recycling. Nat Rev Mol Cell Biol *10*, 597-608.

Greenaway, J., Lawler, J., Moorehead, R., Bornstein, P., Lamarre, J., and Petrik, J. (2007). Thrombospondin-1 inhibits VEGF levels in the ovary directly by binding and internalization via the low density lipoprotein receptor-related protein-1 (LRP-1). J Cell Physiol *210*, 807-818.

Greene, J., Wang, M., Liu, Y.E., Raymond, L.A., Rosen, C., and Shi, Y.E. (1996). Molecular cloning and characterization of human tissue inhibitor of metalloproteinase 4. J Biol Chem *271*, 30375-30380.

Gunther, M., Haubeck, H.D., van de Leur, E., Blaser, J., Bender, S., Gutgemann, I., Fischer, D.C., Tschesche, H., Greiling, H., Heinrich, P.C*., et al.* (1994). Transforming growth factor beta 1 regulates tissue inhibitor of metalloproteinases-1 expression in differentiated human articular chondrocytes. Arthritis Rheum *37*, 395-405.

Haas, J., Beer, A.G., Widschwendter, P., Oberdanner, J., Salzmann, K., Sarg, B., Lindner, H., Herz, J., Patsch, J.R., and Marschang, P. (2011). LRP1b shows restricted expression in human tissues and binds to several extracellular ligands, including fibrinogen and apoE-carrying lipoproteins. Atherosclerosis *216*, 342-347.

Haddock, G., Cross, A.K., Allan, S., Sharrack, B., Callaghan, J., Bunning, R.A., Buttle, D.J., and Woodroofe, M.N. (2007). Brevican and phosphacan expression and localization following transient middle cerebral artery occlusion in the rat. Biochem Soc Trans *35*, 692-694.

Hahn-Dantona, E., Ruiz, J.F., Bornstein, P., and Strickland, D.K. (2001). The low density lipoprotein receptor-related protein modulates levels of matrix metalloproteinase 9 (MMP-9) by mediating its cellular catabolism. J Biol Chem *276*, 15498-15503.

Hamze, A.B., Wei, S., Bahudhanapati, H., Kota, S., Acharya, K.R., and Brew, K. (2007). Constraining specificity in the N-domain of tissue inhibitor of metalloproteinases-1; gelatinase-selective inhibitors. Protein Sci *16*, 1905-1913.

Han, C.Z., and Ravichandran, K.S. (2011). Metabolic Connections during Apoptotic Cell Engulfment. Cell *147*, 1442-1445.

Hanover, J.A., Willingham, M.C., and Pastan, I. (1983). Receptor-mediated endocytosis of alpha 2-macroglobulin: solubilization and partial purification of the fibroblast alpha 2-macroglobulin receptor. Ann N Y Acad Sci *421*, 410-423.

Harpel, P.C. (1973). Studies on human plasma alpha 2-macroglobulin-enzyme interactions. Evidence for proteolytic modification of the subunit chain structure. J Exp Med *138*, 508-521.

Harrison, I.P., and McKnight, A. (2011). Cellular entry via an actin and clathrin-dependent route is required for Lv2 restriction of HIV-2. Virology *415*, 47-55.

Hartmann, D., de Strooper, B., Serneels, L., Craessaerts, K., Herreman, A., Annaert, W., Umans, L., Lubke, T., Lena Illert, A., von Figura, K*., et al.* (2002). The disintegrin/metalloprotease ADAM 10 is essential for Notch signalling but not for alpha-secretase activity in fibroblasts. Hum Mol Genet *11*, 2615-2624.

Hayakawa, T., Yamashita, K., Tanzawa, K., Uchijima, E., and Iwata, K. (1992). Growth-promoting activity of tissue inhibitor of metalloproteinases-1 (TIMP-1) for a wide range of cells. A possible new growth factor in serum. FEBS Lett *298*, 29-32.

Heerklotz, H. (2002). Triton promotes domain formation in lipid raft mixtures. Biophys J *83*, 2693-2701.

Heerklotz, H., Szadkowska, H., Anderson, T., and Seelig, J. (2003). The sensitivity of lipid domains to small perturbations demonstrated by the effect of Triton. J Mol Biol *329*, 793-799.

Henne, W.M., Boucrot, E., Meinecke, M., Evergren, E., Vallis, Y., Mittal, R., and McMahon, H.T. (2010). FCHo proteins are nucleators of clathrin-mediated endocytosis. Science *328*, 1281-1284.

Herz, J., Clouthier, D.E., and Hammer, R.E. (1992). LDL receptor-related protein internalizes and degrades uPA-PAI-1 complexes and is essential for embryo implantation. Cell *71*, 411-421.

Herz, J., Hamann, U., Rogne, S., Myklebost, O., Gausepohl, H., and Stanley, K.K. (1988). Surface location and high affinity for calcium of a 500-kd liver membrane protein closely related to the LDL-receptor suggest a physiological role as lipoprotein receptor. Embo J *7*, 4119-4127.

Herz, J., Kowal, R.C., Ho, Y.K., Brown, M.S., and Goldstein, J.L. (1990). Low density lipoprotein receptor-related protein mediates endocytosis of monoclonal antibodies in cultured cells and rabbit liver. J Biol Chem *265*, 21355-21362.

Herz, J., and Strickland, D.K. (2001). LRP: a multifunctional scavenger and signaling receptor. J Clin Invest *108*, 779-784.

Hiesberger, T., Trommsdorff, M., Howell, B.W., Goffinet, A., Mumby, M.C., Cooper, J.A., and Herz, J. (1999). Direct binding of Reelin to VLDL receptor and ApoE receptor 2 induces tyrosine phosphorylation of disabled-1 and modulates tau phosphorylation. Neuron *24*, 481-489.

Higazi, A.A., Mazar, A., Wang, J., Reilly, R., Henkin, J., Kniss, D., and Cines, D. (1996). Single-chain urokinase-type plasminogen activator bound to its receptor is relatively resistant to plasminogen activator inhibitor type 1. Blood *87*, 3545-3549.

Hill, K.E., Zhou, J., McMahan, W.J., Motley, A.K., Atkins, J.F., Gesteland, R.F., and Burk, R.F. (2003). Deletion of selenoprotein P alters distribution of selenium in the mouse. J Biol Chem *278*, 13640-13646.

Hinshaw, J.E., and Schmid, S.L. (1995). Dynamin self-assembles into rings suggesting a mechanism for coated vesicle budding. Nature *374*, 190-192.

Hobbs, H.H., Russell, D.W., Brown, M.S., and Goldstein, J.L. (1990). The LDL receptor locus in familial hypercholesterolemia: mutational analysis of a membrane protein. Annu Rev Genet *24*, 133-170.

Holmen, S.L., Giambernardi, T.A., Zylstra, C.R., Buckner-Berghuis, B.D., Resau, J.H., Hess, J.F., Glatt, V., Bouxsein, M.L., Ai, M., Warman, M.L.*, et al.* (2004). Decreased BMD and limb deformities in mice carrying mutations in both Lrp5 and Lrp6. J Bone Miner Res *19*, 2033-2040.

Honing, S., Ricotta, D., Krauss, M., Spate, K., Spolaore, B., Motley, A., Robinson, M., Robinson, C., Haucke, V., and Owen, D.J. (2005). Phosphatidylinositol-(4,5)-bisphosphate regulates sorting signal recognition by the clathrin-associated adaptor complex AP2. Mol Cell *18*, 519-531.

Hopkins, C.R., Miller, K., and Beardmore, J.M. (1985). Receptor-mediated endocytosis of transferrin and epidermal growth factor receptors: a comparison of constitutive and ligand-induced uptake. J Cell Sci Suppl *3*, 173-186.

Horn, I.R., van den Berg, B.M., Moestrup, S.K., Pannekoek, H., and van Zonneveld, A.J. (1998). Plasminogen activator inhibitor 1 contains a cryptic high affinity receptor binding site that is exposed upon complex formation with tissue-type plasminogen activator. Thromb Haemost *80*, 822-828.

Hosaka, K., Takeda, T., Iino, N., Hosojima, M., Sato, H., Kaseda, R., Yamamoto, K., Kobayashi, A., Gejyo, F., and Saito, A. (2009). Megalin and nonmuscle myosin heavy chain IIA interact with the adaptor protein Disabled-2 in proximal tubule cells. Kidney Int *75*, 1308-1315.

Hu, K., Yang, J., Tanaka, S., Gonias, S.L., Mars, W.M., and Liu, Y. (2006). Tissue-type plasminogen activator acts as a cytokine that triggers intracellular signal transduction and induces matrix metalloproteinase-9 gene expression. J Biol Chem *281*, 2120-2127.

Hu, Y., Sun, H., Owens, R.T., Gu, Z., Wu, J., Chen, Y.Q., O'Flaherty, J.T., and Edwards, I.J. (2010). Syndecan-1-dependent suppression of PDK1/Akt/bad signaling by docosahexaenoic acid induces apoptosis in prostate cancer. Neoplasia *12*, 826-836.

Huang, S.S., Ling, T.Y., Tseng, W.F., Huang, Y.H., Tang, F.M., Leal, S.M., and Huang, J.S. (2003). Cellular growth inhibition by IGFBP-3 and TGF-beta1 requires LRP-1. Faseb J *17*, 2068-2081.

Huotari, J., and Helenius, A. (2011). Endosome maturation. Embo J *30*, 3481-3500.

Hurskainen, T.L., Hirohata, S., Seldin, M.F., and Apte, S.S. (1999). ADAM-TS5, ADAM-TS6, and ADAM-TS7, novel members of a new family of zinc metalloproteases. General features and genomic distribution of the ADAM-TS family. J Biol Chem *274*, 25555-25563.

Hussain, M.M. (2000). A proposed model for the assembly of chylomicrons. Atherosclerosis *148*, 1-15.

Hussain, M.M., Strickland, D.K., and Bakillah, A. (1999). The mammalian low-density lipoprotein receptor family. Annu Rev Nutr *19*, 141-172.

Iadonato, S.P., Bu, G., Maksymovitch, E.A., and Schwartz, A.L. (1993). Interaction of a 39 kDa protein with the low-density-lipoprotein-receptor-related protein (LRP) on rat hepatoma cells. Biochem J *296 (Pt 3)*, 867-875.

Iijima, H., Miyazawa, M., Sakai, J., Magoori, K., Ito, M.R., Suzuki, H., Nose, M., Kawarabayasi, Y., and Yamamoto, T.T. (1998). Expression and characterization of a very low density lipoprotein receptor variant lacking the O-linked sugar region generated by alternative splicing. J Biochem *124*, 747-755.

Ishibashi, S., Brown, M.S., Goldstein, J.L., Gerard, R.D., Hammer, R.E., and Herz, J. (1993). Hypercholesterolemia in low density lipoprotein receptor knockout mice and its reversal by adenovirus-mediated gene delivery. J Clin Invest *92*, 883-893.

Ishimoto, H., Yanagihara, K., Araki, N., Mukae, H., Sakamoto, N., Izumikawa, K., Seki, M., Miyazaki, Y., Hirakata, Y., Mizuta, Y*., et al.* (2008). Single-cell observation of phagocytosis by human blood dendritic cells. Jpn J Infect Dis *61*, 294-297.

Ito, A., and Nagase, H. (1988). Evidence that human rheumatoid synovial matrix metalloproteinase 3 is an endogenous activator of procollagenase. Arch Biochem Biophys *267*, 211-216.

Itoh, Y., Binner, S., and Nagase, H. (1995). Steps involved in activation of the complex of pro-matrix metalloproteinase 2 (progelatinase A) and tissue inhibitor of metalloproteinases (TIMP)-2 by 4-aminophenylmercuric acetate. Biochem J *308 (Pt 2)*, 645-651.

Jacobsen, L., Madsen, P., Moestrup, S.K., Lund, A.H., Tommerup, N., Nykjaer, A., Sottrup-Jensen, L., Gliemann, J., and Petersen, C.M. (1996). Molecular characterization of a novel human hybrid-type receptor that binds the alpha2-macroglobulin receptor-associated protein. J Biol Chem *271*, 31379-31383.

Jensen, J.K., Dolmer, K., and Gettins, P.G. (2009). Specificity of binding of the low density lipoprotein receptor-related protein to different conformational states of the clade E serpins plasminogen activator inhibitor-1 and proteinase nexin-1. J Biol Chem *284*, 17989-17997.

Jensen, P.H., Christensen, E.I., Ebbesen, P., Gliemann, J., and Andreasen, P.A. (1990). Lysosomal degradation of receptor-bound urokinase-type plasminogen activator is enhanced by its inhibitors in human trophoblastic choriocarcinoma cells. Cell Regul *1*, 1043-1056.

Johnson, E.B., Hammer, R.E., and Herz, J. (2005). Abnormal development of the apical ectodermal ridge and polysyndactyly in Megf7-deficient mice. Hum Mol Genet *14*, 3523-3538.

Jung, K.K., Liu, X.W., Chirco, R., Fridman, R., and Kim, H.R. (2006). Identification of CD63 as a tissue inhibitor of metalloproteinase-1 interacting cell surface protein. Embo J *25*, 3934-3942.

Jung, N., Wienisch, M., Gu, M., Rand, J.B., Muller, S.L., Krause, G., Jorgensen, E.M., Klingauf, J., and Haucke, V. (2007). Molecular basis of synaptic vesicle cargo recognition by the endocytic sorting adaptor stonin 2. J Cell Biol *179*, 1497-1510.

Kadomatsu, K. (2005). The midkine family in cancer, inflammation and neural development. Nagoya J Med Sci *67*, 71-82.

Kanekiyo, T., Zhang, J., Liu, Q., Liu, C.C., Zhang, L., and Bu, G. (2011). Heparan sulphate proteoglycan and the low-density lipoprotein receptor-related protein 1 constitute major pathways for neuronal amyloid-beta uptake. J Neurosci *31*, 1644-1651.

Kang, D.E., Pietrzik, C.U., Baum, L., Chevallier, N., Merriam, D.E., Kounnas, M.Z., Wagner, S.L., Troncoso, J.C., Kawas, C.H., Katzman, R.*, et al.* (2000). Modulation of amyloid beta-protein clearance and Alzheimer's disease susceptibility by the LDL receptor-related protein pathway. J Clin Invest *106*, 1159-1166.

Kang, D.E., Saitoh, T., Chen, X., Xia, Y., Masliah, E., Hansen, L.A., Thomas, R.G., Thal, L.J., and Katzman, R. (1997). Genetic association of the low-density lipoprotein receptor-related protein gene (LRP), an apolipoprotein E receptor, with late-onset Alzheimer's disease. Neurology *49*, 56-61.

Kang, K.H., Park, S.Y., Rho, S.B., and Lee, J.H. (2008). Tissue inhibitor of metalloproteinases-3 interacts with angiotensin II type 2 receptor and additively inhibits angiogenesis. Cardiovasc Res *79*, 150-160.

Kanse, S.M., Kost, C., Wilhelm, O.G., Andreasen, P.A., and Preissner, K.T. (1996). The urokinase receptor is a major vitronectin-binding protein on endothelial cells. Exp Cell Res *224*, 344-353.

Kartenbeck, J., Stukenbrok, H., and Helenius, A. (1989). Endocytosis of simian virus 40 into the endoplasmic reticulum. J Cell Biol *109*, 2721-2729.

Kashiwagi, M., Enghild, J.J., Gendron, C., Hughes, C., Caterson, B., Itoh, Y., and Nagase, H. (2004). Altered proteolytic activities of ADAMTS-4 expressed by C-terminal processing. J Biol Chem *279*, 10109-10119.

Kashiwagi, M., Tortorella, M., Nagase, H., and Brew, K. (2001). TIMP-3 is a potent inhibitor of aggrecanase 1 (ADAM-TS4) and aggrecanase 2 (ADAM-TS5). J Biol Chem *276*, 12501-12504.

Kawata, K., Kubota, S., Eguchi, T., Aoyama, E., Moritani, N.H., Kondo, S., Nishida, T., and Takigawa, M. (2012). Role of LRP1 in transport of CCN2 protein in chondrocytes. J Cell Sci *125*, 2965-2972.

Kerr, C.A., Dunne, R., Hines, B.M., Zucker, M., Cosgrove, L., Ruszkiewicz, A., Lockett, T., and Head, R. (2009). Measuring the combinatorial expression of solute transporters and metalloproteinases transcripts in colorectal cancer. BMC Res Notes *2*, 164.

Kim, D.H., Iijima, H., Goto, K., Sakai, J., Ishii, H., Kim, H.J., Suzuki, H., Kondo, H., Saeki, S., and Yamamoto, T. (1996). Human apolipoprotein E receptor 2. A novel lipoprotein receptor of the low density lipoprotein receptor family predominantly expressed in brain. J Biol Chem *271*, 8373-8380.

Kim, J.R., and Kim, C.H. (2004). Association of a high activity of matrix metalloproteinase-9 to low levels of tissue inhibitors of metalloproteinase-1 and -3 in human hepatitis B-viral hepatoma cells. Int J Biochem Cell Biol *36*, 2293-2306.

Kinoshita, A., Whelan, C.M., Smith, C.J., Mikhailenko, I., Rebeck, G.W., Strickland, D.K., and Hyman, B.T. (2001). Demonstration by fluorescence resonance energy transfer of two sites of interaction between the low-density lipoprotein receptor-related protein and the amyloid precursor protein: role of the intracellular adapter protein Fe65. J Neurosci *21*, 8354-8361.

Kirkham, M., Fujita, A., Chadda, R., Nixon, S.J., Kurzchalia, T.V., Sharma, D.K., Pagano, R.E., Hancock, J.F., Mayor, S., and Parton, R.G. (2005). Ultrastructural identification of uncoated caveolin-independent early endocytic vehicles. J Cell Biol *168*, 465-476.

Kjoller, L. (2002). The urokinase plasminogen activator receptor in the regulation of the actin cytoskeleton and cell motility. Biol Chem *383*, 5-19.

Kjoller, L., Engelholm, L.H., Hoyer-Hansen, M., Dano, K., Bugge, T.H., and Behrendt, N. (2004). uPARAP/endo180 directs lysosomal delivery and degradation of collagen IV. Exp Cell Res *293*, 106-116.

Knauer, M.F., Orlando, R.A., and Glabe, C.G. (1996). Cell surface APP751 forms complexes with protease nexin 2 ligands and is internalized via the low density lipoprotein receptor-related protein (LRP). Brain Res *740*, 6-14.

Knäuper, V., Will, H., Lopez-Otin, C., Smith, B., Atkinson, S.J., Stanton, H., Hembry, R.M., and Murphy, G. (1996). Cellular mechanisms for human procollagenase-3 (MMP-13) activation. Evidence that MT1-MMP (MMP-14) and gelatinase a (MMP-2) are able to generate active enzyme. J Biol Chem *271*, 17124-17131.

Knight, C.G. (1991). A quenched fluorescent substrate for thimet peptidase containing a new fluorescent amino acid, DL-2-amino-3-(7-methoxy-4-coumaryl)propionic acid. Biochem J *274 (Pt 1)*, 45-48.

Kolsch, H., Ptok, U., Mohamed, I., Schmitz, S., Rao, M.L., Maier, W., and Heun, R. (2003). Association of the C766T polymorphism of the low-density lipoprotein receptor-related protein gene with Alzheimer's disease. Am J Med Genet B Neuropsychiatr Genet *121B*, 128-130.

Koskivirta, I., Kassiri, Z., Rahkonen, O., Kiviranta, R., Oudit, G.Y., McKee, T.D., Kyto, V., Saraste, A., Jokinen, E., Liu, P.P.*, et al.* (2010). Mice with tissue inhibitor of metalloproteinases 4 (Timp4) deletion succumb to induced myocardial infarction but not to cardiac pressure overload. J Biol Chem *285*, 24487-24493.

Kossakowska, A.E., Urbanski, S.J., and Edwards, D.R. (1991). Tissue inhibitor of metalloproteinases-1 (TIMP-1) RNA is expressed at elevated levels in malignant non-Hodgkin's lymphomas. Blood *77*, 2475-2481.

Kounnas, M.Z., Chappell, D.A., Wong, H., Argraves, W.S., and Strickland, D.K. (1995). The cellular internalization and degradation of hepatic lipase is mediated by low density lipoprotein receptor-related protein and requires cell surface proteoglycans. J Biol Chem *270*, 9307-9312.

Kounnas, M.Z., Church, F.C., Argraves, W.S., and Strickland, D.K. (1996). Cellular internalization and degradation of antithrombin III-thrombin, heparin cofactor II-thrombin, and alpha 1-antitrypsin-trypsin complexes is mediated by the low density lipoprotein receptor-related protein. J Biol Chem *271*, 6523-6529.

Kounnas, M.Z., Henkin, J., Argraves, W.S., and Strickland, D.K. (1993). Low density lipoprotein receptor-related protein/alpha 2-macroglobulin receptor mediates cellular uptake of pro-urokinase. J Biol Chem *268*, 21862-21867.

Kounnas, M.Z., Morris, R.E., Thompson, M.R., FitzGerald, D.J., Strickland, D.K., and Saelinger, C.B. (1992). The alpha 2-macroglobulin receptor/low density lipoprotein receptor-related protein binds and internalizes Pseudomonas exotoxin A. J Biol Chem *267*, 12420-12423.

Kruse, K., Janko, C., Urbonaviciute, V., Mierke, C.T., Winkler, T.H., Voll, R.E., Schett, G., Munoz, L.E., and Herrmann, M. (2010). Inefficient clearance of dying cells in patients with SLE: anti-dsDNA autoantibodies, MFG-E8, HMGB-1 and other players. Apoptosis *15*, 1098-1113.

Kuhn, P.H., Wang, H., Dislich, B., Colombo, A., Zeitschel, U., Ellwart, J.W., Kremmer, E., Rossner, S., and Lichtenthaler, S.F. (2010). ADAM10 is the physiologically relevant, constitutive alpha-secretase of the amyloid precursor protein in primary neurons. Embo J *29*, 3020-3032.

Kurokawa, S., Hill, K.E., McDonald, W.H., and Burk, R.F. (2012). Long Isoform Mouse Selenoprotein P (Sepp1) Supplies Rat Myoblast L8 Cells with Selenium via Endocytosis Mediated by Heparin Binding Properties and Apolipoprotein E Receptor-2 (ApoER2). J Biol Chem *287*, 28717-28726.

Laemmli, U.K. (1970). Cleavage of structural proteins during the assembly of the head of bacteriophage T4. Nature *227*, 680-685.

Lafourcade, C., Sobo, K., Kieffer-Jaquinod, S., Garin, J., and van der Goot, F.G. (2008). Regulation of the V-ATPase along the endocytic pathway occurs through reversible subunit association and membrane localization. PLoS One *3*, e2758.

Lalazar, A., Weisgraber, K.H., Rall, S.C., Jr., Giladi, H., Innerarity, T.L., Levanon, A.Z., Boyles, J.K., Amit, B., Gorecki, M., Mahley, R.W*., et al.* (1988). Site-specific mutagenesis of human apolipoprotein E. Receptor binding activity of variants with single amino acid substitutions. J Biol Chem *263*, 3542-3545.

Lamaze, C., Dujeancourt, A., Baba, T., Lo, C.G., Benmerah, A., and Dautry-Varsat, A. (2001). Interleukin 2 receptors and detergent-resistant membrane domains define a clathrin-independent endocytic pathway. Mol Cell *7*, 661-671.

Lampugnani, M.G., Orsenigo, F., Gagliani, M.C., Tacchetti, C., and Dejana, E. (2006). Vascular endothelial cadherin controls VEGFR-2 internalization and signaling from intracellular compartments. J Cell Biol *174*, 593-604.

Langbein, S., Szakacs, O., Wilhelm, M., Sukosd, F., Weber, S., Jauch, A., Lopez Beltran, A., Alken, P., Kalble, T., and Kovacs, G. (2002). Alteration of the LRP1B gene region is associated with high grade of urothelial cancer. Lab Invest *82*, 639-643.

Langlois, B., Perrot, G., Schneider, C., Henriet, P., Emonard, H., Martiny, L., and Dedieu, S. (2010). LRP-1 promotes cancer cell invasion by supporting ERK and inhibiting JNK signaling pathways. PLoS One *5*, e11584.

Lawler, J. (2002). Thrombospondin-1 as an endogenous inhibitor of angiogenesis and tumor growth. J Cell Mol Med *6*, 1-12.

Le Gall, S.M., Bobe, P., Reiss, K., Horiuchi, K., Niu, X.D., Lundell, D., Gibb, D.R., Conrad, D., Saftig, P., and Blobel, C.P. (2009). ADAMs 10 and 17 represent differentially regulated components of a general shedding machinery for membrane proteins such as transforming growth factor alpha, L-selectin, and tumor necrosis factor alpha. Mol Biol Cell *20*, 1785-1794.

Leco, K.J., Waterhouse, P., Sanchez, O.H., Gowing, K.L., Poole, A.R., Wakeham, A., Mak, T.W., and Khokha, R. (2001). Spontaneous air space enlargement in the lungs of mice lacking tissue inhibitor of metalloproteinases-3 (TIMP-3). J Clin Invest *108*, 817-829.

Lee, D.C., Sunnarborg, S.W., Hinkle, C.L., Myers, T.J., Stevenson, M.Y., Russell, W.E., Castner, B.J., Gerhart, M.J., Paxton, R.J., Black, R.A*., et al.* (2003). TACE/ADAM17 processing of EGFR ligands indicates a role as a physiological convertase. Ann N Y Acad Sci *995*, 22-38.

Lee, J.A., Croucher, D.R., and Ranson, M. (2010). Differential endocytosis of tissue plasminogen activator by serpins PAI-1 and PAI-2 on human peripheral blood monocytes. Thromb Haemost *104*, 1133-1142.

Lee, M.H., Atkinson, S., and Murphy, G. (2007). Identification of the extracellular matrix (ECM) binding motifs of tissue inhibitor of metalloproteinases (TIMP)-3 and effective transfer to TIMP-1. J Biol Chem *282*, 6887-6898.

Lee, S.H., Suh, H.N., Lee, Y.J., Seo, B.N., Ha, J.W., and Han, H.J. (2011). Midkine prevented hypoxic injury of mouse embryonic stem cells through activation of Akt and HIF-1alpha via low-density lipoprotein receptor-related protein-1. J Cell Physiol.

Leheste, J.R., Melsen, F., Wellner, M., Jansen, P., Schlichting, U., Renner-Muller, I., Andreassen, T.T., Wolf, E., Bachmann, S., Nykjaer, A*., et al.* (2003). Hypocalcemia and osteopathy in mice with kidney-specific megalin gene defect. Faseb J *17*, 247-249.

Leheste, J.R., Rolinski, B., Vorum, H., Hilpert, J., Nykjaer, A., Jacobsen, C., Aucouturier, P., Moskaug, J.O., Otto, A., Christensen, E.I*., et al.* (1999). Megalin knockout mice as an animal model of low molecular weight proteinuria. Am J Pathol *155*, 1361-1370.

Lenting, P.J., Neels, J.G., van den Berg, B.M., Clijsters, P.P., Meijerman, D.W., Pannekoek, H., van Mourik, J.A., Mertens, K., and van Zonneveld, A.J. (1999). The light chain of factor VIII comprises a binding site for low density lipoprotein receptor-related protein. J Biol Chem *274*, 23734-23739.

Levy, G.G., Nichols, W.C., Lian, E.C., Foroud, T., McClintick, J.N., McGee, B.M., Yang, A.Y., Siemieniak, D.R., Stark, K.R., Gruppo, R*., et al.* (2001). Mutations in a member of the ADAMTS gene family cause thrombotic thrombocytopenic purpura. Nature *413*, 488-494.

Li, W.Q., Dehnade, F., and Zafarullah, M. (2001). Oncostatin M-induced matrix metalloproteinase and tissue inhibitor of metalloproteinase-3 genes expression in chondrocytes requires Janus kinase/STAT signaling pathway. J Immunol *166*, 3491-3498.

Lillis, A.P., Mikhailenko, I., and Strickland, D.K. (2005). Beyond endocytosis: LRP function in cell migration, proliferation and vascular permeability. J Thromb Haemost *3*, 1884-1893.

Lillis, A.P., Van Duyn, L.B., Murphy-Ullrich, J.E., and Strickland, D.K. (2008). LDL receptor-related protein 1: unique tissue-specific functions revealed by selective gene knockout studies. Physiol Rev *88*, 887-918.

Limana, F., Esposito, G., D'Arcangelo, D., Di Carlo, A., Romani, S., Melillo, G., Mangoni, A., Bertolami, C., Pompilio, G., Germani, A*., et al.* (2011). HMGB1 attenuates cardiac remodelling in the failing heart via enhanced cardiac regeneration and miR-206-mediated inhibition of TIMP-3. PLoS One *6*, e19845.

Lin, E.A., and Liu, C.J. (2010). The role of ADAMTSs in arthritis. Protein Cell *1*, 33-47.

Liu, C.J., Kong, W., Ilalov, K., Yu, S., Xu, K., Prazak, L., Fajardo, M., Sehgal, B., and Di Cesare, P.E. (2006a). ADAMTS-7: a metalloproteinase that directly binds to and

degrades cartilage oligomeric matrix protein. FASEB journal : official publication of the Federation of American Societies for Experimental Biology *20*, 988-990.

Liu, C.J., Kong, W., Xu, K., Luan, Y., Ilalov, K., Sehgal, B., Yu, S., Howell, R.D., and Di Cesare, P.E. (2006b). ADAMTS-12 associates with and degrades cartilage oligomeric matrix protein. J Biol Chem *281*, 15800-15808.

Liu, C.X., Li, Y., Obermoeller-McCormick, L.M., Schwartz, A.L., and Bu, G. (2001). The putative tumor suppressor LRP1B, a novel member of the low density lipoprotein (LDL) receptor family, exhibits both overlapping and distinct properties with the LDL receptor-related protein. J Biol Chem *276*, 28889-28896.

Liu, C.X., Musco, S., Lisitsina, N.M., Forgacs, E., Minna, J.D., and Lisitsyn, N.A. (2000a). LRP-DIT, a putative endocytic receptor gene, is frequently inactivated in non-small cell lung cancer cell lines. Cancer Res *60*, 1961-1967.

Liu, Q., Zhang, J., Tran, H., Verbeek, M.M., Reiss, K., Estus, S., and Bu, G. (2009). LRP1 shedding in human brain: roles of ADAM10 and ADAM17. Mol Neurodegener *4*, 17.

Liu, X.W., Bernardo, M.M., Fridman, R., and Kim, H.R. (2003). Tissue inhibitor of metalloproteinase-1 protects human breast epithelial cells against intrinsic apoptotic cell death via the focal adhesion kinase/phosphatidylinositol 3-kinase and MAPK signaling pathway. J Biol Chem *278*, 40364-40372.

Liu, X.W., Taube, M.E., Jung, K.K., Dong, Z., Lee, Y.J., Roshy, S., Sloane, B.F., Fridman, R., and Kim, H.R. (2005). Tissue inhibitor of metalloproteinase-1 protects human breast epithelial cells from extrinsic cell death: a potential oncogenic activity of tissue inhibitor of metalloproteinase-1. Cancer Res *65*, 898-906.

Liu, Y., Jones, M., Hingtgen, C.M., Bu, G., Laribee, N., Tanzi, R.E., Moir, R.D., Nath, A., and He, J.J. (2000b). Uptake of HIV-1 tat protein mediated by low-density lipoprotein receptor-related protein disrupts the neuronal metabolic balance of the receptor ligands. Nat Med *6*, 1380-1387.

Lohi, J., Wilson, C.L., Roby, J.D., and Parks, W.C. (2001). Epilysin, a novel human matrix metalloproteinase (MMP-28) expressed in testis and keratinocytes and in response to injury. J Biol Chem *276*, 10134-10144.

Loukinova, E., Ranganathan, S., Kuznetsov, S., Gorlatova, N., Migliorini, M.M., Loukinov, D., Ulery, P.G., Mikhailenko, I., Lawrence, D.A., and Strickland, D.K. (2002). Platelet-derived growth factor (PDGF)-induced tyrosine phosphorylation of the low

density lipoprotein receptor-related protein (LRP). Evidence for integrated co-receptor function betwenn LRP and the PDGF. J Biol Chem *277*, 15499-15506.

Lum, L., Reid, M.S., and Blobel, C.P. (1998). Intracellular maturation of the mouse metalloprotease disintegrin MDC15. J Biol Chem *273*, 26236-26247.

Mahley, R.W., and Huang, Y. (2007). Atherogenic remnant lipoproteins: role for proteoglycans in trapping, transferring, and internalizing. J Clin Invest *117*, 94-98.

Mantuano, E., Inoue, G., Li, X., Takahashi, K., Gaultier, A., Gonias, S.L., and Campana, W.M. (2008). The hemopexin domain of matrix metalloproteinase-9 activates cell signaling and promotes migration of schwann cells by binding to low-density lipoprotein receptor-related protein. J Neurosci *28*, 11571-11582.

Marchenko, G.N., and Strongin, A.Y. (2001). MMP-28, a new human matrix metalloproteinase with an unusual cysteine-switch sequence is widely expressed in tumors. Gene *265*, 87-93.

Marchenko, N.D., Marchenko, G.N., Weinreb, R.N., Lindsey, J.D., Kyshtoobayeva, A., Crawford, H.C., and Strongin, A.Y. (2004). Beta-catenin regulates the gene of MMP-26, a novel metalloproteinase expressed both in carcinomas and normal epithelial cells. Int J Biochem Cell Biol *36*, 942-956.

Marzolo, M.P., and Bu, G. (2009). Lipoprotein receptors and cholesterol in APP trafficking and proteolytic processing, implications for Alzheimer's disease. Semin Cell Dev Biol *20*, 191-200.

Mast, A.E., Enghild, J.J., Pizzo, S.V., and Salvesen, G. (1991). Analysis of the plasma elimination kinetics and conformational stabilities of native, proteinase-complexed, and reactive site cleaved serpins: comparison of alpha 1-proteinase inhibitor, alpha 1-antichymotrypsin, antithrombin III, alpha 2-antiplasmin, angiotensinogen, and ovalbumin. Biochemistry *30*, 1723-1730.

Maurer, M.E., and Cooper, J.A. (2006). The adaptor protein Dab2 sorts LDL receptors into coated pits independently of AP-2 and ARH. J Cell Sci *119*, 4235-4246.

Maxfield, F.R., and McGraw, T.E. (2004). Endocytic recycling. Nat Rev Mol Cell Biol *5*, 121-132.

May, P., Woldt, E., Matz, R.L., and Boucher, P. (2007). The LDL receptor-related protein (LRP) family: an old family of proteins with new physiological functions. Ann Med *39*, 219-228.

Mayor, S., and Pagano, R.E. (2007). Pathways of clathrin-independent endocytosis. Nat Rev Mol Cell Biol *8*, 603-612.

Meems, H., van den Biggelaar, M., Rondaij, M., van der Zwaan, C., Mertens, K., and Meijer, A.B. (2011). C1 domain residues Lys 2092 and Phe 2093 are of major importance for the endocytic uptake of coagulation factor VIII. Int J Biochem Cell Biol *43*, 1114-1121.

Migliorini, M.M., Behre, E.H., Brew, S., Ingham, K.C., and Strickland, D.K. (2003). Allosteric modulation of ligand binding to low density lipoprotein receptor-related protein by the receptor-associated protein requires critical lysine residues within its carboxyl-terminal domain. J Biol Chem *278*, 17986-17992.

Mikhailenko, I., Kounnas, M.Z., and Strickland, D.K. (1995). Low density lipoprotein receptor-related protein/alpha 2-macroglobulin receptor mediates the cellular internalization and degradation of thrombospondin. A process facilitated by cell-surface proteoglycans. J Biol Chem *270*, 9543-9549.

Moake, J.L. (2004). von Willebrand factor, ADAMTS-13, and thrombotic thrombocytopenic purpura. Semin Hematol *41*, 4-14.

Moestrup, S.K., Gliemann, J., and Pallesen, G. (1992). Distribution of the alpha 2-macroglobulin receptor/low density lipoprotein receptor-related protein in human tissues. Cell Tissue Res *269*, 375-382.

Mohammed, F.F., Smookler, D.S., Taylor, S.E., Fingleton, B., Kassiri, Z., Sanchez, O.H., English, J.L., Matrisian, L.M., Au, B., Yeh, W.C.*, et al.* (2004). Abnormal TNF activity in Timp3-/- mice leads to chronic hepatic inflammation and failure of liver regeneration. Nat Genet *36*, 969-977.

Montesano, R., Roth, J., Robert, A., and Orci, L. (1982). Non-coated membrane invaginations are involved in binding and internalization of cholera and tetanus toxins. Nature *296*, 651-653.

Moses, M.A., Sudhalter, J., and Langer, R. (1990). Identification of an inhibitor of neovascularization from cartilage. Science *248*, 1408-1410.

Muramatsu, H., Zou, K., Sakaguchi, N., Ikematsu, S., Sakuma, S., and Muramatsu, T. (2000). LDL receptor-related protein as a component of the midkine receptor. Biochem Biophys Res Commun *270*, 936-941.

Murphy, A.N., Unsworth, E.J., and Stetler-Stevenson, W.G. (1993a). Tissue inhibitor of metalloproteinases-2 inhibits bFGF-induced human microvascular endothelial cell proliferation. J Cell Physiol *157*, 351-358.

Murphy, G. (2008). The ADAMs: signalling scissors in the tumour microenvironment. Nat Rev Cancer *8*, 929-941.

Murphy, G. (2009). Regulation of the proteolytic disintegrin metalloproteinases, the 'Sheddases'. Semin Cell Dev Biol *20*, 138-145.

Murphy, G., Houbrechts, A., Cockett, M.I., Williamson, R.A., O'Shea, M., and Docherty, A.J. (1991). The N-terminal domain of tissue inhibitor of metalloproteinases retains metalloproteinase inhibitory activity. Biochemistry *30*, 8097-8102.

Murphy, G., and Nagase, H. (2008a). Progress in matrix metalloproteinase research. Molecular aspects of medicine *29*, 290-308.

Murphy, G., and Nagase, H. (2008b). Reappraising metalloproteinases in rheumatoid arthritis and osteoarthritis: destruction or repair? Nature clinical practice Rheumatology *4*, 128-135.

Murphy, G., Segain, J.P., O'Shea, M., Cockett, M., Ioannou, C., Lefebvre, O., Chambon, P., and Basset, P. (1993b). The 28-kDa N-terminal domain of mouse stromelysin-3 has the general properties of a weak metalloproteinase. J Biol Chem *268*, 15435-15441.

Nagase, H. (1997). Activation mechanisms of matrix metalloproteinases. Biol Chem *378*, 151-160.

Nagase, H., Visse, R., and Murphy, G. (2006). Structure and function of matrix metalloproteinases and TIMPs. Cardiovasc Res *69*, 562-573.

Nagase, H., and Woessner, J.F., Jr. (1999). Matrix metalloproteinases. J Biol Chem *274*, 21491-21494.

Nakagawa, T., Pimkhaokham, A., Suzuki, E., Omura, K., Inazawa, J., and Imoto, I. (2006). Genetic or epigenetic silencing of low density lipoprotein receptor-related protein 1B expression in oral squamous cell carcinoma. Cancer Sci *97*, 1070-1074.

Nakayama, M., Nakajima, D., Nagase, T., Nomura, N., Seki, N., and Ohara, O. (1998). Identification of high-molecular-weight proteins with multiple EGF-like motifs by motif-trap screening. Genomics *51*, 27-34.

Nakopoulou, L., Giannopoulou, I., Stefanaki, K., Panayotopoulou, E., Tsirmpa, I., Alexandrou, P., Mavrommatis, J., Katsarou, S., and Davaris, P. (2002). Enhanced mRNA expression of tissue inhibitor of metalloproteinase-1 (TIMP-1) in breast carcinomas is correlated with adverse prognosis. J Pathol *197*, 307-313.

Naslavsky, N., Weigert, R., and Donaldson, J.G. (2004). Characterization of a nonclathrin endocytic pathway: membrane cargo and lipid requirements. Mol Biol Cell *15*, 3542-3552.

Nauwynck, H.J., Duan, X., Favoreel, H.W., Van Oostveldt, P., and Pensaert, M.B. (1999). Entry of porcine reproductive and respiratory syndrome virus into porcine alveolar macrophages via receptor-mediated endocytosis. J Gen Virol *80 (Pt 2)*, 297-305.

Neels, J.G., van Den Berg, B.M., Mertens, K., ter Maat, H., Pannekoek, H., van Zonneveld, A.J., and Lenting, P.J. (2000). Activation of factor IX zymogen results in exposure of a binding site for low-density lipoprotein receptor-related protein. Blood *96*, 3459-3465.

Newby, A.C., Pauschinger, M., and Spinale, F.G. (2006). From tadpole tails to transgenic mice: metalloproteinases have brought about a metamorphosis in our understanding of cardiovascular disease. Cardiovasc Res *69*, 559-561.

Nguyen, D.H., Webb, D.J., Catling, A.D., Song, Q., Dhakephalkar, A., Weber, M.J., Ravichandran, K.S., and Gonias, S.L. (2000). Urokinase-type plasminogen activator stimulates the Ras/Extracellular signal-regulated kinase (ERK) signaling pathway and MCF-7 cell migration by a mechanism that requires focal adhesion kinase, Src, and Shc. Rapid dissociation of GRB2/Sps-Shc complex is associated with the transient phosphorylation of ERK in urokinase-treated cells. J Biol Chem *275*, 19382-19388.

Nielsen, M.S., Nykjaer, A., Warshawsky, I., Schwartz, A.L., and Gliemann, J. (1995). Analysis of ligand binding to the alpha 2-macroglobulin receptor/low density lipoprotein receptor-related protein. Evidence that lipoprotein lipase and the

carboxyl-terminal domain of the receptor-associated protein bind to the same site. J Biol Chem *270*, 23713-23719.

Nilsson, S.K., Lookene, A., Beckstead, J.A., Gliemann, J., Ryan, R.O., and Olivecrona, G. (2007). Apolipoprotein A-V interaction with members of the low density lipoprotein receptor gene family. Biochemistry *46*, 3896-3904.

Nimpf, J., and Schneider, W.J. (2000). From cholesterol transport to signal transduction: low density lipoprotein receptor, very low density lipoprotein receptor, and apolipoprotein E receptor-2. Biochim Biophys Acta *1529*, 287-298.

Nishimura, H., Kim, E., Nakanishi, T., and Baba, T. (2004). Possible function of the ADAM1a/ADAM2 Fertilin complex in the appearance of ADAM3 on the sperm surface. J Biol Chem *279*, 34957-34962.

Nishimura, H., Myles, D.G., and Primakoff, P. (2007). Identification of an ADAM2-ADAM3 complex on the surface of mouse testicular germ cells and cauda epididymal sperm. J Biol Chem *282*, 17900-17907.

Niu, S., Renfro, A., Quattrocchi, C.C., Sheldon, M., and D'Arcangelo, G. (2004). Reelin promotes hippocampal dendrite development through the VLDLR/ApoER2-Dab1 pathway. Neuron *41*, 71-84.

Novak, S., Hiesberger, T., Schneider, W.J., and Nimpf, J. (1996). A new low density lipoprotein receptor homologue with 8 ligand binding repeats in brain of chicken and mouse. J Biol Chem *271*, 11732-11736.

Nykjaer, A., Petersen, C.M., Moller, B., Andreasen, P.A., and Gliemann, J. (1992a). Identification and characterization of urokinase receptors in natural killer cells and T-cell-derived lymphokine activated killer cells. FEBS Lett *300*, 13-17.

Nykjaer, A., Petersen, C.M., Moller, B., Jensen, P.H., Moestrup, S.K., Holtet, T.L., Etzerodt, M., Thogersen, H.C., Munch, M., Andreasen, P.A*., et al.* (1992b). Purified alpha 2-macroglobulin receptor/LDL receptor-related protein binds urokinase.plasminogen activator inhibitor type-1 complex. Evidence that the alpha 2-macroglobulin receptor mediates cellular degradation of urokinase receptor-bound complexes. J Biol Chem *267*, 14543-14546.

Ogawa, T., Tsubota, Y., Hashimoto, J., Kariya, Y., and Miyazaki, K. (2007). The short arm of laminin gamma2 chain of laminin-5 (laminin-332) binds syndecan-1 and

regulates cellular adhesion and migration by suppressing phosphorylation of integrin beta4 chain. Mol Biol Cell *18*, 1621-1633.

Ohlsson, K., Ganrot, P.O., and Laurell, C.B. (1971). In vivo interaction beween trypsin and some plasma proteins in relation to tolerance to intravenous infusion of trypsin in dog. Acta Chir Scand *137*, 113-121.

Ohno, H., Fournier, M.C., Poy, G., and Bonifacino, J.S. (1996). Structural determinants of interaction of tyrosine-based sorting signals with the adaptor medium chains. J Biol Chem *271*, 29009-29015.

Ohno, H., Stewart, J., Fournier, M.C., Bosshart, H., Rhee, I., Miyatake, S., Saito, T., Gallusser, A., Kirchhausen, T., and Bonifacino, J.S. (1995). Interaction of tyrosine-based sorting signals with clathrin-associated proteins. Science *269*, 1872-1875.

Olson, T.M., Hirohata, S., Ye, J., Leco, K., Seldin, M.F., and Apte, S.S. (1998). Cloning of the human tissue inhibitor of metalloproteinase-4 gene (TIMP4) and localization of the TIMP4 and Timp4 genes to human chromosome 3p25 and mouse chromosome 6, respectively. Genomics *51*, 148-151.

Orth, K., Willnow, T., Herz, J., Gething, M.J., and Sambrook, J. (1994). Low density lipoprotein receptor-related protein is necessary for the internalization of both tissue-type plasminogen activator-inhibitor complexes and free tissue-type plasminogen activator. J Biol Chem *269*, 21117-21122.

Overton, C.D., Yancey, P.G., Major, A.S., Linton, M.F., and Fazio, S. (2007). Deletion of macrophage LDL receptor-related protein increases atherogenesis in the mouse. Circ Res *100*, 670-677.

Parks, W.C., Wilson, C.L., and Lopez-Boado, Y.S. (2004). Matrix metalloproteinases as modulators of inflammation and innate immunity. Nat Rev Immunol *4*, 617-629.

Patterson, M.L., Atkinson, S.J., Knauper, V., and Murphy, G. (2001). Specific collagenolysis by gelatinase A, MMP-2, is determined by the hemopexin domain and not the fibronectin-like domain. FEBS Lett *503*, 158-162.

Pavloff, N., Staskus, P.W., Kishnani, N.S., and Hawkes, S.P. (1992). A new inhibitor of metalloproteinases from chicken: ChIMP-3. A third member of the TIMP family. J Biol Chem *267*, 17321-17326.

Payne, C.K., Jones, S.A., Chen, C., and Zhuang, X. (2007). Internalization and trafficking of cell surface proteoglycans and proteoglycan-binding ligands. Traffic *8*, 389-401.

Pearse, B.M. (1976). Clathrin: a unique protein associated with intracellular transfer of membrane by coated vesicles. Proc Natl Acad Sci U S A *73*, 1255-1259.

Pei, D., and Weiss, S.J. (1995). Furin-dependent intracellular activation of the human stromelysin-3 zymogen. Nature *375*, 244-247.

Pelkmans, L., Kartenbeck, J., and Helenius, A. (2001). Caveolar endocytosis of simian virus 40 reveals a new two-step vesicular-transport pathway to the ER. Nat Cell Biol *3*, 473-483.

Pelkmans, L., Puntener, D., and Helenius, A. (2002). Local actin polymerization and dynamin recruitment in SV40-induced internalization of caveolae. Science *296*, 535-539.

Pendas, A.M., Knauper, V., Puente, X.S., Llano, E., Mattei, M.G., Apte, S., Murphy, G., and Lopez-Otin, C. (1997). Identification and characterization of a novel human matrix metalloproteinase with unique structural characteristics, chromosomal location, and tissue distribution. J Biol Chem *272*, 4281-4286.

Pho, M.T., Ashok, A., and Atwood, W.J. (2000). JC virus enters human glial cells by clathrin-dependent receptor-mediated endocytosis. J Virol *74*, 2288-2292.

Ploug, M., Ronne, E., Behrendt, N., Jensen, A.L., Blasi, F., and Dano, K. (1991). Cellular receptor for urokinase plasminogen activator. Carboxyl-terminal processing and membrane anchoring by glycosyl-phosphatidylinositol. J Biol Chem *266*, 1926-1933.

Polavarapu, R., Gongora, M.C., Yi, H., Ranganthan, S., Lawrence, D.A., Strickland, D., and Yepes, M. (2007). Tissue-type plasminogen activator-mediated shedding of astrocytic low-density lipoprotein receptor-related protein increases the permeability of the neurovascular unit. Blood *109*, 3270-3278.

Poller, W., Willnow, T.E., Hilpert, J., and Herz, J. (1995). Differential recognition of alpha 1-antitrypsin-elastase and alpha 1-antichymotrypsin-cathepsin G complexes by the low density lipoprotein receptor-related protein. J Biol Chem *270*, 2841-2845.

Porter, S., Clark, I.M., Kevorkian, L., and Edwards, D.R. (2005). The ADAMTS metalloproteinases. Biochem J *386*, 15-27.

Powelka, A.M., Sun, J., Li, J., Gao, M., Shaw, L.M., Sonnenberg, A., and Hsu, V.W. (2004). Stimulation-dependent recycling of integrin beta1 regulated by ARF6 and Rab11. Traffic *5*, 20-36.

Prazeres, H., Torres, J., Rodrigues, F., Pinto, M., Pastoriza, M.C., Gomes, D., Cameselle-Teijeiro, J., Vidal, A., Martins, T.C., Sobrinho-Simoes, M.*, et al.* (2011). Chromosomal, epigenetic and microRNA-mediated inactivation of LRP1B, a modulator of the extracellular environment of thyroid cancer cells. Oncogene *30*, 1302-1317.

Primakoff, P., Hyatt, H., and Tredick-Kline, J. (1987). Identification and purification of a sperm surface protein with a potential role in sperm-egg membrane fusion. J Cell Biol *104*, 141-149.

Puxeddu, I., Pang, Y.Y., Harvey, A., Haitchi, H.M., Nicholas, B., Yoshisue, H., Ribatti, D., Clough, G., Powell, R.M., Murphy, G.*, et al.* (2008). The soluble form of a disintegrin and metalloprotease 33 promotes angiogenesis: implications for airway remodeling in asthma. J Allergy Clin Immunol *121*, 1400-1406, 1406 e1401-1404.

Qi, J.H., Ebrahem, Q., Moore, N., Murphy, G., Claesson-Welsh, L., Bond, M., Baker, A., and Anand-Apte, B. (2003). A novel function for tissue inhibitor of metalloproteinases-3 (TIMP3): inhibition of angiogenesis by blockage of VEGF binding to VEGF receptor-2. Nat Med *9*, 407-415.

Quinn, K.A., Grimsley, P.G., Dai, Y.P., Tapner, M., Chesterman, C.N., and Owensby, D.A. (1997). Soluble low density lipoprotein receptor-related protein (LRP) circulates in human plasma. J Biol Chem *272*, 23946-23951.

Qureshi, H.Y., Sylvester, J., El Mabrouk, M., and Zafarullah, M. (2005). TGF-beta-induced expression of tissue inhibitor of metalloproteinases-3 gene in chondrocytes is mediated by extracellular signal-regulated kinase pathway and Sp1 transcription factor. J Cell Physiol *203*, 345-352.

Radhakrishna, H., and Donaldson, J.G. (1997). ADP-ribosylation factor 6 regulates a novel plasma membrane recycling pathway. J Cell Biol *139*, 49-61.

Rahmatpanah, F.B., Carstens, S., Guo, J., Sjahputera, O., Taylor, K.H., Duff, D., Shi, H., Davis, J.W., Hooshmand, S.I., Chitma-Matsiga, R.*, et al.* (2006). Differential DNA

methylation patterns of small B-cell lymphoma subclasses with different clinical behavior. Leukemia *20*, 1855-1862.

Ranganathan, S., Cao, C., Catania, J., Migliorini, M., Zhang, L., and Strickland, D.K. (2011a). Molecular basis for the interaction of low density lipoprotein receptor-related protein 1 (LRP1) with integrin alphaMbeta2: identification of binding sites within alphaMbeta2 for LRP1. J Biol Chem *286*, 30535-30541.

Ranganathan, S., Liu, C.X., Migliorini, M.M., Von Arnim, C.A., Peltan, I.D., Mikhailenko, I., Hyman, B.T., and Strickland, D.K. (2004). Serine and threonine phosphorylation of the low density lipoprotein receptor-related protein by protein kinase Calpha regulates endocytosis and association with adaptor molecules. J Biol Chem *279*, 40536-40544.

Ranganathan, S., Noyes, N.C., Migliorini, M., Winkles, J.A., Battey, F.D., Hyman, B.T., Smith, E., Yepes, M., Mikhailenko, I., and Strickland, D.K. (2011b). LRAD3, a novel low-density lipoprotein receptor family member that modulates amyloid precursor protein trafficking. J Neurosci *31*, 10836-10846.

Riento, K., Frick, M., Schafer, I., and Nichols, B.J. (2009). Endocytosis of flotillin-1 and flotillin-2 is regulated by Fyn kinase. J Cell Sci *122*, 912-918.

Rodenburg, K.W., Kjoller, L., Petersen, H.H., and Andreasen, P.A. (1998). Binding of urokinase-type plasminogen activator-plasminogen activator inhibitor-1 complex to the endocytosis receptors alpha2-macroglobulin receptor/low-density lipoprotein receptor-related protein and very-low-density lipoprotein receptor involves basic residues in the inhibitor. Biochem J *329 (Pt 1)*, 55-63.

Rohlmann, A., Gotthardt, M., Hammer, R.E., and Herz, J. (1998). Inducible inactivation of hepatic LRP gene by cre-mediated recombination confirms role of LRP in clearance of chylomicron remnants. J Clin Invest *101*, 689-695.

Rohrs, S., Dirks, W.G., Meyer, C., Marschalek, R., Scherr, M., Slany, R., Wallace, A., Drexler, H.G., and Quentmeier, H. (2009). Hypomethylation and expression of BEX2, IGSF4 and TIMP3 indicative of MLL translocations in acute myeloid leukemia. Mol Cancer *8*, 86.

Rosenberg, R.D., and Damus, P.S. (1973). The purification and mechanism of action of human antithrombin-heparin cofactor. J Biol Chem *248*, 6490-6505.

Rosenzweig, S.D., and Holland, S.M. (2011). Recent insights into the pathobiology of innate immune deficiencies. Curr Allergy Asthma Rep *11*, 369-377.

Rothberg, K.G., Heuser, J.E., Donzell, W.C., Ying, Y.S., Glenney, J.R., and Anderson, R.G. (1992). Caveolin, a protein component of caveolae membrane coats. Cell *68*, 673-682.

Rothnie, A., Clarke, A.R., Kuzmic, P., Cameron, A., and Smith, C.J. (2011). A sequential mechanism for clathrin cage disassembly by 70-kDa heat-shock cognate protein (Hsc70) and auxilin. Proc Natl Acad Sci U S A *108*, 6927-6932.

Rozanov, D.V., Hahn-Dantona, E., Strickland, D.K., and Strongin, A.Y. (2004). The low density lipoprotein receptor-related protein LRP is regulated by membrane type-1 matrix metalloproteinase (MT1-MMP) proteolysis in malignant cells. J Biol Chem *279*, 4260-4268.

Rubin, L.L., and Staddon, J.M. (1999). The cell biology of the blood-brain barrier. Annu Rev Neurosci *22*, 11-28.

Ryu, O.H., Fincham, A.G., Hu, C.C., Zhang, C., Qian, Q., Bartlett, J.D., and Simmer, J.P. (1999). Characterization of recombinant pig enamelysin activity and cleavage of recombinant pig and mouse amelogenins. J Dent Res *78*, 743-750.

Sabharanjak, S., Sharma, P., Parton, R.G., and Mayor, S. (2002). GPI-anchored proteins are delivered to recycling endosomes via a distinct cdc42-regulated, clathrin-independent pinocytic pathway. Dev Cell *2*, 411-423.

Sadler, J.E. (1998). Biochemistry and genetics of von Willebrand factor. Annu Rev Biochem *67*, 395-424.

Saenko, E.L., Yakhyaev, A.V., Mikhailenko, I., Strickland, D.K., and Sarafanov, A.G. (1999). Role of the low density lipoprotein-related protein receptor in mediation of factor VIII catabolism. J Biol Chem *274*, 37685-37692.

Saffarian, S., Cocucci, E., and Kirchhausen, T. (2009). Distinct dynamics of endocytic clathrin-coated pits and coated plaques. PLoS Biol *7*, e1000191.

Sagare, A., Deane, R., Bell, R.D., Johnson, B., Hamm, K., Pendu, R., Marky, A., Lenting, P.J., Wu, Z., Zarcone, T.*, et al.* (2007). Clearance of amyloid-beta by circulating lipoprotein receptors. Nat Med *13*, 1029-1031.

Sahebjam, S., Khokha, R., and Mort, J.S. (2007). Increased collagen and aggrecan degradation with age in the joints of Timp3(-/-) mice. Arthritis Rheum *56*, 905-909.

Saito, A., Pietromonaco, S., Loo, A.K., and Farquhar, M.G. (1994). Complete cloning and sequencing of rat gp330/"megalin," a distinctive member of the low density lipoprotein receptor gene family. Proc Natl Acad Sci U S A *91*, 9725-9729.

Sakai, J., Hoshino, A., Takahashi, S., Miura, Y., Ishii, H., Suzuki, H., Kawarabayasi, Y., and Yamamoto, T. (1994). Structure, chromosome location, and expression of the human very low density lipoprotein receptor gene. J Biol Chem *269*, 2173-2182.

Sakamoto, K., Bu, G., Chen, S., Takei, Y., Hibi, K., Kodera, Y., McCormick, L.M., Nakao, A., Noda, M., Muramatsu, T.*, et al.* (2011). Premature ligand-receptor interaction during biosynthesis limits the production of growth factor midkine and its receptor LDL receptor-related protein 1. J Biol Chem *286*, 8405-8413.

Salicioni, A.M., Gaultier, A., Brownlee, C., Cheezum, M.K., and Gonias, S.L. (2004). Low density lipoprotein receptor-related protein-1 promotes beta1 integrin maturation and transport to the cell surface. J Biol Chem *279*, 10005-10012.

Salicioni, A.M., Mizelle, K.S., Loukinova, E., Mikhailenko, I., Strickland, D.K., and Gonias, S.L. (2002). The low density lipoprotein receptor-related protein mediates fibronectin catabolism and inhibits fibronectin accumulation on cell surfaces. J Biol Chem *277*, 16160-16166.

Sandvig, K., Pust, S., Skotland, T., and van Deurs, B. (2011). Clathrin-independent endocytosis: mechanisms and function. Curr Opin Cell Biol *23*, 413-420.

Sandvig, K., Torgersen, M.L., Raa, H.A., and van Deurs, B. (2008). Clathrin-independent endocytosis: from nonexisting to an extreme degree of complexity. Histochem Cell Biol *129*, 267-276.

Sarafanov, A.G., Ananyeva, N.M., Shima, M., and Saenko, E.L. (2001). Cell surface heparan sulfate proteoglycans participate in factor VIII catabolism mediated by low density lipoprotein receptor-related protein. J Biol Chem *276*, 11970-11979.

Sarrazin, S., Lamanna, W.C., and Esko, J.D. (2011). Heparan sulfate proteoglycans. Cold Spring Harb Perspect Biol *3*.

Sauvonnet, N., Dujeancourt, A., and Dautry-Varsat, A. (2005). Cortactin and dynamin are required for the clathrin-independent endocytosis of gammac cytokine receptor. J Cell Biol *168*, 155-163.

Scherzer, C.R., Offe, K., Gearing, M., Rees, H.D., Fang, G., Heilman, C.J., Schaller, C., Bujo, H., Levey, A.I., and Lah, J.J. (2004). Loss of apolipoprotein E receptor LR11 in Alzheimer disease. Arch Neurol *61*, 1200-1205.

Schlondorff, J., and Blobel, C.P. (1999). Metalloprotease-disintegrins: modular proteins capable of promoting cell-cell interactions and triggering signals by protein-ectodomain shedding. J Cell Sci *112 (Pt 21)*, 3603-3617.

Schlossman, D.M., Schmid, S.L., Braell, W.A., and Rothman, J.E. (1984). An enzyme that removes clathrin coats: purification of an uncoating ATPase. J Cell Biol *99*, 723-733.

Schmid, S.L., Braell, W.A., Schlossman, D.M., and Rothman, J.E. (1984). A role for clathrin light chains in the recognition of clathrin cages by 'uncoating ATPase'. Nature *311*, 228-231.

Schwartz, A.L., and Broze, G.J., Jr. (1997). Tissue factor pathway inhibitor endocytosis. Trends Cardiovasc Med *7*, 234-239.

Seals, D.F., and Courtneidge, S.A. (2003). The ADAMs family of metalloproteases: multidomain proteins with multiple functions. Genes Dev *17*, 7-30.

Segarini, P.R., Nesbitt, J.E., Li, D., Hays, L.G., Yates, J.R., 3rd, and Carmichael, D.F. (2001). The low density lipoprotein receptor-related protein/alpha2-macroglobulin receptor is a receptor for connective tissue growth factor. J Biol Chem *276*, 40659-40667.

Selaru, F.M., Olaru, A.V., Kan, T., David, S., Cheng, Y., Mori, Y., Yang, J., Paun, B., Jin, Z., Agarwal, R.*, et al.* (2009). MicroRNA-21 is overexpressed in human cholangiocarcinoma and regulates programmed cell death 4 and tissue inhibitor of metalloproteinase 3. Hepatology *49*, 1595-1601.

Selvais, C., D'Auria, L., Tyteca, D., Perrot, G., Lemoine, P., Troeberg, L., Dedieu, S., Noel, A., Nagase, H., Henriet, P.*, et al.* (2011). Cell cholesterol modulates metalloproteinase-dependent shedding of low-density lipoprotein receptor-related protein-1 (LRP-1) and clearance function. Faseb J *25*, 2770-2781.

Selvais, C., Gaide Chevronnay, H.P., Lemoine, P., Dedieu, S., Henriet, P., Courtoy, P.J., Marbaix, E., and Emonard, H. (2009). Metalloproteinase-dependent shedding of low-density lipoprotein receptor-related protein-1 ectodomain decreases endocytic clearance of endometrial matrix metalloproteinase-2 and -9 at menstruation. Endocrinology *150*, 3792-3799.

Shapiro, S.D., Doyle, G.A., Ley, T.J., Parks, W.C., and Welgus, H.G. (1993). Molecular mechanisms regulating the production of collagenase and TIMP in U937 cells: evidence for involvement of delayed transcriptional activation and enhanced mRNA stability. Biochemistry *32*, 4286-4292.

Shen, G.M., Zhao, Y.Z., Chen, M.T., Zhang, F.L., Liu, X.L., Wang, Y., Liu, C.Z., Yu, J., and Zhang, J.W. (2011). Hypoxia inducible factor 1 (HIF1) promotes LDL and VLDL uptake through inducing VLDLR under hypoxia. Biochem J.

Shevchenko, A., Wilm, M., Vorm, O., Jensen, O.N., Podtelejnikov, A.V., Neubauer, G., Mortensen, P., and Mann, M. (1996). A strategy for identifying gel-separated proteins in sequence databases by MS alone. Biochem Soc Trans *24*, 893-896.

Shibata, M., Yamada, S., Kumar, S.R., Calero, M., Bading, J., Frangione, B., Holtzman, D.M., Miller, C.A., Strickland, D.K., Ghiso, J.*, et al.* (2000). Clearance of Alzheimer's amyloid-ss(1-40) peptide from brain by LDL receptor-related protein-1 at the blood-brain barrier. J Clin Invest *106*, 1489-1499.

Shibata, Y., Muramatsu, T., Hirai, M., Inui, T., Kimura, T., Saito, H., McCormick, L.M., Bu, G., and Kadomatsu, K. (2002). Nuclear targeting by the growth factor midkine. Mol Cell Biol *22*, 6788-6796.

Shipley, J.M., Wesselschmidt, R.L., Kobayashi, D.K., Ley, T.J., and Shapiro, S.D. (1996). Metalloelastase is required for macrophage-mediated proteolysis and matrix invasion in mice. Proc Natl Acad Sci U S A *93*, 3942-3946.

Sid, B., Dedieu, S., Delorme, N., Sartelet, H., Rath, G.M., Bellon, G., and Martiny, L. (2006). Human thyroid carcinoma cell invasion is controlled by the low density lipoprotein receptor-related protein-mediated clearance of urokinase plasminogen activator. Int J Biochem Cell Biol *38*, 1729-1740.

Simons, K., and Ikonen, E. (1997). Functional rafts in cell membranes. Nature *387*, 569-572.

Simons, K., and Toomre, D. (2000). Lipid rafts and signal transduction. Nat Rev Mol Cell Biol *1*, 31-39.

Simons, K., and van Meer, G. (1988). Lipid sorting in epithelial cells. Biochemistry *27*, 6197-6202.

Skeldal, S., Larsen, J.V., Pedersen, K.E., Petersen, H.H., Egelund, R., Christensen, A., Jensen, J.K., Gliemann, J., and Andreasen, P.A. (2006). Binding areas of urokinase-type plasminogen activator-plasminogen activator inhibitor-1 complex for endocytosis receptors of the low-density lipoprotein receptor family, determined by site-directed mutagenesis. Febs J *273*, 5143-5159.

Somerville, R.P., Longpre, J.M., Apel, E.D., Lewis, R.M., Wang, L.W., Sanes, J.R., Leduc, R., and Apte, S.S. (2004). ADAMTS7B, the full-length product of the ADAMTS7 gene, is a chondroitin sulfate proteoglycan containing a mucin domain. J Biol Chem *279*, 35159-35175.

Song, B., Wang, C., Liu, J., Wang, X., Lv, L., Wei, L., Xie, L., Zheng, Y., and Song, X. (2010). MicroRNA-21 regulates breast cancer invasion partly by targeting tissue inhibitor of metalloproteinase 3 expression. J Exp Clin Cancer Res *29*, 29.

Song, H., Li, Y., Lee, J., Schwartz, A.L., and Bu, G. (2009). Low-density lipoprotein receptor-related protein 1 promotes cancer cell migration and invasion by inducing the expression of matrix metalloproteinases 2 and 9. Cancer Res *69*, 879-886.

Song, R.H., Tortorella, M.D., Malfait, A.M., Alston, J.T., Yang, Z., Arner, E.C., and Griggs, D.W. (2007). Aggrecan degradation in human articular cartilage explants is mediated by both ADAMTS-4 and ADAMTS-5. Arthritis Rheum *56*, 575-585.

Sonoda, I., Imoto, I., Inoue, J., Shibata, T., Shimada, Y., Chin, K., Imamura, M., Amagasa, T., Gray, J.W., Hirohashi, S*., et al.* (2004). Frequent silencing of low density lipoprotein receptor-related protein 1B (LRP1B) expression by genetic and epigenetic mechanisms in esophageal squamous cell carcinoma. Cancer Res *64*, 3741-3747.

Sorvillo, N., Pos, W., van den Berg, L.M., Fijnheer, R., Martinez-Pomares, L., Geijtenbeek, T.B., Herczenik, E., and Voorberg, J. (2012). The macrophage mannose receptor promotes uptake of ADAMTS13 by dendritic cells. Blood *119*, 3828-3835.

Sottrup-Jensen, L. (1989). Alpha-macroglobulins: structure, shape, and mechanism of proteinase complex formation. J Biol Chem *264*, 11539-11542.

Sottrup-Jensen, L., Gliemann, J., and Van Leuven, F. (1986). Domain structure of human alpha 2-macroglobulin. Characterization of a receptor-binding domain obtained by digestion with papain. FEBS Lett *205*, 20-24.

Spoelgen, R., von Arnim, C.A., Thomas, A.V., Peltan, I.D., Koker, M., Deng, A., Irizarry, M.C., Andersen, O.M., Willnow, T.E., and Hyman, B.T. (2006). Interaction of the cytosolic domains of sorLA/LR11 with the amyloid precursor protein (APP) and beta-secretase beta-site APP-cleaving enzyme. J Neurosci *26*, 418-428.

Stahl, A., and Mueller, B.M. (1995). The urokinase-type plasminogen activator receptor, a GPI-linked protein, is localized in caveolae. J Cell Biol *129*, 335-344.

Stan, R.V., Roberts, W.G., Predescu, D., Ihida, K., Saucan, L., Ghitescu, L., and Palade, G.E. (1997). Immunoisolation and partial characterization of endothelial plasmalemmal vesicles (caveolae). Mol Biol Cell *8*, 595-605.

Stanford, K.I., Bishop, J.R., Foley, E.M., Gonzales, J.C., Niesman, I.R., Witztum, J.L., and Esko, J.D. (2009). Syndecan-1 is the primary heparan sulfate proteoglycan mediating hepatic clearance of triglyceride-rich lipoproteins in mice. J Clin Invest *119*, 3236-3245.

Starkey, P.M., and Barrett, A.J. (1973). Inhibition by alpha-macroglobulin and other serum proteins. Biochem J *131*, 823-831.

Staskus, P.W., Masiarz, F.R., Pallanck, L.J., and Hawkes, S.P. (1991). The 21-kDa protein is a transformation-sensitive metalloproteinase inhibitor of chicken fibroblasts. J Biol Chem *266*, 449-454.

Stefansson, S., Muhammad, S., Cheng, X.F., Battey, F.D., Strickland, D.K., and Lawrence, D.A. (1998). Plasminogen activator inhibitor-1 contains a cryptic high affinity binding site for the low density lipoprotein receptor-related protein. J Biol Chem *273*, 6358-6366.

Stetler-Stevenson, W.G., Krutzsch, H.C., and Liotta, L.A. (1989). Tissue inhibitor of metalloproteinase (TIMP-2). A new member of the metalloproteinase inhibitor family. J Biol Chem *264*, 17374-17378.

Stowell, M.H., Marks, B., Wigge, P., and McMahon, H.T. (1999). Nucleotide-dependent conformational changes in dynamin: evidence for a mechanochemical molecular spring. Nat Cell Biol *1*, 27-32.

Strickland, D.K., Ashcom, J.D., Williams, S., Burgess, W.H., Migliorini, M., and Argraves, W.S. (1990). Sequence identity between the alpha 2-macroglobulin receptor and low density lipoprotein receptor-related protein suggests that this molecule is a multifunctional receptor. J Biol Chem *265*, 17401-17404.

Strongin, A.Y., Collier, I., Bannikov, G., Marmer, B.L., Grant, G.A., and Goldberg, G.I. (1995). Mechanism of cell surface activation of 72-kDa type IV collagenase. Isolation of the activated form of the membrane metalloprotease. J Biol Chem *270*, 5331-5338.

Su, S., Dehnade, F., and Zafarullah, M. (1996). Regulation of tissue inhibitor of metalloproteinases-3 gene expression by transforming growth factor-beta and dexamethasone in bovine and human articular chondrocytes. DNA Cell Biol *15*, 1039-1048.

Suzuki, J., Takahashi, S., Oida, K., Shimada, A., Kohno, M., Tamai, T., Miyabo, S., Yamamoto, T., and Nakai, T. (1995). Lipid accumulation and foam cell formation in Chinese hamster ovary cells overexpressing very low density lipoprotein receptor. Biochem Biophys Res Commun *206*, 835-842.

Swanson, J.A., and Watts, C. (1995). Macropinocytosis. Trends Cell Biol *5*, 424-428.

Sweitzer, S.M., and Hinshaw, J.E. (1998). Dynamin undergoes a GTP-dependent conformational change causing vesiculation. Cell *93*, 1021-1029.

Tacken, P.J., Teusink, B., Jong, M.C., Harats, D., Havekes, L.M., van Dijk, K.W., and Hofker, M.H. (2000). LDL receptor deficiency unmasks altered VLDL triglyceride metabolism in VLDL receptor transgenic and knockout mice. J Lipid Res *41*, 2055-2062.

Takahashi, S., Kawarabayasi, Y., Nakai, T., Sakai, J., and Yamamoto, T. (1992). Rabbit very low density lipoprotein receptor: a low density lipoprotein receptor-like protein with distinct ligand specificity. Proc Natl Acad Sci U S A *89*, 9252-9256.

Taube, M.E., Liu, X.W., Fridman, R., and Kim, H.R. (2006). TIMP-1 regulation of cell cycle in human breast epithelial cells via stabilization of p27(KIP1) protein. Oncogene *25*, 3041-3048.

Torgersen, M.L., Skretting, G., van Deurs, B., and Sandvig, K. (2001). Internalization of cholera toxin by different endocytic mechanisms. J Cell Sci *114*, 3737-3747.

Traub, L.M. (2003). Sorting it out: AP-2 and alternate clathrin adaptors in endocytic cargo selection. J Cell Biol *163*, 203-208.

Traub, L.M. (2009). Tickets to ride: selecting cargo for clathrin-regulated internalization. Nat Rev Mol Cell Biol *10*, 583-596.

Troeberg, L., Fushimi, K., Khokha, R., Emonard, H., Ghosh, P., and Nagase, H. (2008). Calcium pentosan polysulfate is a multifaceted exosite inhibitor of aggrecanases. Faseb J *22*, 3515-3524.

Troeberg, L., Fushimi, K., Scilabra, S.D., Nakamura, H., Dive, V., Thogersen, I.B., Enghild, J.J., and Nagase, H. (2009). The C-terminal domains of ADAMTS-4 and ADAMTS-5 promote association with N-TIMP-3. Matrix Biol *28*, 463-469.

Ueki, T., Toyota, M., Sohn, T., Yeo, C.J., Issa, J.P., Hruban, R.H., and Goggins, M. (2000). Hypermethylation of multiple genes in pancreatic adenocarcinoma. Cancer Res *60*, 1835-1839.

Ulery, P.G., Beers, J., Mikhailenko, I., Tanzi, R.E., Rebeck, G.W., Hyman, B.T., and Strickland, D.K. (2000). Modulation of beta-amyloid precursor protein processing by the low density lipoprotein receptor-related protein (LRP). Evidence that LRP contributes to the pathogenesis of Alzheimer's disease. J Biol Chem *275*, 7410-7415.

Ungewickell, E., Ungewickell, H., Holstein, S.E., Lindner, R., Prasad, K., Barouch, W., Martin, B., Greene, L.E., and Eisenberg, E. (1995). Role of auxilin in uncoating clathrin-coated vesicles. Nature *378*, 632-635.

van den Biggelaar, M., Sellink, E., Klein Gebbinck, J.W., Mertens, K., and Meijer, A.B. (2011). A single lysine of the two-lysine recognition motif of the D3 domain of receptor-associated protein is sufficient to mediate endocytosis by low-density lipoprotein receptor-related protein. Int J Biochem Cell Biol *43*, 431-440.

Van den Steen, P.E., Van Aelst, I., Hvidberg, V., Piccard, H., Fiten, P., Jacobsen, C., Moestrup, S.K., Fry, S., Royle, L., Wormald, M.R*., et al.* (2006). The hemopexin and O-glycosylated domains tune gelatinase B/MMP-9 bioavailability via inhibition and binding to cargo receptors. J Biol Chem *281*, 18626-18637.

van Kerkhof, P., Lee, J., McCormick, L., Tetrault, E., Lu, W., Schoenfish, M., Oorschot, V., Strous, G.J., Klumperman, J., and Bu, G. (2005). Sorting nexin 17 facilitates LRP recycling in the early endosome. Embo J *24*, 2851-2861.

Van Wart, H.E., and Birkedal-Hansen, H. (1990). The cysteine switch: a principle of regulation of metalloproteinase activity with potential applicability to the entire matrix metalloproteinase gene family. Proc Natl Acad Sci U S A *87*, 5578-5582.

Vassar, R., Bennett, B.D., Babu-Khan, S., Kahn, S., Mendiaz, E.A., Denis, P., Teplow, D.B., Ross, S., Amarante, P., Loeloff, R.*, et al.* (1999). Beta-secretase cleavage of Alzheimer's amyloid precursor protein by the transmembrane aspartic protease BACE. Science *286*, 735-741.

Vater, C.A., Mainardi, C.L., and Harris, E.D., Jr. (1979). Inhibitor of human collagenase from cultures of human tendon. J Biol Chem *254*, 3045-3053.

Velasco, G., Pendas, A.M., Fueyo, A., Knauper, V., Murphy, G., and Lopez-Otin, C. (1999). Cloning and characterization of human MMP-23, a new matrix metalloproteinase predominantly expressed in reproductive tissues and lacking conserved domains in other family members. J Biol Chem *274*, 4570-4576.

Visse, R., and Nagase, H. (2003). Matrix metalloproteinases and tissue inhibitors of metalloproteinases: structure, function, and biochemistry. Circ Res *92*, 827-839.

von Arnim, C.A., Kinoshita, A., Peltan, I.D., Tangredi, M.M., Herl, L., Lee, B.M., Spoelgen, R., Hshieh, T.T., Ranganathan, S., Battey, F.D.*, et al.* (2005). The low density lipoprotein receptor-related protein (LRP) is a novel beta-secretase (BACE1) substrate. J Biol Chem *280*, 17777-17785.

Walling, H.W., Raggatt, L.J., Irvine, D.W., Barmina, O.Y., Toledano, J.E., Goldring, M.B., Hruska, K.A., Adkisson, H.D., Burdge, R.E., Gatt, C.J., Jr.*, et al.* (2003). Impairment of the collagenase-3 endocytotic receptor system in cells from patients with osteoarthritis. Osteoarthritis and cartilage / OARS, Osteoarthritis Research Society *11*, 854-863.

Wang, B., Hsu, S.H., Majumder, S., Kutay, H., Huang, W., Jacob, S.T., and Ghoshal, K. (2010). TGFbeta-mediated upregulation of hepatic miR-181b promotes hepatocarcinogenesis by targeting TIMP3. Oncogene *29*, 1787-1797.

Wang, S., Herndon, M.E., Ranganathan, S., Godyna, S., Lawler, J., Argraves, W.S., and Liau, G. (2004). Internalization but not binding of thrombospondin-1 to low density lipoprotein receptor-related protein-1 requires heparan sulfate proteoglycans. J Cell Biochem *91*, 766-776.

Wang, T., Yamashita, K., Iwata, K., and Hayakawa, T. (2002). Both tissue inhibitors of metalloproteinases-1 (TIMP-1) and TIMP-2 activate Ras but through different pathways. Biochem Biophys Res Commun *296*, 201-205.

Wang, Y., Herrera, A.H., Li, Y., Belani, K.K., and Walcheck, B. (2009). Regulation of mature ADAM17 by redox agents for L-selectin shedding. J Immunol *182*, 2449-2457.

Webb, D.J., Nguyen, D.H., and Gonias, S.L. (2000). Extracellular signal-regulated kinase functions in the urokinase receptor-dependent pathway by which neutralization of low density lipoprotein receptor-related protein promotes fibrosarcoma cell migration and matrigel invasion. J Cell Sci *113 (Pt 1)*, 123-134.

Webb, D.J., Nguyen, D.H., Sankovic, M., and Gonias, S.L. (1999). The very low density lipoprotein receptor regulates urokinase receptor catabolism and breast cancer cell motility in vitro. J Biol Chem *274*, 7412-7420.

Weeber, E.J., Beffert, U., Jones, C., Christian, J.M., Forster, E., Sweatt, J.D., and Herz, J. (2002). Reelin and ApoE receptors cooperate to enhance hippocampal synaptic plasticity and learning. J Biol Chem *277*, 39944-39952.

Werb, Z., Vu, T.H., Rinkenberger, J.L., and Coussens, L.M. (1999). Matrix-degrading proteases and angiogenesis during development and tumor formation. Apmis *107*, 11-18.

Westein, E., Denis, C.V., Bouma, B.N., and Lenting, P.J. (2002). The alpha -chains of C4b-binding protein mediate complex formation with low density lipoprotein receptor-related protein. J Biol Chem *277*, 2511-2516.

Wewer, U.M., Morgelin, M., Holck, P., Jacobsen, J., Lydolph, M.C., Johnsen, A.H., Kveiborg, M., and Albrechtsen, R. (2006). ADAM12 is a four-leafed clover: the excised prodomain remains bound to the mature enzyme. J Biol Chem *281*, 9418-9422.

Wight, T.N., and Merrilees, M.J. (2004). Proteoglycans in atherosclerosis and restenosis: key roles for versican. Circ Res *94*, 1158-1167.

Williams, S.E., Ashcom, J.D., Argraves, W.S., and Strickland, D.K. (1992). A novel mechanism for controlling the activity of alpha 2-macroglobulin receptor/low density lipoprotein receptor-related protein. Multiple regulatory sites for 39-kDa receptor-associated protein. J Biol Chem *267*, 9035-9040.

Williams, S.E., Inoue, I., Tran, H., Fry, G.L., Pladet, M.W., Iverius, P.H., Lalouel, J.M., Chappell, D.A., and Strickland, D.K. (1994). The carboxyl-terminal domain of lipoprotein lipase binds to the low density lipoprotein receptor-related protein/alpha 2-macroglobulin receptor (LRP) and mediates binding of normal very low density lipoproteins to LRP. J Biol Chem *269*, 8653-8658.

Williamson, R.A., Marston, F.A., Angal, S., Koklitis, P., Panico, M., Morris, H.R., Carne, A.F., Smith, B.J., Harris, T.J., and Freedman, R.B. (1990). Disulphide bond assignment in human tissue inhibitor of metalloproteinases (TIMP). Biochem J *268*, 267-274.

Willnow, T.E., Armstrong, S.A., Hammer, R.E., and Herz, J. (1995). Functional expression of low density lipoprotein receptor-related protein is controlled by receptor-associated protein in vivo. Proc Natl Acad Sci U S A *92*, 4537-4541.

Willnow, T.E., Goldstein, J.L., Orth, K., Brown, M.S., and Herz, J. (1992). Low density lipoprotein receptor-related protein and gp330 bind similar ligands, including plasminogen activator-inhibitor complexes and lactoferrin, an inhibitor of chylomicron remnant clearance. J Biol Chem *267*, 26172-26180.

Willnow, T.E., and Herz, J. (1994). Genetic deficiency in low density lipoprotein receptor-related protein confers cellular resistance to Pseudomonas exotoxin A. Evidence that this protein is required for uptake and degradation of multiple ligands. J Cell Sci *107 (Pt 3)*, 719-726.

Willnow, T.E., Moehring, J.M., Inocencio, N.M., Moehring, T.J., and Herz, J. (1996). The low-density-lipoprotein receptor-related protein (LRP) is processed by furin in vivo and in vitro. Biochem J *313 (Pt 1)*, 71-76.

Wilsie, L.C., Gonzales, A.M., and Orlando, R.A. (2006). Syndecan-1 mediates internalization of apoE-VLDL through a low density lipoprotein receptor-related protein (LRP)-independent, non-clathrin-mediated pathway. Lipids Health Dis *5*, 23.

Wisniewska, M., Goettig, P., Maskos, K., Belouski, E., Winters, D., Hecht, R., Black, R., and Bode, W. (2008). Structural determinants of the ADAM inhibition by TIMP-3: crystal structure of the TACE-N-TIMP-3 complex. J Mol Biol *381*, 1307-1319.

Woessner, J.F., Jr., and Nagase, H. (2000). Matrix metalloproteinases and TIMPs. Protein Profile *Oxford University Press*.

Wolfsberg, T.G., Bazan, J.F., Blobel, C.P., Myles, D.G., Primakoff, P., and White, J.M. (1993). The precursor region of a protein active in sperm-egg fusion contains a

metalloprotease and a disintegrin domain: structural, functional, and evolutionary implications. Proc Natl Acad Sci U S A *90*, 10783-10787.

Woolley, D.E., Roberts, D.R., and Evanson, J.M. (1975). Inhibition of human collagenase activity by a small molecular weight serum protein. Biochem Biophys Res Commun *66*, 747-754.

Wyckoff, M., Rodbard, D., and Chrambach, A. (1977). Polyacrylamide gel electrophoresis in sodium dodecyl sulfate-containing buffers using multiphasic buffer systems: properties of the stack, valid Rf- measurement, and optimized procedure. Anal Biochem *78*, 459-482.

Wygrecka, M., Wilhelm, J., Jablonska, E., Zakrzewicz, D., Preissner, K.T., Seeger, W., Guenther, A., and Markart, P. (2011). Shedding of low-density lipoprotein receptor-related protein-1 in acute respiratory distress syndrome. Am J Respir Crit Care Med *184*, 438-448.

Yamamoto, K., Troeberg, L., Scilabra, S.D., Pelosi, M., Murphy, C.L., Strickland, D.K., and Nagase, H. (2012). LRP-1-mediated endocytosis regulates extracellular activity of ADAMTS-5 in articular cartilage. In revision.

Yamazaki, H., Bujo, H., Kusunoki, J., Seimiya, K., Kanaki, T., Morisaki, N., Schneider, W.J., and Saito, Y. (1996). Elements of neural adhesion molecules and a yeast vacuolar protein sorting receptor are present in a novel mammalian low density lipoprotein receptor family member. J Biol Chem *271*, 24761-24768.

Yanagishita, M. (1992). Glycosylphosphatidylinositol-anchored and core protein-intercalated heparan sulfate proteoglycans in rat ovarian granulosa cells have distinct secretory, endocytotic, and intracellular degradative pathways. J Biol Chem *267*, 9505-9511.

Yancey, P.G., Ding, Y., Fan, D., Blakemore, J.L., Zhang, Y., Ding, L., Zhang, J., Linton, M.F., and Fazio, S. (2011). Low-density lipoprotein receptor-related protein 1 prevents early atherosclerosis by limiting lesional apoptosis and inflammatory Ly-6Chigh monocytosis: evidence that the effects are not apolipoprotein E dependent. Circulation *124*, 454-464.

Yang, M., and Kurkinen, M. (1998). Cloning and characterization of a novel matrix metalloproteinase (MMP), CMMP, from chicken embryo fibroblasts. CMMP, Xenopus XMMP, and human MMP19 have a conserved unique cysteine in the catalytic domain. J Biol Chem *273*, 17893-17900.

Yang, T.T., and Hawkes, S.P. (1992). Role of the 21-kDa protein TIMP-3 in oncogenic transformation of cultured chicken embryo fibroblasts. Proc Natl Acad Sci U S A *89*, 10676-10680.

Yang, X., Wang, J., Guo, S.L., Fan, K.J., Li, J., Wang, Y.L., and Teng, Y. (2011). miR-21 promotes keratinocyte migration and re-epithelialization during wound healing. Int J Biol Sci *7*, 685-690.

Yang, Z., Strickland, D.K., and Bornstein, P. (2001). Extracellular matrix metalloproteinase 2 levels are regulated by the low density lipoprotein-related scavenger receptor and thrombospondin 2. J Biol Chem *276*, 8403-8408.

Yepes, M., Sandkvist, M., Moore, E.G., Bugge, T.H., Strickland, D.K., and Lawrence, D.A. (2003). Tissue-type plasminogen activator induces opening of the blood-brain barrier via the LDL receptor-related protein. J Clin Invest *112*, 1533-1540.

Yu, W.H., and Woessner, J.F., Jr. (2000). Heparan sulfate proteoglycans as extracellular docking molecules for matrilysin (matrix metalloproteinase 7). J Biol Chem *275*, 4183-4191.

Yu, X.F., Yang, C., Liang, L.H., Liu, B., Zhou, B., Li, B., and Han, Z.C. (2006). Inhibition of human leukemia xenograft in nude mice by adenovirus-mediated tissue inhibitor of metalloproteinase-3. Leukemia *20*, 1-8.

Zhang, L., Zhao, L., Zhao, D., Lin, G., Guo, B., Li, Y., Liang, Z., Zhao, X.J., and Fang, X. (2010). Inhibition of tumor growth and induction of apoptosis in prostate cancer cell lines by overexpression of tissue inhibitor of matrix metalloproteinase-3. Cancer Gene Ther *17*, 171-179.

Zheng, G., Bachinsky, D.R., Stamenkovic, I., Strickland, D.K., Brown, D., Andres, G., and McCluskey, R.T. (1994). Organ distribution in rats of two members of the low-density lipoprotein receptor gene family, gp330 and LRP/alpha 2MR, and the receptor-associated protein (RAP). J Histochem Cytochem *42*, 531-542.

Appendix

Matrix Biology 28 (2009) 463–469

Contents lists available at ScienceDirect

Matrix Biology

journal homepage: www.elsevier.com/locate/matbio

The C-terminal domains of ADAMTS-4 and ADAMTS-5 promote association with N-TIMP-3

Linda Troeberg [a], Kazunari Fushimi [a], Simone D. Scilabra [a], Hiroyuki Nakamura [a], Vincent Dive [b], Ida B. Thøgersen [c], Jan J. Enghild [c], Hideaki Nagase [a,*]

[a] Kennedy Institute of Rheumatology, Imperial College London, 65 Aspenlea Road, Hammersmith, London, W6 8LH, UK
[b] CEA, iBiTecS, Service d'Ingénierie Moleculaires des Protéines, Gif Sur Yvette, F-91191, France
[c] Department of Molecular Biology and Interdisciplinary Nanoscience Centre (iNANO), University of Aarhus, Gustav Wieds Vej 10C, DK-8000 Aarhus C, Denmark

ARTICLE INFO

Article history:
Received 8 April 2009
Received in revised 20 July 2009
Accepted 20 July 2009

Keywords:
Aggrecanase
Inhibition kinetics
MMPs

ABSTRACT

We investigated whether the affinity of tissue inhibitor of metalloproteinases (TIMP)-3 for adamalysins with thrombospondin motifs (ADAMTS)-4 and ADAMTS-5 is affected by the non-catalytic ancillary domains of the enzymes. For this purpose, we first established a novel method of purifying recombinant FLAG-tagged TIMP-3 and its inhibitory N-terminal domain (N-TIMP-3) by treating transfected HEK293 cells with sodium chlorate to prevent heparan sulfate proteoglycan-mediated TIMP-3 internalization. TIMP-3 and N-TIMP-3 affinity for selected matrix metalloproteinases and forms of ADAMTS-4 and -5 lacking sequential C-terminal domains was determined. TIMP-3 and N-TIMP-3 displayed similar affinity for various matrix metalloproteinases as has been previously reported for *E. coli*-expressed N-TIMP-3. ADAMTS-4 and -5 were inhibited more strongly by N-TIMP-3 than by full-length TIMP-3. The C-terminal domains of the enzymes enhanced interaction with N-TIMP-3 and to a lesser extent with the full-length inhibitor. For example, N-TIMP-3 had 7.5-fold better K_i value for full-length ADAMTS-5 than for the catalytic and disintegrin domain alone. We propose that the C-terminal domains of the enzymes affect the structure around the active site, favouring interaction with TIMP-3.

1. Introduction

In addition to their catalytic domains, proteolytic enzymes often have non-catalytic ancillary domains that modulate interaction of the enzyme with substrates or inhibitors. Indeed, almost all members of the metzincin family of metalloproteinases have such ancillary domains, and they have been shown to mediate recognition and cleavage of numerous substrates. For example, the hemopexin domain of matrix metalloproteinase 1 (MMP-1) is required for cleavage of collagen (Clark and Cawston, 1989). Among the related adamalysins with thrombospondin motifs (ADAMTSs), the C-terminal domains of ADAMTS-4 and ADAMTS-5 have been shown to promote aggrecan cleavage (Kashiwagi et al., 2004; Gendron et al., 2007; Fushimi et al., 2008), the C-terminal spacer domain of ADAMTS13 promotes cleavage of von Willebrand factor (Gao et al., 2008) and C-terminal domains of ADAMTS-2 modulate processing of the N-terminal propeptide of procollagen (Colige et al., 2005). These ancillary domains have also been shown to modulate interaction of some metzincins with the endogenous tissue inhibitors of metalloproteinases (TIMPs). For example, the MMP-2 hemopexin domain interacts strongly with TIMP-2 (Murphy et al., 1992; Butler et al., 1999; Morgunova et al., 2002). While the MMPs are inhibited by all four of the mammalian TIMPs, most adamalysins and ADAMTSs are inhibited only by TIMP-3. Compared to the MMPs, the adamalysins and ADAMTSs have a greater number and diversity of C-terminal ancillary domains and the role of these in modulating interactions with TIMP-3 is largely unknown, as a lack of sensitive substrates has hampered in-depth kinetic analysis. Good substrates are available for ADAM17, or tumour necrosis factor-α converting enzyme (TACE) and the C-terminal domains of this enzyme have been shown to reduce the affinity of the enzyme for both full-length TIMP-3 and N-TIMP-3 by 10-fold (Lee et al., 2002).

ADAMTS-4 and -5 cleave the cartilage matrix proteoglycan aggrecan at various sites, releasing the chondroitin and keratan sulfate-bearing region of the molecule from the tissue. This is an early and crucial step in the development of osteoarthritis as it reduces the ability of the tissue to resist compressive loads. Both enzymes are readily proteolyzed to smaller isoforms, which have altered proteolytic activity (Gao et al., 2004). Here we investigate TIMP-3 inhibition of the isoforms, with an

Abbreviations: ADAM, adamalysin; ADAMTS, adamalysin with thrombospondin motifs; cat, catalytic domain; CysR, cysteine-rich; Dis, disintegrin; LRP, low-density lipoprotein receptor-related protein; MMP, matrix metalloproteinase; N-TIMP, N-terminal domain of TIMP; RAP, receptor-associated protein; Sp, spacer; TACE, tumour necrosis factor-α converting enzyme; TIMP, tissue inhibitor of metalloproteinase; TS, thrombospondin; VAP, vascular apoptosis-inducing protein.

* Corresponding author. Tel.: +44 020 8383 4488; fax: +44 020 8383 4994.
E-mail address: h.nagase@imperial.ac.uk (H. Nagase).

0945-053X/$ – see front matter © 2009 Elsevier B.V. All rights reserved.
doi:10.1016/j.matbio.2009.07.005

aim to understanding whether, as in the case of ADAM17, the C-terminal ancillary domains of the enzymes regulate TIMP-3 binding to the active site. To do this, we developed a novel method of purifying sufficient soluble full-length TIMP-3 and its inhibitory N-terminal domain (N-TIMP-3) for kinetic analysis.

N-TIMP-3 can be successfully expressed in *Escherichia coli* and refolded *in vitro* (Kashiwagi et al., 2001), but we have not been able to refold full-length TIMP-3 using this system. Unlike the other TIMPs, TIMP-3 binds tightly to the extracellular matrix and is not readily soluble (Lee et al., 2007; Yu et al., 2000). It is thus difficult to recombinantly express TIMP-3 in mammalian cells, and to date full-length TIMP-3 has only been recombinantly produced in NSO mouse myeloma cells, which do not produce an extracellular matrix (Apte et al., 1995). Here we describe successful purification of full-length TIMP-3 and N-TIMP-3 recombinantly expressed in human embryonic kidney HEK293 cells. Recently developed synthetic fluorescent quenched substrates allowed us to determine the inhibition constants of both TIMP-3 and N-TIMP-3 for various forms of ADAMTS-4 and ADAMTS-5.

2. Results

2.1. Purification of recombinant TIMP-3 and N-TIMP-3

This study describes a novel method of purifying soluble full-length TIMP-3. No TIMP-3 is observed in the conditioned medium of transfected HEK293 cells, and we have previously shown that TIMP-3 is rapidly endocytosed after secretion from the cell by a scavenger endocytic receptor of the low-density lipoprotein receptor-related protein (LRP) family (Troeberg et al., 2008). TIMP-3 accumulates in the conditioned medium if this endocytic pathway is blocked, for example by the addition of receptor-associated protein (RAP), an inhibitor of LRP-mediated endocytosis (Troeberg et al., 2008). Heparin also causes an accumulation of TIMP-3, indicating that a heparan sulfate proteoglycan co-receptor is possibly required for LRP-mediated endocytosis as has been reported for other LRP ligands (Godyna et al., 1995; Sarafanov et al., 2001). However, heparin binds to TIMP-3 tightly and purification of TIMP-3 from heparin-treated cells proved difficult. To keep recombinantly expressed TIMP-3 in the medium, we treated transfected cells with sodium chlorate ($NaClO_3$), which blocks sulfation of cell surface glycosaminoglycans (Baeuerle and Huttner, 1986; Safaiyan et al., 1999). This resulted in the accumulation of FLAG-tagged TIMP-3 and N-TIMP-3 in the conditioned medium of transfected cells. Both proteins were purified from the conditioned medium by anti-FLAG affinity chromatography (Fig. 1A). As previously reported for full-length ADAMTS-4 (Kashiwagi et al., 2004), substantial processing of the C-terminal FLAG-tag occurred, reducing the yield to approximately 50 μg of purified protein per litre of conditioned medium. Both TIMP-3 and N-TIMP-3 expressed in HEK293 were confirmed to have the expected N-terminal sequence ^{1}CTCSPSHPQD and to react with a polyclonal anti-TIMP-3 antibody (Fig 1B). Titration against a known concentration of MMP-1 showed all preparations of TIMP-3 to be 100% active.

TIMP-3 contains a single N-glycosylation site in its C-terminal domain (Apte et al., 1995) and various possible O-glycosylation sites. Various cell types have been shown to express both a 27 kDa glycosylated and a 24 kDa non-glycosylated form (Apte et al., 1995; Fabunmi et al., 1996; Langton et al., 1998). Transfected HEK293 cells also synthesized both glycosylated and non-glycosylated forms, but only the glycosylated form remained after purification, with the non-glycosylated form possibly lost due to increased "stickiness". Indeed, we obtained lower yields when we treated cells with tunicamycin to obtain only the non-N-glycosylated form. N-TIMP-3 was expressed primarily as a non-glycosylated form, with a lower amount of a higher molecular mass glycosylated form present. Since N-TIMP-3 contains no N-glycosylation sites, this possibly reflects O-glycosylation.

2.2. $K_{i(app)}$ of TIMP-3 and N-TIMP-3 for selected MMPs

We compared the inhibitory activity of our mammalian-expressed TIMP-3 and N-TIMP-3 with the previously characterized *E. coli*-expressed N-TIMP-3 with a C-terminal His-tag (Kashiwagi et al., 2001). $K_{i(app)}$ values determined in the current study for *E. coli*-expressed N-TIMP-3 agreed well with previously published values for this protein (Kashiwagi et al., 2001). Although we determined a 6-fold lower $K_{i(app)}$ value for N-TIMP-3 inhibition of the catalytic domain of MMP-3 (MMP-3_{cat}), our results agree with that found in the previous study that N-TIMP-3 is a weaker inhibitor of MMP-3_{cat} than of the catalytic domain of MMP-1 (MMP-1_{cat}) or MMP-2 (Table 1).

We found that mammalian-expressed N-TIMP-3 had essentially identical inhibitory properties to the *E. coli*-expressed N-TIMP-3, being a strong inhibitor of MMP-1_{cat} and MMP-2, and a 10-fold weaker inhibitor of MMP-3_{cat}.

MMP-1_{cat} was equally well inhibited by N-TIMP-3 and full-length TIMP-3. MMP-3_{cat}, however, was more strongly inhibited by full-length TIMP-3 than by N-TIMP-3, implying that the C-terminal domain of the inhibitor contributes to binding. The MMP-2 catalytic domain (MMP-2_{cat}) was equally well inhibited by N-TIMP-3 and full-length TIMP-3, but the full-length enzyme was more strongly inhibited by the full-length TIMP-3 than by N-TIMP-3. This indicates that the C-terminal domain of TIMP-3 interacts with the C-terminal hemopexin domain of MMP-2.

2.3. K_i of TIMP-3 and N-TIMP-3 for ADAMTS-4 and ADAMTS-5

We analyzed TIMP-3 and N-TIMP-3 inhibition of various isoforms (Fig. 2) of ADAMTS-4 and -5 lacking C-terminal ancillary domains. Fig. 3 shows representative data for four enzyme isoforms fitted to the tight-binding equation (Bieth, 1995). All isoforms of ADAMTS-4 and -5 were effectively inhibited by TIMP-3 and N-TIMP-3, with K_i values in the sub-nanomolar range. All ADAMTS-5 isoforms were inhibited more strongly by N-TIMP-3 than by full-length TIMP-3 (Table 2). The C-terminal domains of ADAMTS-5 enhanced inhibition by N-TIMP-3, with full-length ADAMTS-5 (ADAMTS5-1) having a 7.5-fold better K_i value than ADAMTS5-5, which consists of the catalytic and disintegrin domain. The C-terminal domains of the enzyme had a similar, although less marked, effect on association with the full-length inhibitor. The C-terminal domains of ADAMTS-4 also had a similar effect on association with full-length and N-TIMP-3 (Table 2).

Glycosylation had little effect on TIMP-3 or N-TIMP-3 inhibition of ADAMT5-2 or ADAMTS4-2 (Table 3).

The isolated catalytic domains of ADAMTS-4 and -5 (ADAMTS4-5 and ADAMTS5-6) had only minimal activity on natural substrates and the synthetic substrates used, so their inhibition by TIMP-3 could not be analyzed by enzyme inhibition kinetics.

3. Discussion

Here we report a novel method to generate recombinant TIMP-3 protein by treating transfected HEK293 cells with sodium chlorate. Our initial attempts to express TIMP-3 in HEK293 or HTB94 chondrosarcoma cells were hampered by the observation that, although these cells transcribe a considerable amount of TIMP-3 mRNA, no TIMP-3 accumulates in the conditioned medium. We have previously reported that TIMP-3 is normally internalized but accumulates in medium in the presence of an antagonist of the LRP endocytic receptor or heparin (Troeberg et al., 2008). We thus treated cells with sodium chlorate, which blocks sulfation of cell surface glycosaminoglycans (Baeuerle and Huttner, 1986; Safaiyan et al., 1999) and observed accumulation of soluble TIMP-3 in the medium. TIMP-3 has previously been purified from the conditioned medium of transfected NSO mouse myeloma cells (Apte et al., 1995), which appear to lack this endocytic pathway. Our transfected cells showed no signs of TIMP-3-induced apoptosis (Bond et al., 2000) in the absence of sodium chlorate, but exhibited

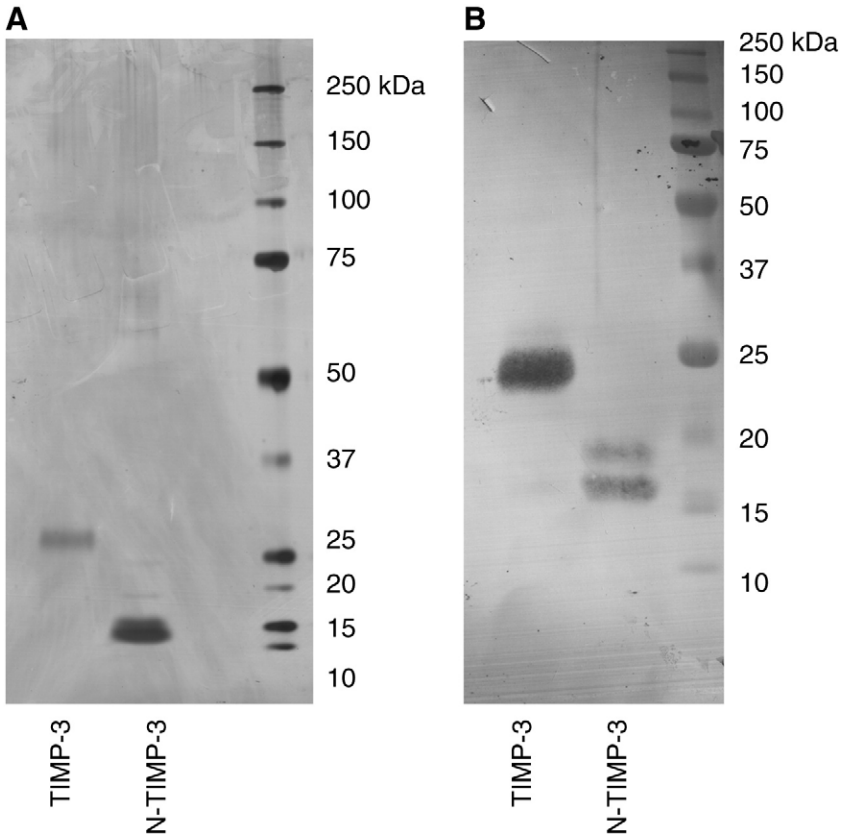

Fig. 1. Purification of TIMP-3 and N-TIMP-3. FLAG-tagged glycosylated human TIMP-3 and N-TIMP-3 were expressed by treating transfected HEK293 with 30 mM sodium chlorate in serum-free DMEM and purified from the conditioned medium by FLAG affinity chromatography and cation exchange chromatography. A. Silver-stained 10% polyacrylamide SDS-PAGE gel of TIMP-3 (100 ng) and N-TIMP-3 (100 ng). B. Immuoblot of 12% polyacrylamide SDS-PAGE gel of TIMP-3 (100 ng) and N-TIMP-3 (100 ng) stained using a polyclonal rabbit anti-TIMP-3 antibody.

increased cell death once chlorate was added and TIMP-3 accumulated in the medium.

Our values for TIMP-3 inhibition of ADAMTS-5 ($K_i = 0.1–1.2$ nM, Table 2) are in agreement with the previously reported value of 0.66 nM (Kashiwagi et al., 2001). Our K_i values for TIMP-3 inhibition of ADAMTS-4 ($K_i = 0.1–0.7$ nM) are also in agreement with that reported by Kashiwagi et al. (2001), although higher values of 4–8 nM have been reported in other studies (Hashimoto et al., 2001; Wayne et al., 2007).

C-terminal domains distal to the disintegrin domain are required for ADAMTS-4 and -5 activity on aggrecan and various other protein substrates, but these domains had little effect on hydrolysis of the synthetic substrates used in this study (data not shown). The isolated catalytic domains of ADAMTS-4 and -5 had negligible activity on these synthetic substrates. To date, the catalytic domain alone has not been shown to effectively cleave protein substrates such as aggrecan, suggesting that the disintegrin domain may be part of the minimal catalytic unit. This view is supported by the crystal structures of ADAMTS-4 and -5, which show that the disintegrin domain is located close to the catalytic domain and may act as an extension of the catalytic cleft (Mosyak et al., 2008).

The inhibitory machinery of TIMPs is contained in their N-terminal domains, and in most cases, the C-terminal domains of both MMPs and TIMPs have a minimal effect on complex formation (Brew et al., 2000). There are some notable exceptions to this, in which interactions other than binding of the N-terminal TIMP domain to the catalytic domain of the enzyme contribute substantially to the overall binding energy. In particular, the C-terminal domains of TIMP-2, TIMP-3 and TIMP-4 bind strongly to the MMP-2 hemopexin domain (Butler et al., 1999; Lee et al., 2001; Morgunova et al., 2002; Murphy et al., 1992; Troeberg et al., 2002) and the C-terminal domain of TIMP-1 binds to the hemopexin domain of MMP-9 (Bodden et al., 1994).

While the C-terminal domains of MMPs either have little effect or strengthen binding to TIMPs, the C-terminal domains of ADAM17 weaken interaction with both full-length TIMP-3 and N-TIMP-3 by 10-fold (Lee et al., 2002). Also, the ADAM17 catalytic domain interacts more strongly with the prodomain than the enzyme with disintegrin and cysteine-rich domains attached to the catalytic domain (Milla et al., 1999). Lee et al. (2002) postulated that the C-terminal domains of the enzyme may sterically hinder access to the catalytic site. The spatial orientation of the ADAM17 C-terminal domains is not known, as crystal structures are only available for the catalytic domain in complex with either a hydroxamate inhibitor or N-TIMP-3 (Maskos et al., 1998; Wisniewska et al., 2008). However, for the related snake venom metalloproteinases, called vascular apoptosis-inducing proteins (VAPs), crystal structures are available showing the catalytic, disintegrin and cysteine-rich domains (Igarashi et al., 2007; Igarashi et al., 2006; Takeda, 2008). These structures support Lee et al.'s (2002) proposal that the C-terminal domains of ADAM17 may sterically hinder TIMP-3 access to the active site as the C-terminal VAP domains

Table 1
$K_{i(app)}$ values[a] (nM) for TIMP-3 and N-TIMP-3 inhibition of selected MMPs.

	Kashiwagi et al. *E. coli*-expressed N-TIMP-3	Current study *E. coli*-expressed N-TIMP-3	Mammalian-expressed N-TIMP-3	Mammalian-expressed TIMP-3
MMP-1_{cat}	1.2	0.8 ± 0.4	0.9 ± 0.6	1. 1 ± 0.6
MMP-2	4.3	1.3 ± 0.5	0.9 ± 0.3	<0.1
MMP-2_{cat}	ND	0.8 ± 0.1	1.0 ± 0.3	0.9 ± 0.3
MMP-3_{cat}	66.9	11.1 ± 5.0	9.1 ± 3.3	1.0 ± 0.4

[a] $K_{i(app)}$ given as mean ± standard deviation ($n = 4–6$).

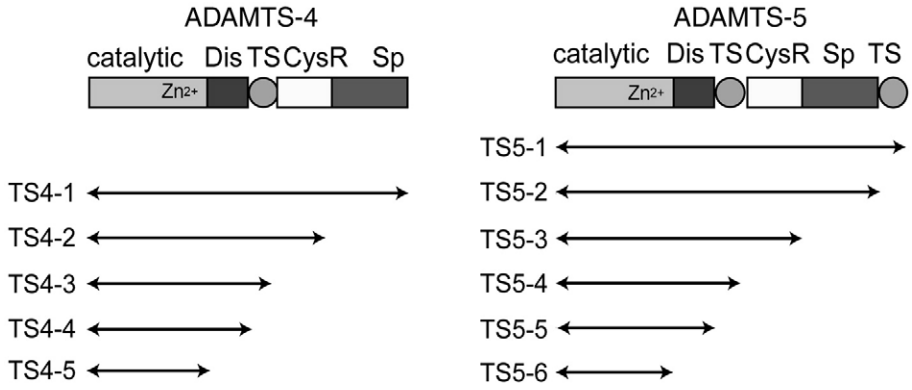

Fig. 2. ADAMTS-4 and ADAMTS-5 isoforms analyzed. Each isoform has a FLAG-tag at its C-terminus and was purified from the conditioned medium of transfected HEK293 cells by FLAG affinity chromatography. Dis, disintegrin domain; TS, thrombospondin domain; CysR, cysteine-rich domain; Sp, spacer domain.

adopt a C-shaped conformation, with the concave surface of the cysteine-rich domain being located near to and facing the catalytic domain (Igarashi et al., 2007). Additionally, there is a "hinge" region between the catalytic and disintegrin domains and the 6 available VAP structures indicate flexibility in the orientation of the catalytic domain relative to the C-terminal domains.

In contrast to ADAM17, we found that the ADAMTS-4 and -5 C-terminal domains increase association with N-TIMP-3 by 5–7-fold (Table 2). The C-terminal domains also increase association with full-length TIMP-3, albeit to a lesser extent (K_i for ADAMTS-4 and -5 improves 2-fold). This is in agreement with the report of Wayne et al. (2007). In particular, our data suggest that the TS domains of ADAMTS-4 and -5 are involved in interaction with TIMP-3. Deletion of the C-terminal TS domain of ADAMTS-5 increases K_i for N-TIMP-3 by 3-fold. Further deletion of the Sp and CysR domains has minimal effect on K_i, but deletion of the first TS domain results in a further increase in K_i for N-TIMP-3. K_i values for ADAMTS-4 deletion mutants show the same result, with deletion of the TS domain increasing K_i for N-TIMP-3 by 6-fold, while deletion of the Sp and CysR domains had little effect. Interestingly, the TS domains have also been shown to play a role in substrate recognition and cleavage (Tortorella et al., 2000; Fushimi et al., 2008).

The domain architecture of the full-length ADAMTSs is not known, as three-dimensional structures are only available for the catalytic and disintegrin domains of ADAMTS-1, -4 and -5 (Gerhardt et al., 2007; Mosyak et al., 2008; Shieh et al., 2008). Although the ADAMTS and VAP disintegrin domains share sequence homology, it is not possible to extrapolate to the ADAMTSs from the available VAP structures as their domain arrangements are dissimilar and may adopt a different

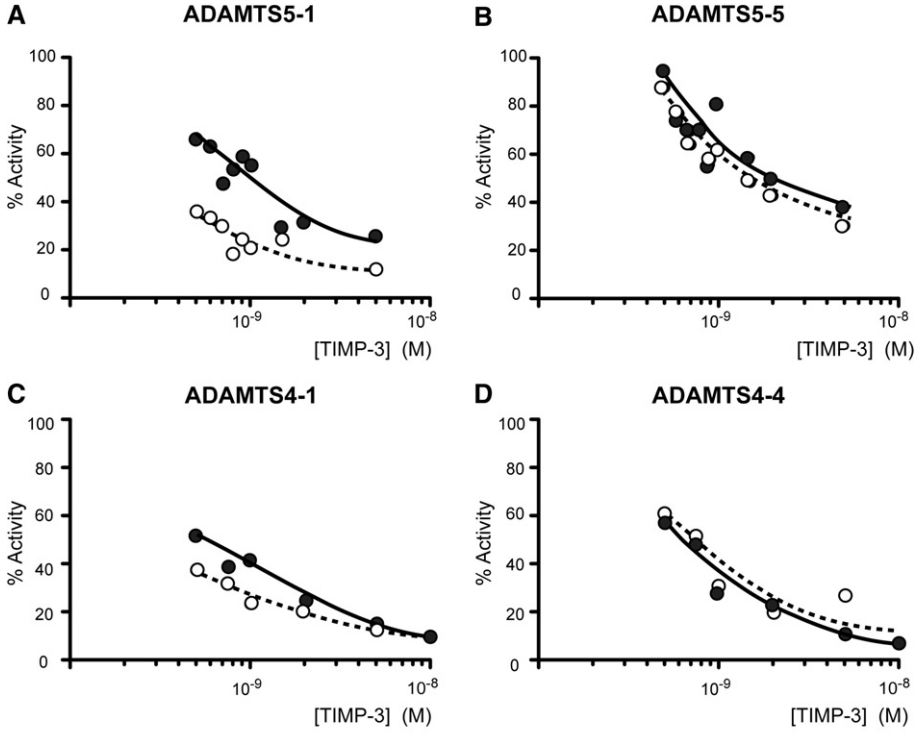

Fig. 3. Inhibition of ADAMTS-4 and ADAMTS-5 by TIMP-3 and N-TIMP-3. ADAMTS5-1 (A, 0.5 nM) and ADAMTS5-5 (B, 0.5 nM) were incubated with 0.5–5 nM TIMP-3 (●) or N-TIMP-3 (○) for 1 h at 37 °C and residual activity against Abz-TESE~SRGAIY-Dpa-KK determined (18 h, 37 °C). TIMP-3 and N-TIMP-3 had $K_{i(app)}$ values of 0.70 ± 0.04 nM and 0.14 ± 0.02 nM respectively for ADAMTS5-1, and 1.89 ± 0.06 nM and 1.35 ± 0.04 nM respectively for ADAMTS5-5. ADAMTS4-1 (C, 0.5 nM) and ADAMTS4-4 (D, 0.5 nM) were incubated with 0.25–10 nM TIMP-3 (●) or N-TIMP-3 (○) for 1 h at 37 °C and residual activity against FAM-AE~LQGRPISIAK-TAMRA (1 μM) determined (18 h, 37 °C). TIMP-3 and N-TIMP-3 had $K_{i(app)}$ values of 0.39 ± 0.03 nM and 0.19 ± 0.04 nM respectively for ADAMTS4-1, and 0.38 ± 0.04 nM and 0.55 ± 0.05 nM respectively for ADAMTS4-4. The error values given are the standard errors on the fit of the data to the tight-binding equation (Eq. (2)) (Bieth, 1995).

Table 2
K_i values (nM)[a] for mammalian-expressed TIMP-3 and N-TIMP-3 inhibition of ADAMTS-4 and ADAMTS-5.

	N-TIMP-3	TIMP-3		N-TIMP-3	TIMP-3
ADAMTS5-1	0.13 ± 0.06	0.63 ± 0.17			
ADAMTS5-2	0.35 ± 0.03	0.72 ± 0.17	ADAMTS4-1	0.13 ± 0.06	0.22 ± 0.15
ADAMTS5-3	0.29 ± 0.08	1.00 ± 0.39	ADAMTS4-2	0.18 ± 0.02	0.22 ± 0.07
ADAMTS5-4	0.40 ± 0.18	1.13 ± 0.37	ADAMTS4-3	0.10 ± 0.01	0.40 ± 0.07
ADAMTS5-5	1.01 ± 0.45	1.17 ± 0.33	ADAMTS4-4	0.64 ± 0.15	0.51 ± 0.21

[a] K_i values given as mean ± standard deviation ($n = 4$–6).

orientation relative to the catalytic domain (Gerhardt et al., 2007; Takeda, 2008). The crystal structures of the catalytic and disintegrin domains of ADAMTS-4 with and without a low molecular weight inhibitor determined by Mosyak et al. (2008) indicated an 'open' and a 'closed' form, respectively. In the latter form, the residues Asp^{328} and Thr^{329} in the so-called S2′ loop of ^{322}CGXXXCDTL^{330} are around the catalytic zinc and the side chain of Asp^{328} chelates the Zn^{2+} ion and that of Thr^{329} fills the space at the mouth of the S1′ pocket. Thus, the S2′ loop remains as an auto-inhibitor unless structural re-arrangements occur around this region and disrupt the interaction between Asp^{328} and the Zn^{2+} ion. However, as proposed by Mosyak et al. (2008), the active open form and the inactive closed form may exist in equilibrium. Full-length ADAMTS-4 and ADAMTS-5 are highly active against a natural substrate, aggrecan, but deletion of the C-terminal non-catalytic domains of the enzymes greatly reduces their activity (Kashiwagi et al., 2004; Gendron et al., 2007; Fushimi et al., 2008). This suggests that these domains alone or substrate binding to these non-catalytic domains may shift the equilibrium to the more open form. Our data support this possibility, since the presence of the C-terminal domains enhances association with N-TIMP-3. Also, agents that interact with the ADAMTS C-terminal domains, such as calcium pentosan polysulfate and aggrecan, improve affinity for TIMP-3 (Troeberg et al., 2008; Wayne et al., 2007).

It is unclear why the C-terminal domains favour association with N-TIMP-3 more than with full-length TIMP-3. Given that N-TIMP-3 is a slightly better inhibitor of full-length ADAMTS-4 and -5 than full-length TIMP-3 (Table 2), steric clashes may occur between the C-terminal domain of TIMP-3 and the ADAMTS non-catalytic domains. Alternatively, a surface available in N-TIMP-3 but not full-length TIMP-3 may enhance interaction with the non-catalytic domains of the enzyme, which in turn, could increase the affinity of binding to the active site. Interestingly, N-TIMP-4 is also a better inhibitor of ADAM17 than full-length TIMP-4 (Lee et al., 2005). The opposite is true for ADAM10, which is not inhibited by N-TIMP-1 or N-TIMP-3, but is effectively inhibited by full-length TIMP-1 and TIMP-3 (Rapti et al., 2008). The ADAMs and the ADAMTSs analyzed to date thus vary considerably in their affinity for N-TIMP-3 relative to full-length TIMP-3, possibly reflecting conformational diversity of their C-terminal domains. Structural studies of the complex formed between full-length ADAMTS-4 or -5 and TIMP-3 are necessary to obtain further information on these molecular interactions.

Table 3
Effect of glycosylation on TIMP-3 and N-TIMP-3 inhibition of ADAMTS4-2 and ADAMTS5-2.

	N-TIMP-3 K_i[a]		TIMP-3 K_i[a]	
	Glycosylated[b]	Non-glycosylated[c]	Glycosylated[b]	Non-glycosylated[d]
ADAMTS5-2	0.35 ± 0.03	0.32 ± 0.12	0.72 ± 0.17	1.37 ± 0.4
ADAMTS4-2	0.18 ± 0.02	0.79 ± 0.02	0.22 ± 0.07	0.20 ± 0.08

[a] K_i values (nM) are expressed as mean ± standard deviation ($n = 4$).
[b] Glycosylated TIMP-3 and N-TIMP-3 were expressed in HEK293 cells.
[c] Non-glycosylated N-TIMP-3 was expressed in *E. coli*.
[d] Non-glycosylated TIMP-3 was expressed in HEK293 cells treated with 5 μg/ml tunicamycin.

4. Experimental procedures

4.1. Preparation of TIMP-3 and N-TIMP-3 from HEK293

Recombinant human C-terminally FLAG-tagged TIMP-3 and N-TIMP-3 were expressed using pCEP4-based expression vectors (Invitrogen, Paisley, UK) constructed by the PCR method. The TIMP-3 expression vector was constructed using the sense primer 5′-CTCGAGTCCC-TTTTTTTTCCACAGGAGCTC*GCCGCCACC*ATGACCCCTTGGCTCGGGCT-CATCGTGCTC-3′ containing an XhoI site (underlined), Kozak consensus sequence (in italics) and TIMP-3N-terminal sequence, and the anti-sense primer 5′-CTCGAG*CTACTTATCGTCGTCATCCTTGTAATC*GGGGTCTGTGG-CATTGATGATGCTTTTATCCGG-3′ containing an XhoI site (underlined), FLAG epitope (Asp-Tyr-Lys-Asp-Asp-Asp-Asp-Lys-stop) (in italics) and the C-terminal sequence of TIMP-3, with a TIMP-3 vector kindly provided by Prof M. Seiki (University of Tokyo, Japan) as a template. The N-TIMP-3 (residues 1–121, from ^{1}CTCSPS to HLGCN^{121}) vector was constructed using the same sense primer and the anti-sense primer 5′-CTCGAGC-*TACTTATCGTCGTCATCCTTGTAATC*GTTACAACCCAGGTGATACCGATAGTT-CAGCC-3′ containing an XhoI site (underlined), FLAG epitope (in italics) and the C-terminal sequence of N-TIMP3. PCR fragments were ligated into pCEP4 at the XhoI site.

Human embryonic kidney HEK293 cells were transfected with the expression plasmids by lipofection with FuGENE6 (Roche Applied Science, Basel, Switzerland) and transfected cells selected by treatment with 800 μg/ml hygromycin B (PAA Laboratories GmbH, Pasching, Austria) over 3 weeks. Transfected cell lines were maintained under standard cell culture conditions in Dulbecco's modified Eagle's medium (DMEM) containing 10% (v/v) fetal calf serum, penicillin (100 units/ml), streptomycin (100 units/ml), 250 μg/ml G418 (PAA Laboratories GmbH, Pasching, Austria) and 800 μg/ml hygromycin B.

For expression of recombinant FLAG-tagged TIMP-3 and N-TIMP-3, transfected cells were treated with 30 mM sodium chlorate ($NaClO_3$, Sigma-Aldrich, Dorset, UK) in serum-free DMEM. Non-glycosylated full-length human TIMP-3 was prepared by treating transfected HEK293 cells with 5 μg/ml tunicamycin in addition to sodium chlorate. In all cases, medium was changed every 2 days to reduce TIMP-3-induced apoptosis (Bond et al., 2000). Conditioned media (0.5–1 l) were centrifuged to remove cell debris and applied to a column of anti-FLAG M2-agarose (1.5 ml, Sigma-Aldrich, Dorset, UK). The column was washed with 50 mM Tris–HCl, pH 7.5, 1 M NaCl, 10 mM $CaCl_2$, 0.05% Brij-35, 0.02% NaN_3. Bound proteins were eluted with 200 μg/ml FLAG peptide (Sigma-Aldrich, Dorset, UK) in TNC buffer (50 mM Tris–HCl, pH 7.5, 150 mM NaCl, 10 mM $CaCl_2$, 0.05% Brij-35 and 0.02% NaN_3). To remove the FLAG peptide, the eluate was applied to a Macro-Prep 25 S resin (400 μl, BioRad, Hemel Hempstead, UK) equilibrated in TNC buffer. Recombinant protein was eluted with 50 mM Tris–HCl, pH 7.5, 1 M NaCl, 10 mM $CaCl_2$, 0.05% Brij-35 and 0.02% NaN_3. Finally, the buffer was exchanged for TNC buffer using a PD-10 desalting column (GE Healthcare, Bucks, UK).

The purity of recombinant TIMP-3 and N-TIMP-3 was confirmed by reducing SDS-PAGE (Bury, 1981) and their active concentrations determined by titration with known concentrations of the catalytic domain of MMP-1. The identity of the purified proteins was confirmed using a commercial rabbit polyclonal antibody (AbCam, Cambridge, UK, catalogue number ab39184) and M2 anti-FLAG antibody (Sigma-Aldrich, Dorset, UK).

N-terminal analysis was carried out on TIMP-3 and N-TIMP-3 prepared from HEK293. Samples were denatured in SDS sample buffer at 80 °C in the presence of 50 mM dithiothreitol. SDS-PAGE was performed on a 10% gel (10 cm × 10 cm × 0.15 cm) according to Bury (1981). The gel was electroblotted to Immobilon-P membrane (Millipore) in 10 mM CAPS 10% methanol pH 11 (Matsudaira, 1987) and stained for protein using Coomassie Brilliant Blue. Bands of interest were excised and placed directly onto a Polybrene-treated glass filter. Samples were analyzed by automated Edman degradation using an

Applied Biosystems Procise 494HT sequencer with on-line phenylthiohydantoin HPLC analysis. The instruments were operated according to the manufacturers' instructions.

4.2. Preparation of E. coli-expressed N-TIMP-3, ADAMTSs and MMPs

The N-terminal domain of human TIMP-3 with C-terminal His-tag was expressed in *E. coli*, purified and folded *in vitro* (Kashiwagi et al., 2001). Human ADAMTS-4 and ADAMTS-5 deletion mutants (Fig. 2) were expressed and purified as previously described (Fushimi et al., 2008). The catalytic domains of human MMP-1 (MMP-1_{cat}) and MMP-3 (MMP-3_{cat}) were prepared as described (Chung et al., 2000; Suzuki et al., 1998). Human proMMP-2 and the pro-form of the MMP-2 catalytic domain (proMMP-2ΔC, lacking hemopexin-domain residues 466 to 660) were expressed in HEK293 cells using pCEP4-based expression vectors. The proMMP-2ΔC expression plasmid was constructed from the proMMP-2/pCEP4 plasmid by PCR mutagenesis using the sense primer 5′-CAGTACATCAAGTGTATCATATGCCAAGTCCGCCCC-3′ and the anti-sense primer 5′-GCCAAGGTCAATAAGCTTTCATCACCCATAGAGCTC-3′. The resulting PCR product was digested with KpnI and HindIII and ligated into similarly cut pCEP4. Both vectors were transfected into HEK293 cells and transfected cells selected by treatment with 1000 μg/ml hygromycin B as described for TIMP-3 above. Recombinant proMMP-2 and proMMP-2_{cat} were purified from the conditioned medium by gelatin affinity chromatography and gel filtration chromatography (Itoh et al., 1995). Active forms of the enzymes were prepared by treatment with 1 mM 4-aminophenylmercuric acetate (ICN Biochemicals, Solon, OH, USA) for 60 min at 37 °C, after which the buffer was exchanged for TNC buffer using a PD-10 desalting column (GE Healthcare, Bucks, UK). Active concentrations of all enzymes were determined by titration against a known concentration of *E. coli*-expressed N-TIMP-3 (for ADAMTS-4 and -5) or TIMP-1 (for MMPs).

4.3. Measurement of inhibition constant, K_i

All enzyme assays were conducted in TNC buffer (50 mM Tris–HCl, pH 7.5, 150 mM NaCl, 10 mM $CaCl_2$, 0.05% Brij-35 and 0.02% NaN_3) at 37 °C, using a Gemini microplate spectrofluorometer (Molecular Devices, Sunnyvale, CA, USA).

The activity of ADAMTS-4 was monitored using the fluorescent peptide substrate carboxyfluorescein-Ala-Glu~Leu-Asn-Gly-Arg-Pro-Ile-Ser-Ile-Ala-Lys-N,N,N',N'-tetramethyl-6-carboxyrhodamine (FAM-AE~LQGRPISIAK-TAMRA) at a final concentration of 0.5 μM with an excitation wavelength of 485 nm and an emission wavelength of 538 nm (495 nm cut-off) (Wayne et al., 2007).

The activity of ADAMTS-5 was monitored using the fluorescent peptide substrate ortho-aminobenzoyl-Thr-Glu-Ser-Glu~Ser-Arg-Gly-Ala-Ile-Tyr-(*N*-3-[2,4-dinitrophenyl]-L-2,3-diaminopropionyl)-Lys-Lys-NH_2 [Abz-TESE~SRGAIY-Dpa-KK] (kindly provided by Dr. Andrew Parker, AstraZeneca, Macclesfield, UK). This peptide is based on the ADAMTS-4 cleavage site in rat brevican (Nakamura et al., 2000; Matthews et al., 2000). ADAMTS-5 has been predicted to also cleave at this site (Nakada et al., 2005) and we found that recombinant ADAMTS-5 cleaved this substrate more readily than ADAMTS-4 *in vitro*. The substrate was used at a final concentration of 20 μM with an excitation wavelength of 300 nm and an emission wavelength of 430 nm (420 nm cut-off). Substrate hydrolysis by 0.5 nM ADAMTS-5 was confirmed to be linear for 18 h at 37 °C.

Activities of MMP-1 and MMP-2 were measured using the fluorescent quenched peptide substrate (7-methoxycoumarin-4-yl) acetyl-Pro-Leu-Gly-Leu-(*N*-3-[2,4-dinitrophenyl]-L-2,3-diaminopropionyl)-Ala-Arg-NH_2 (Mca-PLGL-Dpa-AR) at 1.5 μM final concentration (Knight et al., 1992). Activity of MMP-3_{cat} was measured using the fluorescent quenched substrate NFF-3, Mca-Arg-Pro-Lys-Pro-Val-Glu-Nva-Trp-Arg-Lys(2,4-dinitrophenyl)-NH_2 at 1.5 μM final concentration (Nagase et al., 1994).

K_i values of TIMP-3 for various isoforms of ADAMTS-4 and ADAMTS-5 were determined under equilibrium kinetic conditions (Bieth, 1995). Final enzyme concentrations for K_i determinations were as follows: ADAMTS-4 and -5 were used at 0.5 nM, MMP-1, MMP-1_{cat} and MMP-3_{cat} were used at 1 nM, and MMP-2 and MMP-2_{cat} were used at 0.125 nM. Enzymes were pre-incubated (1 h, 37 °C) with TIMP-3 (0.5–100 nM final concentration) and equilibrium rate of substrate hydrolysis (v_s) determined (18 h, 37 °C). Prism software (GraphPad, La Jolla, CA, USA) was used to fit the data to the tight-binding equation (Bieth, 1995):

$$\frac{v_s}{v_o} = 1 - \frac{(E_o + I_o + K_{i(app)} - [(E_o + I_o + K_{i(app)})^2 - 4E_oK_{i(app)}]^{\frac{1}{2}}}{2E_o} \quad (1)$$

where v_o is equilibrium rate of substrate hydrolysis in the absence of inhibitor, E_o is the total enzyme concentration, I_o is the total inhibitor concentration and $K_{i(app)}$ is the apparent inhibition constant.

To determine K_i from $K_{i(app)}$, the K_m of the enzymes for the substrates used must be known (Bieth, 1995). Wayne et al. (2007) determined a K_m value of 15 μM for ADAMTS-4 cleavage of FAM-AE~LQGRPISIAK-TAMRA, which we used at 0.5 μM. We determined a K_m value of 76 μM for ADAMTS-5 cleavage of Abz-TESE~SRGAIY-Dpa-KK (data not shown), used at 20 μM. K_i was then calculated from the equation:

$$K_i = \frac{K_{i(app)}}{1 + \frac{[S]}{K_m}} \quad (2)$$

where K_i is the inhibition constant, [*S*] is the initial substrate concentration and K_m is the Michaelis constant for the substrate used. Therefore, $K_{i(app)}$ was divided by 1.033 to determine K_i for ADAMTS-4, and by 1.26 to determine K_i for ADAMTS-5.

Acknowledgements

We thank Dr Andrew Parker (AstraZeneca, Macclesfield, UK) for provision of the Abz-TESE~SRGAIY-Dpa-KK fluorescent substrate and Prof. M. Seiki (University of Tokyo, Japan) for the TIMP-3 vector. This work was supported by the Wellcome Trust (grant 057473) and Award Number AR40994 from the National Institute of Arthritis and Musculoskeletal and Skin Diseases (NIAMS). The content is solely the responsibility of the authors and does not necessarily represent the official views of NIAMS or NIH.

References

Apte, S.S., Olsen, B.R., Murphy, G., 1995. The gene structure of tissue inhibitor of metalloproteinases (TIMP)-3 and its inhibitory activities define the distinct TIMP gene family. J. Biol. Chem. 270, 14313–14318.

Baeuerle, P.A., Huttner, W.B., 1986. Chlorate—a potent inhibitor of protein sulfation in intact cells. Biochem. Biophys. Res. Commun. 141, 870–877.

Bieth, J.G., 1995. Theoretical and practical aspects of proteinase inhibition kinetics meth. Enzymol. 248, 59–84.

Bodden, M.K., Windsor, L.J., Caterina, N.C., Harber, G.J., Birkedal-Hansen, B., Birkedal-Hansen, H., 1994. Human TIMP-1 binds to pro-M(r) 92 K GL (gelatinase B, MMP-9) through the "second disulfide knot". Ann. N. Y. Acad. Sci. 732, 403–407.

Bond, M., Murphy, G., Bennett, M.R., Amour, A., Knauper, V., Newby, A.C., Baker, A.H., 2000. Localization of the death domain of tissue inhibitor of metalloproteinase-3 to the N terminus. Metalloproteinase inhibition is associated with proapoptotic activity. J. Biol. Chem. 275, 41358–41363.

Brew, K., Dinakarpandian, D., Nagase, H., 2000. Tissue inhibitors of metalloproteinases: evolution, structure and function. Biochim. Biophys. Acta 1477, 267–283.

Bury, A.F., 1981. Analysis of protein and peptide mixtures. Evaluation of three sodium dodecyl sulfate-polyacrylamide gels electrophoresis systems. J. Chromatogr. 213, 491–500.

Butler, G.S., Apte, S.S., Willenbrock, F., Murphy, G., 1999. Human tissue inhibitor of metalloproteinases 3 interacts with both the N- and C-terminal domains of gelatinases A and B. Regulation by polyanions. J. Biol. Chem. 274, 10846–10851.

Chung, L., Shimokawa, K., Dinakarpandian, D., Grams, F., Fields, G.B., Nagase, H., 2000. Identification of the (183)RWTNNFREY(191) region as a critical segment of matrix metalloproteinase 1 for the expression of collagenolytic activity. J. Biol. Chem. 275, 29610–29617.

Clark, I.M., Cawston, T.E., 1989. Fragments of human fibroblast collagenase. Purification and characterization. Biochem. J. 263, 201–206.
Colige, A., Ruggiero, F., Vandenberghe, I., Dubail, J., Kesteloot, F., Van Beeumen, J., Beschin, A., Brys, L., Lapière, C.M., Nusgens, B., 2005. Domains and maturation processes that regulate the activity of ADAMTS-2, a metalloproteinase cleaving the aminopropeptide of fibrillar procollagens types I–III and V. J. Biol. Chem. 280, 34397–34408.
Fabunmi, R.P., Baker, A.H., Murray, E.J., Booth, R.F., Newby, A.C., 1996. Divergent regulation by growth factors and cytokines of 95 kDa and 72 kDa gelatinases and tissue inhibitors or metalloproteinases-1, -2, and -3 in rabbit aortic smooth muscle cells. Biochem. J. 315 (Pt 1), 335–342.
Fushimi, K., Troeberg, L., Nakamura, H., Lim, N.H., Nagase, H., 2008. Functional differences of the catalytic and non-catalytic domains in human ADAMTS-4 and ADAMTS-5 in aggrecanolytic activity. J. Biol. Chem. 283, 6706–6716.
Gao, G., Plaas, A., Thompson, V.P., Jin, S., Zuo, F., Sandy, J.D., 2004. ADAMTS4 (aggrecanase-1) activation on the cell surface involves C-terminal cleavage by glycosylphosphatidyl inositol-anchored membrane type 4-matrix metalloproteinase and binding of the activated proteinase to chondroitin sulfate and heparan sulfate on syndecan-1. J. Biol. Chem. 279, 10042–10051.
Gao, W., Anderson, P.J., Sadler, J.E., 2008. Extensive contacts between ADAMTS13 exosites and von Willebrand factor domain A2 contribute to substrate specificity. Blood 112, 1713–1719.
Gendron, C., Kashiwagi, M., Lim, N.H., Enghild, J.J., Thogersen, I.B., Hughes, C., Caterson, B., Nagase, H., 2007. Proteolytic activities of human ADAMTS-5: comparative studies with human ADAMTS-4. J. Biol. Chem. 282, 18294–18306.
Gerhardt, S., Hassall, G., Hawtin, P., McCall, E., Flavell, L., Minshull, C., Hargreaves, D., Ting, A., Pauptit, R.A., Parker, A.E., Abbott, W.M., 2007. Crystal structures of human ADAMTS-1 reveal a conserved catalytic domain and a disintegrin-like domain with a fold homologous to cysteine-rich domains. J. Mol. Biol. 373, 891–902.
Godyna, S., Liau, G., Popa, I., Stefansson, S., Argraves, W.S., 1995. Identification of the low density lipoprotein receptor-related protein (LRP) as an endocytic receptor for thrombospondin-1. J. Cell Biol. 129, 1403–1410.
Hashimoto, G., Aoki, T., Nakamura, H., Tanzawa, K., Okada, Y., 2001. Inhibition of ADAMTS4 (aggrecanase-1) by tissue inhibitors of metalloproteinases (TIMP-1, 2, 3 and 4). FEBS Lett. 494, 192–195.
Igarashi, T., Oishi, Y., Araki, S., Mori, H., Takeda, S., 2006. Crystallization and preliminary X-ray crystallographic analysis of two vascular apoptosis-inducing proteins (VAPs) from *Crotalus atrox* venom. Acta Crystallogr. Sect. F Struct. Biol. Cryst. Commun 62, 688–691.
Igarashi, T., Araki, S., Mori, H., Takeda, S., 2007. Crystal structures of catrocollastatin/VAP2B reveal a dynamic, modular architecture of ADAM/adamalysin/reprolysin family proteins. FEBS Lett. 581, 2416–2422.
Itoh, Y., Binner, S., Nagase, H., 1995. Steps involved in activation of the complex of pro-matrix metalloproteinase 2 (progelatinase A) and tissue inhibitor of metalloproteinases (TIMP)-2 by 4-aminophenylmercuric acetate. Biochem. J. 308 (Pt 2), 645–651.
Kashiwagi, M., Tortorella, M., Nagase, H., Brew, K., 2001. TIMP-3 is a potent inhibitor of aggrecanase 1 (ADAM-TS4) and aggrecanase 2 (ADAM-TS5). J. Biol. Chem. 276, 12501–12504.
Kashiwagi, M., Enghild, J.J., Gendron, C., Hughes, C., Caterson, B., Itoh, Y., Nagase, H., 2004. Altered proteolytic activities of ADAMTS-4 expressed by C-terminal processing. J. Biol. Chem. 279, 10109–10119.
Knight, C.G., Willenbrock, F., Murphy, G., 1992. A novel coumarin-labelled peptide for sensitive continuous assays of the matrix metalloproteinases. FEBS Lett. 296, 263–266.
Langton, K.P., Barker, M.D., McKie, N., 1998. Localization of the functional domains of human tissue inhibitor of metalloproteinases-3 and the effects of a Sorsby's Fundus Dystrophy mutation. J. Biol. Chem. 273, 16778–16781.
Lee, M.H., Knäuper, V., Becherer, J.D., Murphy, G., 2001. Full-length and N-TIMP-3 display equal inhibitory activities toward TNF-alpha convertase. Biochem. Biophys. Res. Commun 280, 945–950.
Lee, M.H., Verma, V., Maskos, K., Becherer, J.D., Knäuper, V., Dodds, P., Amour, A., Murphy, G., 2002. The C-terminal domains of TACE weaken the inhibitory action of N-TIMP-3. FEBS Lett. 520, 102–106.
Lee, M.H., Rapti, M., Murphy, G., 2005. Total conversion of tissue inhibitor of metalloproteinase (TIMP) for specific metalloproteinase targeting: fine-tuning TIMP-4 for optimal inhibition of tumor necrosis factor-(alpha)-converting enzyme. J. Biol. Chem. 280, 15967–15975.
Lee, M.H., Atkinson, S., Murphy, G., 2007. Identification of the extracellular matrix (ECM) binding motifs of tissue inhibitor of metalloproteinases (TIMP)-3 and effective transfer to TIMP-1. J. Biol. Chem. 282, 6887–6898.
Maskos, K., Fernandez-Catalan, C., Huber, R., Bourenkov, G.P., Bartunik, H., Ellestad, G.A., Reddy, P., Wolfson, M.F., Rauch, C.T., Castner, B.J., Davis, R., Clarke, H.R., Petersen, M., Fitzner, J.N., Cerretti, D.P., March, C.J., Paxton, R.J., Black, R.A., Bode, W., 1998. Crystal structure of the catalytic domain of human tumor necrosis factor-alpha-converting enzyme. Proc. Natl Acad. Sci. USA 95, 3408–3412.
Matsudaira, P., 1987. Sequence from picomole quantities of proteins electroblotted onto polyvinylidene difluoride membranes. J. Biol. Chem. 262, 10035–10038.
Matthews, R.T., Gary, S.C., Zerillo, C., Pratta, M., Solomon, K., Arner, E.C., Hockfield, S., 2000. Brain-enriched hyaluronan binding (BEHAB)/brevican cleavage in a glioma cell line is mediated by a disintegrin and metalloproteinase with thrombospondin motifs (ADAMTS) family member. J. Biol. Chem. 275, 22695–22703.
Milla, M.E., Leesnitzer, M.A., Moss, M.L., Clay, W.C., Carter, H.L., Miller, A.B., Su, J.L., Lambert, M.H., Willard, D.H., Sheeley, D.M., Kost, T.A., Burkhart, W., Moyer, M., Blackburn, R.K., Pahel, G.L., Mitchell, J.L., Hoffman, C.R., Becherer, J.D., 1999. Specific sequence elements are required for the expression of functional tumor necrosis factor-alpha-converting enzyme (TACE). J. Biol. Chem. 274, 30563–30570.
Morgunova, E., Tuuttila, A., Bergmann, U., Tryggvason, K., 2002. Structural insight into the complex formation of latent matrix metalloproteinase 2 with tissue inhibitor of metalloproteinase 2. Proc. Natl. Acad. Sci. USA 99, 7414–7419.
Mosyak, L., Georgiadis, K., Shane, T., Svenson, K., Hebert, T., McDonagh, T., Mackie, S., Olland, S., Lin, L., Zhong, X., Kriz, R., Reifenberg, E.L., Collins-Racie, L.A., Corcoran, C., Freeman, B., Zollner, R., Marvell, T., Vera, M., Sum, P.E., LaVallie, E.R., Stahl, M., Somers, W., 2008. Crystal structures of the two major aggrecan degrading enzymes, ADAMTS4 and ADAMTS5. Protein Sci. 17, 16–21.
Murphy, G., Willenbrock, F., Ward, R.V., Cockett, M.I., Eaton, D., Docherty, A.J., 1992. The C-terminal domain of 72 kDa gelatinase A is not required for catalysis, but is essential for membrane activation and modulates interactions with tissue inhibitors of metalloproteinases. Biochem. J. 283 (Pt 3), 637–641.
Nagase, H., Fields, C.G., Fields, G.B., 1994. Design and characterization of a fluorogenic substrate selectively hydrolyzed by stromelysin 1 (matrix metalloproteinase-3). J. Biol. Chem. 269, 20952–20957.
Nakada, M., Miyamori, H., Kita, D., Takahashi, T., Yamashita, J., Sato, H., Miura, R., Yamaguchi, Y., Okada, Y., 2005. Human glioblastomas overexpress ADAMTS-5 that degrades brevican. Acta Neuropathol. 110, 239–246.
Nakamura, H., Fujii, Y., Inoki, I., Sugimoto, K., Tanzawa, K., Matsuki, H., Miura, R., Yamaguchi, Y., Okada, Y., 2000. Brevican is degraded by matrix metalloproteinases and aggrecanase-1 (ADAMTS4) at different sites. J. Biol. Chem. 275, 38885–38890.
Rapti, M., Atkinson, S.J., Lee, M.H., Trim, A., Moss, M., Murphy, G., 2008. The isolated N-terminal domains of TIMP-1 and TIMP-3 are insufficient for ADAM10 inhibition. Biochem J. 411, 433–439.
Safaiyan, F., Kolset, S.O., Prydz, K., Gottfridsson, E., Lindahl, U., Salmivirta, M., 1999. Selective effects of sodium chlorate treatment on the sulfation of heparan sulfate. J. Biol. Chem. 274, 36267–36273.
Sarafanov, A.G., Ananyeva, N.M., Shima, M., Saenko, E.L., 2001. Cell surface heparan sulfate proteoglycans participate in factor VIII catabolism mediated by low density lipoprotein receptor-related protein. J. Biol. Chem. 276, 11970–11979.
Shieh, H.S., Mathis, K.J., Williams, J.M., Hills, R.L., Wiese, J.F., Benson, T.E., Kiefer, J.R., Marino, M.H., Carroll, J.N., Leone, J.W., Malfait, A.M., Arner, E.C., Tortorella, M.D., Tomasselli, A., 2008. High resolution crystal structure of the catalytic domain of ADAMTS-5 (aggrecanase-2). J. Biol. Chem. 283, 1501–1507.
Suzuki, K., Kan, C.C., Hung, W., Gehring, M.R., Brew, K., Nagase, H., 1998. Expression of human pro-matrix metalloproteinase 3 that lacks the N-terminal 34 residues in *Escherichia coli*: autoactivation and interaction with tissue inhibitor of metalloproteinase 1 (TIMP-1). Biol. Chem. 379, 185–191.
Takeda, S., 2008. Three-dimensional domain architecture of the ADAM family proteinases. Semin. Cell Dev. Biol.
Tortorella, M., Pratta, M., Liu, R.Q., Abbaszade, I., Ross, H., Burns, T., Arner, E., 2000. The thrombospondin motif of aggrecanase-1 (ADAMTS-4) is critical for aggrecan substrate recognition and cleavage. J. Biol. Chem. 275, 25791–25797.
Troeberg, L., Tanaka, M., Wait, R., Shi, Y.E., Brew, K., Nagase, H., 2002. *E. coli* expression of TIMP-4 and comparative kinetic studies with TIMP-1 and TIMP-2: insights into the interactions of TIMPs and matrix metalloproteinase 2 (gelatinase A). Biochemistry 41, 15025–15035.
Troeberg, L., Fushimi, K., Khokha, R., Emonard, H., Ghosh, P., Nagase, H., 2008. Calcium pentosan polysulfate is a multifaceted exosite inhibitor of aggrecanases. FASEB J. 22, 3515–3524.
Wayne, G.J., Deng, S.J., Amour, A., Borman, S., Matico, R., Carter, H.L., Murphy, G., 2007. TIMP-3 inhibition of ADAMTS-4 (Aggrecanase-1) is modulated by interactions between aggrecan and the C-terminal domain of ADAMTS-4. J. Biol. Chem. 282, 20991–20998.
Wisniewska, M., Goettig, P., Maskos, K., Belouski, E., Winters, D., Hecht, R., Black, R., Bode, W., 2008. Structural determinants of the ADAM inhibition by TIMP-3: crystal structure of the TACE-N-TIMP-3 complex. J. Mol. Biol. 381, 1307–1319.
Yu, W.H., Yu, S., Meng, Q., Brew, K., Woessner, J.F., 2000. TIMP-3 binds to sulfated glycosaminoglycans of the extracellular matrix. J. Biol. Chem. 275, 31226–31232.

The FASEB Journal article fj.12-216671. Published online October 11, 2012.

LRP-1-mediated endocytosis regulates extracellular activity of ADAMTS-5 in articular cartilage

Kazuhiro Yamamoto,* Linda Troeberg,* Simone D. Scilabra,* Michele Pelosi,* Christopher L. Murphy,* Dudley K. Strickland,† and Hideaki Nagase*,[1]

*Kennedy Institute of Rheumatology, Nuffield Department of Orthopaedics, Rheumatology, and Musculoskeletal Sciences, University of Oxford, London, UK; and †Center for Vascular and Inflammatory Diseases, University of Maryland School of Medicine, Baltimore, Maryland, USA

ABSTRACT **Aggrecan is a major matrix component of articular cartilage, and its degradation is a crucial event in the development of osteoarthritis (OA). Adamalysin-like metalloproteinase with thrombospondin motifs 5 (ADAMTS-5) is a major aggrecan-degrading enzyme in cartilage, but there is no clear correlation between ADAMTS-5 mRNA levels and OA progression. Here, we report that post-translational endocytosis of ADAMTS-5 by chondrocytes regulates its extracellular activity. We found 2- to 3-fold reduced aggrecanase activity when ADAMTS-5 was incubated with live porcine cartilage, resulting from its rapid endocytic clearance. Studies using receptor-associated protein (RAP), a ligand-binding antagonist for the low-density lipoprotein receptor-related proteins (LRPs), and siRNA-mediated gene silencing revealed that the receptor responsible for ADAMTS-5 clearance is LRP-1. Domain-deletion mutagenesis of ADAMTS-5 identified that the noncatalytic first thrombospondin and spacer domains mediate its endocytosis. The addition of RAP to porcine cartilage explants in culture increased the basal level of aggrecan degradation, as well as ADAMTS-5-induced aggrecan degradation. Notably, LRP-1-mediated endocytosis of ADAMTS-5 is impaired in chondrocytes of OA cartilage, with ~90% reduction in protein levels of LRP-1 without changes in its mRNA levels. Thus, LRP-1 dictates physiological and pathological catabolism of aggrecan in cartilage as a key modulator of the extracellular activity of ADAMTS-5.—Yamamoto, K., Troeberg, L., Scilabra, S. D., Pelosi, M., Murphy, C. L., Strickland, D. K., Nagase, H. LRP-1-mediated endocytosis regulates extracellular activity of ADAMTS-5 in articular cartilage. *FASEB J.* 27, 000–000 (2013). www.fasebj.org**

Key Words: aggrecanase · protease · chondrocytes · osteoarthritis

Articular cartilage consists of a sparse population of chondrocytes in an abundant extracellular matrix (ECM), whose major components are collagen fibrils and aggrecan proteoglycans (1). Collagen fibrils, mainly type II collagen, form a meshwork and provide the tissue with tensile strength. Aggrecan, present as large aggregated complexes interacting with hyaluronan and link proteins, forms a hydrated gel within the collagen meshwork and gives cartilage its ability to withstand mechanical compression. Chondrocytes, the only cell type present in articular cartilage, regulate tissue homeostasis by balancing the synthesis and degradation of the ECM macromolecules. A disruption in this balance results in the cartilage destruction seen in rheumatoid arthritis and osteoarthritis (OA), largely due to elevated proteolytic enzyme activities (2, 3). Because the presence of aggrecan prevents collagenolysis by collagenases of the matrix metalloproteinase (MMP) family, aggrecan loss is considered to be a crucial early event in the development of arthritis, particularly OA (4, 5).

The proteinases responsible for aggrecan degradation are MMPs and aggrecanases; the latter being members of the adamalysin with thrombospondin motifs (ADAMTS) family (3). Aggrecanases were defined by their ability to cleave the Glu^{373}-Ala^{374} bond of the aggrecan core protein (6, 7). Elevated aggrecanase-generated aggrecan fragments were found in synovial fluids of patients with OA and inflammatory joint disease (8, 9). These fragments were also detected in normal synovial fluid and serum of animals (7), suggesting that aggrecanases function in both physiological and pathological catabolism of aggrecan.

The ADAMTSs are multidomain metalloproteinases consisting of a metalloproteinase domain, a disintegrin

Abbreviations: β-CD, β-cyclodextrin; ADAM, adamalysin; ADAMTS, adamalysin-like metalloproteinase with thrombospondin motifs; CysR, cysteine-rich; DMEM, Dulbecco's modified Eagle's medium; DMMB, dimethylmethylene blue; ECM, extracellular matrix; EEA1, early endosome antigen 1; FBS, fetal bovine serum; GAG, glycosaminoglycan; IL-1, interleukin-1; LRP, low-density lipoprotein receptor-related protein; MMP, matrix metalloproteinase; OA, osteoarthritis; PCR, polymerase chain reaction; RAP, receptor-associated protein; RPLP0, 60S acidic ribosomal protein P0; Sp, spacer; TIMP, tissue inhibitor of metalloproteinases; TS, thrombospondin

[1] Correspondence: Matrix Biology Section, Kennedy Institute of Rheumatology, Nuffield Department of Orthopaedics, Rheumatology and Musculoskeletal Sciences, University of Oxford, 65 Aspenlea Rd., London, W6 8LH, UK. E-mail: hideaki.nagase@kennedy.ox.ac.uk.

doi: 10.1096/fj.12-216671

domain, a thrombospondin (TS) domain, a cysteine-rich (CysR) domain, a spacer (Sp) domain and a number of additional TS domains (10). Among the ADAMTSs that have aggrecanase activity, ADAMTS-4 and ADAMTS-5 have been considered as the major aggrecanases involved in cartilage matrix turnover because of their effective aggrecanase activity *in vitro* (11, 12). The expression of ADAMTS-4 at mRNA and protein levels correlate with the progression of OA in humans (13). In contrast, ADAMTS-5-null mice, but not ADAMTS-4-null mice, showed protection of their cartilage from destruction when challenged in an OA model induced by surgically induced joint destabilization (14, 15) or antigen-induced arthritis (16), indicating that ADAMTS-5 plays a key role in aggrecan degradation, at least in mice. ADAMTS-5 is ~30 times more active on aggrecan than ADAMTS-4 (12). Nevertheless, mRNA levels for ADAMTS-5 in OA cartilage are not significantly elevated compared to that in normal cartilage (13, 17, 18). Treatment of human chondrocytes with the proinflammatory cytokine interleukin-1 (IL-1) increased ADAMTS-4 mRNA levels (17), but the levels of ADAMTS-5 mRNA were reported to be inconsistent and do not correlate with degradation of aggrecan in cartilage (see ref 19 for review). This led us to postulate that the aggrecanase activity of ADAMTS-5 in cartilage may be regulated at the protein level, and changes at the mRNA level may not be the major factor controlling its aggrecanase activity. The aggrecanase activity of ADAMTS-5 is inhibited by tissue inhibitor of metalloproteinases 3 (TIMP-3), which is expressed in cartilage (20). Furthermore, processing of the C-terminal ancillary domain of ADAMTS-5 reduces the aggrecanase activity (21).

Biochemical characterization of ADAMTS-5 has been carried out *in vitro* using purified monomeric aggrecan as a substrate. These studies do not reflect the complexity of the cartilage matrix where numerous minor ECM components, such as fibromodulin; decorin; biglycan; cartilage oligomeric matrix protein; type VI, IX, and XI collagens; matrillins; and cell surface proteoglycans assemble together with type II collagen fibrils and aggrecan (1). Furthermore, ADAMTS-5 binds to the negatively charged cell surface and ECM molecules (21), and sulfated polysaccharides, such as heparan sulfate, may regulate the aggrecanase activity of ADAMTS-5 (20). Therefore, we tested aggrecanase activity of ADAMTS-5 in the context of the cartilage matrix using dissected porcine articular cartilage, which presents a substrate close to physiological conditions. We confirmed that ADAMTS-5 has a greater aggrecan-degrading activity than ADAMTS-4, MMP-1, or MMP-13, and we found that the aggrecanase activity of ADAMTS-5 was much lower when live cartilage was used as a substrate. This was due to a rapid endocytic clearance and degradation of ADAMTS-5 by chondrocytes, which is mediated by low-density lipoprotein receptor-related protein (LRP)-1, but this endocytic pathway is dysregulated in human OA cartilage due to a loss of LRP-1.

MATERIALS AND METHODS

Reagents and antibodies

The sources of materials used were as follows: dimethylmethylene blue (DMMB), dynasore, β-cyclodextrin (β-CD), polymyxin B, and the anti-FLAG M2 mouse monoclonal antibody from Sigma-Aldrich (Dorset, UK); the anti-early endosome antigen 1 (EEA1) rabbit polyclonal antibody, and the anti-LRP-1 mouse monoclonal antibodies 5A6 and 8G1 from Abcam (Cambridge, UK) and Calbiochem (San Diego, CA, USA); the anti-actin antibody from Santa Cruz Biotechnology (Santa Cruz, CA, USA); the anti-tubulin antibody from Cell Signaling (Danvers, MA, USA); and BC-3 mouse monoclonal antibody that recognizes the N-terminal ^{374}ARGSV generated by aggrecanase cleavage of aggrecan core protein from Abcam. The anti-human ADAMTS-5 catalytic domain rabbit polyclonal antibody was raised in rabbits and characterized (21). Recombinant human ADAMTS-5 and its domain-deletion mutants, ADAMTS-4 lacking the Sp domain, MMP-1, and MMP-13, were prepared as described previously (11, 21, 22). Recombinant human IL-1α was kindly provided by Prof. J. Saklatvala (Kennedy Institute of Rheumatology, London, UK). All other reagents used were of the highest analytical grade available.

Expression and purification of human receptor-associated protein (RAP)

Recombinant human C-terminally His-tagged RAP was expressed in *Escherichia coli* using a pET3a-based expression vector (Novagen/EMD Biosciences, Madison, WI, USA). The human RAP cDNA was isolated by polymerase chain reaction (PCR) using cDNA from HT1080 cells as a template with the sense primer 5′-TGGCATATGTACTCGCGGGAGAAGAACCAGCCCAAGCCGTCCCCGAAACGC-3′ containing an *Nde*I site (underscored) and RAP N-terminal sequence and the antisense primer 5′-CCAGGATCCCT*AATGGTGATGGTGATGGT*GGAGTTCGTTGTGCCGAGCTCT-3′ containing a *Bam*HI site (underscored), a 6-histidine tag (in italics) and the C-terminal sequence of RAP. PCR fragments were ligated into CloneJET cloning vector (Fermentas, Glen Burnie, MD, USA), digested with *Nde*I and *Bam*HI, and ligated into similarly cut pET3a. The sequence was confirmed by DNA sequencing. *E. coli* BL21(DE3) cells were transformed with the RAP expression plasmid, and cultures grown at 37°C in 1 L of Luria-Bertani broth with 50 μg/ml carbenicillin. Once the culture reached an OD_{600} of 0.6, protein expression was induced by addition of 1 mM isopropyl-β-D-thiogalactoside for 3 h at 37°C. Cells were harvested by centrifugation and lysed in 40 ml of phosphate-buffered saline using a French press. The soluble fraction of the cell lysate was applied to nickel-nitrilotriacetic acid Superflow resin (Qiagen, Valencia, CA, USA) equilibrated in 20 mM HEPES (pH 7.5) and 150 mM NaCl. The column was washed in 20 mM HEPES (pH 7.5), 1 M NaCl, and 50 mM imidazole, and further washed with an excess amount of 20 mM HEPES (pH 7.5), 150 mM NaCl, and 60% isopropanol to remove endotoxin (23). Bound protein was eluted in 20 mM HEPES (pH 7.5), 150 M NaCl, and 500 mM imidazole. RAP-containing fractions were pooled and dialyzed against 20 mM HEPES (pH 7.5) and 150 mM NaCl. To ascertain the levels of LPS in the recombinant RAP preparation, the Limulus amoebocyte lysate assay (Cambrex, East Rutherford, NJ, USA) was used, according to the manufacturer's instructions. The recombinant RAP used in this study had an endotoxin level < 10 pg/ml.

Porcine articular cartilage culture

Porcine articular cartilage from the metacarpophalangeal joints of 3- to 9-mo-old pigs was dissected into small pieces (~6 mm^3: 10 mg wet vol). Each piece was placed in one well of a round-bottom 96-well plate and allowed to rest for 24 h in 200 μl of Dulbecco's modified Eagle's medium (DMEM) containing 10% fetal bovine serum (FBS) before use. The medium was then replaced, and the cartilage was rested for a further 24 h in 200 μl of DMEM at 37°C (for fresh live cartilage) before the aggrecan degradation and endocytosis assays. For freeze-thawed cartilage experiments, cartilage pieces were frozen at −80°C and thawed in the same medium and replaced with fresh medium before subjecting to subsequent assays.

Analysis of aggrecan degradation

Each piece of cartilage was incubated in 100 μl of DMEM with or without IL-1α (10 ng/ml) or various concentrations of MMPs and ADAMTSs. Three pieces of cartilage were subjected to each treatment. After incubation for various periods of time, the conditioned media were harvested, and glycosaminoglycan (GAG) released into the medium was measured using the DMMB assay (5). Aggrecan fragments in the medium were deglycosylated, as described previously (11), and analyzed by Western blotting using an anti-ARGSV aggrecan neoepitope antibody. Immunoreactive bands were quantified using ImageJ (U.S. National Institutes of Health, Bethesda, MD, USA) and results are presented as relative intensities.

Isolation of chondrocytes and cell culture

Human articular cartilage was obtained from patients after they provided informed consent and following approval by Riverside ethics committee. Non-OA cartilage was obtained from the knee following amputation due to soft tissue sarcoma and osteosarcoma with no involvement of the cartilage. Tissues were obtained from 8 patients (5 male, 3 female; aged 12–55 yr, mean age 31.6 yr). OA cartilage was obtained from patients undergoing joint replacement surgery. Tissues were obtained from 7 patients (2 male, 5 female; aged 53–66 yr, mean age 61 yr). Chondrocytes were isolated as described previously (20). Primary porcine cells and both primary and passaged human cells were used in the experiments. For the ADAMTS-5 endocytosis assay, cells were plated at a density of 2.5×10^5 cells/well (24-well plate) in DMEM containing 10% FCS.

Analysis of ADAMTS-5 clearance

Cartilage explants or cells were incubated in 100 or 400 μl of DMEM with or without 80 μM dynasore, 10 mM β-CD, or 500 nM RAP. After incubation for 30 min, media were replaced with DMEM containing 10 nM ADAMTS-5 or its domain deletion mutants with or without 80 μM dynasore or 500 nM RAP. Four pieces of cartilage were subjected to each treatment. After incubation for various periods of time, media were collected; the protein was precipitated with TCA and dissolved in 50 μl of 1× SDS sample buffer [50 mM Tris-HCl (pH 6.8)/5% 2-mercaptoethanol, 2% SDS and 10% glycerol]. The cartilage explants and cells were washed with DMEM and lysed in 50 μl of 2× SDS-sample buffer. All samples were analyzed by SDS-PAGE and Western blotting using an anti-ADAMTS-5 catalytic domain antibody. Immunoreactive bands were quantified using ImageJ, and the amounts of ADAMTS-5 remaining in the medium and cell lysate at each time point were calculated as a percentage of the amount of ADAMTS-5 at 0 h.

Immunocytochemical localization of endocytosed ADAMTS-5

Cultured cells on 4-well Lab-Tek chamber slides (Nunc, Roskilde, Denmark) were incubated in DMEM with 10 nM ADAMTS-5 in the absence or presence of 500 nM RAP for 1 h. Cells were washed with DMEM, fixed with 3% paraformaldehyde in Tris-buffered saline (TBS; 10 min, room temperature) and permeabilized with TBS containing 10 mM $CaCl_2$ and 0.1% Triton X-100 (15 min, room temperature). To visualize ADAMTS-5 within the cartilage, porcine articular cartilage explants were incubated as described above for 3 h. Explants were washed with DMEM and fixed with 4% formalin (24 h, room temperature). Explants were then snap-frozen and sectioned (5-μm sections) using a CM1900 cryostat (Leica Microsystems, Wetzlar, Germany). Each sample was incubated with anti-FLAG M2 mouse monoclonal antibody and anti-EEA1 rabbit polyclonal antibody (3 h, room temperature). Alexa Fluor 488-conjugated anti-mouse IgG and Alexa Fluor 568-conjugated anti-rabbit IgG (Molecular Probes, Eugene, OR, USA) were used to visualize the antigen signals (1 h, room temperature). Actin was stained with actin stain 670 phalloidin (Cell Signaling), and nuclei were stained with DAPI. Samples were viewed using a Nikon Eclipse TE2000-U confocal laser scanning microscope (Nikon, Tokyo, Japan). The data were collated using Volocity software (Improvision, Coventry, UK).

siRNA-mediated knockdown of LRP-1 in human articular chondrocytes

siRNA oligonucleotides for LRP-1 (On-TargetPlus SMARTpool siRNA) and nontargeting oligonucleotide were purchased from Thermo Scientific Dharmacon (Lafayette, CO, USA). Human articular chondrocytes were plated at a density of 1.5×10^6 cells/dish (6-cm dish) in DMEM containing 10% FCS and incubated until 50% confluent. Lipofectamine 2000 (Invitrogen, Carlsbad, CA, USA) was used to transfect cells with siRNA at a final concentration of 10 nM in Opti-MEM I. At 4 h after transfection, the Opti-MEM was removed and replaced with DMEM containing 10% FCS.

Quantitative reverse transcriptase–PCR

RNA was extracted and prepared using the RNeasy mini kit (Qiagen, Valencia, CA, USA) following the manufacturer's guidelines. cDNA was generated using a reverse-transcription kit (Applied Biosystems, Foster City, CA, USA) and random primers from 0.5 μg of total RNA. Newly synthesized cDNA was diluted 5-fold in DNase-free water. Four percent of this cDNA was then used for real-time PCR assays using TaqMan technology (Applied Biosystems). The ΔΔ threshold cycle ($\Delta\Delta C_t$) method of relative quantitation was used to calculate relative mRNA levels for each transcript examined. The 60S acidic ribosomal protein P0 (RPLP0) gene was used to normalize the data. Predeveloped primer/probe sets for LRP-1 and RPLP0 were purchased from Applied Biosystems.

Western blotting analysis of LRP-1 protein

Cultured cells (2×10^5) were lysed in 50 μl of 2× SDS-sample buffer without 2-mercaptoethanol, and a portion of the lysates was analyzed by SDS-PAGE and Western blotting using anti-LRP-1 heavy-chain and light-chain antibodies. Immunoreactive bands were quantified using ImageJ, and the amounts of LRP-1 heavy chain and light chain in cell lysates were calculated as a percentage of the amount of LRP-1 or shown as relative LRP-1 expression. Cellular tubulin was used to normalize the data.

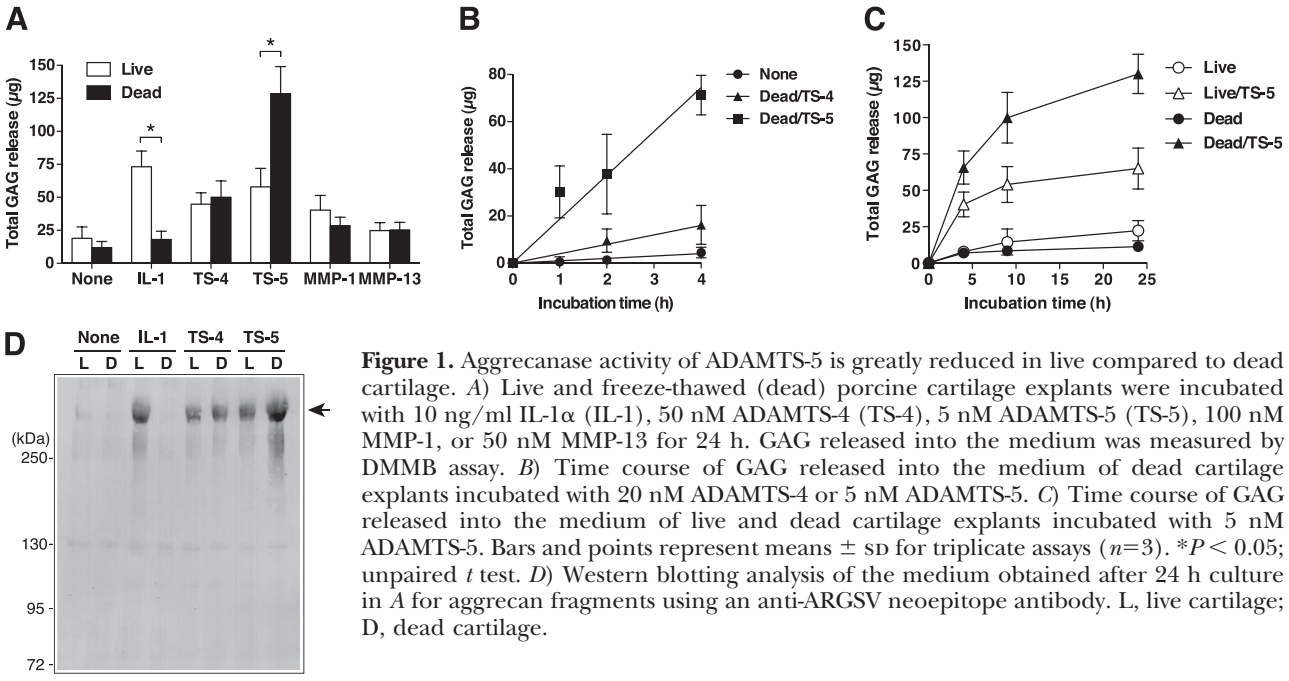

Figure 1. Aggrecanase activity of ADAMTS-5 is greatly reduced in live compared to dead cartilage. *A*) Live and freeze-thawed (dead) porcine cartilage explants were incubated with 10 ng/ml IL-1α (IL-1), 50 nM ADAMTS-4 (TS-4), 5 nM ADAMTS-5 (TS-5), 100 nM MMP-1, or 50 nM MMP-13 for 24 h. GAG released into the medium was measured by DMMB assay. *B*) Time course of GAG released into the medium of dead cartilage explants incubated with 20 nM ADAMTS-4 or 5 nM ADAMTS-5. *C*) Time course of GAG released into the medium of live and dead cartilage explants incubated with 5 nM ADAMTS-5. Bars and points represent means ± SD for triplicate assays (n=3). *$P < 0.05$; unpaired t test. *D*) Western blotting analysis of the medium obtained after 24 h culture in *A* for aggrecan fragments using an anti-ARGSV neoepitope antibody. L, live cartilage; D, dead cartilage.

RESULTS

Aggrecanase activity of ADAMTS-5 is greatly reduced in live compared to dead cartilage

To investigate the ability of ADAMTS-4 and ADAMTS-5 to cleave aggrecan in cartilage, recombinant ADAMTS-4 lacking the C-terminal Sp domain or ADAMTS-5 lacking the C-terminal TS2 domain was added to live or freeze-thawed porcine cartilage explants, and subsequent GAG release was monitored. These two forms of aggrecanases were used as they are readily available in a pure form (11, 21). Freeze-thawed cartilage was used to eliminate the involvement of metabolically active live chondrocytes. Freeze-thawing of cartilage-killed chondrocytes, and these cartilages did not respond to IL-1α stimulation, while live cartilage exhibited a 4.0-fold increase in GAG release into the medium on IL-1α treatment (**Fig. 1*A***). Treatment of dead cartilage with 50 nM ADAMTS-4, 5 nM ADAMTS-5, 100 nM MMP-1, or 50 nM MMP-13 caused a 4.3-, 11.0-, 2.4-, or 2.2-fold increase in GAG release, respectively. When the rate of aggrecan cleavage was compared by measuring GAG release from dead cartilage, ADAMTS-5 cleaved aggrecan fastest, at a rate ~19 times faster than that of ADAMTS-4 (Fig. 1*B*). When live cartilage was used, the amounts of GAG released by ADAMTS-4, MMP-1, or MMP-13 were similar to those released from dead cartilage (Fig. 1*A*). However, ADAMTS-5 showed much lower levels of GAG release when added to live cartilage. A time-course study indicated that ADAMTS-5 digested aggrecan in dead cartilage 1.6- to 2.0-fold more effectively than in live cartilage (Fig. 1*C*). Analysis of aggrecan breakdown products with an anti-ARGSV neoepitope antibody indicated that aggrecan was cleaved at the Glu^{373}-Ala^{374} bond, characteristic of aggrecanase activity (Fig. 1*D*).

Rapid clearance of ADAMTS-5 by articular chondrocytes

To investigate the cause of reduced aggrecanase activity of ADAMTS-5 with live cartilage, we monitored the level of exogenously added ADAMTS-5 in the medium and in the cartilage explants by Western blot analysis. When added to live cartilage, ADAMTS-5 disappeared from the culture medium and was almost completely absent after 4 h without any detectable fragments (**Fig. 2*A, B***). In contrast, relatively large amounts of ADAMTS-5 were detected in the medium of dead cartilage even after 4 h. ADAMTS-5 was also detected in extracts from dead cartilage after 2–4 h, but not in live cartilage. We could not detect endogenous ADAMTS-5, as its level was too low to detect by this method. When ADAMTS-5 was incubated with isolated chondrocytes, it was also depleted from the medium with similar kinetics to that seen in live cartilage, with a half-life of ~80 min. We estimated ~3.5×10^6 ADAMTS-5 molecules were cleared by a single chondrocyte within 1 h (Fig. 2*C*).

LRP-mediated endocytic clearance of ADAMTS-5

To investigate the mechanism of ADAMTS-5 disappearance, we first examined the effect of proteinase inhibitors, but neither the broad-spectrum hydroxamate metalloproteinase inhibitor GM6001 nor a proteinase inhibitor cocktail (mixture of inhibitors for serine, cysteine, and aspartic proteinases) inhibited ADAMTS-5 disappearance. However, dynasore, an inhibitor of dynamin, which is required for most endocytic pathways, including clathrin- and caveolae-mediated endocytosis (24), almost completely inhibited ADAMTS-5 depletion from the medium of live cartilage (**Fig. 3*A***). By contrast, β-CD, which inhibits caveolae-mediated endocytosis by depleting cholesterol from the cell membrane (25), did not inhibit it (Fig. 3*A*), indicating that ADAMTS-5 disappearance is due to a clathrin-dependent endocytic clearance. No significant cytotox-

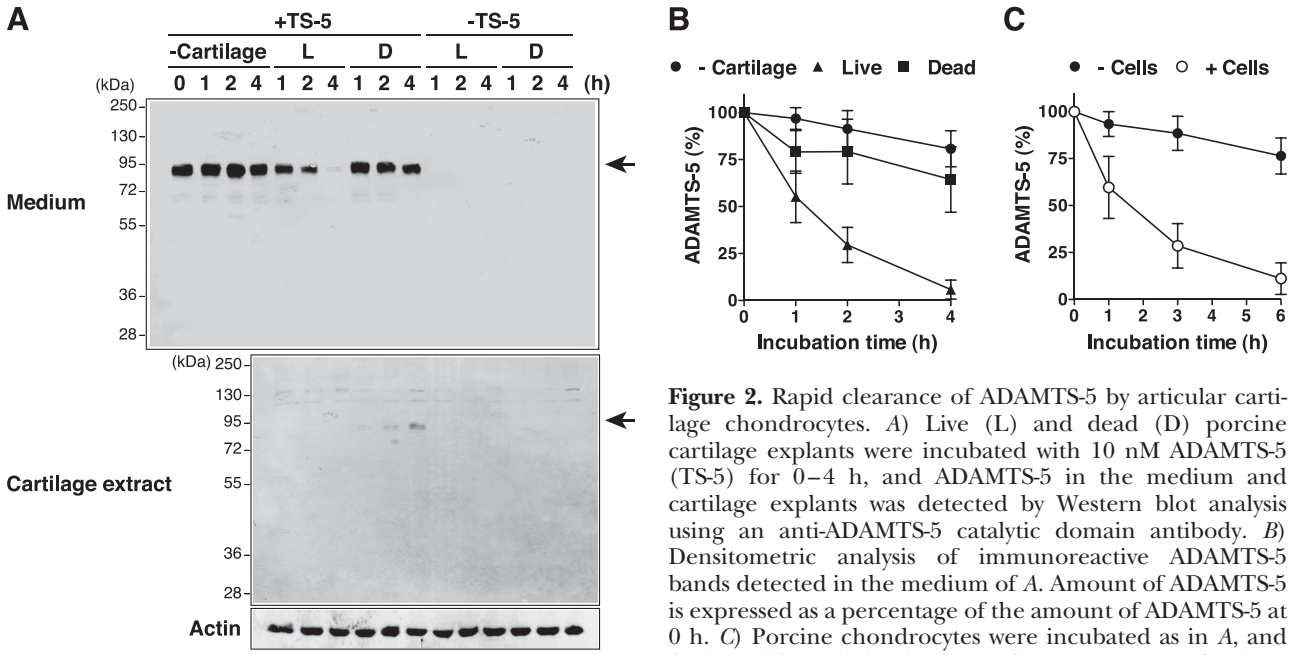

Figure 2. Rapid clearance of ADAMTS-5 by articular cartilage chondrocytes. *A*) Live (L) and dead (D) porcine cartilage explants were incubated with 10 nM ADAMTS-5 (TS-5) for 0–4 h, and ADAMTS-5 in the medium and cartilage explants was detected by Western blot analysis using an anti-ADAMTS-5 catalytic domain antibody. *B*) Densitometric analysis of immunoreactive ADAMTS-5 bands detected in the medium of *A*. Amount of ADAMTS-5 is expressed as a percentage of the amount of ADAMTS-5 at 0 h. *C*) Porcine chondrocytes were incubated as in *A*, and ADAMTS-5 remaining in the medium was measured as in *B*. Points represent means ± SD for triplicate assays (n=3).

icity of dynasore on chondrocytes was found by 3-(4,5-dimethylthiazole-2-yl)-2,5diphenyl tertasolium bromide (MTT) assay (data not shown). We then found that RAP, an antagonist of ligand binding to LRP receptors, inhibited ADAMTS-5 uptake by live cartilage and chondrocytes (Fig. 3*B, C*), suggesting that ADAMTS-5 is endocytosed by a member of the LRPs. The LRP-dependent internalization of ADAMTS-5 was confirmed by immunofluorescent confocal microscopy. Punctate staining of ADAMTS-5 was detected within the cells, and the staining colocalized with EEA1, a marker for early endosomes (Fig. 3*D*). The fluorescent signal of ADAMTS-5 was absent in cells incubated without ADAMTS-5, indicating the specificity of the staining. Consistent with the data from Western blot analysis, the intracellular fluorescent signal for ADAMTS-5 was abolished in the presence of RAP. Heparin also blocked the internalization of ADAMTS-5, suggesting that basic residues of the enzyme are involved in interaction with LRP. When live cartilage was incubated with ADAMTS-5, fluorescent ADAMTS-5 signal was observed within cells located in the superficial zone of the cartilage, and this signal was abolished by RAP (Fig. 3*E*). ADAMTS-5 was internalized even in the presence of 50 μM GM6001 (data not shown), suggesting that the enzyme can penetrate into the cartilage without matrix degradation.

siRNA-mediated knockdown of LRP-1 impairs ADAMTS-5 endocytosis in human chondrocytes

Among the members of the low-density lipoprotein receptor family, LRP-1 is known to mediate endocytosis of a number of proteinases and proteinase-inhibitor complexes (26). Therefore, we silenced LRP-1 in normal human chondrocytes with a gene-specific siRNA to investigate its possible involvement. As shown in **Fig. 4*A***, LRP-1-targeting siRNA-depleted LRP-1 mRNA levels by 93% compared to the nontargeting siRNA control. Western blot analysis of the cell extracts confirmed that the levels of the 515-kDa extracellular heavy chain and the 85-kDa light chain containing the transmembrane domain were reduced by 95 and 80% by targeting siRNA compared to the nontargeting siRNA control (Fig. 4*B*). Cellular uptake of ADAMTS-5 was markedly reduced in LRP-1-depleted cells (Fig. 4*C*). Immunocytochemical analysis further confirmed that ADAMTS-5 endocytosis was impaired in the LRP-1-depleted human chondrocytes (Fig. 4*D*). From these results, we conclude that LRP-1 is the primary endocytic receptor for ADAMTS-5.

TS1 and Sp domains mediate ADAMTS-5 endocytosis

ADAMTS-5 is a multidomain metalloproteinase. Therefore, we searched which domains are required for its endocytosis by testing a series of domain-deletion mutants (**Fig. 5*A***). Since full-length ADAMTS-5 (ADAMTS-5-1) is not available in a high quantity, it was incubated with porcine chondrocytes only for 3 h. The results showed that ~75% of ADAMTS-5-1 disappeared from the medium, and this disappearance was inhibited by RAP (Fig. 5*B*). Domain-deletion mutants were subjected to time-course studies (Fig. 5*C*). Compared to deletion of the TS2 domain alone (ADAMTS-5-2), deletion of both TS2 and Sp domains (ADAMTS-5-3) significantly reduced the rate of endocytosis. Further deletion of the CysR domain resulted in only a slight further reduction. However, the mutant without the TS1 domain (ADAMTS-5-5) was not internalized. When the mutants were tested for their aggrecanase activity using live and dead cartilage explants in culture, all except ADAMTS-5-5 showed a markedly reduced GAG release with live

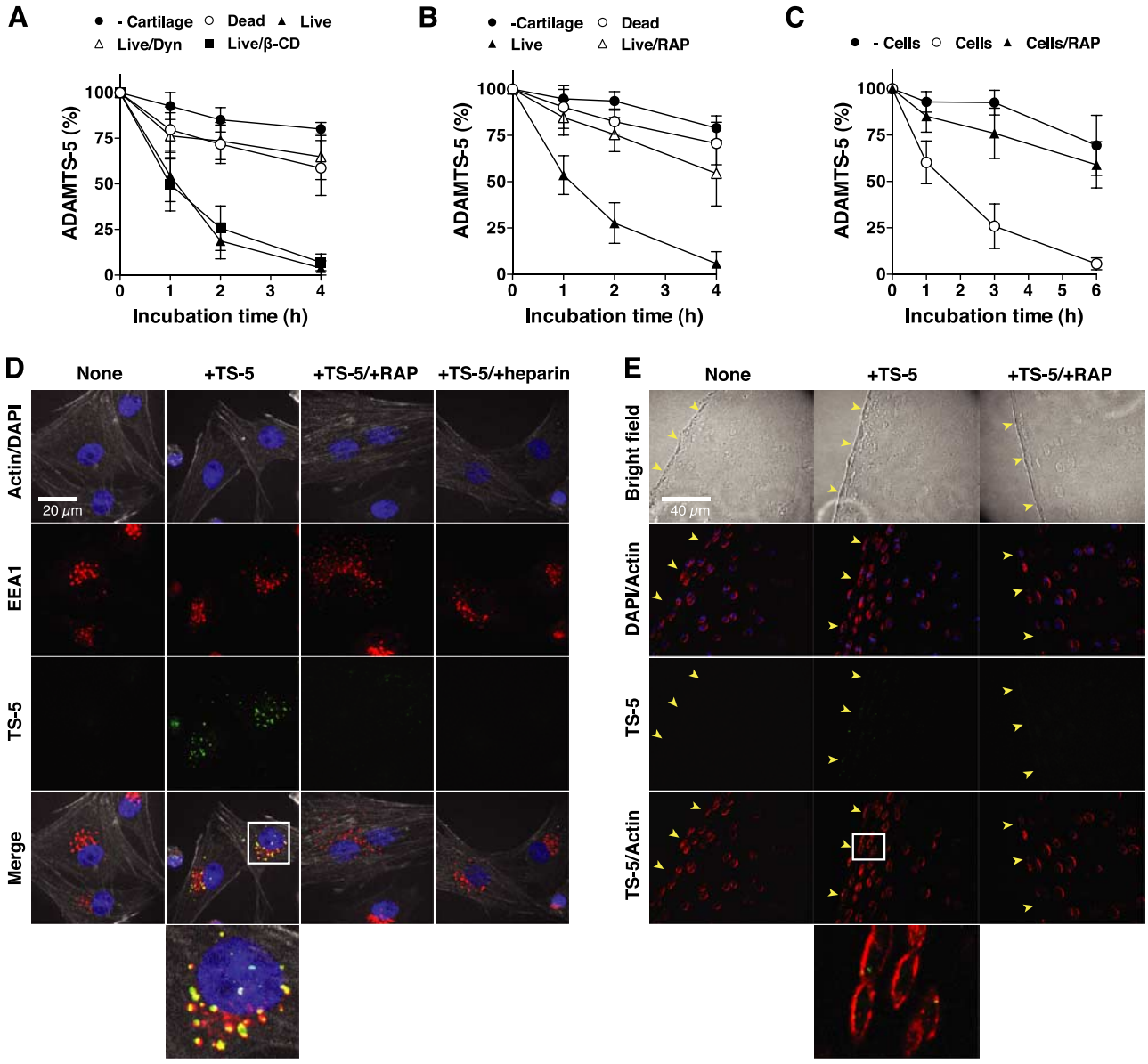

Figure 3. LRP-mediated endocytic clearance of ADAMTS-5. *A*) Live porcine articular cartilage explants were first incubated with 80 μM dynasore or 10 mM β-CD for 30 min. Then, 10 nM ADAMTS-5 was added to the medium and further incubated for 0–4 h. ADAMTS-5 remaining in the medium was measured as in Fig. 2. *B*) Live porcine cartilage explants were incubated with 10 nM ADAMTS-5 in the presence of 500 nM RAP for 0–4 h. *C*) Porcine chondrocytes were incubated as in *B*, and ADAMTS-5 remaining in the medium was measured as in Fig. 2. Points represent means ± SD for triplicate assays (n=3). *D*) Confocal microscopy analysis of ADAMTS-5 endocytosis by porcine chondrocytes. Cells were incubated with 10 nM ADAMTS-5 (TS-5) in the presence or absence of 500 nM RAP or 100 μg/ml heparin for 1 h. Endocytosed ADAMTS-5, EEA1, cytoskeleton and nucleus were visualized as described in Materials and Methods. *E*) Confocal microscopy analysis of ADAMTS-5 endocytosis by porcine cartilage explants. Live cartilage explants were incubated with 10 nM ADAMTS-5 in a similar manner, and endocytosed ADAMTS-5 was detected as in *D*. Yellow arrowheads indicate the intact surface of cartilage explants.

cartilage compared to dead cartilage (Fig. 5*D*). From these data, we conclude that the TS1 domain is essential for ADAMTS-5 endocytosis but that the Sp domain enhances the endocytic process.

Inhibition of ADAMTS-5 endocytosis by RAP enhances aggrecan degradation in articular cartilage

We then examined the effect of RAP on normal turnover of aggrecan in cartilage. The addition of RAP to live porcine cartilage increased the constitutive GAG release an ~2-fold, whereas GAG release from dead cartilage was not enhanced by RAP (**Fig. 6*A***). This effect of RAP was not altered in the presence of polymyxin B, an inhibitor of endotoxin, indicating that the effect was not due to endotoxin contamination in the *E. coli*-expressed RAP preparation. Western blot analysis of the products with an anti-ARGSV antibody indicated that RAP-enhanced aggrecan degradation was due to an increase in aggrecanase activity (Fig. 6*B*). These results suggest that aggrecanases are constitutively produced by normal carti-

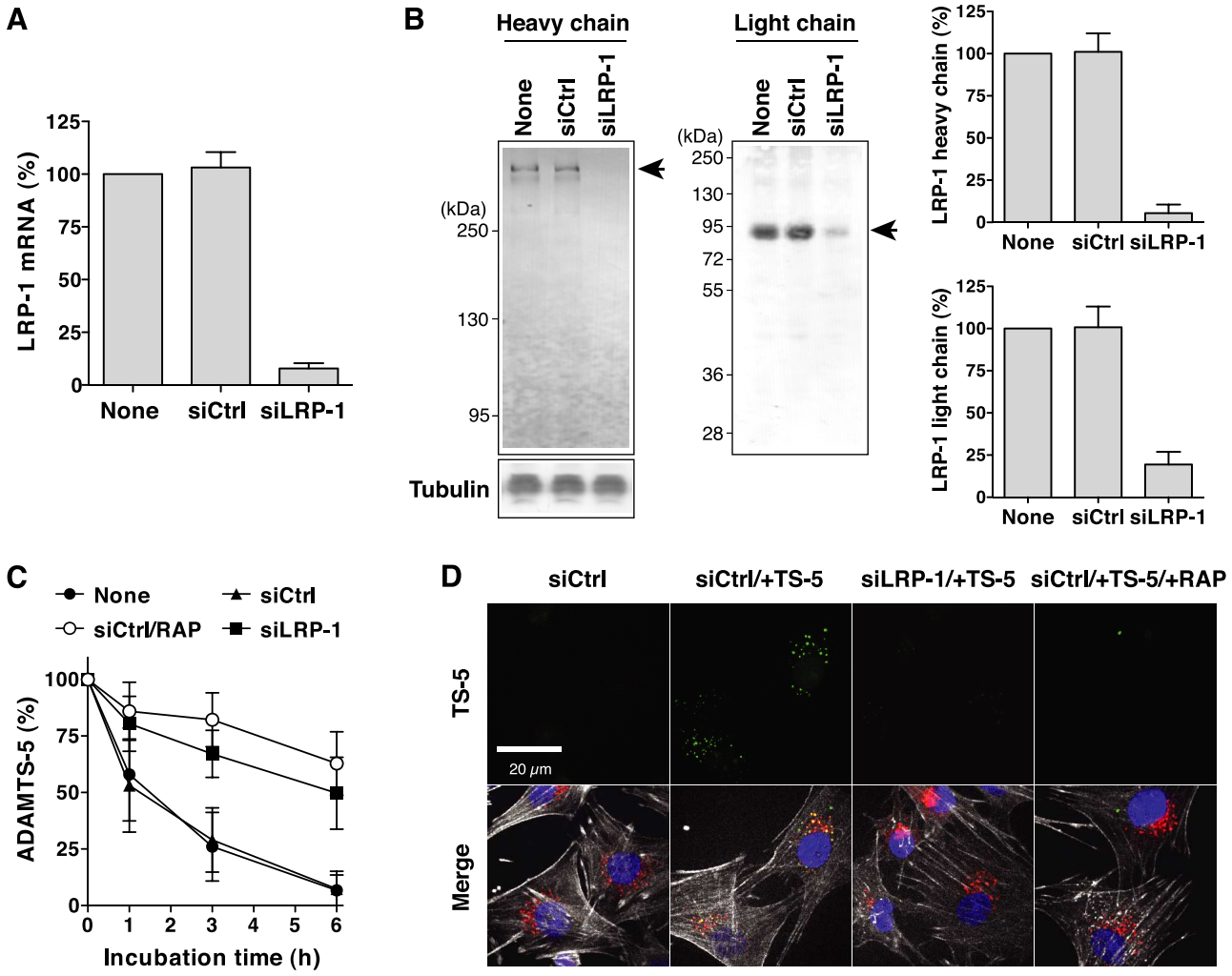

Figure 4. siRNA-mediated knockdown of LRP-1 impairs ADAMTS-5 endocytosis in human chondrocytes. Human chondrocytes transfected with nontargeting siRNA (siCtrl) or LRP-1 targeting siRNA (siLRP-1) were cultured for 2 d in DMEM containing 10% FCS. *A*) Results of TaqMan real-time PCR showing relative levels of mRNA for LRP-1. *B*) Left panels: LRP-1 heavy-chain (515 kDa) and light-chain (85 kDa) in cell lysates were assessed by Western blot analysis using anti-LRP-1 heavy-chain and light-chain antibodies, respectively. Right panels: densitometric analysis of immunoreactive LRP-1 bands detected in the cell lysate. Amount of LRP-1 is expressed as a percentage of the amount of LRP-1 in untransfected cells (none). *C*) Cells were incubated with 10 nM ADAMTS-5 in the presence or absence of 500 nM RAP for 0–6 h, and ADAMTS-5 remaining in the medium was measured as in Fig. 2. Bars and points represent means ± SD for triplicate assays (n=3). *D*) Confocal microscopy analysis of ADAMTS-5 endocytosis by human chondrocytes. Cells were incubated with 10 nM ADAMTS-5 in a similar manner, and endocytosed ADAMTS-5 was detected as in Fig. 3.

lage, but their activities are down-regulated by LRP-1-mediated endocytosis. The addition of 20 nM recombinant ADAMTS-5-4 to dead cartilage caused 1.7-fold higher GAG release over that with live cartilage after 4-h incubation, and this increased to 2.9-fold after 24 h. The addition of RAP to the ADAMTS-5-4-mediated aggrecan degradation system significantly enhanced GAG release from live cartilage but had no effect on GAG release from dead cartilage (Fig. 6*C*). Notably, the level of GAG released from live cartilage in the presence of RAP was equivalent to that from dead cartilage. Western blotting using an anti-ARGSV antibody confirmed that the 3.0-fold increase in aggrecan degradation observed in the presence of RAP is solely due to increased aggrecanase activity of ADAMTS-5 in live cartilage (Fig. 6*D*).

ADAMTS-5 endocytosis is impaired in OA cartilage due to reduced protein levels of LRP-1

Because the extracellular aggrecanase activity of ADAMTS-5 is regulated by LRP-1-mediated endocytosis, we considered whether the increased degradation of aggrecan observed in OA cartilage is due to a dysregulated endocytic pathway. Quantitative mRNA analysis of OA and normal human cartilage showed similar levels of LRP-1 mRNA (**Fig. 7*A***). However, Western blot analysis of LRP-1 protein indicated that OA cartilage has lost most of the receptor protein (Fig. 7*B*). Therefore, we considered the possibility that ADAMTS-5 endocytosis is impaired in OA cartilage, making it more readily susceptible to degradation, while normal human cartilage fully retains this

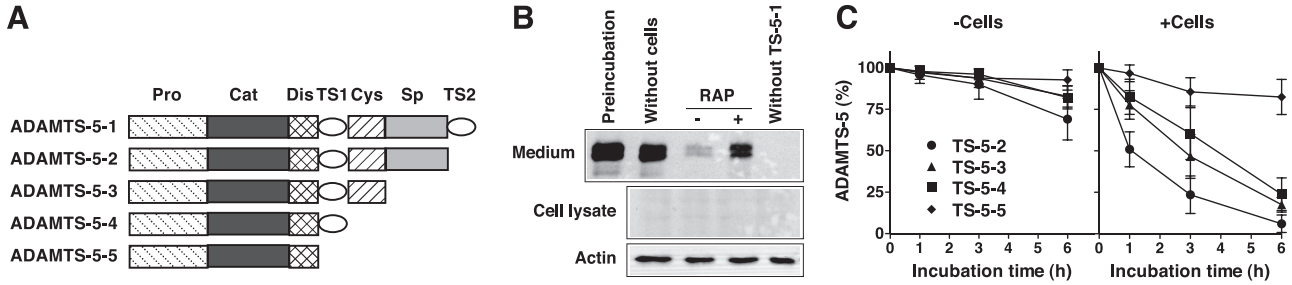

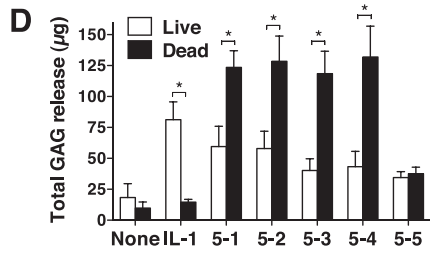

Figure 5. TS1 and spacer domains mediate ADAMTS-5 endocytosis. *A*) Schematic representation of ADAMTS-5 and its domain deletion mutants. Pro, prodomain; Cat, catalytic domain; Dis, disintegrin-like domain; TS1, thrombospondin 1 domain; Cys, cysteine-rich domain; Sp, spacer domain; TS2, thrombospondin 2 domain. *B*) Porcine primary chondrocytes were incubated with 10 nM ADAMTS-5-1 in the presence or absence of 500 nM RAP for 3 h, and ADAMTS-5 in the medium and cell lysate was detected as Fig. 2. *C*) Porcine chondrocytes were incubated with each of 10 nM ADAMTS-5-2, ADAMTS-5-3, ADAMTS-5-4, or ADAMTS-5–5 for 0–6 h, and each ADAMTS-5 mutant remaining in the medium was measured as in Fig. 2. *D*) Live and freeze-thawed (dead) porcine articular cartilage explants were incubated with 10 ng/ml IL-1α, 4 nM ADAMTS-5-1, 5 nM ADAMTS-5-2, 10 nM ADAMTS-5-3, 20 nM ADAMTS-5-4, 50 nM ADAMTS-5-5 for 24 h. GAG released into the medium was measured by DMMB assay. Bars and points represent means ± SD for triplicate assays (n=3). *$P < 0.05$; unpaired t test.

function and efficiently removes aggrecanases from the extracellular space, as demonstrated in Fig. 4. To test this possibility, we examined ADAMTS-5-induced aggrecan degradation in live and freeze-thawed (dead) OA cartilage. We found that the addition of ADAMTS-5 to OA cartilage resulted in a similar release of GAG from the cartilage regardless of whether the tissue was live or dead (Fig. 7*C*). Specific aggrecanase activity detected with these cartilage specimens and the similar susceptibility of live and dead cartilage to degradation was confirmed using an anti-ARGSV antibody (Fig. 7*D*).

DISCUSSION

LRP-1 is a multifunctional endocytic type 1 transmembrane receptor consisting of an extracellular 515-kDa heavy chain and an associated 85-kDa light chain containing the transmembrane and cytoplasmic domains. It mediates internalization of >40 ligands, including lipoproteins, ECM proteins, cell surface receptors, proteinases, and proteinase-proteinase inhibitor complexes (26). The ablation of the LRP-1 gene in mice is embryonically lethal (27), but tissue specific deletion of the LRP-1 gene has indicated that it plays an

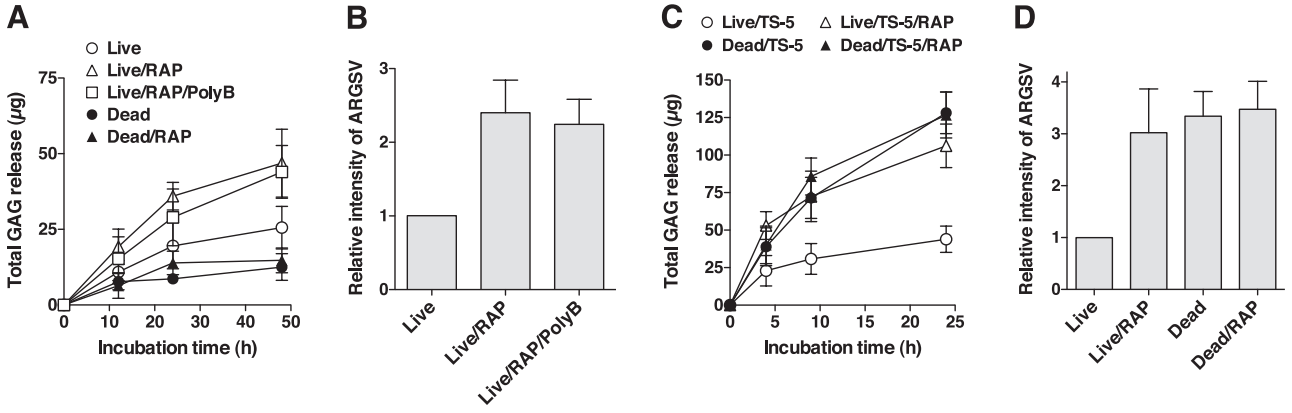

Figure 6. Inhibition of ADAMTS-5 endocytosis by RAP enhances aggrecan degradation in articular cartilage. *A*) Time course of GAG released into the medium of live cartilage explants incubated in the presence or absence of 500 nM RAP. *B*) Densitometric analysis of immunoreactive bands of aggrecan fragments detected in the medium obtained after 48 h culture in *A* by Western blotting using an anti-ARGSV neoepitope antibody. Amount of aggrecan fragment in the medium of live cartilage explants incubated alone was taken as 1. As a control, live cartilage explants were incubated with RAP in the presence of 100 μg/ml polymyxin B (PolyB) for the indicated period of time. *C*) Time course of GAG released into the medium of live and freeze-thawed (dead) cartilage explants incubated with 20 nM ADAMTS-5-4 in the presence or absence of 500 nM RAP. *D*) Amount of aggrecan fragments in the medium obtained after 24 h culture in *C* were measured as in *B*. Amount of aggrecan fragment in the medium of live cartilage explants incubated with 20 nM ADAMTS-5-4 was taken as 1. Bars and points represent means ± SD for triplicate assays (n=3).

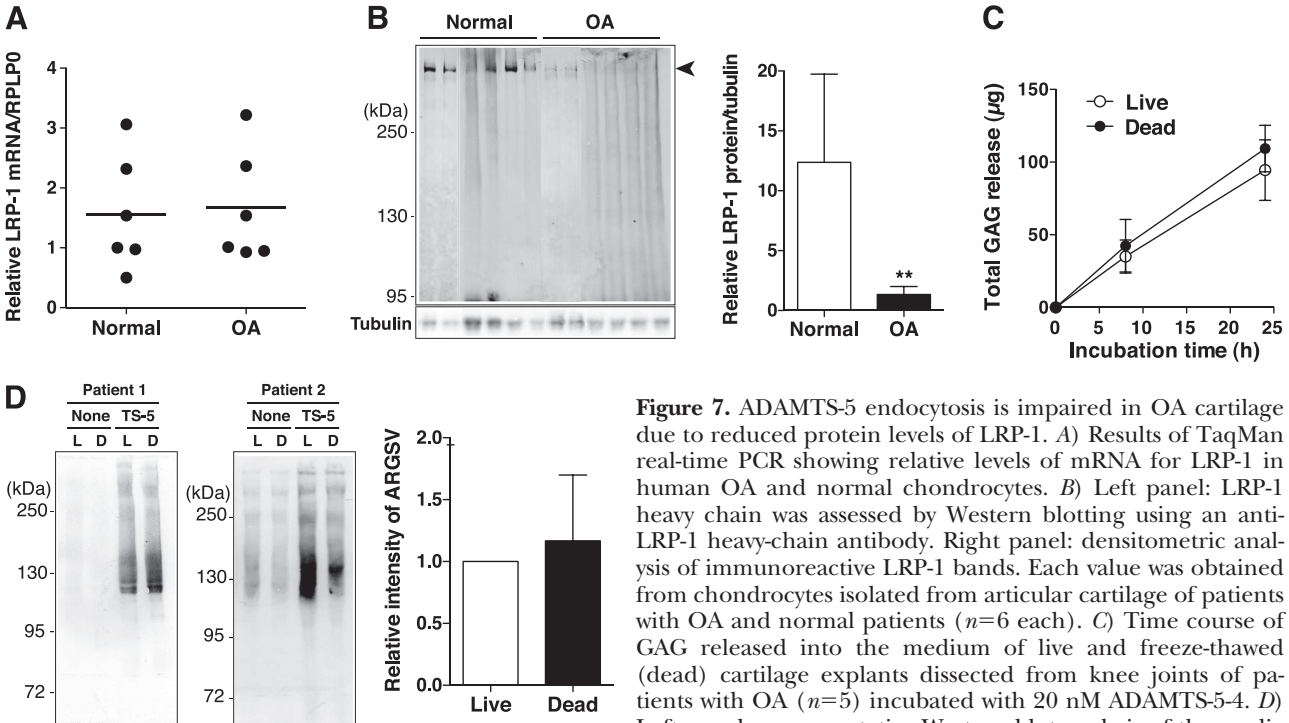

Figure 7. ADAMTS-5 endocytosis is impaired in OA cartilage due to reduced protein levels of LRP-1. *A*) Results of TaqMan real-time PCR showing relative levels of mRNA for LRP-1 in human OA and normal chondrocytes. *B*) Left panel: LRP-1 heavy chain was assessed by Western blotting using an anti-LRP-1 heavy-chain antibody. Right panel: densitometric analysis of immunoreactive LRP-1 bands. Each value was obtained from chondrocytes isolated from articular cartilage of patients with OA and normal patients (n=6 each). *C*) Time course of GAG released into the medium of live and freeze-thawed (dead) cartilage explants dissected from knee joints of patients with OA (n=5) incubated with 20 nM ADAMTS-5-4. *D*) Left panels: representative Western blot analysis of the media obtained from two patients after 24 h culture in *C* for aggrecan fragments using an anti-ARGSV neoepitope antibody. L, live cartilage; D, dead cartilage. Right panel: densitometric analysis of immunoreactive bands of aggrecan fragments (n=4). Amount of aggrecan fragment in the medium of live cartilage explants was taken as 1. Bars and points represent means ± SD. $^{**}P < 0.005$; unpaired t test.

important role in protecting the vasculature, β-amyloid precursor protein trafficking, and lipid metabolism in adipocytes and macrophage biology (see ref. 26 for review). The work presented here demonstrates that LRP-1 also plays a key role in regulating aggrecan turnover in cartilage by internalizing a major aggrecanase, ADAMTS-5.

Many proteinases are internalized by LRP-1 after forming a complex with specific inhibitors, as conformational changes of the inhibitor on complex formation give a signal for LRP-1 recognition (see ref. 26 for review). We considered the possibility that ADAMTS-5 might have been internalized after forming a complex with TIMP-3, as TIMP-3 is also endocytosed by an LRP-1-mediated pathway (ref. 20 and unpublished results). However, we concluded that TIMP-3 is not required for ADAMTS-5 internalization from the following observations: first, GM6001, a broad-spectrum hydroxamate metalloproteinase inhibitor that blocks metalloproteinase-TIMP complex formation, did not block ADAMTS-5 internalization; second, ADAMTS-5-5, consisting of the catalytic and the disintegrin domains, was not internalized, although it can form a complex with TIMP-3; and third, chondrocytes isolated from TIMP-3-null mice internalized ADAMTS-5 (data not shown). Thus, ADAMTS-5 and TIMP-3 can be endocytosed independently or as a complex. Domain deletion mutagenesis studies then indicated that both the TS1 domain and Sp domain are involved in effective binding of ADAMTS-5 to LRP-1, but the TS1 domain alone is sufficient. We postulate that basic residues in these domains are responsible for LRP-1 binding, as ADAMTS-5 internalization is inhibited by heparin. The importance of basic residues for interaction with LRP-1 has been shown for many protein ligands (26). When full-length ADAMTS-5 is secreted from the cell, however, it can bind to sulfated proteoglycans on the cell surface and in the ECM through basic residues in its CysR and Sp domains (21). The CysR and Sp domains are also necessary for the expression of full aggrecanase activity of ADAMTS-5. Therefore, the location of the enzyme and expression of aggrecanase activity is determined by competition between the ECM and LRP-1. However, ADAMTS-5 is internalized by cartilage explants and isolated chondrocytes with similar kinetics (Fig. 2). When live cartilage was incubated with ADAMTS-5, fluorescent ADAMTS-5 signal was observed within chondrocytes but not in the cartilage ECM (Fig. 3*E*). These results suggest that ADAMTS-5 binds loosely to the ECM and thus that the enzyme is readily removed from the tissue by LRP-1. When the spacer domain is removed from ADAMTS-5 (ADAMTS-5-3), its aggrecanase activity reduces only by 25%, but the extracellular half-life increases >3-fold. Deletion of both the CysR and Sp domains (ADAMTS-5-4) results in the loss of most of the aggrecanase activity (only 0.2-0.3% of the original activity remains; ref. 21). This form can diffuse through the interterritorial region of cartilage, as it no longer binds to the ECM. Interestingly, ADAMTS-5-4 retains ~25% of full-length ADAMTS-5 proteolytic activity against biglycan, decorin, and fibromodulin (21). Such processing would have potential to dysregulate tissue matrix turnover and cellu-

lar environments. However, this form of the enzyme is still removed from the tissue by LRP-1, indicating that LRP-1 is therefore an important regulator of normal cartilage homeostasis.

A number of ADAMTS metalloproteinases have been reported to have an important role in development and organ morphogenesis. For example, ADAMTS-1 is essential for normal growth, structure, and function of the kidney, adrenal gland and female reproductive organ, myocardial trabeculation during heart development (see ref. 10 for review), and limb joint development (28). ADAMTS-5 plays a key role in cardiac valve development (29), regression of the interdigital web during mouse limb morphogenesis along with ADAMTS-9 and ADAMTS-20 (30), control of fibroblast-myofibroblast transition (31), and skin excision wound healing (32). In those processes, ADAMTSs function as versican- and aggrecan-cleaving enzymes. Although the role of LRP-1 in post-translational turnover of these ADAMTSs during organ morphogenesis or wound healing is yet to be investigated, our study implies that LRP-1 may regulate the activities of other members of the ADAMTS family, if we consider the importance of LRP-1 in development (27). During morphogenesis and tissue remodeling, timely ECM degradation is essential, and one possible mechanism is endocytosis of matrix-degrading enzymes. The recent study of Sorvillo *et al.* (33) showed that endocytosis of ultralarge von Willebrand factor-cleaving ADAMTS-13 by dendritic cells is mediated by a different scavenger receptor, the macrophage mannose receptor. This process is postulated to be involved in generation of the autoantibodies against the enzyme seen in patients with acquired thrombotic thrombocytopenic purpura (33).

ADAMTS-5 has been implicated in the development of OA, but this is controversial, because no correlation between ADAMTS-5 mRNA levels and OA progression have been reported (13, 17, 18). Our study has provided a new insight into this discrepancy by introducing a role of LRP-1 in the progression of OA. In normal healthy cartilage, the activity of ADAMTS-5 is regulated by endocytosis, as shown by an increased aggrecan turnover on addition of RAP. This pathway is, however, impaired in OA cartilage. This is evident from our observation that there were no significant differences in the ability of exogenously added ADAMTS-5 to digest aggrecan in live or freeze-thawed OA cartilage. A similar impairment of LRP-1-dependent endocytosis of MMP-13 has been reported in OA cartilage without alteration in the mRNA levels of LRP-1 (34), but its mechanism was not known. We have confirmed unaltered mRNA levels of LRP-1 in normal and OA human cartilage and found that levels of LRP-1 protein is substantially lower in OA cartilage. This leads to an increase in extracellular levels of ADAMTS-5, MMP-13, and possibly other metalloproteinase in OA cartilage. Although the mechanism by which OA cartilage loses LRP-1 from the cell surface has yet to be investigated, we postulate that it is due to increased shedding of LRP-1 from the cell surface as has been shown in malignant cells (35, 36) and in cycling human endometrium at menses (37). The shedding of LRP-1 increases under inflammatory conditions, and soluble LRP-1 is elevated in plasma of patients with rheumatoid arthritis and systemic lupus erythematosus (38). Proteinases that were reported to shed LRP-1 include β-amyloid precursor protein-cleaving enzyme (39), MMP-14 (35), ADAM-10 (40), ADAM-12 (36, 37), and ADAM-17 (38, 40). LRP-1 is reported to protect against the progression of atherosclerosis in mice by suppressing the expression of inflammatory mediators, such as monocyte chemoattractant protein 1, tumor necrosis factor α, and MMP-9, while deletion of macrophage LRP-1 increases MMP-9, which is associated with a high frequency to plaque rupture (41). Increased shedding of LRP-1 in chondrocytes will shift the homeostatic balance of ECM turnover to catabolic, resulting in a gradual loss of aggrecan and collagen fibrils. A slight shift in enzymatic balance due to loss of LRP-1 may be an important part of the dysregulation of aggrecanase activity. Identification of the mechanism by which LRP-1 is post-translationally processed will therefore provide further insights into our understanding of the pathogenesis of OA. FJ

The authors thank Dr. Brendan L. Thoms for help with human chondrocyte culture and the Orthopaedic Surgery Department of Charing Cross Hospital (London, UK) for providing human OA cartilage. Normal human cartilage samples were obtained through the Royal National Orthopaedic Hospital (Stanmore, UK). This work was supported by an Arthritis Research UK Core Grant to the Kennedy Institute of Rheumatology, and U.S. National Institutes of Health grants AR40994 (to H.N.), PO1 HL54710 (to D.K.S.), and HL54710 (to D.K.S.). The content is solely the responsibility of the authors and does not necessarily represent the official views of the National Institutes of Health. L.T. is supported by an Arthritis Research UK Career Development Fellowship (grant 19466).

REFERENCES

1. Heinegård, D., and Saxne, T. (2011) The role of the cartilage matrix in osteoarthritis. *Nat. Rev. Rheumatol.* **7,** 50–56
2. Murphy, G., and Nagase, H. (2008) Reappraising metalloproteinases in rheumatoid arthritis and osteoarthritis: destruction or repair? *Nat. Clin. Pract. Rheumatol.* **4,** 128–135
3. Troeberg, L., and Nagase, H. (2012) Proteases involved in cartilage matrix degradation in osteoarthritis. *Biochim. Biophys. Acta* **1824,** 133–145
4. Pratta, M. A., Yao, W., Decicco, C. Tortorella, M. D., Liu, R. Q., Copeland, R. A., Magolda, R. Newton, R. C., Trzaskos, J. M., and Arner, E. C. (2003) Aggrecan protects cartilage collagen from proteolytic cleavage. *J. Biol. Chem.* **278,** 45539–45545
5. Lim, N. H., Kashiwagi, M., Visse, R., Jones, J., Enghild, J. J., Brew, K., and Nagase, H. (2010) Reactive-site mutants of N-TIMP-3 that selectively inhibit ADAMTS-4 and ADAMTS-5: biological and structural implications. *Biochem. J.* **431,** 113–122
6. Sandy, J. D., Neame, P. J., Boynton, R. E., and Flannery, C. R. (1991) Catabolism of aggrecan in cartilage explants. Identification of a major cleavage site within the interglobular domain. *J. Biol. Chem.* **266,** 8683–8685
7. Ilic, M. Z. Handley, C. J., Robinson, H. C., and Mok, M. T. (1992) Mechanism of catabolism of aggrecan by articular cartilage. *Arch. Biochem. Biophys.* **294,** 115–122
8. Sandy, J. D., Flannery, C. R., Neame, P. J., and Lohmander, L. S. (1992) The structure of aggrecan fragments in human synovial fluid. Evidence for the involvement in osteoarthritis of a novel proteinase which cleaves the Glu 373-Ala 374 bond of the interglobular domain. *J. Clin. Invest.* **89,** 1512–1516

9. Lohmander, L. S. Neame, P. J., and Sandy, J. D. (1993) The structure of aggrecan fragments in human synovial fluid. Evidence that aggrecanase mediates cartilage degradation in inflammatory joint disease, joint injury, and osteoarthritis. *Arthritis Rheum.* **36,** 1214–1222
10. Apte, S. S. (2009) A disintegrin-like and metalloprotease (reprolysin-type) with thrombospondin type 1 motif (ADAMTS) superfamily: functions and mechanisms. *J. Biol. Chem.* **284,** 31493–31497
11. Kashiwagi, M. Enghild, J. J., Gendron, C., Hughes, C., Caterson, B., Itoh, Y., and Nagase, H. (2004) Altered proteolytic activities of ADAMTS-4 expressed by C-terminal processing. *J. Biol. Chem.* **279,** 10109–10119
12. Fushimi, K., Troeberg, L., Nakamura, H. Lim, N. H., and Nagase, H. (2008) Functional differences of the catalytic and non-catalytic domains in human ADAMTS-4 and ADAMTS-5 in aggrecanolytic activity. *J. Biol. Chem.* **283,** 6706–6716
13. Naito, S., Shiomi, T., Okada, A., Kimura, T., Chijiiwa, M., Fujita, Y., Yatabe, T., Komiya, K., Enomoto, H., Fujikawa, K., and Okada, Y. (2007) Expression of ADAMTS4 (aggrecanase-1) in human osteoarthritic cartilage. *Pathol. Int.* **57,** 703–711
14. Glasson, S. S., Askew, R., Sheppard, B., Carito, B., Blanchet, T., Ma, H. L., Flannery, C. R., Peluso, D., Kanki, K., Yang, Z., Majumdar, M. K., and Morris, E. A. (2005) Deletion of active ADAMTS5 prevents cartilage degradation in a murine model of osteoarthritis. *Nature* **434,** 644–648
15. Glasson, S. S., Askew, R., Sheppard, B. Carito, B. A., Blanchet, T. Ma, H. L., Flannery, C. R., Kanki, K., Wang, E., Peluso, D., Yang, Z., Majumdar, M. K., and Morris, E. A. (2004) Characterization of and osteoarthritis susceptibility in ADAMTS-4-knockout mice. *Arthritis Rheum.* **50,** 2547–2558
16. Stanton, H. Rogerson, F. M., East, C. J., Golub, S. B., Lawlor, K. E., Meeker, C. T., Little, C. B., Last, K., Farmer, P. J., Campbell, I. K., Fourie, A. M., and Fosang, A. J. (2005) ADAMTS5 is the major aggrecanase in mouse cartilage in vivo and in vitro. *Nature* **434,** 648–652
17. Bau, B. Gebhard, P. M., Haag, J., Knorr, T., Bartnik, E., and Aigner, T. (2002) Relative messenger RNA expression profiling of collagenases and aggrecanases in human articular chondrocytes in vivo and in vitro. *Arthritis Rheum.* **46,** 2648–2657
18. Kevorkian, L. Young, D. A., Darrah, C. Donell, S. T., Shepstone, L., Porter, S. Brockbank, S. M., Edwards, D. R., Parker, A. E., and Clark, I. M. (2004) Expression profiling of metalloproteinases and their inhibitors in cartilage. *Arthritis Rheum.* **50,** 131–141
19. Fosang, A. J. Rogerson, F. M., East, C. J., and Stanton, H. (2008) ADAMTS-5: the story so far. *Eur. Cell. Mater.* **15,** 11–26
20. Troeberg, L., Fushimi, K., Khokha, R., Emonard, H., Ghosh, P., and Nagase, H. (2008) Calcium pentosan polysulfate is a multifaceted exosite inhibitor of aggrecanases. *FASEB J.* **22,** 3515–3524
21. Gendron, C., Kashiwagi, M. Lim, N. H., Enghild, J. J., Thogersen, I. B., Hughes, C., Caterson, B., and Nagase, H. (2007) Proteolytic activities of human ADAMTS-5: comparative studies with ADAMTS-4. *J. Biol. Chem.* **282,** 18294–18306
22. Yu, Z., Visse, R., Inouye, M., Nagase, H., and Brodsky, B. (2012) Defining the requirements for collagenase cleavage in collagen type III using a bacterial collagen system. *J. Biol. Chem.* **287,** 22988–22997
23. Franken, K. L. Hiemstra, H. S., van Meijgaarden, K. E., Subronto, Y. den Hartigh, J., Ottenhoff, T. H., and Drijfhout, J. W. (2000) Purification of his-tagged proteins by immobilized chelate affinity chromatography: the benefits from the use of organic solvent. *Protein Exp. Purif.* **18,** 95–99
24. Kirchhausen, T., Macia, E., and H. E. Pelish. (2008) Use of dynasore, the small molecule inhibitor of dynamin, in the regulation of endocytosis. *Methods Enzymol.* **438,** 77–93
25. Rodal, S. K., Skretting, G., Garred, O., Vilhardt, F. van Deurs, B., and Sandvig, K. (1999) Extraction of cholesterol with methyl-beta-cyclodextrin perturbs formation of clathrin-coated endocytic vesicles. *Mol. Biol. Cell* **10,** 961–974
26. Lillis, A. P., Van Duyn, L. B., Murphy-Ullrich, J. E., and Strickland, D. K. (2008) LDL receptor-related protein 1: unique tissue-specific functions revealed by selective gene knockout studies. *Physiol. Rev.* **88,** 887–918
27. Herz, J. Clouthier, D. E., and Hammer, R. E. (1992) LDL receptor-related protein internalizes and degrades uPA-PAI-1 complexes and is essential for embryo implantation. *Cell* **71,** 411–421
28. Capehart, A. A. (2010) Proteolytic cleavage of versican during limb joint development. *Anat. Rec. (Hoboken)* **293,** 208–214
29. Dupuis, L. E. McCulloch, D. R., McGarity, J. D., Bahan, A., Wessels, A., Weber, D. Diminich, A. M., Nelson, C. M., Apte, S. S., and Kern, C. B. (2011) Altered versican cleavage in ADAMTS5 deficient mice; a novel etiology of myxomatous valve disease. *Dev. Biol.* **357,** 152–164
30. McCulloch, D. R. Nelson, C. M., Dixon, L. J., Silver, D. L., Wylie, J. D., Lindner, V., Sasaki, T. Cooley, M. A., Argraves, W. S., and Apte, S. S. (2009) ADAMTS metalloproteases generate active versican fragments that regulate interdigital web regression. *Dev. Cell* **17,** 687–698
31. Hattori, N. Carrino, D. A., Lauer, M. E., Vasanji, A. Wylie J. D., Nelson, C. M., and Apte, S. S. (2011) Pericellular versican regulates the fibroblast-myofibroblast transition: a role for ADAMTS5 protease-mediated proteolysis. *J. Biol. Chem.* **286,** 34298–34310
32. Velasco, J., Li, J., DiPietro, L. M. A. Stepp, J. D. Sandy, and Plaas, A. (2011) Adamts5 deletion blocks murine dermal repair through CD44-mediated aggrecan accumulation and modulation of transforming growth factor beta1 (TGFβ1) signaling. *J. Biol. Chem.* **286,** 26016–26027
33. Sorvillo, N., Pos, W., van den Berg, L. M., Fijnheer, R., Martinez-Pomares, L., Geijtenbeek, T. B., Herczenik, E., and Voorberg, J. (2012) The macrophage mannose receptor promotes uptake of ADAMTS13 by dendritic cells. *Blood* **119,** 3828–3835
34. Walling, H. W. Raggatt, L. J., Irvine, D. W., Barmina, O. Y., Toledano, J. E., Goldring, M. B., Hruska, K. A., Adkisson, H. D., Burdge, R. E., Gatt, Jr., C. J., Harwood, D. A., and Partridge, N. C. (2003) Impairment of the collagenase-3 endocytotic receptor system in cells from patients with osteoarthritis. *Osteoarthritis Cartilage* **11,** 854–863
35. Rozanov, D. V., Hahn-Dantona, E. Strickland, D. K., and Strongin, A. Y. (2004) The low density lipoprotein receptor-related protein LRP is regulated by membrane type-1 matrix metalloproteinase (MT1-MMP) proteolysis in malignant cells. *J. Biol. Chem.* **279,** 4260–4268
36. Selvais, C. D'Auria, L., Tyteca, D., Perrot, G., Lemoine, P., Troeberg, L., Dedieu, S., Noel, A., Nagase, H., Henriet, P. Courtoy, P. J., Marbaix, E., and Emonard, H. (2011) Cell cholesterol modulates metalloproteinase-dependent shedding of low-density lipoprotein receptor-related protein-1 (LRP-1) and clearance function. *FASEB J.* **25,** 2770–2781
37. Selvais, C. Gaide Chevronnay, H. P., Lemoine, P., Dedieu, S., Henriet, P. Courtoy, P. J., Marbaix, E., and Emonard, H. (2009) Metalloproteinase-dependent shedding of low-density lipoprotein receptor-related protein-1 ectodomain decreases endocytic clearance of endometrial matrix metalloproteinase-2 and -9 at menstruation. *Endocrinology* **150,** 3792–3799
38. Gorovoy, M., Gaultier, A. Campana, W. M., Firestein, G. S., and Gonias, S. L. (2010) Inflammatory mediators promote production of shed LRP1/CD91, which regulates cell signaling and cytokine expression by macrophages. *J. Leukoc. Biol.* **88,** 769–778
39. Von Arnim, C. A., Kinoshita, A., Peltan, I. D., Tangredi, M. M., Herl, L. Lee, B. M., Spoelgen, R., Hshieh, T. T., Ranganathan, S. Battey, F. D., Liu, C. X., Bacskai, B. J., Sever, S., Irizarry, M. C., Strickland, D. K., and Hyman, B. T. (2005) The low density lipoprotein receptor-related protein (LRP) is a novel beta-secretase (BACE1) substrate. *J. Biol. Chem.* **280,** 17777–17785
40. Liu, Q., Zhang, J., Tran, H., Verbeek, M. M., Reiss, K., Estus, S., and Bu, G. (2009) LRP1 shedding in human brain: roles of ADAM10 and ADAM17. *Mol. Neurodegener.* **4,** 17
41. Overton, C. D., Yancey, P. G., Major, A. S., Linton, M. F., and Fazio, S. (2007) Deletion of macrophage LDL receptor-related protein increases atherogenesis in the mouse. *Circ. Res.* **100,** 670–677

Received for publication August 26, 2012.
Accepted for publication October 1, 2012.

JBC Papers in Press. Published on November 19, 2012 as Manuscript M112.393322
The latest version is at http://www.jbc.org/cgi/doi/10.1074/jbc.M112.393322

Differential Regulation of Extracellular Tissue Inhibitor of Metalloproteinases-3 Levels by Cell Membrane-bound And Shed Low Density Lipoprotein Receptor-related Protein 1*

Simone D. Scilabra[1, 2], Linda Troeberg[1, 2], Kazuhiro Yamamoto[2], Hervé Emonard[3], Ida Thøgersen[4], Jan J. Enghild[4], Dudley K. Strickland [5] and Hideaki Nagase[1, 2,*]

[1]Department of Medicine, Imperial College London; London, UK; [2]Kennedy Institute of Rheumatology, University of Oxford, London, UK; [3]University of Reims Champagne-Ardenne, FRE 3481 CNRS, Reims, France; [4]Department of Molecular Biology and Genetics, Aarhus University, Aarhus, Denmark; [5]Department of Surgery, University of Maryland, Baltimore, USA.

*Running title: *TIMP-3 endocytosis by LRP-1*

To whom correspondence should be addressed: Hideaki Nagase, Kennedy Institute of Rheumatology, University of Oxford, 65 Aspenlea Road, London, W6 8LH, UK. Tel: + 44 (0)20 8383 4488, e-mail: hideaki.nagase@kennedy.ox.ac.uk

Background: Tissue inhibitor of metalloproteinases-3 (TIMP-3) is endocytosed, but its regulatory mechanism is not well understood.
Result: TIMP-3 endocytosis occurs mainly through low-density lipoprotein receptor-related protein-1 (LRP-1), but shed sLRP-1 binds TIMP-3.
Conclusion: TIMP-3-sLRP-1 complexes are retained extracellularly with metalloproteinase inhibitory activity.
Significance: LRP-1 is the master regulator of extracellular levels of TIMP-3.

SUMMARY

Tissue inhibitor of metalloproteinases-3 (TIMP-3) plays a key role in regulating extracellular matrix turnover by inhibiting matrix metalloproteinases (MMPs), adamalysins (ADAMs) and adamalysins with thrombospondin motifs (ADAMTSs). We demonstrate that levels of this physiologically important inhibitor can be post-translationally regulated by endocytosis. TIMP-3 was endocytosed and degraded by a number of cell types including chondrocytes, fibroblasts, and monocytes, and we found that the endocytic receptor low-density lipoprotein receptor-related protein-1 (LRP-1) plays a major role in TIMP-3 internalization. However, the cellular uptake of TIMP-3 significantly slowed down after 10 h due to shedding of LRP-1 from the cell surface and formation of soluble LRP-1 (sLRP-1)−TIMP-3 complexes. Addition of TIMP-3 to HTB94 human chondrosarcoma cells increased the release of sLRP-1 fragments of 500, 215, 160 and 110 kDa into the medium in a concentration dependent manner, and all these fragments were able to bind to TIMP-3. TIMP-3 bound to sLRP-1, which was resistant to endocytosis, retained its inhibitory activity against metalloproteinases. Extracellular levels of sLRP-1 can thus increase the half-life of TIMP-3 in the extracellular space, controlling the bioavailability of TIMP-3 to inhibit metalloproteinases.

INTRODUCTION

The tissue inhibitors of metalloproteinases (TIMPs) are a family of proteins that regulate the activity of metalloproteinases through formation of tight, non-covalent complexes in a 1:1 stoichiometry (1). Among the four mammalian TIMPs, TIMP-3 is unique in a number of respects. It has a broader inhibitory profile than the other TIMPs, being able to inhibit matrix metalloproteinases (MMPs) and the related metalloproteinases of the ADAM (a disintegrin and metalloproteinase) and the ADAMTS (a disintegrin and metalloproteinase with thrombospondin motifs) families (1). TIMP-3 is the only member of the family that can bind to the extracellular matrix (ECM) (2,3), while the other TIMPs are readily extracted from the tissue. Studies using TIMP-3-null mice have

indicated that it is the major regulator of metalloproteinase activities *in vivo*. Ablation of the *Timp3* gene leads to a number of defects in mice, including impaired lung development (4), dilated cardiomyopathy (5), increased apoptosis during mammary gland involution (6), and accelerated development of osteoarthritis upon aging (7). These are due to dysregulation of ECM turnover. In addition, uncontrolled activity of ADAMs, particularly ADAM17, resulted in elevated levels of TNFα and increased inflammation in murine models of liver regeneration (8), sepsis (9), and antigen-induced arthritis (7), and the phenotypes of the *Timp3*-null mouse are reflected in a number of human pathologies (see ref. (1) for review). Thus, there is considerable interest in understanding factors regulating TIMP-3 levels, and it has been shown that transcription of TIMP-3 can be increased by the histone deacetylase SirT1 (10) and growth factors such as TGFβ (11) and oncostatin M (12) and reduced by promoter methylation (13). Translation of TIMP-3 can be reduced by miR-21 (14), miR-221 and miR-222 (15), miR-181b (16) and miR-206 (17).

We have recently shown that TIMP-3 levels can be post-translationally regulated by endocytosis and intracellular degradation and suggested that this is an important factor determining extracellular levels of TIMP-3 (18). In the previous studies we used endocytic blockers to demonstrate the cellular uptake of TIMP-3. For example, HTB94 chondrosarcoma cells transfected with an expression plasmid for TIMP-3 produced high levels of *TIMP3* mRNA, but TIMP-3 protein was not detected in the conditioned medium. When heparin, pentosan polysulfate (PPS), or receptor-associated protein (RAP), an antagonist of ligand binding to low-density lipoprotein (LDL) receptor and related receptors, was added to the cells, TIMP-3 accumulated in the medium. These studies suggested that the receptor responsible for TIMP-3 endocytosis is a member of the LDL receptor-related protein (LRP) family (18). There are 13 members in the mammalian LDL receptor family that endocytose a wide variety of ligands and deliver them to endosomes for degradation (19). Among them, LDL receptor-related protein 1 (LRP-1) endocytoses more than 30 ligands, including proteinase-inhibitor complexes and ECM proteins, making it an important regulator of ECM composition and turnover (20). LRP-1 is comprised of 2 chains, a 515 kDa α-chain that interacts with ligands via its 4 clusters of LDL receptor type A repeats, and a non-covalently associated 85 kDa β-chain that tethers the receptor in the membrane and interacts with intracellular adaptors to direct endocytosis via clathrin-coated pits (20). LRP-1 can be shed from cell membranes, releasing a soluble form of the receptor, sLPR-1, that can act as a competitive inhibitor of ligand endocytosis (21,22).

In this report, we used metabolically radiolabelled, isolated recombinant [^{35}S]TIMP-3 to investigate the endocytic pathways for TIMP-3 in more detail and analyzed the distribution of radioactivity in different cell fractions over time. Using LRP-1-deficient cells and sulfated proteoglycan mutant cells, we examined the contribution of LRP-1-dependent and LRP-1-independent pathways of TIMP-3 endocytosis. More importantly, our study has revealed that LRP-1 shed from the cell surface (sLRP-1) also binds to extracellular TIMP-3 and sequesters TIMP-3 in the medium and that TIMP-3 bound to sLRP-1 retained metalloproteinase inhibitory activity. This suggests that LRP-1 is a master regulator of extracellular levels of TIMP-3 and regulates ECM catabolism.

EXPERIMENTAL PROCEDURES

Materials — Heparin, de-N-sulfated heparin, chondroitin sulfate, hyaluronan and pronase were from Sigma-Aldrich (Dorset, UK); dermatan sulfate from Calbiochem (Nottingham, UK); PPS from Arthropharm (Sydney, Australia) and GM6001 from Elastin Products Co (Owensville, MOS, USA). Dulbecco's modified Eagle's medium (DMEM), DMEM without L-glutamine or phenol red, L-glutamine, penicillin/streptomycin, fetal calf serum (FCS), hygromycin B, amphotericin B and trypsin-EDTA from PAA Laboratories (Somerset, UK); DMEM without L-glutamine, cysteine, methionine or cystine from MP Biomedicals (Solon, OH, USA). The catalytic domain of human MMP-1 (24); recombinant His-tagged RAP (25), ADAMTS-4 lacking the C-terminal spacer domain (26) and non-radiolabelled FLAG-tagged TIMP-3 (27) were prepared as previously described.

Cell culture — HTB94 human chondrosarcoma and THP-1 human monocytic acute leukaemia cell lines were from American Culture Type Collection (Manassas, VA, USA). Human uterine cervical fibroblasts were kindly provided by Akira Ito (Tokyo University of Pharmacy and Life Sciences, Japan). CHO-K1

and CHO-745 (28) were generously provided by Jeffrey Esko (Department of Cellular and Molecular Medicine, University of California San Diego, La Jolla, USA). MEF-1 and PEA-13 (homozygous LRP-1-deficient) (29) cells were generated as described previously. Syndecan-4-deficient and wild-type MEF (30) were kindly provided by John R. Couchman (Department of Biomedical Sciences and Biotech Research and Innovation Centre, University of Copenhagen, Copenhagen, Denmark). All cells were maintained in DMEM with 10 % FCS, 100 U/ml penicillin and 100 U/ml streptomycin at 37 ºC in 5 % CO_2.

Porcine articular cartilage chondrocytes were isolated from metacarpophalangeal joints within 24 h of slaughter (31). Cartilage was incubated with 1 mg/ml *Clostridium histolyticum* collagenase (Sigma-Aldrich, Dorset, UK) in 10 ml DMEM with 10 % FCS for 4 h at 37 ºC. The digested material was passed through a cell strainer, washed and cells cultured in DMEM containing 10 % FCS, 100 U/ml penicillin, 100 U/ml streptomycin, 2 mg/ml amphotericin B and 10 mM HEPES at 37 ºC in 5 % CO_2.

Expression and purification of [^{35}S]TIMP-3 and [^{35}S]N-TIMP-3 — [^{35}S]TIMP-3 and [^{35}S]-labelled N-terminal domain of TIMP-3 ([^{35}S]N-TIMP-3) were prepared by metabolic labelling. HEK-293/EBNA cells transfected with a pCEP4-based expression vector for C-terminally FLAG-tagged TIMP-3 (27) were grown to confluence in a 150 cm^2 flask, washed once and starved for 2 h in serum-free DMEM without L-glutamine, cysteine, methionine or cysteine. Cells were then grown for a further 4 days in serum-free DMEM without L-glutamine, cysteine, methionine or cysteine, supplemented with 30 mM sodium chlorate and [^{35}S]Met/[^{35}S]Cys (500 µCi of Redivue Pro-Mix L-[^{35}S] *in vitro* Cell Labelling Mix (GE Healthcare, Buckinghamshire, UK). Conditioned media were collected after 4 days, centrifuged to remove cell debris and applied to a 2 ml anti-FLAG M2-agarose column (Sigma-Aldrich, Dorset, UK). The resin was washed extensively and bound protein eluted with 200 µg/ml FLAG peptide (Sigma-Aldrich, Dorset, UK). The purity of recombinant [^{35}S]TIMP-3 was confirmed by reducing SDS-PAGE and autoradiography. The active concentration of [^{35}S]TIMP-3 was determined by titration against a known concentration of the catalytic domain of MMP-1 (27).

Endocytosis of [^{35}S]TIMP-3 — Cells were plated at a density of $1x10^6$ cells/well and washed three times with serum-free DMEM. For some experiments, cells were then incubated for 1 h at 37 ºC with GM6001 (10 µM), heparin, de-N-sulfated heparin, PPS, chondroitin sulfate, dermatan sulfate, hyaluronan (all at 200 µg/ml) or RAP (500 nM) in DMEM with 0.1 % FCS before addition of [^{35}S]TIMP-3. As a control for agents diluted in DMSO, the equivalent volume of DMSO was added to separate wells. [^{35}S]TIMP-3 (1 nM) was added to cells in 2 ml of DMEM with 0.1% FCS. After 0-24 h incubation, the conditioned medium was removed and 5% (v/v) trichloroacetic acid (TCA) added (4 ºC, overnight). The TCA-soluble fraction (2 ml) was separated from the TCA-insoluble fraction by centrifugation (13000 rpm, 15 min, 4 ºC). The TCA-insoluble pellet was dissolved in 1 N NaOH (500 µl). The cell layer was washed three times with ice-cold PBS and solubilized in 1 N NaOH [1 ml, 1 h, room-temperature (RT)]. Each fraction was mixed with 3 ml of scintillant (Goldstar Multipurpose Liquid Scintillation Cocktail, Meridian, Surrey, UK) and radioactivity counted. TCA-soluble radioactivity present in the [^{35}S]TIMP-3 preparation prior to incubation with cells (5-15% of total radioactivity) was subtracted from the amount of TCA-soluble radioactivity at each time point. The amount of radioactivity in the different fractions was calculated as a percentage of the total amount of [^{35}S]TIMP-3 radioactivity added to the cells.

Endocytosis of surface-bound [^{35}S]TIMP-3 — [^{35}S]TIMP-3 (40 nM) in ice cold TBS was added to cells and incubated for 2 h at 4 ºC. To quantify cell surface binding of [^{35}S]TIMP-3, cells were washed twice in TBS, solubilized in 1 N NaOH (1 ml) and radioactivity quantified. In parallel experiments, endocytosis of cell surface-bound [^{35}S]TIMP-3 was quantified by washing cells in TBS and then incubating them for 2 h at 37 ºC in pre-warmed DMEM with 0.1% FCS. After 2 h, conditioned media were harvested and TCA-precipitated to quantify degraded [^{35}S]TIMP-3 (TCA-soluble counts in medium) and the amount of intact [^{35}S]TIMP-3 released from the cell surface (TCA-insoluble counts in medium). Cell layers were treated with 0.1 % pronase in serum-free DMEM on ice for 10 min, and then centrifuged (5000 rpm, 5 min, 4 ºC) to allow quantification of cell surface-bound [^{35}S]TIMP-3 (pronase-sensitive radioactivity)

and intracellular [^{35}S]TIMP-3 (pronase-resistant radioactivity, solubilized in 1 ml of 1 N NaOH).

Confocal microscopy analysis of TIMP-3 endocytosis — HTB94, MEF-1 and PEA-13 cells were cultured on 18 mm glass cover slips coated with gelatin (0.1 % w/v). Non-radiolabelled TIMP-3 (40 nM) was added to cells either alone or in combination with heparin (200 μg/ml) or RAP (500 nM) in phenol-red free DMEM with 0.1% FCS (2 h, 37 ºC). Cells were then fixed with 3% paraformaldehyde in PBS (10 min, RT) and blocked with 5% (v/v) goat serum, 3% (w/v) bovine serum albumin in PBS (1 h, RT). Cells were permeabilized with PBS containing 0.1% (v/v) Triton X-100 (15 min, RT) and incubated with anti-FLAG M2 antibody (Sigma-Aldrich, UK, F1804, 5 μg/ml, 1 h, RT). Alexa Fluor 488–conjugated goat anti-mouse IgG (Molecular Probes, Cambridge, UK) was used to visualize the antigen signal (5 μg/ml, 1 h, RT). Actin was stained with Alexa Fluor 568-conjugated phalloidin (Molecular Probes, Cambridge, UK). The signals were analyzed using a CCD camera-equipped microscope (Nikon TE-2000) with a 60× objective lens.

siRNA targeting of syndecan-1 expression — HTB94 cells (1-1.5x10^5 cells) were transiently transfected with 50 nM of two siRNAs targeting syndecan-1 (AM12432 and AM142557, Ambion) or scrambled (Ambion) using Lipofectamine 2000 for 3 h. After 24 and 48 h, expression of syndecan-1 was reduced by about 90% compared to the housekeeping gene *GAPDH*.

Isolation of sLRP-1 from plasma — sLRP-1 was isolated from fresh-frozen human plasma by a modification of previously published methods (32). Plasma was diluted 5-fold with equilibration buffer (50 mM citrate, pH 6.0, 75 mM NaCl, 0.02 % NaN_3) supplemented with proteinase inhibitor cocktail (P8340, Sigma-Aldrich, Dorset, UK) and applied to a MacroPrep S ion exchange resin (Bio-Rad, Hemel Hempstead, UK) equilibrated in the same buffer. The resin was extensively washed in equilibration buffer to remove unbound material and bound proteins then eluted in a gradient of 75 to 500 mM NaCl in equilibration buffer over 10 column volumes. Eluted fractions were analyzed by SDS-PAGE with silver staining and immunoblotting for LRP-1 using the 8G1 antibody (Abcam, Cambridge, UK).

ELISA detection of TIMP-3 binding to sLRP-1 — High-binding microtitre plates (Corning, NY, USA) were coated with 0.4 nmol sLRP-1 in 50 mM citrate, pH 6.0, 75 mM NaCl overnight. Wells were blocked using 3 % BSA-PBS (1 h, 37 ºC) and washed in PBS containing 0.1 % (v/v) Tween 20 (Sigma-Aldrich, Dorset, UK) after this and each subsequent step. Wells were then incubated with recombinant TIMP-3 in blocking solution (0.15 - 20 nM, 3 h, 37 ºC). Bound TIMP-3 was detected by incubation of wells with murine M2 anti-FLAG antibody (3 h, 37 ºC) and then with an anti-mouse secondary antibody coupled to horseradish peroxidase (1 h, 37 ºC) (DAKO, Ely, UK). Hydrolysis of tetramethylbenzidine substrate (KPL, Gaithersburg, MA, USA) was measured at 450 nm using a BioTek EL-808 absorbance microplate reader (BioTek, Winooski, VT, USA).

Inhibitory activity of TIMP-3 remnants — HTB94 cells were treated with or without TIMP-3 (1 nM) for 0, 24 or 48 h in serum-free, phenol red-free DMEM. Conditioned media were collected and centrifuged (13000 rpm, 15 min, 4 ºC) to remove cell debris. Recombinant ADAMTS-4 lacking the C-terminal spacer domain (1 nM) was incubated with dilutions of the media or with purified recombinant TIMP-3 in assay buffer (50 mM Tris-HCl, 150 mM NaCl, 10 mM $CaCl_2$, 0.05 % Brij, 0.02 % NaN_3) for 1 h at 37 ºC. Residual activity against the fluorescent peptide substrate carboxyfluorescein-Ala-Glu~Leu-Asn-Gly-Arg-Pro-Ile-Ser-Ile-Ala-Lys-N,N,N',N'-tetramethyl-6-carboxyrhodamine (FAM-AE~LQGRPISIAK-TAMRA, custom synthesized by Bachem, Switzerland) was determined (0.5 μM, excitation wavelength 485 nm, emission wavelength 538 nm with 495 nm cut-off) (27).

Co-immunoprecipitation of sLRP-1 with TIMP-3 — HTB94 cells were incubated in serum-free DMEM for 24 h, the conditioned media collected and centrifuged (13000 rpm, 15 min, 4 ºC) to remove cell debris. TIMP-3-FLAG (1 nM) was added to the conditioned medium (10 ml) and incubated overnight at RT with mixing. The solution was then applied to an anti-FLAG M2-agarose affinity resin (1 ml) equilibrated in TBS and the resin extensively washed with 10 volumes of TBS. Bound proteins were sequentially eluted with 50 mM Tris-HCl, pH 7.5, 10 mM $CaCl_2$, 0.2 % NaN_3 containing 1 M NaCl (2 x 0.5 ml) and then with the same buffer containing 150 mM NaCl and 200 μg/ml FLAG peptide (2 x 0.5 ml). Eluted samples were analysed by SDS-PAGE and immunoblotting using M2 anti-FLAG and 8G1

anti-LRP-1 antibodies. A band corresponding to the LRP-1 immunoreactive band was excised from the silver stained gel, digested with trypsin and analyzed by mass spectrometry.

RESULTS

TIMP-3 is endocytosed by HTB94 cells — Metabolically labelled [^{35}S]TIMP-3 was purified and added to HTB94 cells in culture. The radioactivity in the TCA-insoluble fraction (intact [^{35}S]TIMP-3) of the conditioned medium decreased over 24 h, while that in the TCA-soluble fraction (degraded [^{35}S]TIMP-3 fragments) increased (Fig. 1A). Radioactivity was also detected in the cell and ECM layer (the cell-associated fraction). Treatment of the cell-associated layer with pronase indicated that about half of the [^{35}S]TIMP-3 in this fraction was present within cells, with the remainder was present on the cell surface and in the ECM. These results indicate that [^{35}S]TIMP-3 bound to the cell surface, was endocytosed and degraded by the cells, and peptide fragments were released back into the medium. [^{35}S]N-TIMP-3 was also endocytosed by HTB94 cells with indistinguishable kinetics, suggesting that the N-terminal domain contains the minimal structure required for endocytosis.

We previously reported that TIMP-3 accumulated in the conditioned medium of HTB94 cells in the presence of RAP, an antagonist of ligand binding to the LRP family of endocytic receptors (18). In line with this finding, RAP (500 nM) reduced endocytosis of [^{35}S]TIMP-3 by HTB94 cells, i.e., an increase in TCA-insoluble radioactivity and a decrease in TCA-soluble and cell-associated radioactivity (Fig. 1A). These data suggest that a member of the RAP-sensitive LRP family is involved in TIMP-3 endocytosis. Heparin (200 μg/ml) and PPS (200 μg/ml) similarly reduced endocytosis of [^{35}S]TIMP-3 (Fig. 1A), but de-N-sulfated heparin, dermatan sulfate, chondroitin sulfate and hyaluronan (all at 200 μg/ml) had little effect. [^{35}S]TIMP-3 endocytosis was unaffected by addition of the broad-spectrum metalloproteinase inhibitor GM6001, indicating that TIMP-3 is internalized without forming complexes with metalloproteinases. [^{35}S]TIMP-3 endocytosis and degradation was observed in a variety of other cell types, including porcine articular chondrocytes, human uterine cervical fibroblasts and THP-1 human monocytic leukemia cells.

Cellular uptake of exogenously added TIMP-3 was also investigated by confocal microscopy. After incubation of HTB94 cells with recombinant TIMP-3-FLAG for 2 h at 37 ºC, punctate staining for TIMP-3-FLAG was detected inside of the cells (Fig. 1B). This staining was absent in cells incubated without TIMP-3, indicating the specificity of the staining. The amount of intracellular fluorescent signal was greatly reduced by incubation of cells with RAP (500 nM) and completely abolished by incubation with heparin (200 μg/ml).

TIMP-3 endocytosis is reduced in LRP-1-deficient cells — Since TIMP-3 endocytosis was inhibited by RAP, we postulated that a member of the LRP family of receptors was involved in TIMP-3 endocytosis. We thus compared [^{35}S]TIMP-3 endocytosis by LRP-1-deficient mouse embryonic fibroblasts (PEA-13 cells) and wild-type cells (MEF-1). As shown in Fig. 2A, [^{35}S]TIMP-3 was readily endocytosed by MEF-1 cells with similar kinetics to that observed in HTB94 cells, but [^{35}S]TIMP-3 endocytosis was impaired in PEA-13 cells, with the rate of endocytosis approximately half of that observed in HTB94 and MEF-1 cells (Fig. 2B). This indicates that LRP-1 mediates a major pathway for TIMP-3 endocytosis, but that an LRP-1-independent pathway also operates in these cells. Similar results were obtained using confocal microscopy, with endocytosed TIMP-3-FLAG visible in vesicles within MEF-1 cells, but lower intracellular staining observed in PEA-13 cells (Fig. 2C). RAP inhibited [^{35}S]TIMP-3 endocytosis and degradation by MEF-1 cells to the level observed in PEA-13 cells (Fig. 2A and B). In contrast, RAP had no effect on [^{35}S]TIMP-3 endocytosis by PEA-13 cells. Based on these observation we propose that LRP-1 is the only member within the LRP family that mediates [^{35}S]TIMP-3 endocytosis in these cells.

On the other hand, heparin strongly inhibited [^{35}S]TIMP-3 endocytosis by both MEF-1 and PEA-13 cells (Fig. 2A and B). In this case, only a minimal decrease in TCA-insoluble radioactivity and little increase in TCA-soluble radioactivity in the medium were observed, and [^{35}S]TIMP-3 was barely detectable in the cell-associated layer.

We further investigated the role of LRP-1 in [^{35}S]TIMP-3 surface binding by adding 1 nM [^{35}S]TIMP-3 to cells at 4 ºC. Comparable binding of [^{35}S]TIMP-3 to MEF-1 and PEA-13 cells was observed (Fig. 2D). Upon warming

the cells to 37 ºC, higher radioactivity was observed in MEF-1 cells, confirming their greater ability to endocytose [^{35}S]TIMP-3. Interestingly, both MEF-1 and PEA-13 cells released about a third of the surface-bound radioactivity back into the medium, indicating there was a notable dissociation of [^{35}S]TIMP-3 from the cell surface under these experimental conditions. The release of TCA-soluble radioactivity by MEF-1 and PEA-13 cells was measured following cell surface binding of [^{35}S]TIMP-3 and warming of the cells to 37 ºC. MEF-1 cells released approximately twice as much TCA-soluble radioactivity as PEA-13 cells Fig 2E), confirming the existence of LRP-1-dependent and -independent endocytic pathways for TIMP-3.

Cell surface sulfated GAGs are not involved in TIMP-3 endocytosis — Since highly sulfated polysaccharides (e.g. heparin and PPS) blocked TIMP-3 endocytosis (18), we postulated that HSPGs or CSPGs may be involved in TIMP-3 endocytosis. To test this possibility we compared [^{35}S]TIMP-3 endocytosis by wild-type (CHO-K1) and mutant CHO-745 cells which lack HS and CS chains due to a mutation in xylosyltransferase (28). We observed no significant differences in the rate of [^{35}S]TIMP-3 endocytosis by CHO-K1 and CHO-745 cells Fig. 3A), indicating that neither HSPG nor CSPG are required for the internalization of TIMP-3. [^{35}S]TIMP-3 endocytosis by both CHO-K1 and CHO-745 cells was partially inhibited by RAP (500 nM) (Data not shown). Heparin (200 μg/ml) inhibited [^{35}S]TIMP-3 endocytosis by CHO-745 cells (Figure 3B) indicating that the blocking effect of heparin is independent from the presence of HSPGs or CSPGS on the cell surface. Similarly, heparin blocked [^{35}S]TIMP-3 endocytosis by CHO-K1 cells. Interestingly, both CHO-745 and CHO-K1 exhibited a higher amount of cell-associated radioactivity than HTB94 or MEF cells. [^{35}S]TIMP-3 levels in this fraction were not affected by RAP, but were strongly inhibited by heparin.

We further investigated possible involvement of the syndecan family in TIMP-3 endocytosis, since some protein ligands have been shown to bind to the core protein of these proteoglycans (33). Comparable endocytosis of [^{35}S]TIMP-3 was observed in syndecan-4-deficient and wild-type MEF, and siRNA targeting of syndecan-1 (leading to a 90% reduction in expression), had no effect on [^{35}S]TIMP-3 endocytosis.

Since heparin inhibits TIMP-3 endocytosis by cells lacking HSPG and CSPG, we tested whether heparin can directly interfere the binding of TIMP-3 to LRP-1. We isolated sLRP-1 from human plasma and measured binding of TIMP-3 and TIMP-3-heparin complexes to immobilized sLRP-1 by ELISA. TIMP-3 bound readily to LRP-1, but upon pre-incubation with 100 μg/ml heparin, binding of TIMP-3 to LRP-1 was completely abolished Fig. 3C).

sLRP-1 inhibits TIMP-3 endocytosis — During the course of this study we noticed that for all the cell lines we tested, TIMP-3 endocytosis was initially fast, but decreased over time and little endocytosis was observed after 10 h. [^{35}S]TIMP-3 remaining in the medium at 24 h ([^{35}S]TIMP-3 remnants) appeared intact by reducing SDS-PAGE and autoradiography, with no fragmentation evident. The ability of TIMP-3 remnants to inhibit metalloproteinase activity was assessed by adding 1 nM TIMP-3 to HTB94 cells for 0, 24 or 48 h, after which time TIMP-3 remnants in the media were harvested and titrated against 1 nM ADAMTS-4 *in vitro*. TIMP-3 collected after 0 h incubation on HTB94 cells completely inhibited 1 nM ADAMTS-4 (Fig. 4A). TIMP-3 harvested after 24 and 48 h incubation on HTB94 cells inhibited ADAMTS-4 activity by 60%, indicating that while the concentration of TIMP-3 in the medium had been reduced by endocytosis, the TIMP-3 remnants remaining in the medium retained their full inhibitory activity against metalloproteinases. These data indicate that TIMP-3 remnants had not undergone any substantial structural modification or inactivation.

We therefore considered whether the reduced rate of [^{35}S]TIMP-3 endocytosis was due to a change in the endocytic capacity of the cells. Although TIMP-3 has been shown to induce apoptosis in a variety of cell types (34), we found that incubation of HTB94 cells with 1 nM [^{35}S]TIMP-3 for 24 h had no effect on cell viability as measured by the 3-(4,5-dimethylthiazol-2-yl)-2,5-diphenyltetrazolium bromide (MTT) assay. Furthermore, pre-treatment of HTB94 cells with non-radiolabelled TIMP-3 for 24 h did not alter the rate of endocytosis of subsequently added [^{35}S]TIMP-3.

We then investigated the possibility that TIMP-3 remnants in the medium were resistant

to being taken up by the cells. To test this, [^{35}S]TIMP-3 remnants were added to naïve cells that had not previously been exposed to TIMP-3. Remnants collected from HTB94 cells after 24 h of incubation were largely resistant to endocytosis by naïve HTB94 cells, indicating that the [^{35}S]TIMP-3 remnants had become refractory to endocytosis (Fig. 4B). This phenomenon was further studied by incubating PEA-13 cells, which lack LRP-1, with [^{35}S]TIMP-3 for 24 h, and transferring the conditioned medium containing [^{35}S]TIMP-3 remnants to naïve MEF-1 cells. [^{35}S]TIMP-3 remnants from PEA-13 cells were readily endocytosed by naïve MEF-1 (Fig. 4C), whereas [^{35}S]TIMP-3 remnants from MEF-1 cells were resistant to endocytosis by naïve MEF-1 cells (Fig. 4D). Based on these results, we postulated that TIMP-3 became resistant to endocytosis as a result of association with sLRP-1 shed from cells into the conditioned medium during the culturing period.

sLRP-1 accumulated over time in the conditioned medium harvested from HTB94 cells grown in serum-free medium in the absence of TIMP-3 (Fig. 4E). Binding of TIMP-3 to sLRP-1 was investigated first by incubating TIMP-3-FLAG (1 nM) *in vitro* with the conditioned medium from HTB94 cells. After overnight incubation at ambient temperature, the mixture was applied to an M2 anti-FLAG resin, and bound proteins were eluted with FLAG peptide. Analysis of the eluted samples with the 8G1 anti-LRP-1 antibody indicated that LRP-1 was co-eluted with TIMP-3-FLAG by FLAG-peptide (Fig. 4F). The identity of the eluted LRP-1 band was further confirmed by mass spectrometry, confirming that TIMP-3 can interact with sLRP-1 shed into the conditioned medium of cells.

We also found that addition of TIMP-3 to HTB94 cells increases the release of sLRP-1 fragments of 500, 215, 160 and 110 kDa into the conditioned medium in a concentration-dependent manner, suggesting that the inhibitor can induce shedding and fragmentation of LRP-1 (Fig. 4G). When TIMP-3-FLAG (1 nM) was incubated with HTB94 cells for 24 h and conditioned medium was applied to an M2 anti-FLAG resin column, bound TIMP-3-FLAG co-eluted with the 500 kDa sLRP-1 and with LRP-1 fragments of 215, 160 and 110 kDa (Fig. 4H). This indicates that these fragments generated upon addition of TIMP-3 to the cells are capable of binding to the inhibitor.

DISCUSSION

Our study has revealed a new mechanism for regulating levels of TIMP-3 in the extracellular space. We previously reported that levels of this physiologically and pathologically important inhibitor can be post-translationally regulated by endocytosis (18). TIMP-3 accumulates in the medium of HTB94 chondrosarcoma cells and porcine articular chondrocytes treated with receptor-associated protein (RAP), an antagonist of ligand binding to the LRP family of endocytic receptors (18). Using radiolabelled TIMP-3 we investigated the kinetics of TIMP-3 endocytosis and degradation by LRP-1-deficient PEA-13 mouse embryonic fibroblasts and their wild-type counterpart. TIMP-3 endocytosis was substantially reduced in LRP-1-deficient PEA-13 cells compared to wild-type cells, indicating that LRP-1 is an important component of the TIMP-3 endocytic machinery. RAP, which inhibits ligand binding to all LRPs, had no effect on the residual endocytosis of TIMP-3 by PEA-13 cells, indicating that LRP-1 is the only member of the LRP family that mediates TIMP-3 endocytosis in mouse embryonic fibroblasts.

We compared the endocytosis of TIMP-3 by several cell types, including chondrosarcoma cells, porcine articular chondrocytes, fibroblasts and monocyte-like THP-1 cells. All cell types showed similar kinetics for TIMP-3 endocytosis. The rate of TIMP-3 endocytosis was not constant over 24 h. After addition of [^{35}S]TIMP-3 to cells, endocytosis was initially rapid, but then slowed, so that only minimal endocytosis was observed after 10 h. We demonstrated that this reduction in endocytosis is due to interaction of TIMP-3 with a soluble form of LRP-1 shed from the cell surface into the medium. Different LRP-1 'sheddases' have been described, including ADAM10, ADAM12, ADAM17, MT1-MMP and β-secretase (23,35-38). Although the specific site(s) at which these enzymes cleave LRP-1 have not been characterized, shedding is known to involve cleavage of the β-chain of LRP-1, releasing a fragment of the β-chain in complex with the entire ligand-binding α-chain from the cell membrane (39). Inflammation is a key stimulus for LRP-1 shedding. For example, interferon γ and LPS stimulate LRP-1 shedding by ADAM17 (35). Increased levels of sLRP-1 are detectable in the plasma of patients with rheumatoid arthritis, systemic lupus erythematous (35) and

liver disease (32). sLRP-1 and lower molecular weight fragments of LRP-1 are found in brain and in cerebral spinal fluids, and are increased in older people (23). Cholesterol depletion has also been found to stimulate LRP-1 shedding by MT1-MMP and ADAM12 (36). We observed LRP-1 shedding in the absence of any pro-inflammatory stimuli, and addition of IL-1 had no effect on the rate of TIMP-3 endocytosis by primary chondrocytes (S. Scilabra and H. Nagase, unpublished observations). Since a number of the proposed LRP-1 'sheddases' are metalloproteinases, production of sLRP-1 should be inhibited by metalloproteinase inhibitors such as TIMP-3 and GM6001. However, we found that TIMP-3 could induce shedding of LRP-1 and generation of LRP-1 fragments. A previous report showed that N-TIMP-3 inhibited MT1-MMP- and ADAM12-mediated shedding of LRP-1 (36). We found that, unlike TIMP-3, N-TIMP-3 did not induce shedding and fragmentation of LRP-1 (S. Scilabra and H. Nagase, unpublished observations), therefore we hypothesize that the C-terminal domain of TIMP-3 can play a crucial role in this process. GM6001 has also been shown to inhibit LRP-1 shedding from macrophages and lung fibroblasts (21,35), but we found that GM6001 had no effect on the rate of [^{35}S]TIMP-3 endocytosis by HTB94 cells. This suggests that a GM6001-insensitive sheddase may mediate LRP-1 shedding in HTB94 cells. The stimulus and sheddases responsible for LRP-1 constitutive shedding and TIMP-3 induced shedding in HTB94 cells and chondrocytes are currently under investigation in our laboratory.

Shedding of LRP-1 has numerous consequences. Firstly, it can reduce endocytosis of LRP-1 ligands in a loss-of-function manner by reducing the number of endocytic receptors on the cell surface (21,36,38). Secondly, sLRP-1 can bind to and inhibit endocytosis of its ligands, as we found for TIMP-3, and as has been reported for tPA (32). By antagonizing LRP-1-mediate endocytosis, sLRP-1 can increase the half-life of TIMP-3 in the extracellular space. More importantly, we found that the TIMP-3-sLRP-1 complex is still able to inhibit metalloproteinases. We found that the ratio between cell surface LRP-1 and sLRP-1 is an important factor that regulates the bioavailability of TIMP-3 in the extracellular space, and hence controls ECM proteolysis and proteolysis of cell surface molecules.

In addition to the LRP-1-mediated pathway, we observed LRP-1-independent endocytosis of TIMP-3 in PEA-13 cells and RAP-treated HTB94, MEFs and CHO cells. Although this is a slower process compared with the LRP-1-mediated endocytosis, it is likely to be receptor-mediated. Members belonging to the macrophage mannose receptor protein family may be possible candidates as they have been shown to internalize some LRP-1 ligands and play a crucial role in ECM turnover. For instance, urokinase plasminogen activator receptor-associated protein/endocytic recycling protein Endo180 is expressed in chondrocytes and fibroblasts and is involved in collagen internalization (40,41). TIMP-1 and TIMP-2 are also endocytosed by LRP-1 (42,43). While TIMP-1 is internalized only in complex with MMP-9, with the binding determinants thought to reside on the MMP-9 (42). TIMP-2 can be endocytosed by LRP-1 both as a free inhibitor and in complex with MMP-2 or proMMP-2 (43). Interestingly, binding of TIMP-2 to HT1080 cells was insensitive to RAP, suggesting that TIMP-2 initially binds to a cell surface receptor other than LRP-1 prior to endocytosis (43). Furthermore, endocytosis and degradation of TIMP-2 was only partially inhibited by RAP, indicating that an LRP-1-independent endocytic pathway also occurs (43). These studies thus suggest that both TIMP-2 and TIMP-3 can be endocytosed by LRP-1-dependent and LRP-1-independent pathways. It would be interesting to determine whether TIMP-2 and TIMP-3 share the same the mechanism of LRP-1-independent endocytosis.

Endocytosis of TIMP-3 in all tested cell types was almost completely inhibited by heparin. This suggested that an HSPG or CSPG might participate in TIMP-3 endocytosis, either as a direct endocytic receptor or as a co-receptor of LRP-1. HSPG have been demonstrated to mediate endocytosis of ligands including lipoproteins (44). Alternatively, HSPG might act as co-receptors of LRP-1-mediated endocytosis as proposed for thrombospondin 1 (45), tissue factor pathway inhibitor (46), amyloid-β (47) and factor VIII (48). However, we found that TIMP-3 endocytosis was not affected in xylosyltransferase-deficient CHO-745 cells, indicating that sulfated cell surface proteoglycans are not required for TIMP-3 endocytosis. In line with this finding, TIMP-3 endocytosis was also unimpaired in syndecan-4-null and syndecan-1-silenced cells. We therefore

conclude that cell surface HSPG or CSPG do not mediate the LRP-1-independent pathway of TIMP-3 endocytosis.

The unimpaired endocytosis of TIMP-3 in CHO-745 cells nullified our hypothesis that heparin inhibits TIMP-3 endocytosis by blocking interaction with a sulfated cell surface proteoglycan component of the endocytic pathway. Interestingly, heparin has been shown to directly inhibit interaction of other ligands, including factor IXa (49), apolipoprotein A-V (50), C4b-binding protein (51) and PAI-1 (52), to LRP-1. In the case of PAI-1, the heparin-binding and LRP-1-binding regions have been found to overlap (53,54). Binding of proteins to heparin is commonly mediated by clusters of positively charged residues (55). Similarly, binding of protein ligands to LRP-1 and related LDL receptors is often mediated by positive residues, as has been demonstrated for RAP (56,57) and α_2M (58). In the case of RAP, crystallography and mutagenesis studies have confirmed that K256 and K270 mediate binding to acidic pockets in the ligand binding motifs of the receptor (56,57). Inhibition of TIMP-3 binding to sLRP-1 by heparin suggests that the heparin-binding and LRP-1-binding sites of TIMP-3 may also overlap. The three-dimensional structure of full-length TIMP-3 is currently unavailable, but the protein is predicted to contain an extended patch of basic residues, located on the opposite face of the protein to the inhibitory ridge that interacts with metalloproteinase. This may explain why TIMP-3-sLRP-1 complexes retain metalloproteinases inhibition activity.

The phenotypes of the *Timp3*$^{-/-}$ mouse reveal the central role of TIMP-3 in regulating activity of MMPs, ADAMs and ADAMTSs. Our study has shown that LRP-1 plays an important role in controlling the extracellular levels of TIMP-3. It is well established that TIMP-3 binds to ECM (2,3), but we have shown here that secreted TIMP-3 can be readily internalized via LRP-1, and this process competes with TIMP-3 binding to the ECM. On the other hand, shed sLRP-1 sequesters TIMP-3 from the above two reactions and increases its availability to extracellular MMPs, ADAMs and ADAMTs. It is notable that shedding of LRP-1 is increased under inflammatory conditions. We therefore propose that LPR-1 is a master regulator of extracellular trafficking of TIMP-3 and the ratio of cell surface LPR-1 and sLRP-1 dictates TIMP-3 availability.

Acknoledgements
We thank Prof. John Couchman of Copenhagen University for his provision of syndecan-4-deficient cells, Prof. Akira Ito of Tokyo University for human uterine cervical fibroblasts, and Prof. Jeffrey Esko of University of California San Diego for CHO-K1 and -CHO-745 cells.

References

1. Brew, K., and Nagase, H. (2010) *Biochim. Biophys. Acta* **1803**, 55-71
2. Staskus, P. W., Masiarz, F. R., Pallanck, L. J., and Hawkes, S. P. (1991) *J. Biol. Chem.* **266**, 449-454
3. Yu, W. H., Yu, S., Meng, Q., Brew, K., and Woessner, J. F. (2000) *J Biol Chem.* **275**, 31226-31232
4. Leco, K. J., Waterhouse, P., Sanchez, O. H., Gowing, K. L., Poole, A. R., Wakeham, A., Mak, T. W., and Khokha, R. (2001) *J. Clin. Invest.* **108**, 817-829
5. Fedak, P. W., Smookler, D. S., Kassiri, Z., Ohno, N., Leco, K. J., Verma, S., Mickle, D. A., Watson, K. L., Hojilla, C. V., Cruz, W., Weisel, R. D., Li, R. K., and Khokha, R. (2004) *Circulation* **110**, 2401-2409
6. Fata, J. E., Leco, K. J., Voura, E. B., Yu, H. Y., Waterhouse, P., Murphy, G., Moorehead, R. A., and Khokha, R. (2001) *J. Clin. Invest.* **108**, 831-841
7. Sahebjam, S., Khokha, R., and Mort, J. S. (2007) *Arthritis Rheum.* **56**, 905-909
8. Mohammed, F. F., Smookler, D. S., Taylor, S. E., Fingleton, B., Kassiri, Z., Sanchez, O. H., English, J. L., Matrisian, L. M., Au, B., Yeh, W. C., and Khokha, R. (2004) *Nat Genet* **36**, 969-977

9. Martin, E. L., Moyer, B. Z., Pape, M. C., Starcher, B., Leco, K. J., and Veldhuizen, R. A. (2003) *Am J Physiol Lung Cell Mol Physiol* **285**, L1222-1232
10. Cardellini, M., Menghini, R., Martelli, E., Casagrande, V., Marino, A., Rizza, S., Porzio, O., Mauriello, A., Solini, A., Ippoliti, A., Lauro, R., Folli, F., and Federici, M. (2009) *Diabetes* **58**, 2396-2401
11. Su, S., DiBattista, J. A., Sun, Y., Li, W. Q., and Zafarullah, M. (1998) *J Cell Biochem* **70**, 517-527
12. Li, W. Q., and Zafarullah, M. (1998) *J. Immunol.* **161**, 5000-5007
13. Darnton, S. J., Hardie, L. J., Muc, R. S., Wild, C. P., and Casson, A. G. (2005) *Int J Cancer* **115**, 351-358
14. Gabriely, G., Wurdinger, T., Kesari, S., Esau, C. C., Burchard, J., Linsley, P. S., and Krichevsky, A. M. (2008) *Mol. Cell. Biol.* **28**, 5369-5380
15. Garofalo, M., Di Leva, G., Romano, G., Nuovo, G., Suh, S. S., Ngankeu, A., Taccioli, C., Pichiorri, F., Alder, H., Secchiero, P., Gasparini, P., Gonelli, A., Costinean, S., Acunzo, M., Condorelli, G., and Croce, C. M. (2009) *Cancer Cell* **16**, 498-509
16. Wang, B., Hsu, S. H., Majumder, S., Kutay, H., Huang, W., Jacob, S. T., and Ghoshal, K. (2010) *Oncogene* **29**, 1787-1797
17. Limana, F., Esposito, G., D'Arcangelo, D., Di Carlo, A., Romani, S., Melillo, G., Mangoni, A., Bertolami, C., Pompilio, G., Germani, A., and Capogrossi, M. C. (2011) *PLoS One* **6**, e19845
18. Troeberg, L., Fushimi, K., Khokha, R., Emonard, H., Ghosh, P., and Nagase, H. (2008) *FASEB J.* **22**, 3515-3524
19. Strickland, D. K., Gonias, S. L., and Argraves, W. S. (2002) *Trends Endocrinol. Metab.* **13**, 66-74
20. Lillis, A. P., Mikhailenko, I., and Strickland, D. K. (2005) *J Thromb Haemost* **3**, 1884-1893
21. Wygrecka, M., Wilhelm, J., Jablonska, E., Zakrzewicz, D., Preissner, K. T., Seeger, W., Guenther, A., and Markart, P. (2011) *Am J Respir Crit Care Med* **184**, 438-448
22. Selvais, C., Gaide Chevronnay, H. P., Lemoine, P., Dedieu, S., Henriet, P., Courtoy, P. J., Marbaix, E., and Emonard, H. (2009) *Endocrinology* **150**, 3792-3799
23. Liu, Q., Zhang, J., Tran, H., Verbeek, M. M., Reiss, K., Estus, S., and Bu, G. (2009) *Mol Neurodegener* **4**, 17
24. Chung, L., Shimokawa, K., Dinakarpandian, D., Grams, F., Fields, G. B., and Nagase, H. (2000) *J. Biol.Chem.* **275**, 29610-29617
25. Nielsen, M. S., Nykjaer, A., Warshawsky, I., Schwartz, A. L., and Gliemann, J. (1995) *J. Biol. Chem.* **270**, 23713-23719
26. Kashiwagi, M., Enghild, J. J., Gendron, C., Hughes, C., Caterson, B., Itoh, Y., and Nagase, H. (2004) *J. Biol. Chem.* **279**, 10109-10119
27. Troeberg, L., Fushimi, K., Scilabra, S. D., Nakamura, H., Dive, V., Thogersen, I. B., Enghild, J. J., and Nagase, H. (2009) *Matrix Biol.* **28**, 463-469
28. Esko, J. D., Stewart, T. E., and Taylor, W. H. (1985) *Proc. Natl. Acad. Sci. U. S. A.* **82**, 3197-3201
29. Willnow, T. E., and Herz, J. (1994) *J. Cell Sci.* **107** 719-726
30. Ishiguro, K., Kadomatsu, K., Kojima, T., Muramatsu, H., Tsuzuki, S., Nakamura, E., Kusugami, K., Saito, H., and Muramatsu, T. (2000) *J. Biol. Chem.* **275**, 5249-5252
31. Gendron, C., Kashiwagi, M., Hughes, C., Caterson, B., and Nagase, H. (2003) *FEBS Lett.* **555**, 431-436
32. Quinn, K. A., Grimsley, P. G., Dai, Y. P., Tapner, M., Chesterman, C. N., and Owensby, D. A. (1997) *J. Biol. Chem.* **272**, 23946-23951
33. Echtermeyer, F., Baciu, P. C., Saoncella, S., Ge, Y., and Goetinck, P. F. (1999) *J Cell Sci* **112 (Pt 20)**, 3433-3441
34. Ahonen, M., Poukkula, M., Baker, A. H., Kashiwagi, M., Nagase, H., Eriksson, J. E., and Kahari, V. M. (2003) *Oncogene* **22**, 2121-2134
35. Gorovoy, M., Gaultier, A., Campana, W. M., Firestein, G. S., and Gonias, S. L. (2010) *J. Leukocyte Biol.* **88**, 769-778

36. Selvais, C., D'Auria, L., Tyteca, D., Perrot, G., Lemoine, P., Troeberg, L., Dedieu, S., Noel, A., Nagase, H., Henriet, P., Courtoy, P. J., Marbaix, E., and Emonard, H. (2011) *FASEB J.* **25**, 2770-2781
37. von Arnim, C. A., Kinoshita, A., Peltan, I. D., Tangredi, M. M., Herl, L., Lee, B. M., Spoelgen, R., Hshieh, T. T., Ranganathan, S., Battey, F. D., Liu, C. X., Bacskai, B. J., Sever, S., Irizarry, M. C., Strickland, D. K., and Hyman, B. T. (2005) *J Biol Chem.* **280**, 17777-17785
38. Rozanov, D. V., Hahn-Dantona, E., Strickland, D. K., and Strongin, A. Y. (2004) *J. Biol. Chem.* **279**, 4260-4268
39. Quinn, K. A., Pye, V. J., Dai, Y. P., Chesterman, C. N., and Owensby, D. A. (1999) *Exp. Cell Res.* **251**, 433-441
40. Engelholm, L. H., List, K., Netzel-Arnett, S., Cukierman, E., Mitola, D. J., Aaronson, H., Kjoller, L., Larsen, J. K., Yamada, K. M., Strickland, D. K., Holmbeck, K., Dano, K., Birkedal-Hansen, H., Behrendt, N., and Bugge, T. H. (2003) *J Cell Biol* **160**, 1009-1015
41. Kjoller, L., Engelholm, L. H., Hoyer-Hansen, M., Dano, K., Bugge, T. H., and Behrendt, N. (2004) *Exp Cell Res* **293**, 106-116
42. Hahn-Dantona, E., Ruiz, J. F., Bornstein, P., and Strickland, D. K. (2001) *J. Biol. Chem.* **276**, 15498-15503
43. Emonard, H., Bellon, G., Troeberg, L., Berton, A., Robinet, A., Henriet, P., Marbaix, E., Kirkegaard, K., Patthy, L., Eeckhout, Y., Nagase, H., Hornebeck, W., and Courtoy, P. J. (2004) *J. Biol. Chem.* **279**, 54944-54951
44. Stanford, K. I., Bishop, J. R., Foley, E. M., Gonzales, J. C., Niesman, I. R., Witztum, J. L., and Esko, J. D. (2009) *J. Clin. Invest.* **119**, 3236-3245
45. Wang, S., Herndon, M. E., Ranganathan, S., Godyna, S., Lawler, J., Argraves, W. S., and Liau, G. (2004) *J. Cell. Biochem.* **91**, 766-776
46. Schwartz, A. L., and Jr, B. G. J. (1997) *Trends Cardiovasc Med* **7**, 234-239
47. Kanekiyo, T., Zhang, J., Liu, Q., Liu, C. C., Zhang, L., and Bu, G. (2011) *J. Neurosci.* **31**, 1644-1651
48. Sarafanov, A. G., Ananyeva, N. M., Shima, M., and Saenko, E. L. (2001) *J. Biol. Chem.* **276**, 11970-11979
49. Neels, J. G., van Den Berg, B. M., Mertens, K., ter Maat, H., Pannekoek, H., van Zonneveld, A. J., and Lenting, P. J. (2000) *Blood* **96**, 3459-3465
50. Nilsson, S. K., Lookene, A., Beckstead, J. A., Gliemann, J., Ryan, R. O., and Olivecrona, G. (2007) *Biochemistry* **46**, 3896-3904
51. Westein, E., Denis, C. V., Bouma, B. N., and Lenting, P. J. (2002) *J Biol Chem* **277**, 2511-2516
52. Nykjaer, A., Petersen, C. M., Møller, B., Jensen, P. H., Moestrup, S. K., Holtet, T. L., Etzerodt, M., Thøgersen, H. C., Munch, M., Andreasen, P. A., and Gliemann, J. (1992) *J Biol Chem* **267**, 14543-14546
53. Horn, I. R., van Den Berg, B. M., Moestrup, S. K., Pannekoek, H., and van Zonneveld, A. J. (1998) *Thromb Haemost* **80**, 822-828
54. Stefansson, S., Muhammad, S., Cheng, X. F., Battey, F. D., Strickland, D. K., and Lawrence, D. A. (1998) *J Biol Chem* **273**, 6358-6366
55. Gandhi, N. S., and Mancera, R. L. (2008) *Chem Biol Drug Des.* **72**, 455-482
56. Fisher, C., Beglova, N., and Blacklow, S. C. (2006) *Molecular Cell* **22**, 277-283
57. van den Bigglelaar, M., Sellink, E., Klein Gebbinck, J. W. T. M., Mertens, K., and Meijer, A. B. (2011) *Int J Biochem Cell Biol* **43**, 431-440
58. Arandjelovic, S., Hall, B. D., and Gonias, S. L. (2005) *Arch Biochem Biophys* **438**, 29-35

FOOTNOTES

Linda Troeberg is the recipient of an Arthritis Research UK Career Development Fellowship (grant 19466). Hideaki Nagase is supported by Arthritis Research UK Core Grant to the Kennedy Institute of Rheumatology, and grant AR40994 from the National Institute of Arthritis and Musculoskeletal and Skin Diseases (NIAMS). The content is solely the responsibility of the authors and does not necessarily represent the official views of NIAMS or NIH.

Abbreviations used are: ADAM, a disintegrin and metalloproteinase; ADAMTS, adamalysin with thrombospondin motifs; CSPG, chondroitin sulfate proteoglycan; ECM, extracellular matrix; GAG, glycosaminoglycan; HSPG, heparan sulfate proteoglycan; LDL, low-density lipoprotein; LRP-1, low-density lipoprotein receptor-related protein-1; MMP, matrix metalloproteinase; N-TIMP, N-terminal domain of TIMP; PPS, pentosan polysulfate; RAP, receptor associated protein; sLRP-1, soluble LRP-1; TCA, trichloroacetic acid; TIMP, tissue inhibitor of metalloproteinase.

FIGURE LEGENDS

Figure 1: TIMP-3 is endocytosed by HTB94 chondrosarcoma cells. *A*, [^{35}S]TIMP-3 (1 nM) was added to HTB94 chondrosarcoma cells in the absence or presence of RAP (500 nM) or heparin (200 μg/ml), and radioactivity in different cell fractions monitored over time *(n=3)*. TIMP-3, black symbols; TIMP-3 plus 500 nM RAP, open symbols; TIMP-3 plus heparin, grey symbols. *B*, Confocal microscopy analysis of TIMP-3 endocytosis by HTB94 cells. Cells were incubated for 2 h at 37 °C with TIMP-3-FLAG (40 nM), either alone or with heparin (200 μg/ml) or RAP (500 nM). Control cells were incubated without TIMP-3-FLAG. Cells were washed and permeabilized, and endocytosed TIMP-3-FLAG vizualised using an M2 anti-FLAG antibody and an Alexa 488-labelled secondary antibody (green channel). The cytoskeleton was visualized using Alexa 568-labelled phalloidin (red channel). Images were gathered using a 60× objective lens. Scale bar: 41 μm

Figure 2: LRP-1 contributes to [^{35}S]TIMP-3 endocytosis. *A-B*, [^{35}S]TIMP-3 (1 nM) was added to MEF-1 (*A*) or PEA-13 (*B*) cells for 0-24 h and radioactivity in the cell-associated fraction (triangles), as well as in the TCA-insoluble (squares) and TCA-soluble (circles) fractions of the conditioned media were quantified by scintillation counting *(n =3)*. TIMP-3, black symbols; TIMP-3 plus 500 nM RAP, open symbols; TIMP-3 plus 200 μg/ml heparin, grey symbols. *C*, Confocal microscopy analysis of TIMP-3 endocytosis by MEF-1 and PEA-13 cells. Cells were incubated for 2 h at 37 °C with TIMP-3-FLAG (40 nM), washed and permeabilized, and endocytosed TIMP-3-FLAG vizualised using an M2 anti-FLAG antibody and an Alexa 488-labelled secondary antibody (green channel). The cytoskeleton was visualized using Alexa 568-labelled phalloidin (red channel). Images were gathered using a 60× objective lens. Scale bar: 41 μm. *D*, [^{35}S]TIMP-3 (10 nM) was added to MEF-1 (closed bars) or PEA-13 (open bars) cells at 4 °C for 2 h to allow surface binding. Cells were warmed to 37 °C for 2 h, and surface bound (pronase-sensitive), intracellular (pronase-resistant), degraded (TCA-soluble medium) and intact-released (TCA-insoluble medium) radioactivity was quantified, (this result is representative of two separate experiments). *E*, TCA-soluble radioactivity released by MEF-1 (solid squares) and PEA-13 (open squares) cells after surface binding of [^{35}S]TIMP-3, (this result is representative of two separate experiments).

Figure 3: Cell surface HSPGs and CSPGs are not required for TIMP-3 endocytosis. *A-B,* [^{35}S]TIMP-3 (1 nM) was added to CHO-K1 (*A, B,* solid lines and symbols), CHO-745 (A, dashed lines and open symbols) or heparin treated CHO-745 (*B,* dashed lines and open symbols) cells for 0-24 h and radioactivity in the cell-associated fraction (triangles), as well as in the TCA-insoluble (squares) and TCA-soluble (circles) fractions of the conditioned media were quantified by scintillation counting (*n* =3). *C*, Shed LRP purified from human plasma was coated onto microtitre plates and binding of TIMP-3 (0.1 – 40 nM) in the absence (■) and presence (□) of 100 μg/ml heparin was measured using an M2 anti-FLAG antibody and a horseradish peroxidase-conjugate secondary antibody. Control wells (○) were not coated with sLRP.

Figure 4: sLRP-1 interacts with TIMP-3 and inhibits its endocytosis. *A*, ADAMTS-4 (1 nM) was incubated (1 h, 37 °C) with dilutions of recombinant TIMP-3 in TNC buffer (from 1 nM, □) or with dilutions of TIMP-3 (1 nM) incubated on HTB94 cells for 0 h (■), 24 h (▲) or 48 h (●). As a control, ADAMTS-4 was incubated with conditioned medium from HTB94 cells incubated in serum-free medium without TIMP-3 for 24 h (○) or 48 h (△). Residual activity against FAM-AE~LQGRPISIAK-TAMRA was determined. *B*, [^{35}S]TIMP-3 (1 nM) was added to HTB94 cells for 24 h, after which conditioned media were harvested and transferred to naïve HTB94 cells for a further 0-24 h.

Radioactivity in the cell-associated fraction (▲), as well as in the TCA-insoluble (■) and TCA-soluble (●) fractions of the conditioned media were quantified by counting radioactivity (this result is representative of three separate experiments). *C*, [^{35}S]TIMP-3 (1 nM) was added to PEA-13 cells for 24 h, after which conditioned media were harvested and transferred to fresh MEF-1 cells. Radioactivity in the cell-associated fraction (▲), as well as in the TCA-insoluble (■) and TCA-soluble (●) fractions of the conditioned media were quantified by scintillation counting (representative of two separate experiments). *D*, [^{35}S]TIMP-3 (1 nM) was added to MEF-1 cells for 24 h, after which conditioned media were harvested and transferred to naïve MEF-1 cells. Radioactivity in the cell-associated fraction (▲), as well as in the TCA-insoluble (■) and TCA-soluble (●) fractions of the conditioned media were quantified by scintillation counting (this result is representative of two separate experiments). *E*, Conditioned medium harvested from HTB94 cells at different times was analyzed by SDS-PAGE and immunoblotting using 8G1 anti-LRP-1 antibody. *F*, Conditioned medium collected from HTB94 cells was incubated with or without TIMP-3-FLAG (1 nM, overnight, RT) applied to an M2 anti-FLAG resin. The resin was extensively washed with TBS and then with 1 M NaCl in TBS to remove unspecific binding. Subsequently the resin was sequentially eluted with 200 μg/ml FLAG peptide in TBS (2 x 0.5 ml, lanes 1 and 2). Eluted samples were analyzed by SDS-PAGE and immunoblotting using M2 anti-FLAG and 8G1 anti-LRP-1 antibodies. *G*, Different concentrations of TIMP-3 (0 to 25 nM) were incubated with HTB94 cells (24 h, 37 °C). Conditioned media were harvested and analyzed by SDS-PAGE and immunoblotting using 8G1 anti-LRP-1 antibody. *H*, TIMP-3-FLAG was incubated with HTB94 cells (1 nM, 24 h, 37 °C). The conditioned medium containing TIMP-3-FLAG remnants was harvested and applied to an M2 anti-FLAG resin. The resin was extensively washed with TBS and then with 1 M NaCl in TBS to remove unspecific binding. Subsequently the resin was sequentially eluted with 200 μg/ml FLAG peptide in TBS (2 x 0.5 ml, lanes 1 and 2). Eluted samples were analyzed by SDS-PAGE and immunoblotting using M2 anti-FLAG and 8G1 anti-LRP-1 antibodies.

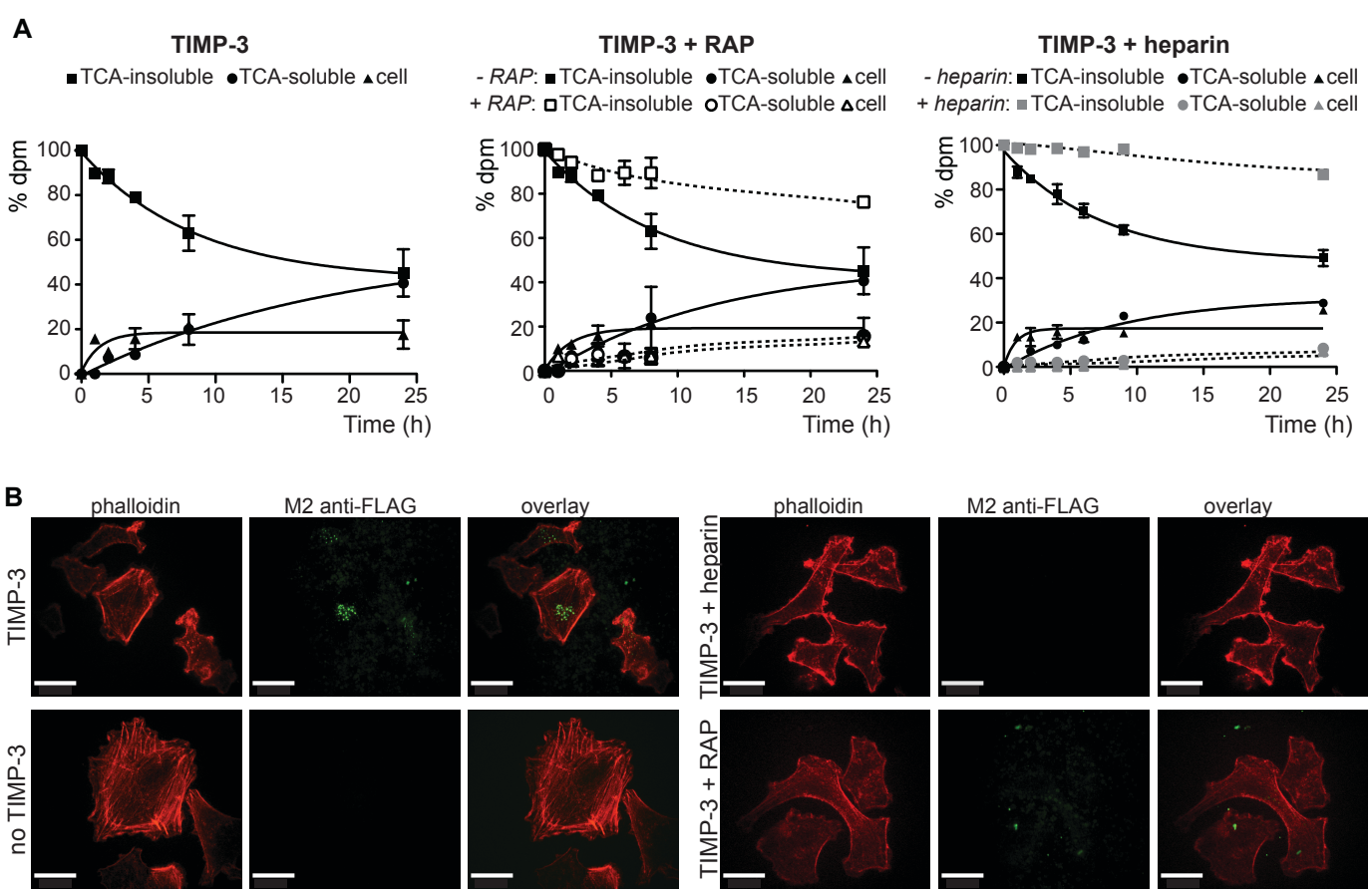
A
TIMP-3
■TCA-insoluble ●TCA-soluble ▲cell
% dpm
Time (h)
TIMP-3 + RAP
- RAP: ■TCA-insoluble ●TCA-soluble ▲cell
+ RAP: □TCA-insoluble ○TCA-soluble △cell
TIMP-3 + heparin
- heparin: ■TCA-insoluble ●TCA-soluble ▲cell
+ heparin: ■TCA-insoluble ●TCA-soluble ▲cell

B
phalloidin
M2 anti-FLAG
overlay
TIMP-3
no TIMP-3
TIMP-3 + heparin
TIMP-3 + RAP

Figure 1

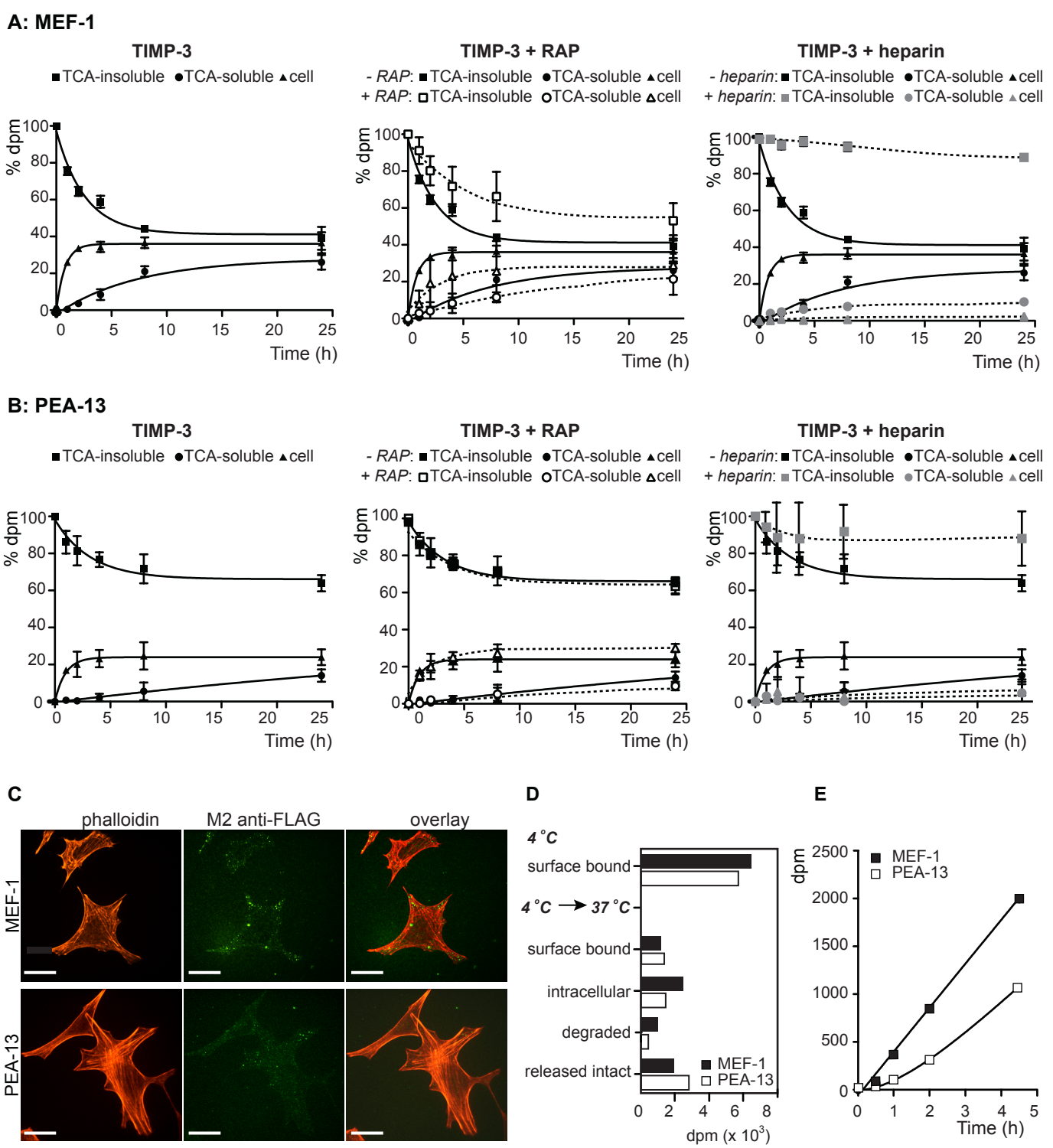
A: MEF-1
TIMP-3
TIMP-3 + RAP
TIMP-3 + heparin
■TCA-insoluble ●TCA-soluble ▲cell
- RAP: ■TCA-insoluble ●TCA-soluble ▲cell
+ RAP: □TCA-insoluble ○TCA-soluble △cell
- heparin: ■TCA-insoluble ●TCA-soluble ▲cell
+ heparin: ■TCA-insoluble ●TCA-soluble ▲cell
% dpm
Time (h)
B: PEA-13
TIMP-3
TIMP-3 + RAP
TIMP-3 + heparin
■TCA-insoluble ●TCA-soluble ▲cell
- RAP: ■TCA-insoluble ●TCA-soluble ▲cell
+ RAP: □TCA-insoluble ○TCA-soluble △cell
- heparin: ■TCA-insoluble ●TCA-soluble ▲cell
+ heparin: ■TCA-insoluble ●TCA-soluble ▲cell
% dpm
Time (h)
C
phalloidin
M2 anti-FLAG
overlay
MEF-1
PEA-13
D
4 ˚C
surface bound
4 ˚C → 37 ˚C
surface bound
intracellular
degraded
released intact
MEF-1
PEA-13
dpm (x 10^3)
E
dpm
MEF-1
PEA-13
Time (h)

Figure 2

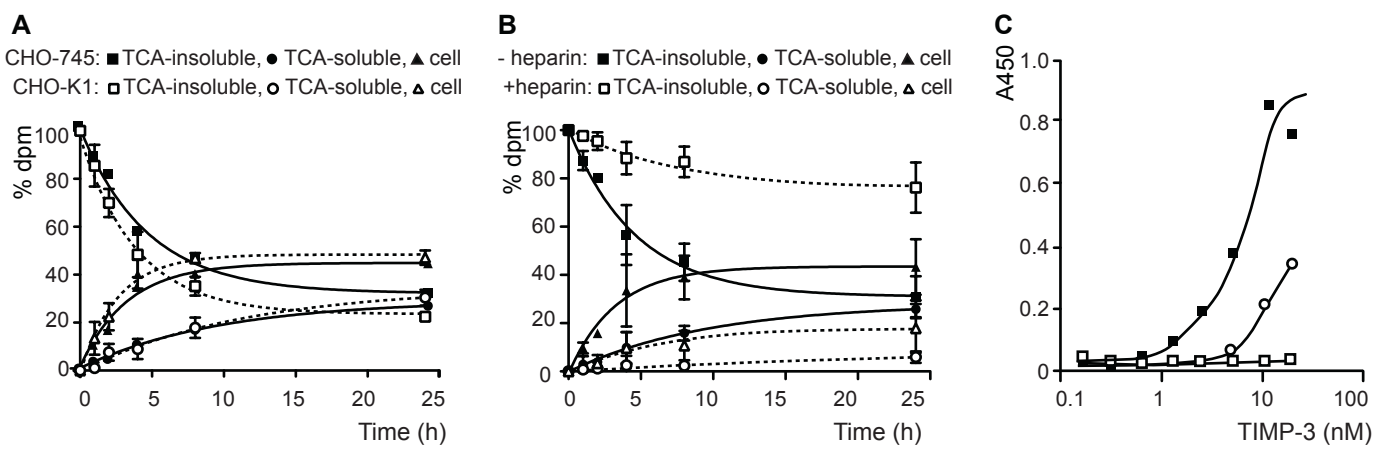
A
CHO-745: ■ TCA-insoluble, ● TCA-soluble, ▲ cell
CHO-K1: □ TCA-insoluble, ○ TCA-soluble, △ cell
% dpm
Time (h)
B
- heparin: ■ TCA-insoluble, ● TCA-soluble, ▲ cell
+heparin: □ TCA-insoluble, ○ TCA-soluble, △ cell
% dpm
Time (h)
C
A450
TIMP-3 (nM)

Figure 3

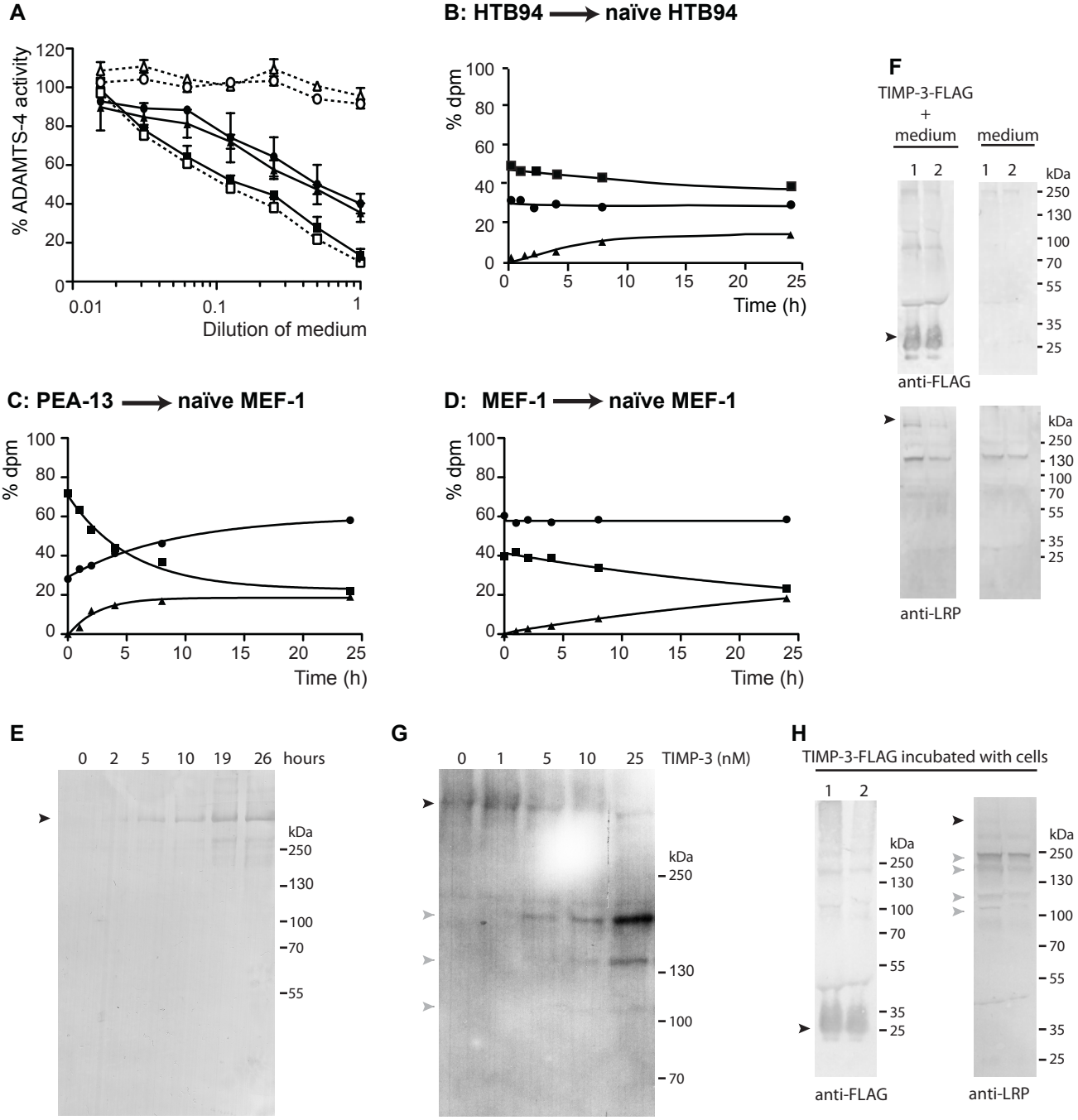
A
% ADAMTS-4 activity
Dilution of medium
B: HTB94 → naïve HTB94
% dpm
Time (h)
F
TIMP-3-FLAG
+
medium
medium
kDa
anti-FLAG
anti-LRP
C: PEA-13 → naïve MEF-1
D: MEF-1 → naïve MEF-1
E
hours
G
TIMP-3 (nM)
H
TIMP-3-FLAG incubated with cells

Figure 4